CHEMICAL REVIEWS

pubs.acs.org/CR

Review

Electrolytes in Organic Batteries

Mengjie Li, Robert Paul Hicks, Zifeng Chen, Chao Luo,* Juchen Guo,* Chunsheng Wang, and Yunhua Xu*

Cite This: *Chem. Rev.* 2023, 123, 1712−1773

Read Online

ACCESS | Metrics & More | Article Recommendations

ABSTRACT: Organic batteries using redox-active polymers and small organic compounds have become promising candidates for next-generation energy storage devices due to the abundance, environmental benignity, and diverse nature of organic resources. To date, tremendous research efforts have been devoted to developing advanced organic electrode materials and understanding the material structure−performance correlation in organic batteries. In contrast, less attention was paid to the correlation between electrolyte structure and battery performance, despite the critical roles of electrolytes for the dissolution of organic electrode materials, the formation of the electrode−electrolyte interphase, and the solvation/desolvation of charge carriers. In this review, we discuss the prospects and challenges of organic batteries with an emphasis on electrolytes. The differences between organic and inorganic batteries in terms of electrolyte property requirements and charge storage mechanisms are elucidated. To provide a comprehensive and thorough overview of the electrolyte development in organic batteries, the electrolytes are divided into four categories including organic liquid electrolytes, aqueous electrolytes, inorganic solid electrolytes, and polymer-based electrolytes, to introduce different components, concentrations, additives, and applications in various organic batteries with different charge carriers, interphases, and separators. The perspectives and outlook for the future development of advanced electrolytes are also discussed to provide a guidance for the electrolyte design and optimization in organic batteries. We believe that this review will stimulate an in-depth study of electrolytes and accelerate the commercialization of organic batteries.

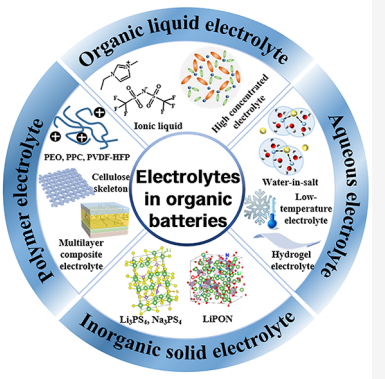

CONTENTS

Received: June 4, 2022
Published: February 3, 2023

https://doi.org/10.1021/acs.chemrev.2c00374
Chem. Rev. 2023, 123, 1712−1773

1. INTRODUCTION

With the fast development of smart technologies, electric transportations and renewable energies, the demands for high-performance and sustainable energy storage are surging.[1] To date, lithium ion batteries (LIBs) are still regarded as promising energy storage systems for future applications because of their high energy density, high operating voltages, and excellent cycling stability.[2] Although the actual energy density of LIBs with optimized inorganic electrode materials and cell architectures can reach 300 Wh kg^{-1}, the search for advanced batteries with higher energy densities is still ongoing.[3] So far, achieving batteries with energy densities approaching to 500 Wh kg^{-1}, a value doggedly pursued by researchers worldwide, has met many challenges relying on current battery chemistries.[4] Commercially ubiquitous battery architectures utilizing cobalt-, nickel-, and manganese-containing lithium transition metal oxide cathodes commonly deliver a practical capacity lower than 200 mAh g^{-1}, limiting the battery energy density. In addition, these inorganic materials are mainly produced from non-renewable and scarce resources.[5,6] Although the development of spent LIBs recycling technology like hydrometallurgical and pyrometallurgical processes provides a new way to realize resource sustainability, low recovery efficiency, high energy consumption, and environmental pollution during the recovery process still pose many challenges in industrial-scale recycling.[7,8] Therefore, considerable research efforts have been devoted to developing novel low-cost, high-capacity, long cyclic stability, and safe battery systems based on renewable and abundant electrode materials and more aggressive battery chemistries.

In contrast to inorganic electrode materials, organic electrode materials are endowed with various merits of facile synthesis, abundant and easily accessible resources, and versatile and flexible structures.[9,10] Organic compounds are mainly composed of naturally abundant lightweight elements (e.g., C, H, N, O, and S) and some of them could be degraded into amino acids on demand after operation,[11] which are potentially low-cost and environmentally benign.[12] Additionally, many organic materials can be derived from biomass or synthesized through mild synthesis processes below 200 °C, in contrast to inorganic materials whose production processes usually require high-temperature annealing.[13,14] Furthermore, the structures of organic molecules are highly tunable, enabling the rational design of high-capacity organic electrode materials.[15] Most intriguingly, due to their universal conversion reaction mechanisms in lieu of the intercalation or displacement mechanisms in inorganic electrode materials, organic electrode materials are electrochemically active in metal ion battery systems beyond LIBs, including naturally abundant alkali metal ions (Na^+ and K^+) and multivalent ions (Zn^{2+}, Mg^{2+}, Ca^{2+}, Al^{3+}, etc.). It is feasible to apply the same organic molecule in various metal ion batteries, which paves the way for developing new battery systems.[16−19]

However, organic batteries still face significant challenges, one of which is the serious dissolution of organic electrode materials in liquid electrolytes. During dissolution, the electrochemically active materials deleteriously migrate from the current collectors, resulting in irreversible capacity decay for the organic electrode. In addition, the dissolved material can diffuse to and corrode the counter electrode, resulting in further degradation of the electrochemical performance of the cells. Based on the perspective of organic electrode materials, a series of strategies have been developed to minimize the dissolution of organic compounds into the electrolytes, such as polymerization with high molecular weight,[20] forming salts with increased polarity,[21,22] designing molecules with large π-conjugated structures[23−26] and immobilizing small molecules with advanced conductive carbon.[27,28] Although encouraging results have been obtained, the introduction of inactive ingredients leads to a decrease in practical capacity. To further optimize previous strategies, the design of novel electrolyte/separator pairings is considered as one of the most effective strategies to mitigate electrode dissolution while maintaining optimal capacity.

Electrolyte composition is a critical, even decisive component in all battery systems, the importance of which cannot be underestimated regarding the development of high-energy-density and functional organic batteries. As well documented, the structures and compositions of electrolytes in inorganic batteries have been widely acknowledged and extensively researched, promoting the performance of high-energy inorganic batteries.[29−31] In the past few decades, various electrolytes, such as aqueous electrolytes, organic liquid electrolytes, inorganic solid electrolytes, polymer electrolytes and polymer/inorganic composite electrolytes have also been studied to enhance the performance of organic batteries. Optimization of a range of electrolytes suitable for different organic electrodes and battery configurations is the key to developing organic batteries which exhibit excellent performance. As proof of principle, based on the general theory of the empirical "like-dissolves-like" rule, most organic electrode materials show lower solubility in aqueous electrolytes and better cyclic performance than that in organic liquid electrolytes. However, the narrow electrochemical stability window (1.23 V) of water is unable to endure the large voltage differences between the cathode and anode in a commercially relevant cell.[32] Although organic liquid electrolytes can enlarge the working voltage window, the severe dissolution challenge still needs to be addressed. In addition, most of the organic batteries are cycled at ultrafast rates (>2 C) in order to minimize the dissolution degree and side reactions. An alternative strategy is the introduction of solid electrolytes that can essentially avoid the dissolution of organic electrodes. However, solid electrolytes harbor their own disadvantages, primarily due to their high mechanical strength and rigid structure, which affects interfacial contact, resulting in poor compatibility with electrodes.

To date, many reviews on organic electrode materials have been published.[9,33−41] However, these reviews have restricted their comprehensive summarization of research efforts by focusing only on four facets: materials structure design, electrode preparation, electrochemical performance, and storage mechanism. Although some electrolytes in specific research fields of organic batteries are briefly discussed in some review articles,[42−45] there is no systematical and comprehensive treatise about electrolytes in organic batteries so far. In addition, the significant difference in requirements of electrolytes between organic and inorganic batteries, owing to drastically different chemical and physical properties of electrodes, must be clarified and addressed to promote greater developments in the field.

https://doi.org/10.1021/acs.chemrev.2c00374
Chem. Rev. 2023, 123, 1712−1773

Scheme 1. Structures and Abbreviations of Organic Electrode Materials

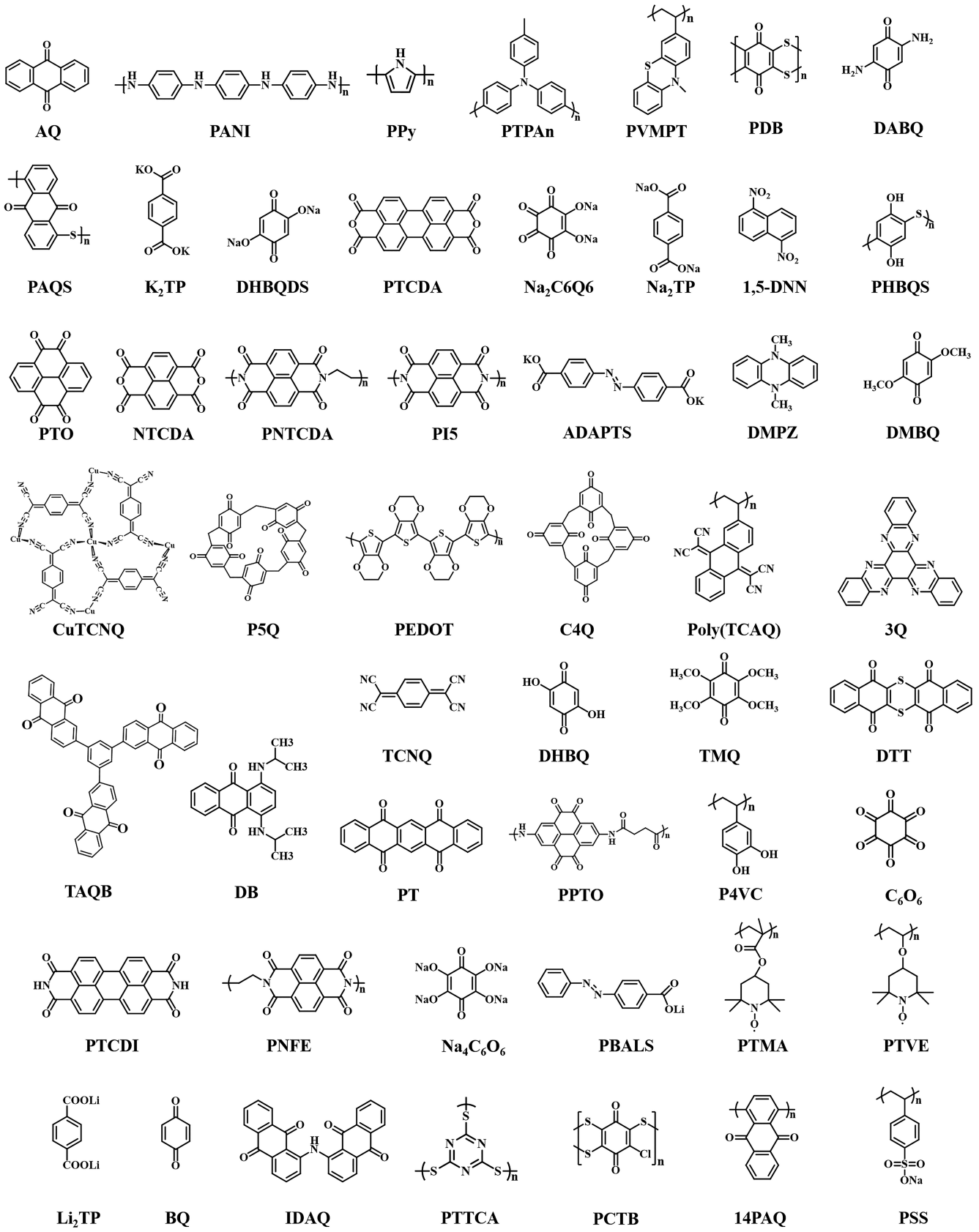

Therefore, a comprehensive summary and in-depth analysis of electrolytes for organic batteries is demanded to provide guidance for their rational design. In this review, we summarize the research progress of electrolytes and separators in organic

https://doi.org/10.1021/acs.chemrev.2c00374
Chem. Rev. 2023, 123, 1712−1773

Scheme 2. Structures and Abbreviations of Solvents and Polymer Matrices in Electrolytes

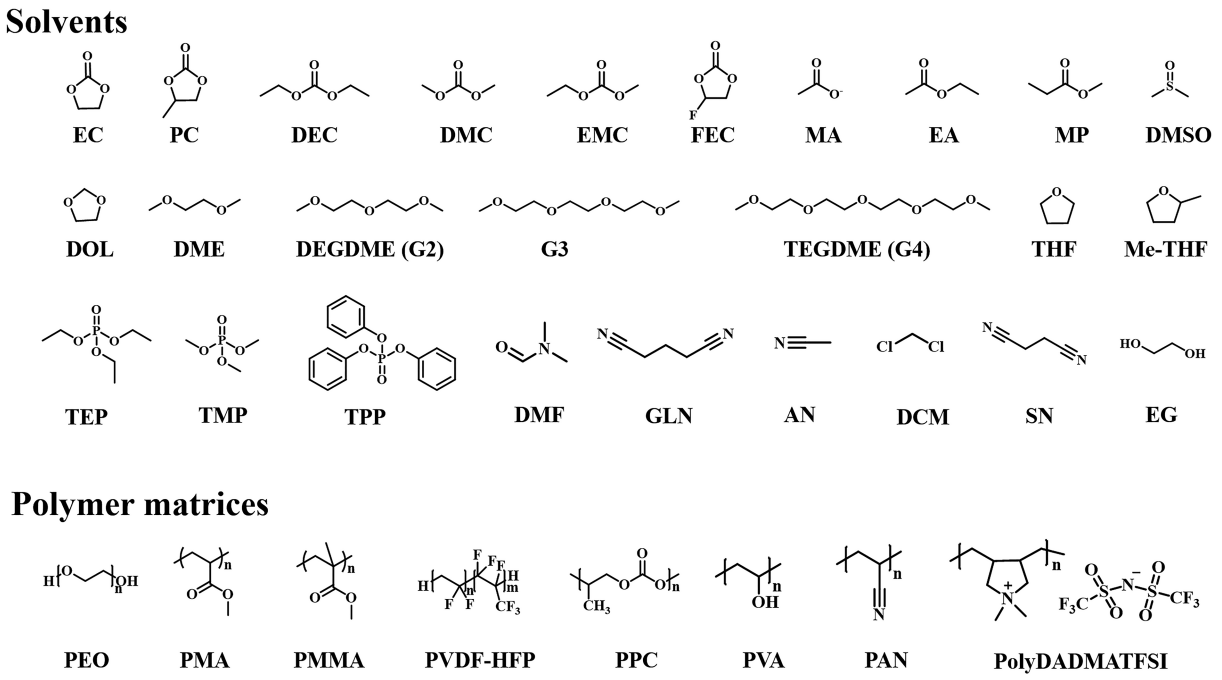

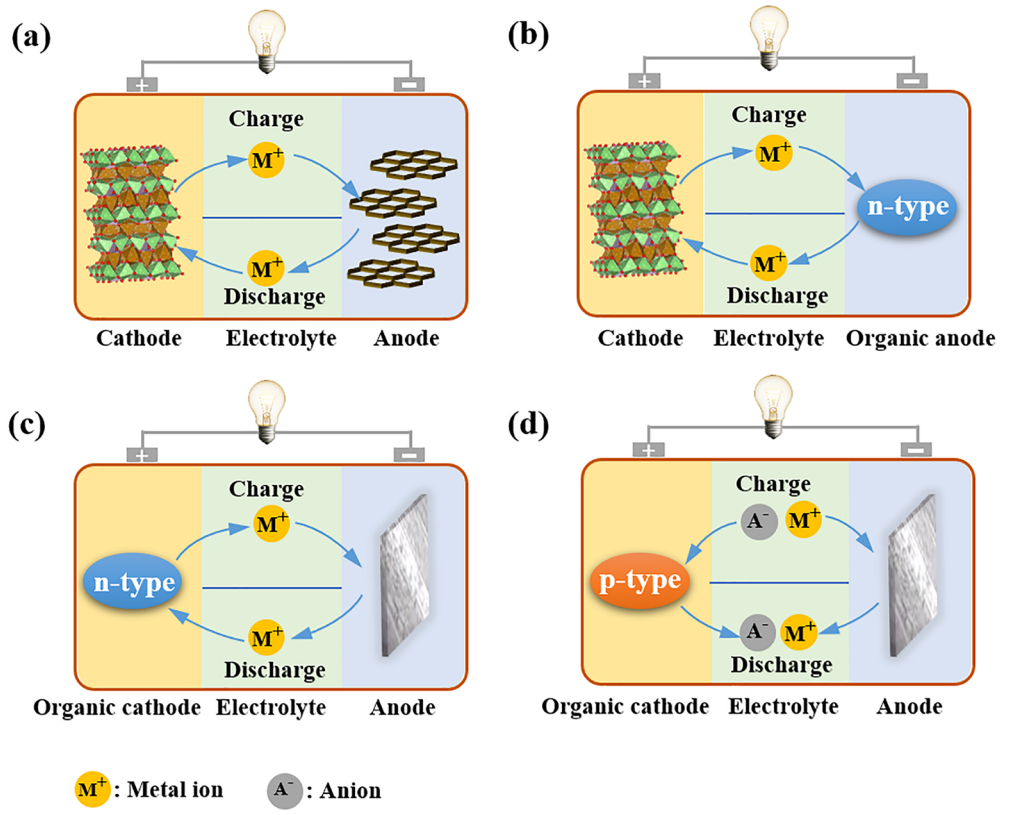

Figure 1. Cell configurations and operation mechanisms of rechargeable batteries based on (a) inorganic cathode, (b) n-type organic anode, (c) n-type organic cathode, and (d) p-type organic cathode.

batteries. Part one discusses the differences of reaction mechanisms and performance requirements between organic and inorganic batteries. Afterward, various electrolytes are summarized and discussed, including organic liquid electrolytes, aqueous electrolytes, inorganic solid electrolytes, and polymer-based electrolytes. In addition, the influence of membrane modification on the performance of organic batteries is discussed. In the last section, the challenges and research directions of organic batteries are also discussed. Structures and abbreviations of organic electrode materials, solvents and

https://doi.org/10.1021/acs.chemrev.2c00374
Chem. Rev. 2023, 123, 1712−1773

polymer matrices in the electrolytes discussed in this review are listed in Schemes 1 and 2, respectively.

2. ORGANIC VERSUS INORGANIC BATTERIES

2.1. Reaction Mechanisms

The charge storage mechanism of conventional inorganic electrodes is based on the reversible intercalation/deintercalation of charge carriers (metal cations, metal complexes, anions, protons, etc.), along with the valence change of transition metals. During the process of energy storage, metal-based structures react with ions to form intercalated compounds, which leads to variation in the crystal structures and chemical/physical properties of electrode materials. Due to the intercalation reaction kinetics of inorganic electrode materials is strongly related to the ionic radius of the insertion ion and the interspace within crystalline structure, only very few ions can be stored with high selectivity and reversibility. In contrast, organic electrode materials are mostly based on reversible electrochemical redox reactions, rather than crystallographic structures, which store charge via changes in the covalent state of electroactive organic groups (carbonyl, nitroxide, organosulfide, etc.). Therefore, the electrochemical activities of most organic electrodes are not sensitive to the radius and type of charge carriers, making organic electrodes amenable universal for different metal ion batteries (Li^+, Na^+, K^+, Mg^{2+}, Ca^{2+}, etc.).

The structure of conventional inorganic-based batteries is shown in Figure 1a, in which metal ions are inserted and stored within the anode and cathode during operation. Generally, the cathode materials are transition metal-containing inorganic compounds, and the anodes are mainly graphitic carbon or alloy-based materials.[46] In organic batteries, organic electrode materials can be categorized into n-type, p-type, and bipolar-type organics according to the charge-state change of active sites.[47] Among them, the n-type electrodes can be used either as anodes or cathodes depending on the actual redox potentials (Figure 1b,c). As shown in Figure 1c, when used as the cathode materials, n-type electrodes are reduced to anions and combined with metal ions such as Li^+ and Na^+ during the discharge process. Due to the higher redox potentials compared with the n-type electrodes, the p-type organics are generally used as cathode materials, which are oxidized and yield cations by reacting with anions like PF_6^- and ClO_4^- in the electrolyte during the charge process. As shown in Figure 1d, for the p-type electrodes, the electrolyte is responsible for transporting metal ions between the anode and the electrolyte, as well as anions between the electrolyte and cathode at the same time. Batteries in which electrolyte salts provide both the cations and anions to be stored in electrodes are called "dual-ion batteries".[48,49] Bipolar-type organic molecules (such as nitronyl nitroxide) can be oxidized or reduced, depending on the applied voltage.[50] The various reaction mechanisms in organic batteries offer numerous opportunities for the design and synthesis of high-performance organic electrode materials to achieve cost-effective and sustainable batteries.

Organic electrode materials can undergo multielectron reactions and exhibit high energy density, while inorganic electrode materials have limited ion selectivity. As a result, transcending the commercially relevant operating voltages and specific capacities have been proven to be relatively difficult for inorganic batteries. Furthermore, the redox reactions of many organic electrode materials are often accompanied by highly reversible bond rearrangement and minimal structural changes with fast reaction kinetics and excellent performances in high-power energy storage devices.[33] Recently, researchers have explored new ways to further improve the rate performance of organic materials by employing extended conjugation systems.[51] In contrast, inorganic electrodes operate via intercalation/conversion/alloying reactions, and the insertion of cations readily leads to the deformation of the lattice structure. The relatively slow reaction kinetics and the easily compromised electrode structure under a high current density adversely affect the cyclic stability and rate performance of the battery.

In addition to the rate performance, the different reaction mechanisms between organic and inorganic electrode materials also affect the performance of the battery under extreme environmental conditions. Major research interest has been invested in the development of batteries which can reliably operate in low-temperature conditions, like ocean exploration and polar expeditions. Although the use of low-freezing-point esters and ionic liquids (ILs) lowers the melting point of the electrolytes and improves ionic conductivity at low temperatures, the traditional transition metal-based inorganic materials are limited by their intrinsic grain boundary resistance and slow diffusion rate of metal ions in the inorganic lattice. Not surprisingly, charge transfer in the electrode becomes more difficult at low temperatures, resulting in the rapid deterioration of battery performance.[52] Relying on current inorganic materials, it is difficult to realize the application of rechargeable batteries in ultralow-temperature conditions (≤ -40 °C). On the contrary, organic electrode materials undergo conversion reactions, especially the amorphous conjugated carbonyl polymers, and are regarded as promising electrode materials for low-temperature applications. The highly reversible keto/enolate pair results in faster redox kinetics than the current intercalation/deintercalation paradigm of transition metal-based inorganic materials. For dual-ion organic batteries, the ion radius of anions is significantly larger than that of cations, so the desolvation energy is also relatively lower, which greatly reduces the dependence of electrode materials on the solvation/desolvation process and improves the performance of the battery at low temperatures. Therefore, exploring the low-temperature performance of organic electrode materials and electrolytes is a promising research direction for the development of organic batteries.

To further expand the application of organic batteries, the energy density needs to be further improved, which is closely related to the specific capacity and working potential of electrodes. As shown in Figure 2, the working potential of the inorganic cathode is usually higher than 3.5 V versus Li^+/Li, and the cutoff potentials of some ternary materials like $LiNi_{0.895}Co_{0.085}Mn_{0.02}O_2$[53] and "Li-rich" materials[54] can even reach 4.8 V versus Li^+/Li. However, the high working voltage of inorganic cathode materials often leads to continuous electrolyte decomposition, resulting in poor cycling stability of the battery. Although p-type cathode materials own high voltage comparable to conventional inorganic cathodes, most of them can only provide a limited specific capacity, usually less than 100 mAh g^{-1}, which makes them less appealing to obtain a satisfactory energy density. For n-type cathode materials, the working potentials are usually within the range of 1.8−3.5 V versus Li^+/Li, which is significantly lower than that of inorganic cathode materials, limiting the high energy density of organic batteries. Efforts to tune the working potentials of n-type organic electrode materials have been realized by introducing electron-withdrawing or electron-donating groups into the electrode

https://doi.org/10.1021/acs.chemrev.2c00374
Chem. Rev. 2023, 123, 1712−1773

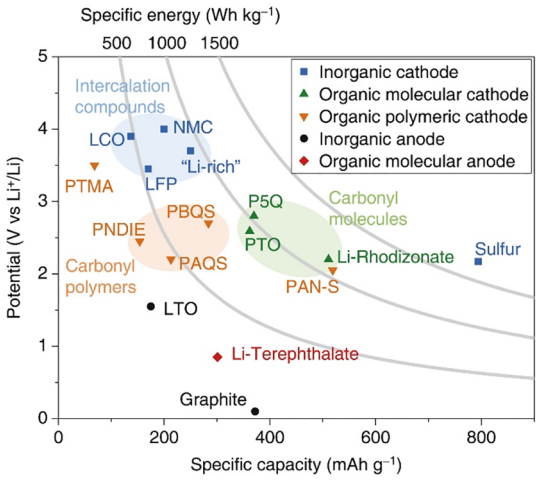

Figure 2. Redox potentials and specific capacities of selected inorganic and organic electrode materials. Reproduced with permission from ref 33. Copyright 2018 Elsevier.

materials,[55,56] changing the relative position and number of active groups,[57,58] and designing different conjugated structures.[59] For example, by introducing relatively strong electronegative atoms (O, N, or S) into 9,10-anthraquinone (AQ), the energy level of the lowest unoccupied molecular orbital (LUMO) of the obtained heteroaromatic compounds is decreased, which generally results in higher reduction potentials.[55] It is worth noting that the improvement of the working potentials of organic cathode materials should not compromise the chemical and electrochemical stability of electrolytes. Therefore, developing high-voltage and high-capacity organic electrode materials, accompanied by the design of suitable electrolyte systems, is another pivotal research direction for the large-scale application of high-performance and sustainable organic batteries.

In addition, the poor cyclability and increased self-discharge effect due to the dissolution of organic molecules in polar organic electrolytes are fundamental shortcomings that must be addressed to ensure the viability of organic materials in future battery design. Dissolved active materials often peel away from the current collector and can even shuttle to the counter electrode and cause side-reactions, resulting in irreversible capacity loss and poor cycle life. To solve the dissolution problem, various strategies have been developed, including electrode material design and electrolyte modification. Many research efforts have been reported on the design of electrodes to suppress or prevent the dissolution of organic active materials. Additionally, many reviews have been published on this aspect,[47,60] and this is not the emphasis of this paper. We will, instead, discuss the electrolytes in organic batteries in detail.

2.2. Electrical Conductivity

The electronic conductivity of the electrode material greatly affects the charge and discharge rates of the battery. For electrode materials with poor conductivity, it is often necessary to add a large amount of conductive additive to promote electronic and ionic transport, achieving fast and reversible redox reactions. Compared with inorganic electrodes, organic electrode materials (except for conductive polymers like polyacetylene, polyaniline (PANI), polypyrrole (PPy),[61] poly-paraphenylene,[62] polythiophene, and polytriphenylamine (PTPAn)[63]) generally exhibit lower intrinsic electronic conductivity.[36] The insulating nature of many organic molecules strongly affects efficient ion/electron transport in organic electrodes while also hindering the full utilization of the active materials. A common strategy to curtail the insulative properties of organic materials is to add more conductive agents during electrode preparation. For example, approximately 80 wt % conductive carbon additive was added to the nitroxyl polyradical cathode for the stable free radical organic batteries in 2002.[64] Though increasing the content of conductive carbon in the organic electrodes can improve the conductivity, it sacrifices the gravimetric and volumetric energy densities of the organic batteries. Hence, minimizing the carbon content but retaining the high conductivity of organic electrodes is crucial for the large-scale application of organic batteries.

At present, the conductivity of the organic electrodes are generally enhanced by the following methods: 1) coating with a conductive layer; 2) introducing conductive moieties;[65] 3) adding highly conductive materials (such as carbon nanotubes,[66,67] graphene,[68,69] and carbon fibers) on a molecular level; 4) constructing single-ion conducting materials;[57] 5) adopting organics with a large π-conjugated structure;[70] 6) performing annealing treatments to promote π-electron delocalization;[71] 7) forming organic charge transfer composites (OCTCs).[72] In OCTCs, monomers with different electron accepting and donating capabilities interact each other by π donor−acceptor interaction, forming molecular layers with high structural stability. The relatively strong intercomponent interactions between the orderly stacked layers could form a relatively dense electron cloud, providing a rapid and short electron transfer pathway and elevating the electronic conductivity of OCTCs. Significant progress has been made to improve the conductivity of organic electrodes, establishing a solid foundation for the practical application of organic batteries.

2.3. Mechanical Properties

Organic compounds, especially polymers, are promising for portable electronic applications due to their excellent flexibility, easy processing, and facile design. In particular, aqueous Zn-organic batteries have been successfully applied in wearable electronic devices.[73] Furthermore, in solid-state organic batteries, the inherent low Young's modulus of organic electrode materials could efficiently prevent the contact loss at the interface between the electrode and the solid-state electrolyte, while maintaining intimate interfacial contact during cell cycling.[74,75] In contrast, inorganic electrode materials with high Young's modulus are less likely to maintain adequate electrochemical performance after repeated cycling. The degradation in capacity for inorganic electrode materials is generally attributed to local stress caused by intercalation related volume changes which may lead to cracks at the interface, and eventually result in the loss of mechanical contact with the substrate, particle level cracking, and electronic isolation.[76,77]

2.4. Materials Resources and Costs

It is estimated that a Li-ion battery with a 100 kg cathode requires 6−12 kg of cobalt and 36−48 kg of nickel.[78] At present, the battery industry accounts for about 50% of the total consumption for cobalt, while approximately 70% of the world cobalt resources are located in Congo (Kinshasa).[79] Furthermore, the demand for cobalt and nickel resources will exceed production within 20 years if their use continues to increase.[78] The limited production and uneven distribution, combined with the low recovery and high cost of these transition metals have become increasingly prominent problems with the development of large-scale energy storage technology (Figure 3),[79,80] which

https://doi.org/10.1021/acs.chemrev.2c00374
Chem. Rev. 2023, 123, 1712−1773

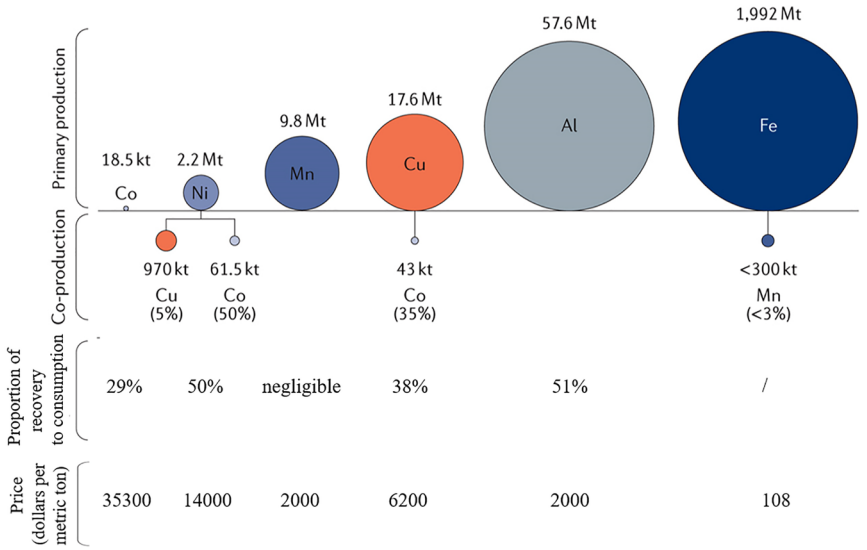

Figure 3. Global annual (co)production from mineral mining, recovery rate, and price of several metals. Reproduced with permission from ref 80. Copyright 2018 Springer Nature. (The output of metallic elements comes from ref 80. The proportion of recovered metal to apparent consumption and price come from ref 79.)

may lead to high and unstable production costs for batteries. In addition, the use of large amounts of transition metals not only consumes nonrenewable mineral resources, but also causes severe environmental degradation due to the excessive exploitation of the heavy metals combined with the energy consumption and greenhouse gas emission in the process of synthesis and recovery.

To address these challenges, organic electrode materials are promising alternatives to inorganic electrode materials for battery industries to achieve cost-effective and sustainable energy storage. Organic compounds are primarily composed of naturally abundant elements (C, H, N, O, S), which are considered with respect to inorganic metals as relatively sustainable, environmentally friendly, and low-cost materials for batteries. Some electrode materials for organic batteries have even been directly extracted from natural biomass,[81] which is conducive to sustainable development. In addition, because the synthetic processes for organic materials are flexible and more easily controlled, than with respect to inorganic materials, optimizing energy use and resource utilization is theoretically easier to achieve. Since most organic electrode materials are not yet commercially available or mass-produced, it is difficult to estimate their costs. Lu et al.[36] calculated the costs of several organic batteries by using BatPaC software and compared them with two inorganic battery systems of $LiNi_{0.6}Co_{0.2}Mn_{0.2}O_2$ (NCM622)-Li and NCM622-graphite. The results show that the cost of batteries using high-voltage n-type organic cathode materials (especially carbonyl compounds like 1,4-benzoquinone) and Li anodes is lower than that of the NCM622-graphite system and equivalent to that of the NCM622-Li system, indicating great economic prospects for organic electrode materials in practical applications.

2.5. Requirements for Electrolytes

To enhance electrochemical performance, appropriate electrolytes are required for both organic and inorganic batteries. Though there are four types of electrolytes, including organic liquid electrolytes, aqueous electrolytes, inorganic solid electrolytes, and polymer-based electrolytes, advanced electrolytes should have the following features to satisfy the needs of rechargeable batteries.

(1) **High ionic conductivity and low electronic conductivity**: An idea electrolyte is expected to possess high ionic conductivity to efficiently transfer ionic charges between electrodes, and negligible electronic conductivity to prevent internal short-circuits and self-discharge. Liquid electrolytes often have low viscosity and exhibit suitable solvation characteristics, to achieve the rapid ion transport during the charge−discharge process. In contrast, solid polymer electrolytes typically exhibit low ionic conductivity, which can be improved by adding solvents and/or inorganic fillers, or increasing the operating temperature. For inorganic solid-state electrolytes, increasing the sintering density and reducing the grain boundary resistance can improve the ionic conductivity.[82] In addition, recent studies have shown that reducing the electronic conductivity of solid-state electrolytes is critical to prevent the formation of dendrites inside the electrolyte.[83]

(2) **Suitable electrochemical stability window**: The electrochemical window of the electrolyte should be wider than the operating voltage range of the battery in order to minimize electrolyte decomposition. Though the electrolyte decomposition in the first charge/discharge cycle generates the solid electrolyte interphase (SEI) on the anode and cathode electrolyte interphase (CEI) on the cathode to enlarge the stability window of the electrolytes in practical applications, a stable electrolyte is required to avoid continuous electrolyte decomposition and achieve high Coulombic efficiency upon long-term cycling. Compared with inorganic electrode materials, the working potential of organic electrode materials is generally lower, and many aqueous, organic liquid, and solid-state electrolytes which are incompatible in the inorganic system become uniquely accessible in organic batteries. For some high-voltage electrodes, it is necessary to design electrolytes with high oxidation resistance to match them.

https://doi.org/10.1021/acs.chemrev.2c00374
Chem. Rev. 2023, 123, 1712−1773

(3) **Excellent compatibility with the electrode**: Electrolyte/electrode compatibility is the precondition of developing high energy density batteries with excellent electrochemical performance. For example, maintaining effective and uniform ion transport at the electrolyte/electrode interface is critical when employing a solid-state electrolyte to achieve a high-energy density battery.
(4) **Good thermal stability**: The development of batteries that can operate under wide operating temperature ranges requires the implementation of electrolytes that maintain adequate compatibility with the electrode materials as well as high ionic conductivity over those ranges.
(5) **Low cost, simple preparation, and low toxicity**: These are regarded as the primary metrics for the commercial application of rechargeable batteries, especially for the deployment in stationary electric energy storage, where the cost and toxicity are critical factors for grid-scale applications.

2.5.1. Liquid Electrolytes. The performances of liquid electrolytes are closely related to the characteristics of solvents and salts. In organic batteries, the choice of solvents is often the same as that of inorganic batteries, and for both types of batteries, the solvents need to have a low viscosity, an adequate solvation relationship with the salts, and sufficient electrochemical stability in the working potential window. However, the use of solvents optimized for inorganic batteries readily leads to the spontaneous dissolution of active materials in organic batteries. Using ILs as the solvent, increasing the salt concentration or incorporating additives such as fluoroethylene carbonate (FEC) can significantly reduce the solubility of some organic materials and improve the cyclic stability of the organic batteries.

In commercial inorganic batteries, the electrolyte solvents are mainly selected from the carbonate esters due to their wide electrochemical stability window and formation of the stable SEI. To satisfy the application requirements of electrolytes in terms of dielectric constant, viscosity, ionic conductivity, melting point, and so on, the electrolyte solvents are often a mixture of cyclic and linear carbonates. The mixed organic carbonate solvents are implemented more often than the ether-based solvents such as 1,3-dioxolane (DOL) and 1,2-dimethoxyethane (DME), because the latter are usually unstable at the working potential above 4.0 V and cannot be used in high-voltage batteries. Intriguingly, the ether-based electrolytes exhibit better performance than carbonate-based electrolytes in organic batteries. Compared to carbonate solvents, electrolytes based on ether solvents exhibit relatively better compatibility with organic electrodes, resulting in increased cycling stability. The increased compatibility can be attributed to diminished solubility of active organic materials and the formation of a relatively stable SEI layer.

In addition to the solvents, the selection criteria of electrolyte salts used in inorganic and organic batteries differs, mainly depending on the type and desired dissociation characteristics of metal ions. Traditional LIBs are generally fabricated using transition metal oxides as the cathode and graphite or alkali metal as the anode. The operating principles of LIBs are usually reliant on lithium-based electrolytes, which means the cations in the salts are Li ions, and the anions are generally PF_6^-, ClO_4^-, BF_4^-, $TFSI^-$ for nonaqueous electrolytes or Cl^-, NO_3^-, SO_4^{2-}, $TFSI^-$ for aqueous electrolytes. Likewise, in organic batteries, the electrochemical redox reactions result in the transition between the neutral state and the negatively charged state of the n-type organic electrode materials, which using cations in the electrolyte to balance the charge. In addition, for many n-type organic materials, Li^+ can be replaced by other alkali ions (such as Na^+ and K^+) or even H^+ without significantly affecting the electrochemical behavior. This is different from inorganic intercalation compounds, which are very sensitive to cationic radii. In contrast, p-type organic electrode materials usually act as cathode materials for batteries and mainly rely on anions in the electrolyte to balance the charges. During the charging process, the p-type organic electrode materials will lose electrons, and the anions in the electrolyte will participate in the electrode reaction to maintain charge neutrality.

2.5.2. Solid-State Electrolytes. Compared with liquid electrolytes, solid-state electrolytes can completely solve the dissolution challenge of organic electrode materials, but introduce high interfacial resistance. At present, the application of solid-state electrolytes in organic batteries draws heavily from previous research work done on the all-solid-state inorganic LIBs or Na-ion batteries (NIBs). However, the requirements for solid-state electrolytes in organic and inorganic batteries are different and are summarized below.

There are many reports about ceramic solid-state electrolytes for inorganic electrode materials, such as sulfide electrolytes, oxide electrolytes, halide electrolytes, perovskite/antiperovskite, garnet, and lithium phosphorus oxynitride (LiPON).[31,84−86] For solid-state NIBs, β-alumina is also a commonly used electrolyte.[87] Nevertheless, in solid-state organic batteries, only the sulfide electrolytes, LiPON, and β-alumina were reported to couple with n-type materials. Sulfide-based electrolytes exhibit high ionic conductivity, on par with that of conventional liquid electrolytes. In addition, even at room temperature, sulfide-based electrolytes can be easily processed into dense films and maintain intimate contact with electrodes, showing low grain boundary resistance and excellent ductility.[88] For LiPON, with high redox stability, its combination with organic electrodes holds the potential for thin-film all-solid-state batteries with high volumetric and specific energy densities. The reports of other ceramic electrolytes (such as perovskite/antiperovskite, NASICON-like and garnet) for organic batteries are rare. In addition, the p-type organics are much more difficult to be combined with inorganic solid-state electrolytes, because the redox reactions of p-type organic electrode materials rely on anions in the electrolyte to balance the charge, while traditional ceramic and glassy solid-state electrolytes are single ion conductors that only transfer cations.

Compared with organic cathode materials, the oxidizing potentials of intercalation-type inorganic cathodes are generally higher,[88,89] requiring electrolytes with wider electrochemical stability windows to avoid side reactions. Some electrolytes with low anodic decomposition potentials, such as sulfide electrolytes, readily form a resistive interfacial layer between the electrode and the electrolyte when they are coupled with an transition metal oxide-based cathode, resulting in reduced capacities.[90,91] Furthermore, the formation of a highly resistive space-charge layer hinders ion transport.[92] Therefore, it is necessary to add a chemically inert coating layer like $LiNbO_3$[93] or Li_3PO_4[94] on the surface of the cathode particles to maintain the electrochemical and chemical compatibility of the interface. The development of halide solid-state electrolytes with high ionic conductivity and high chemical and electrochemical stability provides an effective strategy to realize high-voltage all-solid-state batteries without interfacial coatings on the cathode materials.[95] However, the poor electrochemical

https://doi.org/10.1021/acs.chemrev.2c00374
Chem. Rev. 2023, 123, 1712−1773

Table 1. Key Physical Properties, LUMO, and HOMO Energy Levels of the Organic Solvents and Additives for Electrolytes in Organic Batteries

Solvent	Dipole moment [debye]	Viscosity at 25 °C [cP]	Dielectric constant at 25 °C	Density at 25 °C [g mL^{-1}]	LUMO [eV][a]	HOMO [eV][a]
Ethylene carbonate (EC)	4.61	1.90 (40 °C)	89.78	1.32	1.089	−7.924
Propylene carbonate (PC)	4.81	2.53	64.92	1.20	1.112	−7.870
Diethyl carbonate (DEC)	0.96	0.75	2.805	0.97	1.254	−7.633
Ethyl methyl carbonate (EMC)	0.89	0.65	2.9	1.01	1.222	−7.675
Dimethyl carbonate (DMC)	0.76	0.59 (20 °C)	3.107	1.06	1.189	−7.718
1,3-Dioxolane (DOL)	1.25	0.59	7.1	1.06	3.049	−6.639
Ethylene glycol dimethyl ether (DME)	1.15	0.46	7.2	0.86	2.532	−6.695
Diethylene glycol dimethyl ether (G2 or DEGDME)	–	0.94	7.4	1.1	2.312	−6.698
Tetraethylene glycol dimethyl ether (G4 or TEGDME)	2.45	1.01	7.5	3.4	2.186	−6.613
Tetrahydrofuran (THF)	1.63	0.5	7.1	0.5	2.707	−6.353
Acetonitrile (AN)	3.92	0.3	36.6	0.78	1.087	−8.905
Fluoroethylene carbonate (FEC)	–	2.4	109.4	1.45	0.696	−8.315
Triethyl phosphate (TEP)	–	1.7	–	1.07	1.751	−7.633
Trimethyl phosphate (TMP)	–	2.0	–	1.20	1.599	−7.728

[a]LUMO and HOMO energy values of the solvent were calculated by applying the density functional theory (DFT) method with the hybrid density functional B3LYP and the 6-31G(d, p) basis set using Gaussian g09 software package.[109]

reduction stability of halide electrolytes impairs their compatibility with metal anodes. It is necessary to develop strategies to stabilize the interface with metal anodes and explore large-scale and low-cost preparation processes to realize the practical application of halide electrolytes.[96] Organic electrode materials, with lower operating voltages, are relatively more compatible with electrolytes featuring low anodic decomposition potentials and do not necessitate the use of complex surface treatments for the electrode materials.

In addition, the interfacial performances are also different in organic and inorganic solid-state batteries. Inorganic electrode materials usually have a high Young's modulus. During the repeated intercalation/deintercalation processes in an inorganic battery, the electrode materials are prone to lose interparticle contact with the electrolyte as a result of structural damage accrued from mechanical stresses due to volume changes.[97−99] However, organic electrode materials have low mechanical strength, which can effectively relieve interfacial stress and maintain intimate contact between the active material and the electrolyte without additional interfacial modification treatment. To promote the development of all-solid-state organic batteries for safe, sustainable, and high-energy-density energy storage, advanced organic electrode materials with new redox chemistries and high compatibility to the solid-state electrolytes are demanded. Moreover, exploring the organic electrode−electrolyte interaction and stability, as well as the interfacial chemistry, are promising research directions for all-solid-state organic batteries.

3. ELECTROLYTES IN ORGANIC BATTERIES

The electrolyte as an indispensable and decisive component in rechargeable batteries plays an important role in balancing the charge via ion transport between the cathode and the anode.[29,100] The choice of the electrolyte directly affects the energy density, cycle life, safety, and working conditions of the battery. For organic batteries, the type and concentration of the electrolyte, the choice of the solvent and salt, and the use of additives all affect the reversible capacity, solubility of electrode materials, and interfacial stability between the electrode and the electrolyte. Therefore, choosing an appropriate electrolyte system is essential for obtaining an organic battery with excellent overall performances.

3.1. Organic Liquid Electrolytes

Organic liquid electrolytes based on organic solvents and inorganic salts function as bridges for ion transport between cathodes and anodes, and prevent deleterious electron transport inside rechargeable batteries. During the initial discharge/charge cycles, organic liquid electrolytes are decomposed at low (<1 V versus Li/Li$^+$) and high (>3.5 V versus Li/Li$^+$) reaction potentials to form electronic insulating but ionic conductive passivation layers. The layers are known as SEI, on the anode surface and CEI on the cathode surface. The SEI/CEI layers are critical components in the optimal functioning of commercially viable batteries. The layers block the physical contact between electrodes and electrolytes, and minimize continuous side reactions, resulting in improved Coulombic efficiency and capacity retention of the electrodes. As it is well-documented, the formation of stable and robust SEI/CEI layers is paramount for inorganic batteries to exhibit high cyclability and high Coulombic efficiency.[101,102] Similarly, organic liquid electrolytes also play a critical role in the formation of SEI/CEI in organic batteries, which will impact the cycle life and Coulombic efficiency. Therefore, it is of great significance to gain fundamental insight into the correlation between the structure of organic liquid electrolytes and the electrochemical performance of organic batteries for rational electrolyte design and organic battery performance optimization.

3.1.1. Effects of the Solvent. Organic solvents are the main components in the liquid electrolytes, which are critical for defining the overall battery performance. According to past research experiences, the selected organic solvents should exhibit the following features: 1) a high dielectric constant to enhance the solubility of inorganic salts and ensure a high ionic conductivity; 2) a relatively low viscosity over a wide operating temperature range; 3) a high electrochemical and chemical stability within the operating voltage range.

In the past few decades, a variety of solvents have been used in electrolytes for batteries, including carbonate-based solvents such as ethylene carbonate (EC), propylene carbonate (PC),

https://doi.org/10.1021/acs.chemrev.2c00374
Chem. Rev. 2023, 123, 1712−1773

Table 2. Comparison of the Physical Properties of Several Charge Carriers for Rechargeable Batteries; Reproduced from Ref 110, Copyright 2020 American Chemical Society

	Li^+	Na^+	K^+	Mg^{2+}	Al^{3+}	Ca^{2+}
Relative atomic mass	6.94	23.00	39.10	24.31	26.58	40.08
Mass-to-charge ratio	6.94	23.00	39.10	12.16	8.86	20.04
Theoretical gravimetric capacity of $ACoO_2$[a] (mAh g^{-1})	274	235	206	260	268	242
Theoretical volumetric capacity of $ACoO_2$[a] (mAh cm^{-3})	1378	1193	906			
E^0 (A/A^+_{aq}) (V vs SHE)	−3.04	−2.71	−2.93	−2.4	−1.7	−2.9
E^0 (A/A^+_{PC}) (V vs Li/Li^+_{PC})	0	0.23	−0.09			
Shannon's ionic radii (Å)	0.76	1.02	1.38	0.72	0.54	1.06
Stokes radii in water (Å)	2.38	1.84	1.25	3.47	4.39	3.10
Stokes radii in PC (Å)	4.8	4.6	3.6			
limiting molar ionic conductivity in PC (S cm^2 mol^{-1})	8.3	9.1	15.2			
Desolvation energy in PC (kJ mol^{-1})	215.8	158.2	119.2	569.4		
Melting point (°C)	180.5	97.8	63.4	650	660	842

[a]Theoretical capacities of $ACoO_2$ with the multivalent ions are estimated based on $Mg_{0.5}CoO_2$, $Al_{1/3}CoO_2$, and $Ca_{0.5}CoO_2$.

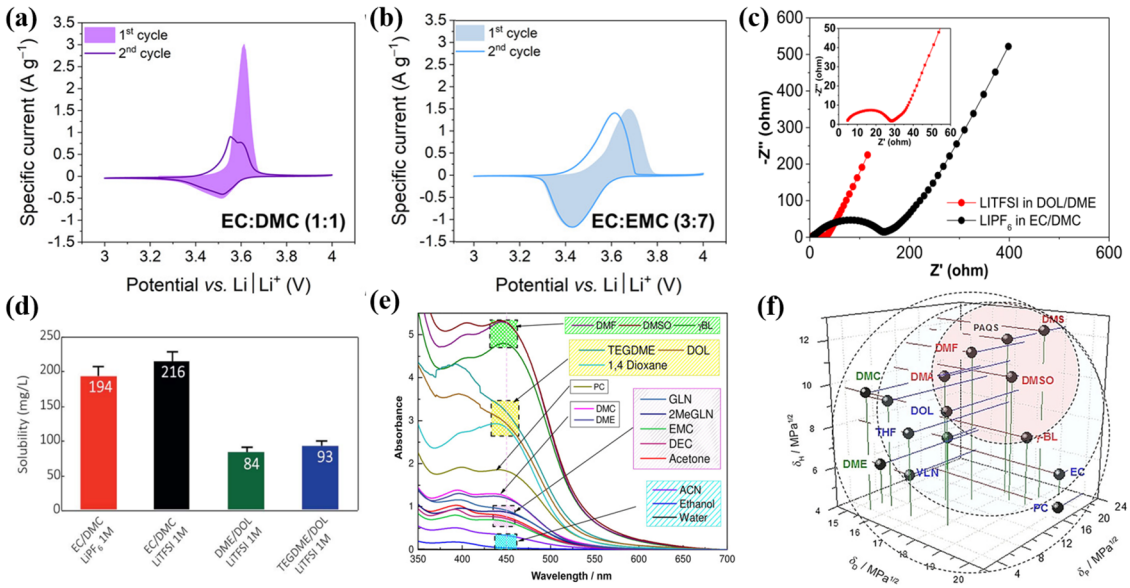

Figure 4. Effects of the solvent in organic liquid electrolytes on electrode/electrolyte interfacial compatibility and solubility of organic electrodes. Cyclic voltammetry (CV) curves of the PVMPT electrode using 1 M $LiPF_6$ in (a) EC/DMC (1:1) and (b) EC/EMC (3:7) electrolytes. Reproduced from ref 111. Copyright 2021 American Chemical Society. (c) Electrochemical impedance spectroscopy (EIS) profiles of fresh cells in different electrolytes. The inset shows the enlarged EIS plot of the cell with LiTFSI-DOL/DME electrolyte. Reproduced with permission from ref 112. Copyright 2018 Wiley-VCH. (d) Saturated concentrations of DABQ in different electrolytes. Reproduced with permission from ref 113. Copyright 2019 Royal Society of Chemistry. (e) Solubility test of PAQS in various solvents. (f) Location of various solvents in Hansen space. Reproduced with permission from ref 115. Copyright 2018 Wiley-VCH.

diethyl carbonate (DEC), dimethyl carbonate (DMC), ethyl methyl carbonate (EMC),[57] and ether-based solvents such as DOL, DME, diethylene glycol dimethyl ether (DEGDME or G2), triethylene glycol dimethyl ether (G3), tetraethylene glycol dimethyl ether (TEGDME or G4),[103] tetrahydrofuran (THF), and methyltetrahydrofuran (Me-THF). Recently, fluorinated ether solvents such as triethylene glycol[104] and fluorinated 1,4-dimethoxylbutane[105] were reported to exhibit excellent compatibility with the Li metal anode and high stability at high redox potentials. A common practice to obtain an advanced electrolyte with a high dielectric constant and a low viscosity is to use multisolvents in one electrolyte and take the advantage of the special feature of each solvent to satisfy the requirements of high-performance batteries. For example, the mixture of EC (high dielectric constant, but high viscosity) and DMC (low viscosity, but insufficient dielectric constant) in a ratio of 1:1 has been widely used in commercial LIBs. In addition, some fire-retardant solvents such as triethyl phosphate (TEP),[106] trimethyl phosphate (TMP),[107] and triphenyl phosphate (TPP)[108] also endow the electrolyte with nonflammability, which greatly improves the battery safety. Key physical properties, LUMO, and the highest occupied molecular orbital (HOMO) energy levels of the common organic solvents and additives for electrolytes are summarized in Table 1.[29,109]

For metal-ion batteries beyond LIBs, the development of electrolytes is different from conventional LIBs due to the intrinsic differences of ionic radius, standard potential, and ionic charge distribution between Li^+ and other metal ions. Table 2 shows the comparison of physical and chemical properties of several metal ion charge carriers for rechargeable batteries.[110] Since Na^+ and K^+ have identical cationic charge, similar redox potentials (vs Li^+/Li) and electrochemistry behaviors to Li^+, the

https://doi.org/10.1021/acs.chemrev.2c00374
Chem. Rev. 2023, 123, 1712−1773

selection of electrolyte solvents in organic batteries based on Na^+ or K^+ could be similar to conventional Li-based electrolytes. However, for the battery systems involving Zn^{2+}, Mg^{2+}, Ca^{2+}, and Al^{3+}, the selection of electrolyte solvents is different. Although the development of electrolytes for organic batteries has attracted some interests from the battery field, the basic research is still not sufficient. Here, we summarized the various electrolyte systems in organic batteries, and related research results are also discussed below.

For p-type electrodes with high redox potentials, ester-based electrolytes with a wide electrochemical stability window are often selected. While for n-type electrodes, the cycling stability of organic batteries containing ether-based electrolytes surpasses those containing carbonate-based electrolytes. The use of ester-based electrolytes has been linked to a greater degree of active material dissolution, diminished compatibility and inadequate SEI layer formation, with respect to the organic electrodes.

3.1.1.1. Reducing Dissolution of Active Materials. In general, except certain compounds with a highly extended conjugation structure and some organic salts, small organic molecules like quinone derivatives, acid anhydride compounds, and some low-molecular-weight polymers suffer from the dissolution challenge. Suitable solvents for the electrolytes could reduce the dissolution of these materials to a certain extent.

It was reported that the solubility of the poly(3-vinyl-*N*-methylphenothiazine) (PVMPT) electrode can be significantly reduced by reducing the content of cyclic carbonate EC and selecting asymmetric linear carbonate EMC instead of symmetric linear carbonate DMC in the solvent mixture.[111] Compared with the 1 M (where M is molar concentration, mol L^{-1}) $LiPF_6$ in EC/DMC (1:1) electrolyte, the irreversible capacity decay of the PVMPT electrode in the 1 M $LiPF_6$ in EC/EMC (3:7) electrolyte is greatly reduced due to the decrease of solubility (Figure 4a,b). Xie et al.[112] ascribed the reasons for the poor cycling performance of the poly(2,3-dithiino-1,4-benzoquinone) (PDB) electrode in carbonate-based electrolytes to two aspects: 1) the dissolution of PDB in the carbonate-based electrolyte is more severe than that in the ether-based electrolyte as evidenced by the obvious color change of the two separators from cycled batteries; 2) the poor compatibility of the carbonate-based electrolyte with the PDB electrode results in higher interfacial resistance and sluggish reaction kinetics (Figure 4c).

To improve the electrochemical performance of organic batteries and mitigate the high solubility of organic electrode materials in liquid electrolytes, it is critical to gain fundamental insight into the correlation between electrolyte solvents and organic material solubility. Vlad and colleagues[113] explored the reason for the high solubility of 2,5-diamino-1,4-benzoquinone (DABQ) in carbonate-based electrolytes and found a clear correlation between the dipole moment of the solvent and the solubility. The relatively low dipole moments of DOL (1.25 D), DME (1.15 D), and TEGDME (2.45 D) result in less damage to the H-bond-based crystallinity of DABQ. However, the high dipole moment (up to 4.61 D) of EC results in the formation of H-bonds between the carbonyl groups in EC and the amine groups in DABQ, thereby increasing the solubility of DABQ in the EC-based electrolyte. Therefore, electrolytes based on DOL/DME and DOL/TEGDME solvents showed lower solubility than the EC/DMC-based electrolyte at the same salt concentration (Figure 4d) and the cyclic stability of the corresponding battery was better. It is noteworthy that DMC has the lowest dipole momentum of 0.76 D among all the tested electrolyte solvents. Correspondingly, DABQ also shows a low solubility in the DMC-based electrolyte, which can be attributed to the relatively large polarity difference between DMC and DABQ. Therefore, the development of a battery system based on organic electrode materials and electrolytes with opposite polarities is expected to mitigate the dissolution in organic batteries. To this end, Renault et al.[114] introduced ionic auxiliary groups to small polyimide (PI) molecules to drastically increase the polarity of the organic electrode material and coupled the material with low polarity electrolyte of 1 M lithium bis(trifluoromethanesulfonyl)imide (LiTFSI) in DMC to maximize the expected polarity difference. However, it is not accurate to predict the solubility of organic materials based on the dipole moment or the dielectric constant of the solvents alone. Phadke et al.[115] analyzed the solubility of polyanthraquinone sulfide (PAQS) in 17 different solvents (Figure 4e) and found that although *N*,*N*-dimethylformamide (DMF) and glutaronitrile (GLN) have similar dielectric constants and showed similar polarity, the solubility of PAQS in DMF is much higher than that in GLN. To accurately predict the trends of solubility, Hansen solubility parameters (HSPs) analysis was employed. In 1967, HSPs were proposed by Hansen to predict miscibility between different material systems, in which the total cohesive energy of a species is the sum of three individual energetic components of hydrogen bonding (δ_h), dispersion interaction (δ_d), and polar cohesive energy (δ_p).[116] Since the change in solubility is mainly attributed to different intermolecular interactions, the HSPs can be used to predict the solubilities of polymers in different solvents.[117] The Hansen space was established with δ_h, δ_d, and δ_p as three coordinates. When the values of δ_h, δ_d, and δ_p of the solvent are similar to those of PAQS, the distance between the solvent and PAQS molecule is small, indicating that PAQS has a higher solubility in the solvent (Figure 4f).[115] However, the polarity of organic electrode materials will change dramatically during the charge and discharge processes. Though the organic electrode materials are insoluble in the optimized electrolytes, the charged or discharged states of the materials could be soluble, resulting in poor cyclic stability. Hence, it is difficult to establish a reliable correlation between the polarity of active materials or electrolytes and the cyclic stability of organic batteries.

3.1.1.2. Constructing a Stable SEI. In addition to the high solubility challenge of organic electrode materials, the choice of the solvent also affects the wettability of electrolytes and the formation of the SEI. Lei et al.[118] compared the electrochemical performances of the dipotassium terephthalate (K_2TP) electrode in two different types of electrolytes and found that DME-based electrolyte resulted in better rate capability and cycling performance with respect to carbonate-based electrolytes. The superior performance of the DME-based electrolyte was attributed to two factors: 1) the excellent wettability of the DME-based electrolyte in the K_2TP electrode enables the contact angle close to 0°, while the poor wettability of carbonate-based electrolytes results in poor interfacial contact between the electrode and the electrolyte; 2) the SEI film formed by the DME-based electrolyte is smooth and robust, allowing for the fast transfer of K^+ ions. In contrast, the surfaces of cycled electrodes in carbonate-based electrolytes are seamed and rough because of the formation of dynamically unstable and thick SEI films. Seamed and rough SEIs generally result in larger charge transfer resistance and lead to large voltage polarization.

https://doi.org/10.1021/acs.chemrev.2c00374
Chem. Rev. 2023, 123, 1712−1773

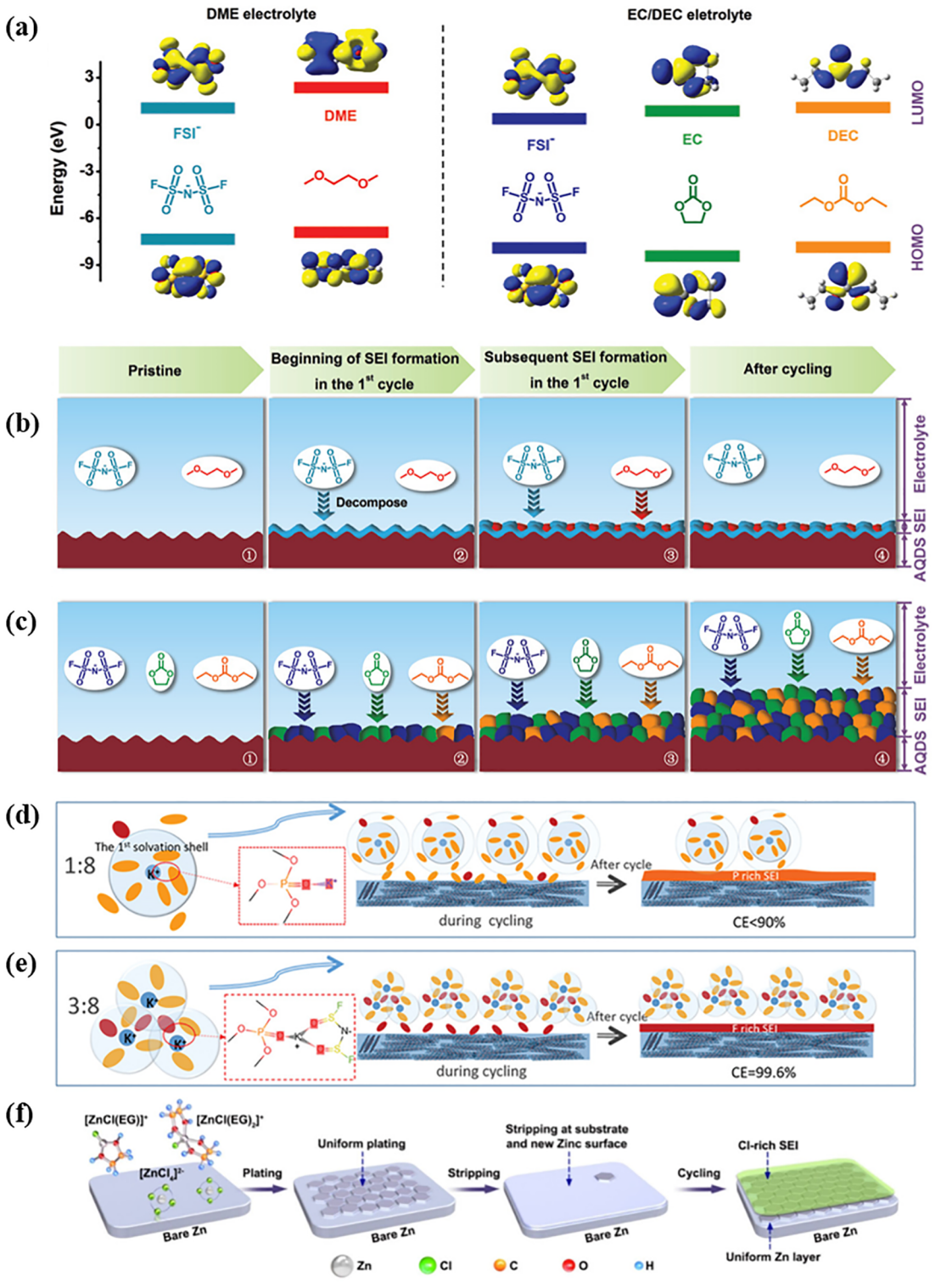

Figure 5. Effects of the solvent in organic liquid electrolytes on SEI formation. (a) HOMO and LUMO energy levels of solvents and potassium salts (FSI^- and DME in DME-based electrolyte; FSI^-, EC, and DEC in EC/DEC-based electrolyte). The process of the SEI formation during the first cycle and its growth in the following cycles with (b) DME electrolyte and (c) EC/DEC electrolyte. Reproduced with permission from ref 119. Copyright 2019 Wiley-VCH. Schematic diagrams of the solvation structure and SEI formation on graphite in (d) 1:8 (KFSI:TMP) electrolyte and (e) 3:8 (KFSI:TMP) electrolyte, respectively. Reproduced with permission from ref 107. Copyright 2021 Wiley-VCH. (f) Schematic illustration of Zn plating/stripping in $ZnCl_2$-EG electrolyte. Reproduced with permission from ref 125. Copyright 2022 Wiley-VCH.

Since the operating potentials of n-type organic cathode materials are usually in the range of 1.8 to 3.5 V versus Li^+/Li, most organic liquid electrolytes are thermodynamically stable against the organic cathodes. Therefore, in contrast to the SEI, the study on the formation and optimization of CEI is scarce. The selection of the solvents and salts for the electrolytes

https://doi.org/10.1021/acs.chemrev.2c00374
Chem. Rev. 2023, 123, 1712−1773

determines the composition of the SEI due to the different LUMO energy levels of the solvent and salt molecules.[119] Theoretical calculations, for the formation of a desirable SEI, show that the LUMO energy level of FSI^- is much lower than that of DME molecules in the potassium bis(fluorosulfonyl)-imide (KFSI)-DME electrolyte (Figure 5a), indicating the preferential decomposition of KFSI during the first cycle. The inorganic-rich inner SEI layer can effectively protect the electrode and effectively alleviate the subsequent decomposition of DME molecules (Figure 5b), thus enhancing the electrochemical stability of the battery. In contrast, in the KFSI-EC/DEC electrolyte system, the LUMO energy levels among FSI^-, EC, and DEC are relatively similar, and they are decomposed simultaneous in the first cycle, resulting in a random distribution of inorganic and organic components in the SEI layer (Figure 5c). During subsequent cycles, cracks are formed in the mosaic structure of the SEI due to the large volume change caused by the repeated potassiation/depotassiation process. At the same time, the electrolyte penetrates the SEI through the cracks and directly contact with the anode surface, leading to continuous decomposition of the electrolyte, large irreversible capacity loss, and poor cyclability. Similar results were reported for NIBs using sodium hexafluorophosphate ($NaPF_6$)-DEGDME and $NaPF_6$-EC/DEC electrolytes.[120] Since the LUMO energy level of PF_6^- is lower than that of DEGDME, an inorganic-rich SEI layer is formed in the ether-based electrolyte as a result of the preferential decomposition of $NaPF_6$. In contrast, because of the similar LUMO energy levels of PF_6^-, EC, and DEC in the EC/DEC electrolyte, simultaneous decomposition of these chemicals occurs, resulting in the formation of an unstable mosaic structure SEI layer, the continuous growth of the SEI, and poor cycle life. Therefore, developing organic liquid electrolytes composed of low LUMO energy level salts and high LUMO energy level solvents is a promising research direction for high-performance organic batteries.[109,121,122] It is noteworthy that the frontier orbital characters in the electrolyte can be modified by changing the electrolyte concentration and adjusting the solvation structure, which is discussed in Section 3.1.3.

To improve the performance of organic batteries, other ether and carbonate solvents such as Me-THF and FEC were also employed in electrolytes. Armand and co-workers[123] studied a series of redox-active Schiff-base polymers for NIBs coupled with $NaPF_6$-EC/DMC, sodium bis(fluorosulfonyl)imide (NaFSI)-(PC or DEGDME or Me-THF) and sodium bis-(trifluoromethanesulfonyl)imide (NaTFSI)-(DEGDME or Me-THF) to optimize the performance of organic batteries. The results indicated the battery system based on the NaFSI in Me-THF electrolyte exhibited the highest capacity and best cyclic stability. Luo et al.[124] systematically compared the effects of FEC/DMC and EC/DMC on the electrochemical performance of a 2,5-dihydroxy-1,4-benzoquinone disodium salt (DHBQDS) nanorod electrode, and found that regardless of whether poly(vinylidene difluoride) (PVDF) or sodium alginate was used as the binder, the sodium perchlorate ($NaClO_4$)-FEC/DMC electrolyte showed a better cyclic stability compared than the $NaClO_4$-EC/DMC electrolyte. By analyzing the CV result in the first charge/discharge cycle, it was found that there was an extra sodiation plateau centered at 1.4 V in the FEC-based electrolyte, which may be associated with the formation of a thicker and F-rich stable SEI layer. This SEI consequently results in reduced dissolution of the active material and stabilized electrode.

In addition to carbonate- and ether-based electrolytes, electrolytes based on organic phosphates and ethylene glycol (EG) can also be used in organic batteries. Liu et al. found that KFSI-TEP and KFSI-TMP without the need for superhigh-concentration electrolytes could form a stable SEI layer on the graphite surface, which not only effectively suppresses electrolyte decomposition but also enables long cyclability of a 3,4,9,10-pyrenetetracarboxylic dianhydride (PTCDA)-graphite full cell.[106,107] As shown in Figure 5d, when the molar ratio of KFSI to TMP is 1:8, both FSI^- anions and free TMP molecules have similar chances to decompose on the electrode surface, resulting in significant solvent decomposition, the formation of a phosphorus-rich SEI, irreversible capacity loss during cycling, and low Coulombic efficiency of <90%. However, when the KFSI-TMP electrolyte is formulated with a molar ratio of 3:8, almost all TMP molecules are involved in the solvation of K^+ cations, leading to the formation of a fluorine-rich SEI. This effectively suppressed the continuous decomposition of electrolytes on the surface of the graphite anode and resulted in a high Coulombic efficiency of 99.6% (Figure 5e). Very recently, Geng et al.[125] developed a new electrolyte composed of EG and zinc chloride ($ZnCl_2$), which realized dendrite-free Zn anode and long cycle life of Zn-PANI battery. Via the hydrogen-bond interactions between EG molecules and $ZnCl_2$, EG molecules participate in the Zn^{2+} solvation and form $[ZnCl(EG)]^+$ and $[ZnCl(EG)_2]^+$ complex cations, leading to the formation of a Cl-rich organic−inorganic SEI film on the surface of Zn anode, thus realizing reversible and uniform Zn plating/stripping (Figure 5f). Therefore, the formation of a stable and robust SEI layer is critical for the development of high-performance organic batteries.

3.1.1.3. Altering the Reaction Routes. Apart from the influence on the solubility of organic electrode materials and the formation of the SEI layer, the electrolytes also affect the redox potential, phase transformation, structure change, and the reaction mechanism of the active materials.

Lee et al. found that the reversibility of some p-type organic cathodes was significantly affected by the type of the solvent in the electrolyte.[126] Using electrolytes with low-donor-number solvents, like AN and TEGDME, the CV curves of 5,10-dihydro-5,10-dimethyl phenazine cathode showed two pairs of redox peaks, corresponding to two-step one-electron redox reactions. However, with the electrolytes containing high-donor-number solvents, like DMSO and DMF, the second cathodic peaks disappeared, indicating that the multielectron transfer became irreversible. This could be attributed to the redox potential of the electrode exceeding the electrochemical stability window of the electrolyte, resulting in an irreversible capacity loss. Considering that the redox potentials of redox-active organic species decrease with the reduce of the donor numbers of the electrolytes, the redox reaction of the electrode can be adjusted within the stable electrolyte window by choosing the solvent with a lower donor number.[127] Since anions in the electrolyte need to be desolvated to participate in the electrode reaction for p-type electrode materials, the desolvation and binding process would also affect the redox potential of the battery. Compared with the poly(ethylene glycol) (PEG)+H_2O and EMC solvents, the $Zn(CF_3SO_3)_2$ molecules with AN solvent showed the highest desolvated energy, and the corresponding cell had the highest charge and discharge voltage.[128] The above results indicate that the redox potential of the electrode can be altered by adjusting the type of solvents, which provides new insight in developing organic cathodes with high energy density.

https://doi.org/10.1021/acs.chemrev.2c00374
Chem. Rev. 2023, 123, 1712−1773

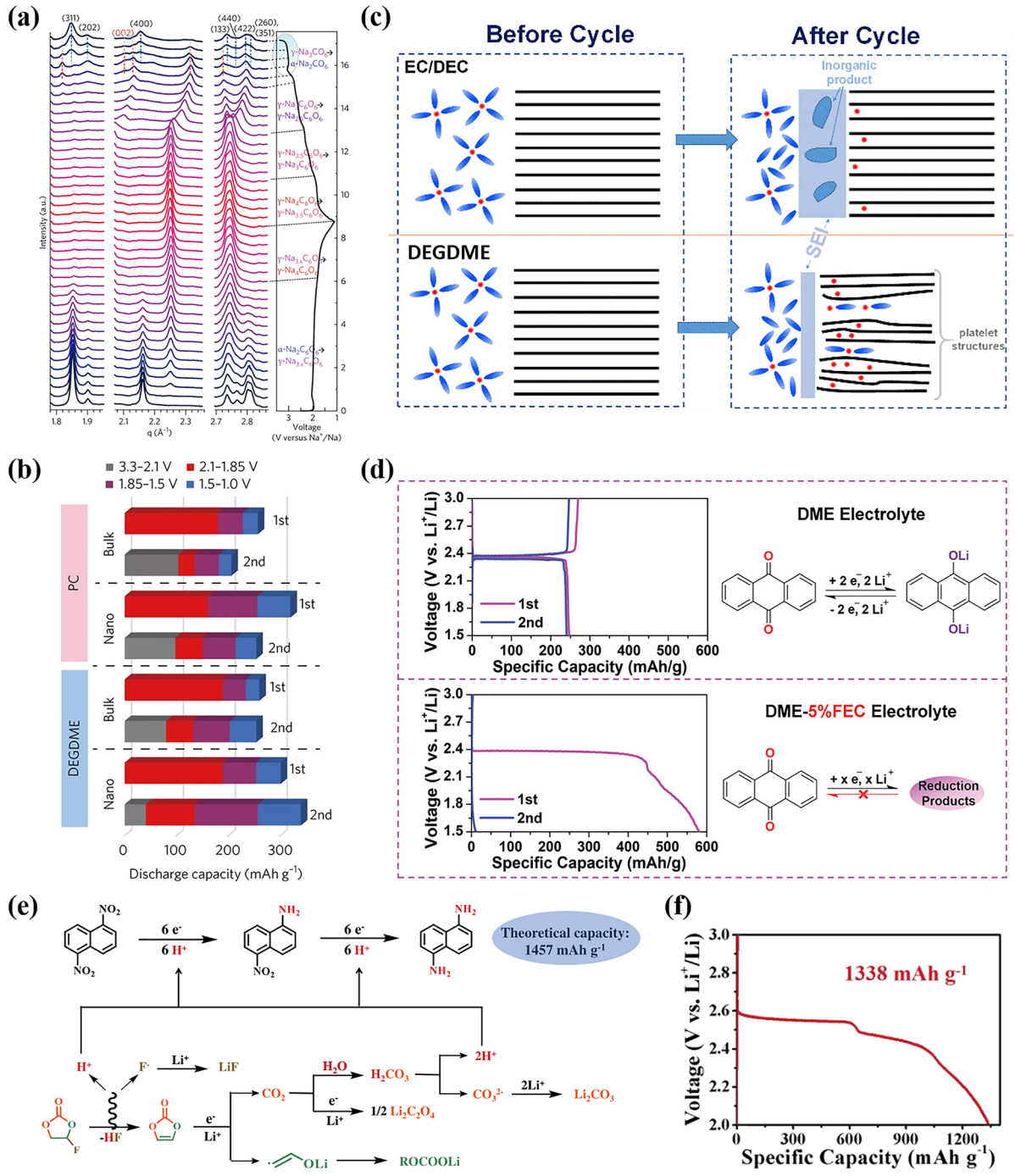

Figure 6. Effects of the solvent in organic liquid electrolytes on the phase transformation, structure change and the reaction mechanism of organic electrodes. (a) In situ synchrotron XRD patterns of $Na_2C_6O_6$ electrode during sodiation/desodiation processes. (b) Comparison of discharge capacities of $Na_2C_6O_6$ electrode for different conditions. Reproduced with permission from ref 129. Copyright 2017 Springer Nature. (c) Schematic illustration of Na^+ storage in Na_2TP using EC/DEC and DEGDME electrolytes. Reproduced with permission from ref 130. Copyright 2020 Elsevier. (d) Galvanostatic charge/discharge curves of AQ in DME and DME-5% FEC electrolytes. Reproduced with permission from ref 131. Copyright 2020 Wiley-VCH. (e) Supposed reduction path and (f) galvanostatic charge/discharge curves of 1,5-DNN in the electrolyte with FEC. Reproduced with permission from ref 132. Copyright 2021 PNAS.

In addition, the choice of the electrolyte also affects the activation barrier in the redox reaction of active materials. A representative example is the perfect combination of a disodium rhodizonate ($Na_2C_6O_6$) cathode and a DEGDME-based electrolyte.[129] The result of the *in situ* synchrotron X-ray diffraction (XRD) (Figure 6a) indicated that the crystalline structure of $Na_2C_6O_6$ changed from γ-$Na_2C_6O_6$ to α-$Na_2C_6O_6$ during the charging (desodiation) process. In contrast, when utilizing a PC-based electrolyte, the transition from γ-$Na_2C_6O_6$ to α-$Na_2C_6O_6$ requires overcoming a large activation energy barrier and usually exhibits a high degree of irreversibility, thus severely restricting the electrochemical performance of

https://doi.org/10.1021/acs.chemrev.2c00374
Chem. Rev. 2023, 123, 1712−1773

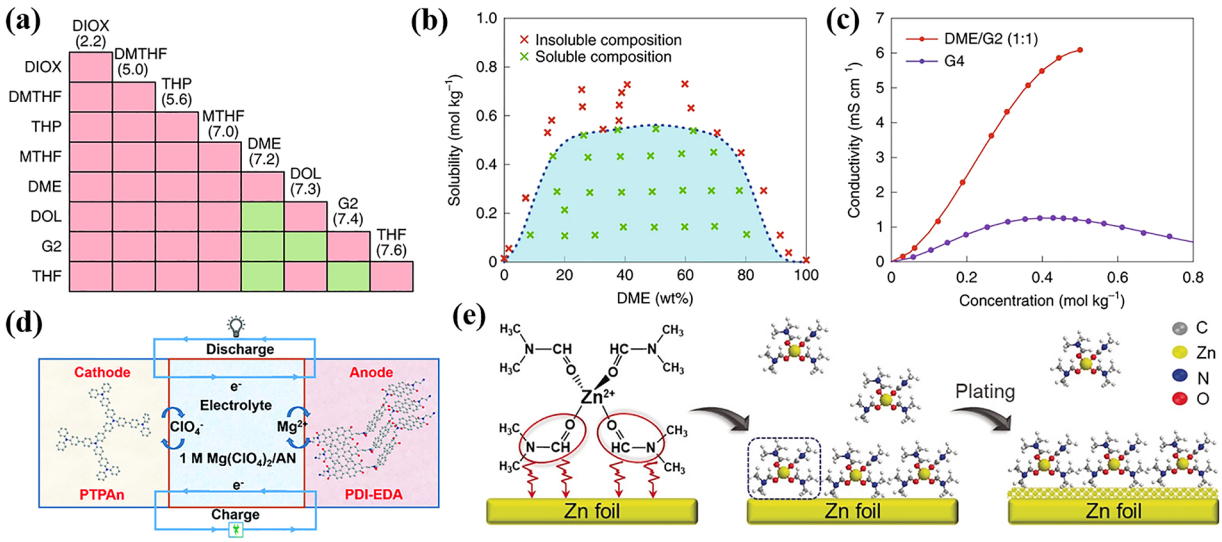

Figure 7. Selection of solvents in multivalent metal-ion organic batteries. (a) The differences of solubility of MMC salt in different mixed solvents. Color codes represent the solubility of MMC: pink (insoluble) and green (soluble). (b) Solubility diagram of MMC in the mixture of DME/G2. (c) Effects of MMC concentrations on the ionic conductivity of electrolytes with G4 solvent and DME/G2 mixed solvent, respectively. Reproduced with permission from ref 139. Copyright 2020 Springer Nature. (d) Schematic illustration of all-organic dual-ion battery using 1 M $Mg(ClO_4)_2$/AN electrolyte. Reproduced with permission from ref 140. Copyright 2018 Royal Society of Chemistry. (e) Schematic diagram of Zn^{2+}-DMF complexes enable the smooth Zn deposition in DMF-based electrolyte. Reproduced with permission from ref 144. Copyright 2020 Wiley-VCH.

$Na_2C_6O_6$. As shown in Figure 6b, decreasing the particle size of $Na_2C_6O_6$ and using DEGDME to replace PC as the electrolyte solvent could effectively improve the reversible capacity of $Na_2C_6O_6$. Researchers attributed the improvement to a lower kinetic barrier of the phase transformation between α-$Na_2C_6O_6$ and γ-$Na_2C_6O_6$ during charge and discharge processes, thereby achieving efficient four-sodium storage with a high reversible specific capacity of 484 mAh g^{-1}. Recent research has also shown that DEGDME-based electrolytes can generate an ultrathin SEI layer and promote beneficial irreversible structure change in graphene/disodium terephthalate (Na_2TP/G) electrodes during the sodiation/desodiation process, which enables the one-step sodium storage process.[130] Compared with the two-step sodium storage process that occurred in the EC/DEC-based electrolytes, the ultrathin SEI layer and one-step sodium storage process in DEGDME-based electrolytes are beneficial to shorten the diffusion length of Na-ions across the SEI and decrease charge transfer impedance, resulting in better electrode kinetics and higher initial Coulombic efficiency (Figure 6c). Hence, the use of different electrolytes can alter the reaction mechanism of organic electrode materials. To further confirm it, Sun et al.[131] found that the reaction mechanism of AQ changed from reversible transformation between carbonyl and enol structures to an irreversible lithiation mechanism when the solvent in the electrolyte was change from pure DME to 5% FEC in DME. The irreversible chemistry of AQ yields a high discharge capacity of 575 mAh g^{-1} and a high energy density of 1300 Wh kg^{-1} (Figure 6d). Similarly, adding FEC in electrolyte could change the reaction mechanism of nitroaromatic electrode materials, converting the reversible one-electron reaction between nitro groups and N-OLi structures into an irreversible six-electron amination reaction (Figure 6e).[132] As a result, the electrode of 1,5-dinitronaphthalene (1,5-DNN) delivered an ultrahigh specific capacity of 1338 mAh g^{-1} and impressive energy density of 3273 Wh kg^{-1} (Figure 6f) which surpassed all reported organic and inorganic cathode materials. The new reaction provides a valuable strategy for manufacturing Li-organic primary batteries with high energy density.

In summary, electrolytes play pivotal roles in the performance of organic batteries in terms of mitigating the electrode solubility, generating robust SEIs, supporting desirable reaction kinetics, and tuning the reaction mechanism. Rational structure design of the liquid electrolytes is paramount for the performance optimization of organic batteries.

3.1.1.4. Solvent Optimization for Multivalent Batteries. Though great success has been achieved for carbonate- and ether-based electrolytes in alkali-ion batteries, simply applying these electrolytes in other battery systems such as multivalent batteries does not guarantee the excellent performance. For example, the carbonate solvents widely used in LIBs are not suitable for rechargeable Mg-organic batteries with Mg metal as the counter electrode. This is because the decomposition of carbonate solvents in Mg batteries form a passivation layer on the surface of the Mg metal, which precludes the migration of Mg^{2+}. The passivation layer, which is rich in MgO, $Mg(OH)_2$, $MgCO_3$, and $(ROCO_2)_2Mg$, not only impedes the continuous reaction between the electrolyte and Mg metal, but also deactivates the Mg-metal anode quickly, resulting in low Coulombic efficiency. In addition, the relatively high reactivity and negative potential of Mg metal render aqueous electrolytes unsuitable. Therefore, in rechargeable Mg-metal batteries, the selection of solvents is mostly limited to ether-based solvents such as THF,[133,134] DME,[135] DEGDME, TEGDME,[136] or their mixed solutions.[137] The ether-based electrolytes could improve the reversibility of Mg plating/stripping and result in high Coulombic efficiency of more than 98%. Bitenc et al.[138] compared the effects of the pure TEGDME solvent and the mixed solvent of TEGDME/DOL on the performance of Mg-poly(hydrobenzoquinonyl-benzoquinonyl sulfide) (PHBQS) batteries. It was found that compared with the TEGDME/DOL-based electrolyte, PHBQS showed a slower activation process and higher final polarization in the pure TEGDME-based electrolyte, because the high viscosity and relatively strong

https://doi.org/10.1021/acs.chemrev.2c00374
Chem. Rev. 2023, 123, 1712−1773

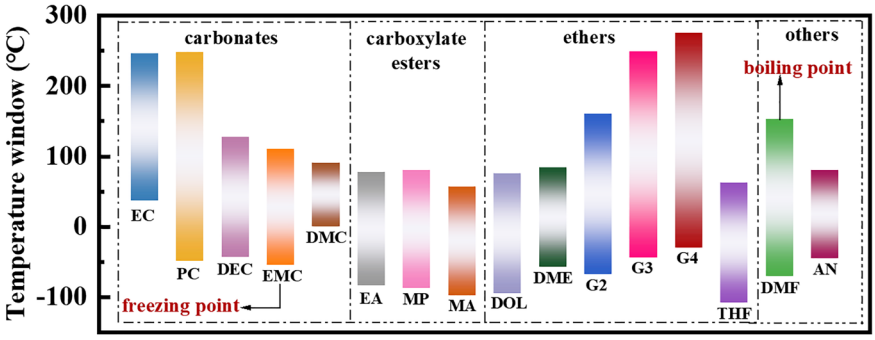

Figure 8. Freezing points and boiling points of several common electrolyte solvents.

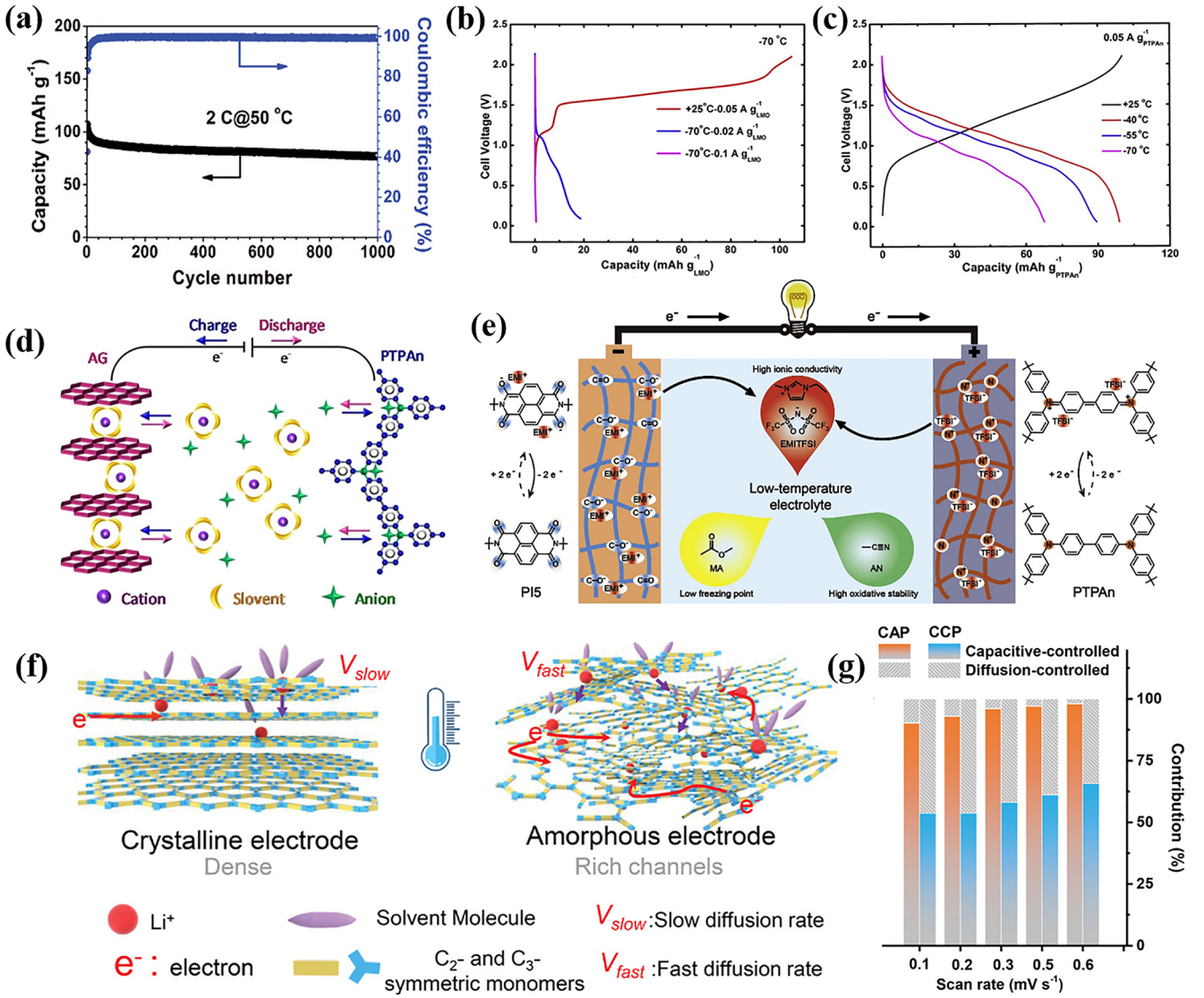

Figure 9. Electrochemical performance of organic batteries with organic liquid electrolytes at high or low temperature conditions. (a) Cycling performance of ADAPTS anode in KPF_6-EC/DEC electrolyte at a high temperature of 50 °C. Reproduced with permission from ref 22. Copyright 2018 Wiley-VCH. Low-temperature performance of the full cells based on (b) intercalation compound electrodes and (c) all-organic electrodes. Reproduced with permission from ref 52. Copyright 2018 Elsevier. (d) Schematic diagram of desolvation-free dual-ion PTPAn-artificial graphite battery with 0.5 M $NaPF_6$-G2 electrolyte. Reproduced with permission from ref 169. Copyright 2021 Wiley-VCH. (e) The composition and reaction schematic of the metal-free PTPAn-PI5 battery with EMITFSI-MA/AN electrolyte. Reproduced with permission from ref 163. Copyright 2020 Elsevier. (f) Difference of ion transport between crystalline and amorphous electrodes at low temperatures. (g) The contribution ratio of the capacitive capacities and diffusion-limited capacities of CCP and covalent amorphous polymer (CAP). Reproduced with permission from ref 171. Copyright 2021 Wiley-VCH.

https://doi.org/10.1021/acs.chemrev.2c00374
Chem. Rev. 2023, 123, 1712−1773

coordination of TEGDME-based electrolyte hinder ion transfer and retard the kinetics at the electrolyte/electrode interface. However, the TEGDME/DOL electrolyte exhibited worse cycling stability and lower Coulombic efficiency than the pure TEGDME electrolyte during cycling, which can be attributed to the side reaction of DOL in TEGDME/DOL electrolyte at above 2.8 V vs Mg^{2+}/Mg. Dong et al.[139] investigated the effect of solvent selection on the solubility of $Mg(CB_{11}H_{12})_2$ (MMC) salt in pyrene-4,5,9,10-tetraone (PTO)-Mg batteries, and screened out an electrolyte based on the mixed solvents of DME/DEGDME with high ionic conductivity. As shown in Figure 7a, compared with pure solvents, increased solubility was found via the use of some mixtures, which provides a key to overcome the solubility limitation of MMC in DME solvent. When the mass ratio of DME to DEGDME is 1:1, the maximum solubility of MMC was achieved (Figure 7b) and the corresponding 0.5 M MMC in DME/DEGDME electrolyte showed a high ionic conductivity of 6.1×10^{-3} S cm^{-1}, which was much higher than that of the pure TEGDME-based electrolyte (Figure 7c). Therefore, solvent mixtures can exhibit characteristics which appear to mask certain undesirable effects exhibited by a single solvent while unlocking useful properties for battery operation.

In addition to ether-based solvents for rechargeable Mg metal batteries, other solvents have also been successfully employed for Mg dual-ion batteries, rechargeable Zn metal batteries, Ca metal batteries, and Al metal batteries. For example, AN can be used in all-organic dual-ion batteries based on Mg^{2+} cations and ClO_4^- anions, because there is no side reaction between the solvent and the electrode (Figure 7d).[140] Aqueous electrolytes are widely used in Zn-organic batteries due to the low cost, fast reaction kinetics, and nonflammability.[141−143] In addition, a recent study has shown that the formation of Zn^{2+}-DMF complexes enable Zn salts with desirable solubility in the DMF solution while also circumventing deleterious Zn dendrite growth and H_2 evolution on the Zn anode (Figure 7e).[144] Moreover, the electrolyte based on 1-ethyl-3-methylimidazolium dicyanamide (EMIDCA) IL was confirmed to be able to maintain stable Zn deposition/dissolution in Zn-organic batteries.[145] Another important multivalent metal anode is Ca metal, which is difficult to be reversibly plated and stripped in traditional organic electrolytes. To date, only a few studies have reported rechargeable Ca batteries based on the $Ca(BF_4)_2$ in the EC/PC electrolyte,[146] $Ca(BH_4)_2$ in the THF electrolyte,[147] and aqueous electrolytes.[148,149] As another promising multivalent battery system, Al-organic batteries face similar challenges as rechargeable Mg-metal batteries in that traditional carbonate solvents generally produce Al^{3+} nonconductive passivation layers on electrode surfaces,[150] which limits the choices of viable electrolyte solvents. Most electrolytes in Al-organic batteries are based on ILs like $AlCl_3$/1-ethyl-3-methylimidazolium chloride (EMICl)[151,152] and $AlCl_3$/1-ethyl-3-methylimidazolium tetrachloroaluminate ($EMIAlCl_4$).[153] More research efforts are demanded to develop cost-effective, noncorrosive, highly compatible, and stable electrolytes for multivalent batteries.

3.1.1.5. Realizing Wide Temperature-Range Application of Batteries. The previous discussion focuses on the research at room temperature. To expand the applications of organic batteries, the wide-temperature-range electrolytes were also exploited. Some unique solvents are suitable in battery operation at extreme conditions of high or low temperatures. Figure 8 summarizes the freezing points and boiling points of several common electrolyte solvents.[154,155] In general, solvents with high boiling points are suitable for electrolytes in high-temperature batteries, while solvents with low freezing points are used in low-temperature batteries.

Traditional ether-based solvents like DOL and DME are difficult to apply in high-temperature electrolytes due to their low boiling points (75.6 °C for DOL and 84 °C for DME), while ester solvents like EC, PC, and DEC with higher boiling points (246 °C for EC, 249.5 °C for PC, and 126.8 °C for DEC) can be applied to the battery system at high operating temperatures over 60 °C. In addition to the risk of solvent evaporation, organic electrode materials suffer from more significant dissolution and shuttle reactions at high temperatures.

Liang et al.[22] designed a K-ion battery with high rate capability and long cycle life at a high temperature using 0.8 M KPF_6 in EC/DEC as the electrolyte. As shown in Figure 9a, the azobenzene-4,4′-dicarboxylic acid potassium salts (ADAPTS) anode could retain a reversible capacity of 77 mAh g^{-1} after 1000 cycles at 50 °C and 2 C. When the operating temperature rises to 60 °C, a reversible capacity of 113 mAh g^{-1} is retained after 80 cycles, which is equivalent to 81% of the initial capacity. The long-term cycling stability of the ADAPTS anode at high temperatures could be attributed to three factors: 1) The electrolyte selected could maintain thermodynamic and electrochemical stability at 60 °C; 2) The long-range delocalized π-conjugated structure in ADAPTS and the surface reaction mechanism between the organic anode and K-ions enable ADAPTS to maintain structure stability during repeated charge/discharge processes even at high temperatures up to 60 °C; 3) The elevated temperature could accelerate the reaction kinetics and significantly reduce the interphase resistance, which is conducive to the diffusion of K^+ in the solvent, thus ensuring higher capacity and better rate performance. In addition to high-temperature K-ion batteries, high operating temperatures (50 °C) are conducive to the complete lithiation of the super-lithiation reaction-based organic anode materials, and higher capacities and power densities are observed compared with room temperature operation.[156,157]

At low temperatures, most traditional solvents exhibit increased viscosity or even partial curing, resulting in a sharp drop in the ionic conductivity, and thus greatly limits the low-temperature battery performance. Additionally, the increased interfacial resistance,[158] sluggish Li^+ desolvation process,[159] limited ion transfer in the electrodes, and uncontrollable Li plating/stripping on the anode surfaces[160,161] greatly affect the performance of the battery at low temperatures. These effects are so pronounced that the discharge capacity of a Li/graphite battery at −20 °C only retains about 12% of the room temperature capacity.[162]

Due to the relatively low freezing points, carboxylate esters like methyl acetate (MA, −98 °C),[163] ethyl acetate (EA, −84 °C),[52] and methyl propionate (MP, −87.5 °C)[164] are usually used as solvents for low-temperature LIBs. Dong et al.[52] found that the electrolyte of 2 m (where m is molality, mol kg^{-1}) LiTFSI-EA was able to maintain a high ionic conductivity of 2×10^{-4} S cm^{-1} at −70 °C, which could meet the requirement of rapid ion transport in electrolytes under cryogenic conditions. However, except for some inorganic electrodes based on intercalation pseudocapacitive behaviors, like the nanosized Ni-based Prussian blue cathode,[165] conventional intercalation inorganic compounds for LIBs suffer from fast capacity fading at low temperatures, owing to the sluggish intercalation/deintercalation kinetics, slow solid diffusion of ions and high energy barrier for the desolvation processes (Figure 9b).[166−168]

https://doi.org/10.1021/acs.chemrev.2c00374
Chem. Rev. 2023, 123, 1712−1773

In sharp contrast, the highly reversible carbonyl/enol couple in amorphous conjugated carbonyl polymers vests them with much faster redox kinetics. Therefore, an all-organic dual-ion battery with a PTPAn cathode and a 1,4,5,8-naphthalenetetracarboxylic dianhydride (NTCDA)-derived polyimide (PNTCDA) anode was constructed. It avoided the sluggish desolvation of Li^+ at the interface between electrolytes and traditional intercalation compound-based electrodes, and greatly enhanced the capacity retention of the battery at low temperatures.[52] As shown in Figure 9c, even at an ultralow temperature of −70 °C, the capacity of the all-organic battery with the LiTFSI-EA electrolyte could still reach 69 mAh g^{-1}, only 30% lower than that at room temperature. However, the narrow electrochemical window (~1.5 V versus Li^+/Li) of the EA-based electrolyte hiders the application of a Li metal anode. Coupled with the low specific capacity of organic electrode materials, the flooded electrolyte and the addition of a large amount of inactive conductive carbon, the energy density of the PTPAn-PNTCDA battery was only 33 Wh kg^{-1}. The relatively low energy density does not meet the requirements for practical battery application.

For this reason, the electrolyte was further optimized as a cosolvent electrolyte of 5 m LiTFSI in EA and dichloromethane (DCM) diluent (1/4, v/v), which exhibited high stability with a Li metal anode and a sufficient ionic conductivity at −70 °C.[155] The prepared PNTCDA-Li organic battery based on such a cosolvent electrolyte displayed relatively high energy density of 178 Wh kg^{-1} and power density of 2877 W kg^{-1} at −70 °C, providing a beneficial battery system that can operate under extreme operating conditions. Besides n-type organic anodes like PNTCDA and Li metal anodes, a dual-ion battery was proposed by using a graphite anode and a p-type organic cathode of PTPAn. Considering the high energy barrier for the desolvation step, and slow cation-intercalation in graphite anode, Chen et al.[169] cleverly utilized the cointercalation of Na^+ with ether solvent molecules to circumvent the desolvation process at the graphite anode, and designed a new desolvation-free sodium dual-ion battery with unique features of fast-charging and low-temperature operation capability (Figure 9d). Additionally, a Zn-organic battery with a phenanthrenequinone macrocyclic trimer cathode was also reported to work well in an ultrawide temperature range from −70 to +150 °C, due to the high boiling point (157.6 °C) and low freezing point (−70.8 °C) of the 0.5 M Zn trifluoromethanesulfonate (ZnTFMS)-DMF electrolyte.[123] This demonstrated a good application prospect for outer space and in the north/south pole areas.

Due to the promise of organic batteries under extreme conditions, more electrolyte systems were exploited to further improve the performance of wide-temperature-range organic batteries. The high ionic conductivity and nonsolvation feature of pure IL electrolytes and the pseudocapacitive electrochemical redox reactions of organic electrodes were combined to fulfill the metal-free and solvent-free battery composed of all-organic electrodes and a 1-ethyl-3-methylimidazolium bis-(trifluoromethanesulfonyl)imide (EMITFSI) electrolyte. This new organic battery showed ultrafast reaction kinetics and excellent cyclic performance at a low temperature of −10 °C.[170] To further improve the performance, Qin et al.[163] took advantage of the low freezing point of MA and high oxidation resistance of AN to decrease the freezing point and viscosity of the EMITFSI-based electrolytes. The high ionic conductivity, good oxidation resistance, and low freezing point of the 1 M EMITFSI in MA/AN (1/2, v/v) electrolyte successfully pushed the working temperature of the all-organic PTPAn/PI5 battery to −80 °C (Figure 9e). Compared to the fast capacity decay of the PTPAn/PI5 battery using 1 M LiTFSI in DOL/DME electrolyte at 20 °C, the battery using the optimized electrolyte showed excellent cycling stability and rate performance at temperatures lower than −60 °C.

In addition to the liquid electrolytes, the structures of organic electrode materials can also impact the low-temperature performance of organic batteries. Zheng et al.[171] used 0.75 M LiTFSI-DOL as the electrolyte and explored the effect of crystallinity of organic electrode materials on low-temperature performance of batteries. The low dielectric constant of DOL reduces the dipole−dipole force between molecules, thus reducing the freezing point of the electrolyte. Furthermore, the low desolvation energy (2.04 eV) of $[Li\text{-}DOL]^+$ is conducive to promoting ion transport at the electrode/electrolyte interface under low temperatures.[167] As shown in Figure 9f, compared with covalent crystalline polymer (CCP) electrodes with a staggered dense frame structure, the channel-rich amorphous structure in the covalent amorphous polymer (CAP) electrode is more beneficial for the fast diffusion of Li-ions in the interstitial space of organic solids under cryogenic conditions, showing faster ion transport dynamics, smaller charge transport impedance, and higher capacitance contribution (Figure 9g).[171] The above results indicate that tailoring the crystal structure of organic electrode materials can affect low-temperature Li^+ transport kinetics, which should be comprehensively considered in the design of low-temperature batteries. These findings may also be applicable to the design and optimization of other metal-ion battery systems operating at low temperatures.

Different from the sluggish desolvation process and slow diffusion in the conventional intercalation-type inorganic electrode materials, organic electrode materials often exhibit fast redox kinetics due to the distinctive reaction mechanism based on rearrangement of chemical bonds. Therefore, they are regarded as promising candidates for low-temperature energy storage devices. Battery systems based on all-organic, organic-artificial graphite, and organic-metal electrodes have been reported with excellent electrochemical performance at low temperatures. However, the solvation/desolvation processes in the organic electrode reaction and the ion transport behavior through the electrode/electrolyte interface at low temperatures are not well understood. There is an urgent need to probe the kinetic process with *in situ* and *operando* characterization methods at low temperatures. Furthermore, the design of electrolyte systems for low-temperature application is mostly driven by reducing the freezing point and viscosity, but few studies focus on the engineering of the solvation structure to decrease the energy barrier of the desolvation. It is essential to gain profound understanding of the interfacial process at low temperatures to develop electrolytes with low desolvation energy and stable SEI.

3.1.2. Effects of Conductive Salt. Conductive salts, as the anion/cation supplier, are critical components in a battery electrolyte. The ideal salt needs to satisfy the requirements of low cost, high abundance, high solubility, excellent thermal stability, environmental benignity, and low- or nontoxicity. More importantly, the salt should exhibit electrochemical stability within the potential voltage window of the battery, good compatibility with electrode materials/binders, and high chemical stability toward other battery accessories such as current collector, separator, stainless steel spacer, spring, and case. In organic electrodes, the cations and/or anions from the electrolyte salt will participate in the electrochemical reaction to

https://doi.org/10.1021/acs.chemrev.2c00374
Chem. Rev. 2023, 123, 1712−1773

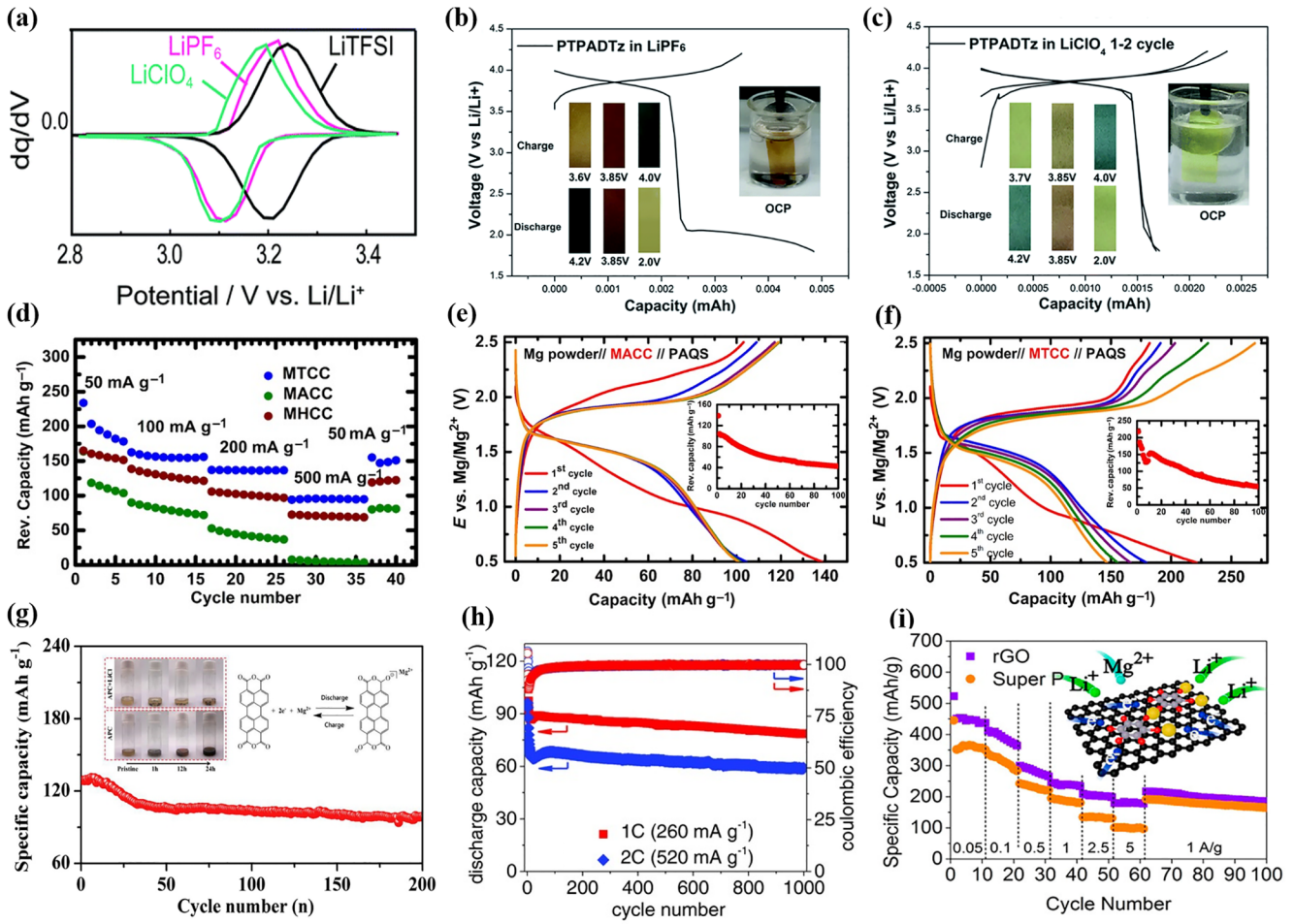

Figure 10. Effects of the salt composition in organic liquid electrolytes on the performance of the battery. (a) CV curves of DMPZ electrodes using electrolytes with different Li salts. Reproduced with permission from ref 126. Copyright 2017 Royal Society of Chemistry. Charge−discharge curves and color change under different voltages of the electrode using (b) $LiPF_6$ and (c) $LiClO_4$ electrolytes. Reproduced with permission from ref 185. Copyright 2019 Royal Society of Chemistry. (d) Rate performance of Mg-PAQS batteries with MTCC, MACC, and MHCC electrolytes. Galvanostatic charge−discharge curves of PAQS cathode during the first five cycles with (e) MACC and (f) MTCC electrolytes. Insets: Discharge capacities of corresponding electrode during the first 100 cycles. Reproduced with permission from ref 194. Copyright 2015 Wiley-VCH. (g) Cycling performance of PTCDA electrode using APC electrolyte with LiCl salt. Insets: Photos of PTCDA dissolved in electrolytes with or without LiCl salt after different soak time and the theoretical reaction mechanism of PTCDA cathode in Mg-organic battery. Reproduced with permission from ref 195. Copyright 2019 Elsevier. (h) Cycling performance of Mg-14PAQ with 0.3 M $Mg(HMDS)_2$-$4MgCl_2$ in THF electrolyte. Reproduced with permission from ref 133. Copyright 2016 Wiley-VCH. (i) Rate performance of $Na_2C_6O_6$ with different carbon additives. Inset: Schematic diagram of cointercalation of Li^+ and Mg^{2+}. Reproduced from ref 69. Copyright 2018 American Chemical Society.

balance the charge formed during the oxidation−reduction processes.

Traditional aprotic metal batteries (e.g., Li/S and Li/air) and aprotic metal-ion batteries (e.g., graphite/$LiCoO_2$ and hard carbon/$Na_3V_2(PO_4)_3$) rely on metal cations as the only charge carrier and the charge balancer in electrode redox processes. Importantly, the anions do not participate in the electrode reactions. It is worth mentioning that the ion transport mechanism is different in rechargeable Al batteries. Due to the high charge density of Al^{3+} ions and its strong coordination affinity with solvents, it is difficult to intercalate/deintercalated Al^{3+} ions in any host structure,[172] the redox reaction of the cathode material mainly depends on the insertion/deinsertion of monovalent species like $AlCl_4^-$ or $AlCl_2^+$.[153,173] Recently, dual-ion batteries based on both graphite electrodes[174,175] or graphite cathodes/Li anodes[176] have been reported, in which metal cations participate in the redox reaction at the anode, and anions participate in the redox reaction at the cathode. However, the anion intercalation reaction with a high working voltage of around 5 V (vs Li^+/Li) often leads to the continuous decomposition of organic electrolytes, resulting in inferior Coulombic efficiency and significant capacity loss during cycling.[175] The use of organic cathodes is expected to store anions at relatively low potentials and obtain more stable dual-ion batteries with high Coulombic efficiency.

3.1.2.1. Single-Salt Systems. For most organic batteries, the choice of electrolyte salt is often similar to the traditional inorganic battery systems. The cations are metal ions (Li^+, Na^+, K^+, etc.) and the anions are generally BF_4^-, ClO_4^-, PF_6^-, FSI^-, and $TFSI^-$ listed in order of increasing polyatomic radius. Significantly, in 2000, a form of magnesium salt-based electrolytes of $Mg(AlCl_2BuEt)_2$-THF and $MgAlCl_3Bu_2$-THF were developed, exhibiting wide electrochemical windows and reversible Mg deposition-stripping behaviors.[177] These electrolytes have been widely used in Mg-organic batteries.[134,178] Generally, an increase of the anionic radius results in slower

https://doi.org/10.1021/acs.chemrev.2c00374
Chem. Rev. 2023, 123, 1712−1773

electron transfer kinetics, and decreases the ionic conductivity of the electrolyte. Furthermore, the shape of anions also affects the electron transfer in organic molecules. Lee et al. found that although the ionic radius of $TFSI^-$ is higher than that of PF_6^-, its V-shaped molecular geometry is more conducive to the rapid electron transfer than the spherical PF_6^-.[179] It is worth noting that for the all-organic battery system, no specific cations or anions are needed in the charge and discharge processes because of the universal electrochemical redox property of organic electrode materials. Because of this property, various cations and anions can be employed as conductive salts in the electrolytes. It has been reported that quaternary ammonium compounds[180,181] and pure ILs[163,170,182] also could be used as ion-conducting charge carriers and show excellent electrochemical properties.

For p-type organic electrode materials, the choice of the anion in the electrolyte greatly impacts the electrochemical performance of the battery, because the anions directly participate in the electrochemical redox reaction. In general, larger anion size triggers greater polarization of the electrode during the charge/discharge process.[183] However, according to the charge/discharge profiles of lithium 4-(10H-phenothiazin-10-yl) benzoate electrode in $LiClO_4$-PC, $LiPF_6$-PC, and LiTFSI-PC electrolytes, the bulky LiTFSI with greater ionic conductivity and faster ion transport performance induced less polarization than the smaller $LiPF_6$, which ultimately led to better electrochemical performance.[184] Furthermore, the type of anion species may affect the redox potential of the electrode. Research results indicated that the redox potential of 5,10-dihydro-5,10-dimethyl phenazine (DMPZ) electrode in the electrolyte containing $TFSI^-$ ions was higher than that in the electrolyte containing PF_6^- or ClO_4^- ions (Figure 10a).[126] Compared with smaller anions, large anions tend to exhibit weaker electrostatic interactions and introduce more significant steric effects with organic redox intermediates, resulting in increased structural deformation, worse stability of the complex, and a higher redox potential in the battery. In addition, for the organic battery with the PF_6^--based electrolyte, trace HF in the system negatively impacts the battery performance.[185] Compared with the $LiClO_4$-based electrolyte, the charge−discharge curves of the organic electrode material containing N-heterocycle functional groups in the $LiPF_6$-based electrolyte displayed a new and uncommon voltage plateau at around 2 V. The voltage plateau was caused by the acid-doping of the trace HF into the triazine group of the organic electrode material (Figure 10b,c).

3.1.2.2. Dual-Salt Systems. In traditional Li secondary batteries, there have been many reports on the design of dual-salt systems to improve the performance of electrolytes,[186−190] such as improving thermal stability, inhibiting corrosion of Al current collector, protecting the Li metal anode, optimizing interfacial layers between the electrolyte and electrodes, and enhancing ionic conductivity.[191] In organic batteries, the reports about dual-salt systems are mostly based on rechargeable Mg batteries. Due to the low-cost, dendrite-less, double-electron redox characteristics, and high volumetric capacity of Mg (3833 mAh cm^{-3} versus 2046 mAh cm^{-3} for Li), rechargeable Mg metal batteries hold great promise for applications in vehicle electrification and large-scale stationary energy storage.[177] However, due to the low redox potential of Mg, electrolytes are readily reduced and decomposed in the vicinity of Mg metal, resulting in the formation of nonconducting passivation films on the surface of Mg anode that hinders the transfer of Mg ions.[192] Thus, the development of an electrolyte with reversible Mg plating/stripping capabilities and a wide electrochemical stability window has become the focus of research in Mg-ion batteries. In addition, the incompatibility of the electrolyte with metal oxide cathode materials is still an enormous challenge for high-energy-density Mg batteries.

Non-nucleophilic electrolytes with high oxidation stability enable the application of organic electrode materials in rechargeable Mg batteries, where weak intermolecular forces enable reversible electrochemical interactions and rapid diffusion of Mg ions. It was found that a novel $[Mg_2(\mu\text{-}Cl)_2]^{2+}$ cation complex with high activity for reversible Mg electrodeposition could be formed through the dehalodimerization of non-nucleophilic $MgCl_2$ with either Mg salts or Lewis acid salts in the DME solvent.[193] Therefore, 0.5 M $Mg(TFSI)_2$-2$MgCl_2$ in DME was used as an optimized electrolyte in the Mg-organic battery with a 2,5-dimethoxy-1,4-benzoquinone (DMBQ) cathode.[135] Compared with the 0.5 M $Mg(TFSI)_2$-DME electrolyte, the Coulombic efficiency of the battery was increased from 58.8% to 98.9%. However, considerable capacity loss was observed after 30 cycles, which may be caused by the dissolution of DMBQ in the electrolyte.

To mitigate the high solubility, using redox-active polymers to replace highly soluble small molecules as organic electrode materials is an effective way to improve the cyclic stability of the Mg-organic battery. Bitenc et al.[194] explored the electrochemical performance of three non-nucleophilic electrolytes in PAQS/Mg batteries using Mg powder as the anode rather than Mg foil to improve the reaction kinetics. The results showed that compared with $MgCl_2$-$AlCl_3$ in THF (named MACC) and $[Mg_2Cl_3\text{-}6THF]$ $[HMDSAlCl_3]$ (HMDS: hexamethyldisilazane) in THF (named MHCC), the battery with an electrolyte composition of 0.37 M $MgCl_2$ and 0.15 M $Mg(TFSI)_2$ in THF/DME (3/2, v/v) (named MTCC) exhibited higher reversible specific capacity and better rate performance (Figure 10d). The initial capacity of the battery using MTCC electrolyte was up to 225 mAh g^{-1}, which was close to the theoretical capacity of PAQS, but its long cyclic stability was not significantly improved (Figure 10e,f). The reversible specific capacity was only about 50 mAh g^{-1} after 100 cycles, which might be due to the unstable reduction state of PAQS during the discharge process. In addition, the worse performance in MACC and MHCC electrolytes was attributed to the formation of Lewis acid−base adducts between the strong Lewis acid $AlCl_3$ and the cathode material.

Another method to mitigate the high solubility of organic electrode materials is to add chlorides (LiCl, NaCl, or KCl) in the electrolytes. The salt-controlled dissolution strategy is expected to inhibit the dissolution of organic electrodes and improve the long-term cyclic stability of Mg-organic batteries. As shown in Figure 10g, Mai and co-workers[195] compared the dissolution of PTCDA in a phenyl complex electrolyte of $PhMgCl/AlCl_3$ (APC) before and after LiCl addition and found that the color of the APC electrolyte containing LiCl was almost unchanged after immersing the PTCDA electrode in the electrolyte for 24 h, demonstrating that the dissolution of PTCDA was inhibited. Moreover, A high capacity, excellent rate performance, and cycling stability of PTCDA in the APC electrolyte with 1 M LiCl were demonstrated, further proving that the addition of soluble salts ameliorates the diffusion and Mg-storage performance. However, it is worth noting that the addition of a large amount of soluble chloride will narrow the voltage stability window on the cathode side and increase the viscosity of the electrolyte. Furthermore, some studies indicate

https://doi.org/10.1021/acs.chemrev.2c00374
Chem. Rev. 2023, 123, 1712−1773

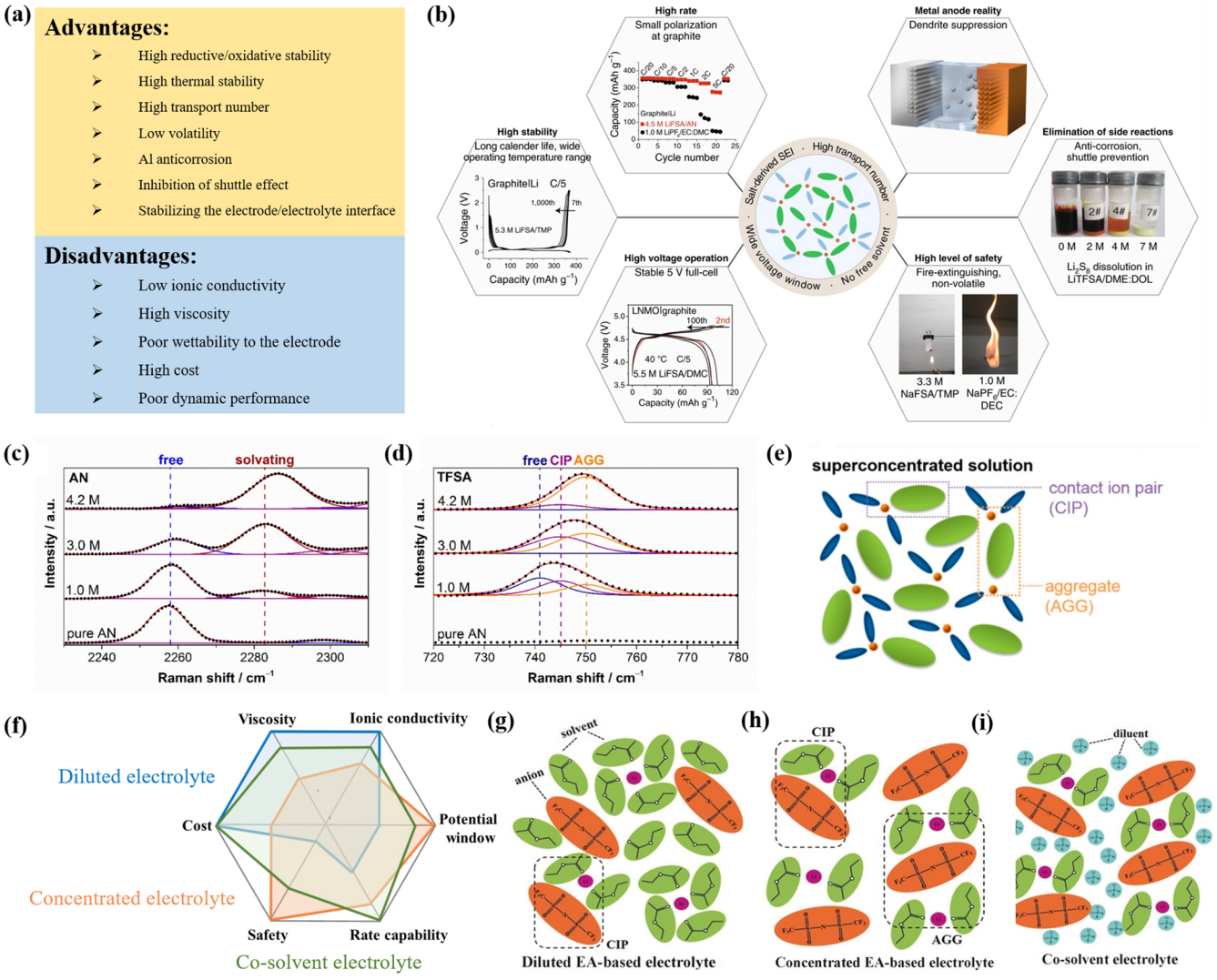

Figure 11. Effects of the salt concentration in organic liquid electrolytes on the performance of the battery. (a) Advantages and disadvantages of concentrated electrolytes. (b) Excellent battery functions realized by concentrated electrolytes. Reproduced with permission from ref 210. Copyright 2019 Springer Nature. Raman spectra of the vibrational band of (c) CN stretching mode from AN molecule and (d) S-N stretching, C-S stretching, and CF_3 bending mode from $TFSI^-$ in LiTFSI-AN solutions with different concentrations. (e) Schematic diagrams of the solvation structure of the salt-superconcentrated solution (4.2 M LiTFSI-AN). Reproduced from ref 218. Copyright 2014 American Chemical Society. (f) Comparison of the properties and performances of diluted electrolyte, concentrated electrolyte, and cosolvent electrolyte. Schematic diagrams of the solvation structure of (g) diluted electrolyte, (h) concentrated electrolyte, and (i) cosolvent electrolyte. Reproduced with permission from ref 155. Copyright 2019 Wiley-VCH.

that the addition of halogenated Li salts to a conventional liquid electrolyte leads to an ultrastable SEI layer, high electrochemical reversibility, and marked stable electrodeposition on the Li metal anode, which may be applicable for developing dendrite-free metal anodes.[196,197]

In addition to the phenyl complex electrolyte, $Mg(HMDS)_2$-$MgCl_2$ in THF is also considered as a promising electrolyte for Mg batteries due to its high ionic conductivity, wide electrochemical stability window, and excellent electrochemical reversibility. The Mg/Mo_6S_8 battery exhibited a high reversible capacity and good rate performance in the $Mg(HMDS)_2$-$MgCl_2$ in THF electrolyte.[198] However, the PAQS-Mg battery with 0.3 M $Mg(HMDS)_2$-$4MgCl_2$ in THF electrolyte exhibited rapid capacity decay due to the severe dissolution of PAQS in discharged states.[133] Replacing PAQS by poly(1,4-anthraquinone) (14PAQ) decreased the degree of dissolution of the anthraquinonyl groups, which is expected to achieve a stable and sustainable Mg-organic battery system (Figure 10h). Besides the organic electrodes based on quinone materials, aromatic dianhydride-derived PIs with reversible multielectron redox properties can also serve as cathode materials for rechargeable Mg batteries.[199] The carbonyl groups and conjugated structures in PIs can provide abundant redox-active centers for Mg^{2+} storage, while the relatively narrow HOMO−LUMO energy gap and tight $\pi-\pi$ stacking structure are conducive to achieving excellent Mg^{2+} storage properties. Compared with the traditional nucleophilic APC electrolyte, the charge transfer impedance of the PI electrode in the non-nucleophilic electrolyte of $Mg(HMDS)_2$-$4MgCl_2$/2THF-$PP_{14}TFSI$ (PP_{14}: 1-butyl-1-methylpiperidinium) was smaller, and the corresponding battery showed higher charge−discharge capacity due to the wide electrochemical window and good interfacial

https://doi.org/10.1021/acs.chemrev.2c00374
Chem. Rev. 2023, 123, 1712−1773

compatibility of non-nucleophilic electrolytes with organic electrodes. By further optimizing the composition of the electrode and electrolyte, the battery exhibited excellent rate performance and long-term cycle stability for 8000 cycles, demonstrating great promise for developing low-cost, high-performance, and sustainable Mg-organic batteries.

Recently, considerable research efforts have extended to Mg-Li and Mg-Na hybrid batteries.[200−202] It was found that conventional intercalation cathode materials developed for LIBs and NIBs were not suitable for Mg storage. This may be due to the significant Coulombic interactions between the intercalation host and Mg ions, resulting in the slow diffusion kinetics of Mg^{2+} in cathode materials and also in large polarizability of the intercalation reaction-based electrodes during charge and discharge processes.[203,204] To address this challenge, Mg-Li or Mg-Na hybrid batteries have exhibited remarkably accelerated kinetics due to the fast intercalation of Li^+ or Na^+ instead of clumsy Mg^{2+} into cathode materials. Hence, Li^+ or Na^+ redox reactions take place in the cathode, while the highly reversible deposition and dissolution of Mg^{2+} occurs at the Mg anode during the cycling process. The hybrid Mg-Li or Mg-Na battery design avoids the poor performance of Mg^{2+} and greatly expands the selection of compatible cathode materials for rechargeable Mg batteries.[205]

To overcome the poor kinetics of Mg^{2+} transport in inorganic cathode materials, Tian et al.[69] reported an organic-Mg battery with multielectron reactions activated by Mg−Li dual-salt electrolyte and used the rhodizonate salt of $Na_2C_6O_6$ as the cathode. Although the reaction was driven by Li^+ dominantly, the cointercalation of Mg^{2+} was beneficial to suppress the exfoliation of rhodizonate dianion ($C_6O_6^{2-}$) layers, which is different from the single intercalation of Li^+ or Na^+ in the dual-salt batteries with inorganic cathodes. As a result, the battery exhibited relatively high stability for 600 cycles. Researchers attributed the high cyclability to the cointercalation of Mg^{2+}, which protects the layered structure of $C_6O_6^{2-}$ and the stable Mg anode without the formation of Mg dendrites. Furthermore, the high intrinsic diffusion coefficient, the pseudocapacitive contribution, and the coating layer of reduced graphene oxide endow $Na_2C_6O_6$ with excellent rate performance. Even at an ultrahigh current density of 5 A g^{-1}, a high capacity of 175 mAh g^{-1} was still achieved (Figure 10i). Therefore, dual-salt electrolytes offer opportunities for the performance optimization of organic multivalent batteries.

These results suggest that selecting an appropriate salt composition for the electrolyte is crucial to fully utilize the redox activity and obtain excellent electrochemical performance of the organic electrodes.

3.1.3. Concentration Optimization. *3.1.3.1. Low-Concentration Electrolytes.* The salt concentration also plays a key role in the electrochemical performance of rechargeable batteries. For most nonaqueous electrolyte systems, maximal ionic conductivity always occurs near a salt concentration of 1 M.[206] In the past few years, research has focused on moderate- and high-concentration electrolytes, but little attention has been paid to low-concentration electrolytes.

Recent work has shown that low-concentration electrolytes possess advantages of low cost and viscosity, enhanced interfacial wettability, and wide operational temperature ranges. At low temperatures, the viscosity of the electrolyte increases sharply with the increase of concentration, resulting in poor ion-transport kinetics in the battery.[207] Considering that low-concentration electrolytes help to mitigate the risk of electrolyte solidification due to the recrystallization of electrolyte salt at low temperatures, Chen et al.[169] reduced the concentration of the $NaPF_6$-DEGDME electrolyte to 0.5 M. The low-concentration electrolyte exhibited higher ionic conductivity and lower electrolyte/electrode interfacial impedance compared to the 1 M $NaPF_6$-DEGDME electrolyte at −40 °C. In addition, a recent study has shown that dilute (0.1 M LiTFSI in DOL/DME with 1 wt % $LiNO_3$) electrolyte with excellent wettability, low viscosity, and high Li-ion transference number also suppressed the shuttle effect and dissolution of polysulfides, which may be attributed to the strong aggregation of short chain polysulfides.[208]

3.1.3.2. High-Concentration Electrolytes. Though some success has been achieved for low-concentration electrolytes, significant efforts have been devoted to the highly concentrated electrolytes because of the unique features like high reduction/oxidation stability, high thermal stability, low volatility, Al anticorrosion, and high transference number (Figure 11a).[209] The performance of the battery could be improved by simply increasing the salt concentration of the electrolyte (Figure 11b).[210] Specifically, the highly concentrated electrolytes in organic batteries could effectively reduce the severe dissolution of active materials and the shuttle effect of dissolved redox-active organic materials/intermediates in the electrolyte, leading to better cycling performance.[211−213] However, the increase of the salt concentration would enhance the viscosity and reduce the ionic conductivity of the electrolyte, resulting in slower reaction kinetics.[110]

Wang et al. used 4 M lithium bis(fluorosulfonyl)imide (LiFSI) in DME[16] and 7 M LiTFSI in DOL/DME[214] as electrolytes for high-performance Li-organic batteries but did not systemically investigate the effect of electrolyte concentration on the battery performance. Zhang et al. prepared an organic−inorganic nanocomposite cathode to couple with the highly concentrated electrolytes for high-performance LIBs[27] and NIBs.[215] The results showed that although the increase of salt concentration reduced the ionic conductivity of the electrolyte, the dissolution of the AQ cathode in the electrolyte was significantly decreased simultaneously, resulting in better cyclic stability. Similar results were reported by Xu et al.[216] The use of a high-concentration electrolyte (5 M LiTFSI in DOL/DME) reduced the initial capacity of the tannic acid cathode, but it was beneficial to prolong the cycle life of the organic battery. Recent research has also shown that the high viscosity of highly concentrated electrolytes could minimize the self-discharge effect and help the organic electrode maintain good stability.[182] Nevertheless, it is worth noting that although the cyclic stability of organic electrodes can be improved by enhancing the electrolyte salt concentration, other factors (such as ionic conductivity, inhibitory effect on the dissolution of active materials, viscosity, cost, etc.) need to be considered when designing and optimizing the concentration of the liquid electrolytes in organic batteries.

Furthermore, the electrolyte concentration influences the formation and stability of the interphase between the electrodes and electrolytes. The highly concentrated electrolyte could suppress the electrochemical decomposition and continuous electrochemical reactions of solvent molecules on the electrode surface.[217,218] Tong et al.[219] used 1, 3, and 5 M potassium bis(trifluoromethanesulfonyl)imide (KTFSI) in DME as the electrolytes for all-organic K-ion batteries, respectively, and discussed the effect of electrolyte concentration on the electrolyte/electrode interface. The results showed that the PTCDA-based polymer electrodes using low- (1 M) and

https://doi.org/10.1021/acs.chemrev.2c00374
Chem. Rev. 2023, 123, 1712−1773

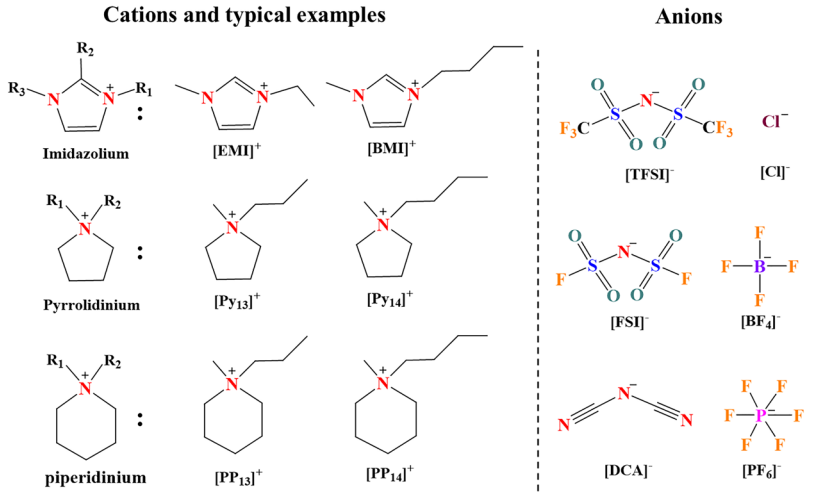

Figure 12. Commonly used cations and anions in ILs for organic batteries.

medium- (3 M) concentration electrolytes suffered from rapid capacity loss. However, batteries with a highly concentrated electrolyte (5 M) delivered a long cycle life of over 1000 cycles, and the Coulombic efficiency was close to 100%, which is attributed to the formation of a compact and uniform SEI. In addition, the solvation structure of the salt in the electrolyte has a significant impact on the battery performance as well. The high-concentration electrolyte exhibited an increased ratio of solvating DME solvent molecules to "free" DME molecules versus the lower concentration electrolyte. The decrease of free DME molecules inhibits the dissolution of organic electrodes, thereby enhancing the electrochemical performance. On the other hand, solvated DME molecules exhibit greater stability with respect to free DME molecules and $TFSI^-$ ions. As a direct result, the KTFSI salt becomes the primary source for electrode/electrolyte interphase generation. The X-ray photoelectron spectroscopy (XPS) results indicated that high-concentration KTFSI electrolyte was able to form a SEI rich in inorganic KF, which could protect the organic cathode materials from corrosion by electrochemical byproducts. Similarly, Huang et al.[220] found that the initial Coulombic efficiency and cyclic stability of the Li-cuprous 7,7,8,8-tetracyanoquinodimethane (CuTCNQ) battery was significantly improved by increasing electrolyte concentrations from 1 to 7 M. The Raman spectrum showed that there were almost no solvating molecules in 7 M $LiClO_4$-EC/PC electrolyte, effectively suppressing the dissolution of TCNQ. In addition, the highly concentrated electrolyte was implicated in the formation of an effective SEI layer on the surface of Li metal, thereby preventing the reduction of the dissolved Cu^{2+}. Furthermore, the highly concentrated electrolytes can also improve the performance of multivalent batteries. For example, Li et al.[221] developed a 3.5 m concentrated electrolyte with $Ca(FSI)_2$ salt dissolved in the carbonate solvents for a Ca-based dual-ion battery, which exhibited enhanced oxidation potential, resulting in good anion intercalation reversibility of the graphite cathode in the dual-ion battery.

As one of the most oxidation-tolerant organic solvents, AN is considered as a promising substitute for carbonate solvents due to its wide electrochemical stability window, high dielectric constant, and excellent ionic transport property. However, the poor reductive stability of AN solvent precludes its use for the Li metal anode, limiting the extensive application of AN-based electrolytes in high-energy-density rechargeable batteries. To circumvent this challenge, a superconcentrated LiTFSI-AN electrolyte was formulated to overcome the low reductive stability of the AN solvent, in which a unique networking structure with Li^+-solvating AN solvent was formed, as confirmed by Raman spectra (Figure 11c,d).[218] With the increase of salt concentration, the ratio of contact ion pairs (CIPs) and aggregates (AGGs) was increased, with free solvent molecules virtually absent when the salt concentration reached 4.2 M (Figure 11e). DFT-based molecular dynamics was applied to further understand the origin of enhanced reductive stability in the highly concentrated LiTFSI-AN solution. In the dilute system with completely dissociated salts, the energy levels of Li^+-solvating or free AN molecules are lower than that of $TFSI^-$ anions at the lowest end of conduction bands, indicating that AN molecules are predominantly reduced on the surface of the graphite electrode. With the solvation structure changing from the solvent-separated ion pairs in the dilute solution to AGGs in the highly concentrated solution, the LUMO shifts from the AN molecules to the $TFSI^-$ anions. In other words, the $TFSI^-$, instead of the AN solvent, is preferentially reduced to form a stable surface film on the graphite electrode, avoiding the reaction between the AN solvent and the intercalated Li.[218] Recently, Zhang et al.[222] applied the above electrolyte to decrease the severe dissolution of the Pillar[5] quinone (P5Q) cathode material in a traditional ester-based electrolyte and achieved excellent battery performance with a high-rate capability and long cycle life.

3.1.3.3. Localized High-Concentration Electrolytes. Although the high-concentration electrolyte could reduce the number of free solvent molecules and change the cation solvation structure to stabilize the high-voltage cathode, the increase of electrolyte concentration would inevitably lead to increased viscosity, reduced ion mobility and conductivity, and poor wettability with electrodes, especially in low-temperature conditions. To address the challenges, Chen et al.[223] proposed the design of localized high-concentration electrolytes. Fluorinated ether with low permittivity and diminished Lewis base character can be used as a cosolvent to dilute the electrolyte without changing the original Li salt-solvent coordination in highly concentrated electrolytes. Adding the fluorinated ether as a cosolvent allows for electrolytes with low salt concentration, low cost, low viscosity, improved conductivity, and good wettability (Figure 11f). Alternatively, Dong et al.[155] added a

https://doi.org/10.1021/acs.chemrev.2c00374
Chem. Rev. 2023, 123, 1712−1773

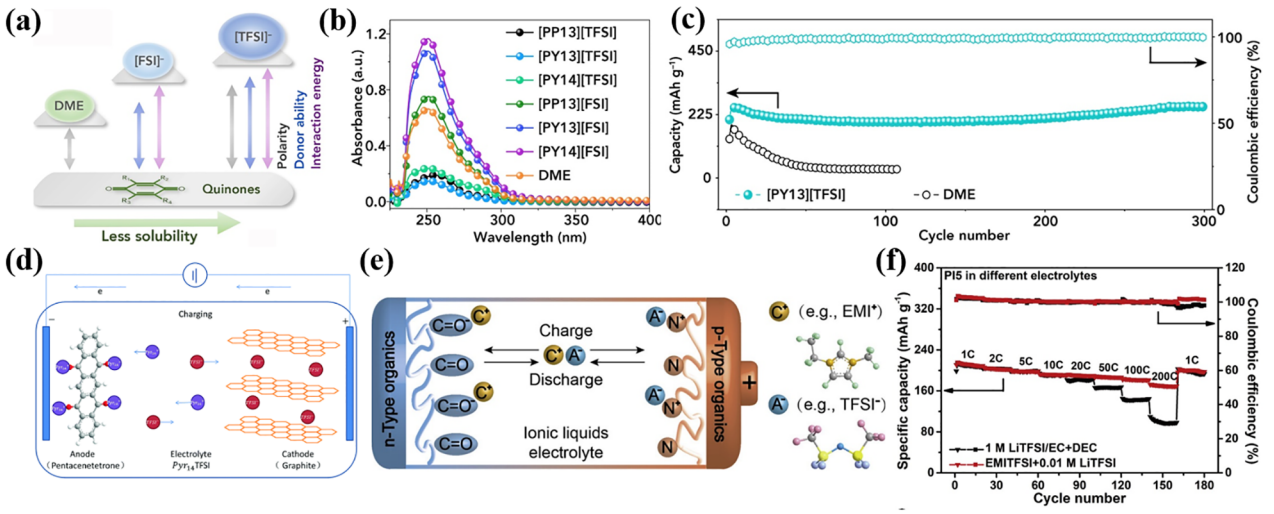

Figure 13. Effects of the IL-based electrolyte on the performance of the battery. (a) Schematic comparison of the factors affecting the solubility of quinones in DME and ILs. (b) UV−vis spectra of C4Q in DME and different ILs. (c) Long-term cycling performance of C4Q cathode with IL-based and DME-based electrolytes. Reproduced with permission from ref 229. Copyright 2019 Elsevier. (d) Schematic illustration of the charging mechanism of the graphite-PT dual-ion battery. Reproduced with permission from ref 231. Copyright 2019 Royal Society of Chemistry. (e) Schematic diagram of the metal-free battery composition and (f) rate performance of PI5 in 1 M LiTFSI/EC+DEC and EMITFSI+0.01 M LiTFSI electrolytes. Reproduced with permission from ref 170. Copyright 2019 Elsevier.

large amount of low-viscosity DCM to the high-concentration electrolyte. The ionic conductivity of the 5 m LiTFSI in EA/DCM (1/4, v/v) electrolyte can exhibit a high ionic conductivity of 6×10^{-4} S cm^{-1} at the ultralow temperature of −70 °C. By means of spectral characterization, molecular dynamics simulation, and first principle analysis, the solvation structure in the diluted, concentrated, and cosolvent electrolytes are shown in Figure 11g−i. It is further confirmed that the addition of DCM diluent has neither dissolved the salt nor destroyed the solvation structure between Li salt and ethyl acetate. The localized high-concentration electrolyte with the cosolvation structure has a wide electrochemical stability window (0−4.85 V) and a high chemical and electrochemical stability with respect to Li metal. Accordingly, localized high-concentration electrolytes are promising alternatives to low-concentration and high-concentration electrolytes for the development of high-performance organic batteries.

3.1.4. Ionic Liquids. Ionic liquids (ILs), also known as room temperature molten salts, are liquid ionic compounds composed of organic cations with specific volumes and inorganic/organic anions. Due to their excellent properties of low vapor pressure, nonflammability, good thermal and chemical stability, as well as electrochemical stability over a wide potential window, ILs have been widely investigated as solvents in electrolytes or plasticizers for various energy storage devices.[224] In organic batteries, IL-based electrolytes have also been reported, and commonly used ILs are shown in Figure 12.

Although the viscosities of ILs are generally high, resulting in low ionic conductivities at room temperature, their excellent thermal stability renders IL-based electrolytes as excellent candidates for optimizing battery performance at high temperatures. Gurkan et al.[225] compared the electrochemical performance of DHBQDS with NaFSI in 1-methyl-1-propylpyrrolidinium bis(fluorosulfonyl)amide (Py_{13}FSI) and NaFSI in EC/PC electrolytes. It was found that the addition of ILs improved the reversible capacity and cyclic stability of the battery. At an operating temperature of 60 °C, a relatively high capacity retention of 83% was achieved for the battery with the IL-based electrolyte after 300 cycles, whereas the battery using the carbonate-based electrolyte exhibited a rapid capacity decline in the first 50 cycles due to the poor thermal stability of the electrolyte. The result proved that the IL-based electrolyte enhances the performance and safety of organic batteries at ambient temperatures and, importantly, at high operating temperatures.

In addition to improving the high-temperature performance of alkali-ion batteries, ILs have also been utilized to enhance the compatibility of electrolytes with the aromatic dianhydride-derived PI cathodes in rechargeable multivalent batteries. Wang et al.[199] developed an IL-modified non-nucleophilic electrolyte to replace the traditional nucleophilic APC electrolyte. The results indicated that the non-nucleophilic electrolyte had a lower charge transfer resistance than the APC electrolyte. At the same current density, the corresponding battery had a higher specific capacity, which was attributed to the larger electrochemical stability window and better interfacial compatibility of non-nucleophilic electrolyte with the electrode.

Additionally, the type of IL also affects the capacity and cyclic stability of polymer electrodes. In the oxidation/reduction process, the anions and cations in the ILs migrate into the polymer electrode to compensate charges, causing swelling of the polymer. Cations with high planarity and small size can more easily intercalate into the conducting polymer, enabling the reaction to occur at more active sites in the polymer and faster ion transport. Therefore, in a Na-organic battery based on a poly(3,4-ethylenedioxythiophene) (PEDOT)/lignin cathode, the imidazolium-based IL electrolyte exhibited higher ionic conductivity and better fluidity compared with the pyrrolidinium-based IL electrolyte, and the corresponding battery showed a higher discharge capacity, better cyclic stability and rate performance.[226]

Besides the inherent properties of high thermal stability and electrochemical stability, ILs are also able to suppress the dissolution of organic electrodes, which was previously attributed to the relatively higher viscosity of IL-based electrolytes.[227] However, recent results indicate that ILs could

https://doi.org/10.1021/acs.chemrev.2c00374
Chem. Rev. 2023, 123, 1712−1773

reduce reactivity of nitroxide radicals without altering the radical structure, which is due to the strong interaction between the radicals in organic materials and ions in ILs.[228] In combination with DFT calculations and spectroscopic exploration, Wang et al. further discovered that ILs with large polarity, weak electron donor ability, and low interaction energy with solvents showed superior inhibition for the dissolution of quinones (Figure 13a).[229] Considering the corrosion of [FSI^-]-based electrolytes to the Al current collectors, less corrosive electrolytes that preserved the beneficial characteristics of the FSI^- ion were necessary. The commonly used 1-methyl-1-propylpyrrolidinium bis(trifluoro-methanesulfonyl)amid (Py_{13}TFSI) IL electrolyte with weak electron donor ability and a large polarity was optimized and showed the greatest compatibility with the calix[4]quinone (C4Q) electrode (Figure 13b). As shown in Figure 13c, the C4Q cathode with 0.3 M NaTFSI in Py_{13}TFSI electrolyte exhibited high capacity (>400 mAh g^{-1}) and excellent capacity retention (99.7% at 130 mA g^{-1} after 300 cycles), significantly outperforming similar batteries using ether-based electrolytes. In addition, AQ, benzoquinone, biphenyl-quinone, naphthoquinone, and phenanthraquinone cathodes also showed improved capacity and better cycling stability in the Py_{13}TFSI-based electrolyte, confirming the general applicability of using ILs to inhibit the dissolution of active materials. Subsequently, the research group designed and synthesized a high-energy cathode material of cyclohexanehexone (C_6O_6) for LIBs, which has the highest theoretical specific capacity (957 mAh g^{-1}) among reported organic cathodes so far.[15] With the electrolyte of 0.3 M LiTFSI-Py_{13}TFSI, the solubility of C_6O_6 was greatly reduced and the battery exhibited a high capacity retention of 82% after 100 cycles, demonstrating relatively good cyclic performance.

Due to the reversible redox reaction between n-type organic molecules and organic cations in ILs, it is feasible to use pure ILs acting as anion/cation suppliers and charge carriers at the same time in the electrolyte. The pure IL with high viscosity could inhibit the dissolution of active materials and improve the cyclic stability of the organic battery. Gerlach et al.[230] revealed the effect of 1-butyl-1-methylpyrro-lidiuniumbis (trifluoromethylsulfonyl)imide (Py_{14}TFSI) on the electrochemical performance of the poly(2,2,6,6-tetramethylpiperidinyl-*N*-oxy-methacrylate) (PTMA) electrode. Compared with the 1 M Py_{14}TFSI-PC electrolyte, the PTMA electrode displayed better cyclic stability in the pure IL-based electrolyte, and the capacity retention increased from 30% to 87% after 10000 cycles at 10 C. In addition, the self-discharge effect of the PTMA electrode was effectively alleviated. The electrode combined with pure Py_{14}TFSI retained about 90% of the initial capacity after 3 days, which was higher than that in the 1 M Py_{14}TFSI-PC electrolyte (70%). Fang et al.[231] designed a novel organic dual-ion battery based on a graphite cathode and a 5,7,12,14-pentacenetetrone (PT) anode (Figure 13d). By comparing the effects of three pure IL-based electrolytes on the electrochemical performance, it was found that the battery with the Py_{14}TFSI electrolyte showed higher specific capacity and better cyclic stability compared with EMITFSI- and PP_{14}TFSI-based electrolytes. These results can be explained as, although EMITFSI with the highest conductivity and the lowest viscosity exhibited a higher initial capacity, its narrow electrochemical window induced irreversible electrolyte decomposition, leading to dramatic capacity decay. For PP_{14}TFSI, its low conductivity adversely affected the high specific capacity of the organic dual-ion battery. Another example of using a pure IL-based electrolyte was reported by Qin et al. They made a metal-free and solvent-free battery based on a PTPAn cathode, a PI5 anode and a pure IL-based electrolyte (Figure 13e).[170] Contrary to previous reports that ILs with high viscosity would decrease the capacity and degrade the rate performance of the battery, organic electrodes exhibited superior rate capability and faster reaction kinetics in ILs than that in traditional carbonate-based electrolytes (Figure 13f), due to the high ionization energy of ILs, the pseudo capacitance behavior of polymer electrodes, and the absence of solvation/desolvation processes. Besides the high specific capacity, the reported all-organic battery also showed excellent cyclic stability and superior low-temperature (−10 °C) performance.

The results demonstrated that the design of solvent-free IL-based electrolytes and all-organic batteries addressed the challenges of the solvation effect and the undesired interaction between the solvent and the electrode. It provided a new strategy to improve the battery energy density based on the wide electrochemical window of ILs and abundant structural diversity of organic electrodes. However, the high cost of ILs has hindered the industrial application of the pure IL-based electrolytes.

3.1.5. Additives. In previous sections, we discussed that optimizing the structure and composition of salts and solvents is an effective method to tune the physicochemical properties of electrolytes. Additives are also widely studied to further improve the interphases and electrochemical performance of organic batteries.

As a common electrolyte additive, $LiNO_3$ is extensively used to protect Li metal, reduce the shuttle effect by forming a layer of Li_xNO_y, and improve Coulombic efficiency of Li secondary batteries.[232−234] Accordingly, Zhang et al.[27] designed and prepared 2 M LiTFSI in DOL/DME electrolytes with different contents of $LiNO_3$ for Li-AQ batteries. The results indicated that with the addition of an appropriate amount of $LiNO_3$, electrolytes can readily form a passivation film on the surface of the Li anode to prevent the continuous shuttle reaction between the dissolved organic electrode material and the Li anode, thus improving the cyclic stability of the battery. This is further confirmed by the surface smoothness of the Li anode after cycling. Among the electrolytes, the battery based on 2 M LiTFSI in DOL/DME electrolytes+1 wt % $LiNO_3$ resulted in the best cycling performance with 94% capacity retention after 20 cycles. When $LiNO_3$ content is further increased to 2 wt %, excessive $LiNO_3$ hinders the migration of Li-ions, which would reduce the specific capacity of the battery and decrease the cyclic stability. Nevertheless, the addition of $LiNO_3$ cannot effectively impede the dissolution of active materials, and $LiNO_3$ would gradually be depleted during the battery cycling, resulting in capacity loss and poor cyclic performance. Therefore, $LiNO_3$ is applied as an additive in synergy with other methods to achieve stable cycle life.[235−237] In addition, LiTFSI was reported as an electrolyte additive to improve the Coulombic efficiency of K-metal batteries due to the reduced parasitic reactions that often occur between the highly reactive K metal and the electrolyte.[238] The addition of 0.05 M LiTFSI into 1 M KPF_6-DME electrolyte significantly improved the Coulombic efficiency of an insoluble organic cathode from 77% to 97% at the second cycle and nearly 100% in the subsequent cycles. Similar results were observed in K-Cu and K-K batteries.[238] The function of the LiTFSI additive can be summarized as follows: 1) Li^+, with a more negative redox potential than K^+, could promote electrostatic shielding to reduce the formation of K dendrites; 2) the cathodic decomposition of $TFSI^-$ is beneficial for the formation of a

https://doi.org/10.1021/acs.chemrev.2c00374
Chem. Rev. 2023, 123, 1712−1773

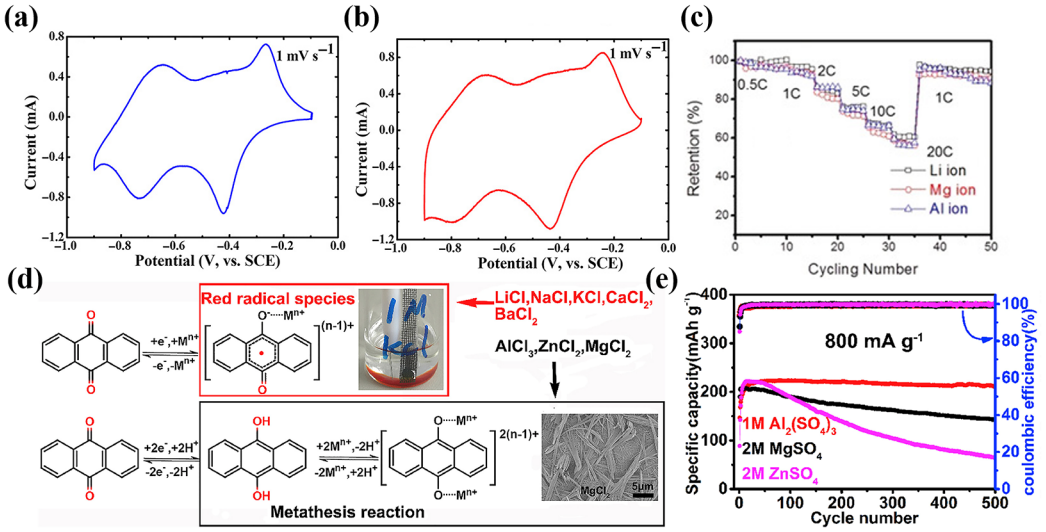

Figure 14. Effects of the cations in aqueous electrolyte on the performance of the battery. CV curves of PI-based electrode in (a) 1 M $LiNO_3$ and (b) 1 M $NaNO_3$ aqueous electrolytes at a scan rate of 1 mV s^{-1}. Reproduced with permission from ref 246. Copyright 2016 American Association. (c) Comparison of rate performance of PI@CNT as three metal ion cathodes. Reproduced with permission from ref 16. Copyright 2018 Wiley-VCH. (d) Metathesis reactions of AQ in different aqueous electrolytes with eight metal ions. Upper inset: Digital photo of three electrode system based on AQ in 1 M KCl aqueous electrolyte after the first cathodic scan. Lower inset: SEM image of AQ surface after first discharging in 1 M $MgCl_2$ electrolyte. (e) Long-term cycle performance of AQ with aqueous multivalent metal-ion electrolytes. Reproduced with permission from ref 248. Copyright 2020 Elsevier.

stable SEI to protect K metal. FEC is another commonly used additive: due to its low LUMO energy level, it is preferentially reduced on the surface of the anode over conventional solvents such as EC and DEC, forming LiF nanoparticles with high mechanical strength and high ionic conductivity, thus reducing the thickness of SEI and stabilizing the Li metal anode.[124]

In summary, organic liquid electrolytes are still the major electrolytes used in organic batteries. Carbonate-, ether-, and IL-based solvents are mostly used in state-of-the-art organic electrolytes. Among the three types of solvents, the use of ILs in the electrolytes can improve the electrochemical performance of the battery at high temperatures, and the non-nucleophilicity of ILs also plays an important role in improving the interfacial compatibility between the electrolyte and the electrode. Although the high viscosity of the ILs leads to a decrease in the initial specific capacity of the organic battery, the slower dissolution kinetics of organic electrode materials in ILs and the interaction between the anions/cations in the ILs and organic molecules reduce the solubility of the organic electrodes and minimize the self-discharge effect, resulting in improved cycling performance of organic batteries. In addition, the low freezing points, poor-solvation or nonsolvation properties, and good electrical conductivities of ILs also allow the electrolytes to retain excellent performance at low temperatures. Some research results indicate that the combination of IL-based electrolytes and organic electrodes with fast oxidation−reduction kinetics has achieved a stable and rapid cyclic performance of the battery at low temperature (0 °C)[182] or even ultralow temperature (−60 °C),[163] and the specific capacities are equivalent to those at room temperature. The selection of solvents and salts for the electrolytes has a significant impact on the electrochemical performance of organic batteries. Some special solvents can enable the operation of batteries under extreme environmental conditions and expand their applications in high-altitude aircrafts, polar exploration, deep sea exploration, and so on. Highly concentrated electrolytes represent another strategy for organic battery development that has resulted in excellent performances via improving cyclic stability and reducing self-discharge of organic electrodes. In the future, exploring the most appropriate electrolyte concentration to maintain optimal battery performances at high current density will be paramount for extending current battery technology. Additionally, the rational design of localized high-concentration electrolytes to improve the wettability of the electrolyte to the electrode and also reduce the cost of ILs and their supporting chemicals will become increasingly relevant for research focused on using highly concentrated electrolytes.

3.2. Aqueous Electrolytes

In recent years, aqueous electrolytes have attracted extensive attention due to their low cost, environmental benignity, nonflammability, high ionic conductivity, and high stability to oxygen and moisture.[239−242] In 1994, Dahn and colleagues[243] assembled the first aqueous rechargeable Li-ion battery, in which the flammable organic electrolyte was replaced by a nonflammable 5 M $LiNO_3$ aqueous solution. The average operating voltage of the $LiMn_2O_4$-VO_2 battery is 1.5 V and the mass energy density could theoretically reach 75 Wh kg^{-1}, higher than current Pb-acid batteries. Since then, various aqueous rechargeable batteries have been studied. State-of-the-art aqueous batteries have shown great potential in high safety and large-scale energy storage devices.

Unsurprisingly, it was found that many inorganic electrode materials, with excellent electrochemical performance in organic liquid electrolytes, were not able to achieve reversible Li-ion insertion/extraction in aqueous electrolytes, exhibiting drawbacks such as low capacity and poor cycling stability.[244] Protons with high activity in aqueous electrolytes may cause significant side reactions to passivate the electrodes before Li-ion intercalation/extraction. Additionally, the structure of the electrode material is easily destroyed during cycling due to the absence of effective protection films on the surface of the electrodes. In addition, water imposes a narrow electrochemical

https://doi.org/10.1021/acs.chemrev.2c00374
Chem. Rev. 2023, 123, 1712−1773

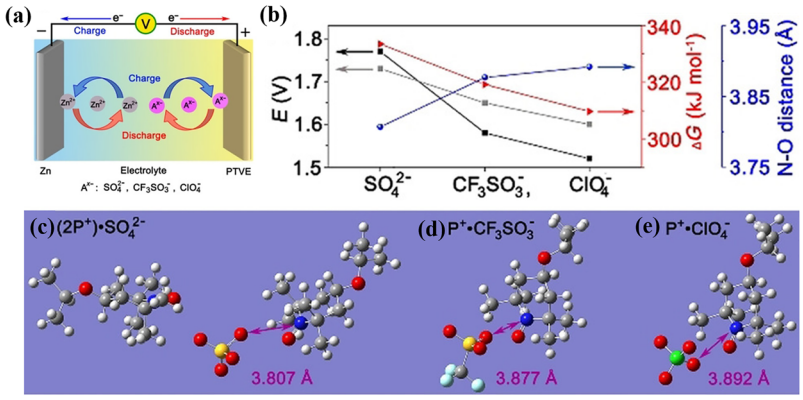

Figure 15. Effects of the anions in aqueous electrolyte on the performance of the battery. (a) Schematic illustration of Zn-PTVE dual-ion battery. (b) Comparison of experimental voltages (black), calculated voltages (gray), Gibbs free-energy changes (red) of the battery reaction in aqueous electrolytes with different anions, and N−O distances (blue) between PTVE and the anions. (c−e) N−O distances and the optimized structures of $(2P^+)\cdot SO_4^{2-}$, $P^+\cdot CF_3SO_3^-$, and $P^+\cdot ClO_4^-$ from DFT calculations. Reproduced with permission from ref 250. Copyright 2020 Wiley-VCH.

stability window of 1.23 V on aqueous electrolytes.[241] The operating voltage of the aqueous LIBs is usually between 1.3 and 2.0 V, which is much lower than that of the nonaqueous LIBs. Therefore, in order to achieve the highest energy density of the battery, it is necessary to use electrode materials with high specific capacities to compensate for the voltage loss. Organic compounds with unique structural diversity and tunability provide a good solution to the problem, which are expected to achieve high specific capacities of more than 900 mAh g^{-1}.[15] In addition, compared with the high solubility of organic electrodes in organic solvents, the lower solubility exhibited in water has also led to widespread interest for organic batteries based on aqueous electrolytes.[245]

3.2.1. Effects of Conductive Salt. *3.2.1.1. Conductive Salts with Different Cations.* Organic electrodes often exhibit similar energy storage behaviors when the metal ions in the conductive salts are bonded with the same anion. As shown in Figure 14a,b, the similar CV curves of PI-based electrodes in $LiNO_3$ and $NaNO_3$ aqueous electrolytes indicate the reversible charge storage of the electrode is not affected by the type of metal cations.[246] Even for high-concentration (5 M) aqueous electrolytes, similar redox peaks of PI electrodes in these two electrolytes indicate similar reaction kinetics.[247] Further research showed that for metal cations with different valences (Li^+, Mg^{2+}, Al^{3+}), fast multivalent insertion/extraction could be achieved in the PIs@CNT cathode through a stable ion-coordination charge storage mechanism, showing similar CV curves and rate performances (Figure 14c), which means PIs are suitable as a universal electrode for different multivalent batteries.[16]

Recent work has shown that organic quinone electrodes exhibit different electrochemical redox mechanisms in different aqueous metal-ion electrolytes. In aqueous electrolytes, different charge carriers exhibit specific physicochemical properties like valence state, ionic radius and hydrolysis characteristics. To explore the ion-pairing effect of charge carriers on the electrochemical performances of organic quinone electrodes, researchers have used AQ as a study model to analyze its redox characteristics in different aqueous electrolytes.[248] As shown in Figure 14d, in 1 M LiCl, NaCl, KCl, $CaCl_2$, and $BaCl_2$ aqueous electrolytes, the AQ molecule undergoes a one-electron redox reaction and becomes a free radical anion $[AQ]^-$. Afterward, a metal ion pairs with $[AQ]^-$ to form red colored $[AQ\text{-}M^{n+}]^{(n-1)+}$, which is easily dissolved in the electrolyte, resulting in poor redox reversibility of the electrode. In contrast, aided by protons, the AQ molecule undergoes two-electron redox reaction in 1 M $AlCl_3$, $MgCl_2$ and $ZnCl_2$ electrolytes. The researchers proposed the substitution reaction between anthrahydroquinone ($AQ\text{-}H_2$) and metal ions could become facile, and the reversible redox reaction of the electrode could be fully realized. Further research found that the AQ electrode showed variable cycling stability in 1 M $Al_2(SO_4)_3$, 2 M $MgSO_4$, and 2 M $ZnSO_4$ even based on the same redox mechanism. The different cycling stabilities were likely caused by the difference in lattice energies of the crystalline and hydrated phases of the ion. As a result, the solubility of AQ-M in the electrolyte differs and AQ in 1 M $Al_2(SO_4)_3$ showed the best cyclability (Figure 14e), which could be attributed to the highest binding energy of AQ-Al compared with AQ-Zn and AQ-Mg.

3.2.1.2. Conductive Salts with Different Anions. Counter anions play an important role in battery performances, even given the same cationic metal. For dual-ion batteries, this is especially true, in which the anions in the electrolyte would participate in the redox reaction at the p-type cathodes. Taking Zn-organic batteries as an example, research showed that in Zn-PANI batteries, the oxidized PANI would act as an electrophile and react with the water in conventional $ZnSO_4$ aqueous electrolyte, resulting in severe capacity fading.[249] In contrast, the bulky $CF_3SO_3^-$ anion, from $Zn(CF_3SO_3)_2$, can stabilize the oxidized PANI by forming hydrogen bonds and reducing the number of water molecules surrounding the oxidized PANI. In addition, $Zn(CF_3SO_3)_2$ electrolytes can passivate Zn foil anodes, inhibit the formation of dendrites, and improve Zn plating/stripping efficiency from 55% to 100%. The use of Zn salts with bulky anions benefits the reactivity and stability of the Zn anode.[249]

Additionally, Luo et al.[250] found that the selection of anions has significant effects on the operating voltage and cyclic stability of dual-ion batteries. Taking the poly(2,2,6,6-tetramethylpiperidinyloxy-4-ylvinylether) (PTVE)-Zn organic battery as an example (Figure 15a), researchers explored the electrostatic interaction between SO_4^{2-}, $CF_3SO_3^-$, and ClO_4^- anions with different molecular electrostatic potentials and the PTVE organic radical. The results showed that the strong electrostatic interaction between anions and PTVE could increase the operating voltage of the Zn-PTVE battery. According to the CV tests, the equilibrium voltages of Zn-PTVE batteries in $ZnSO_4$, $Zn(CF_3SO_3)_2$, and $Zn(ClO_4)_2$ aqueous electrolytes were 1.77,

https://doi.org/10.1021/acs.chemrev.2c00374
Chem. Rev. 2023, 123, 1712−1773

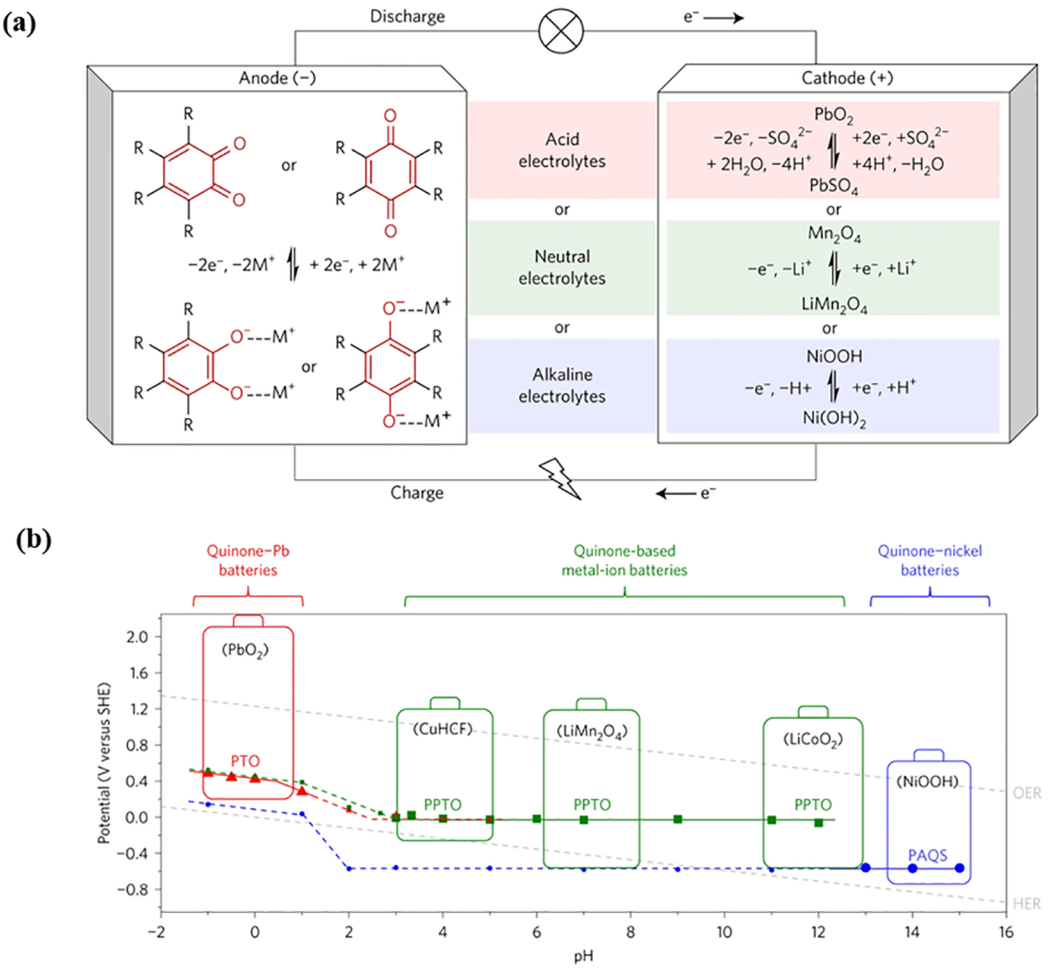

Figure 16. Effects of the aqueous electrolyte PH value on the performance of the battery. (a) Operating schematics of batteries based on quinone anodes in aqueous electrolytes with different pH values. (b) Relationship between the reduction potentials of three quinone anodes and the pH values of aqueous electrolytes. Reproduced with permission from ref 254. Copyright 2017 Springer Nature.

1.58, and 1.53 V, respectively. The CV results were positively correlated with the DFT calculated binding energies of the anions and PTVE (Figure 15b), with the highest binding energy occurring between SO_4^{2-} and PTVE. Compared to $ZnSO_4$ and $Zn(ClO_4)_2$, the battery with the $Zn(CF_3SO_3)_2$ electrolyte exhibited better reversibility and cycling stability, which could be attributed to the well-delocalized electronic structure of $CF_3SO_3^-$ facilitating its more facile dissociation from the PTVE host. For the $ZnSO_4$ electrolyte, the strong Coulombic interaction between SO_4^{2-} and PTVE greatly shortens the distance between them (Figure 15c–e), making it relatively difficult for SO_4^{2-} to dissociate from the $(2P^+)\cdot SO_4^{2-}$ compound and resulting in significant capacity decay of the battery. Although the $Zn(ClO_4)_2$ electrolyte could maintain good cycle stability, the formation of ZnO on the Zn anode would increase the interfacial resistance, resulting in the low specific capacity of the battery.

The previous results demonstrate that, in contrast to inorganic intercalation electrodes, with the rigid crystal structure, some organic electrodes based on reversible electrochemical redox reactions are not sensitive to the ionic radius of the electrolyte salt. For organic electrodes whose redox mechanism and electrochemical performance are greatly affected by electrolyte salts, the selection of conductive salts is particularly important.

3.2.2. Effects of pH. The pH values of electrolytes also play important roles in the performance of the battery. Neutral or weak acid electrolytes are often used in aqueous Zn ion batteries to avoid corrosion of the Zn foil and inhibit Zn dendrite growth.[73,251] However, some organic polymer materials need a high proton (H^+) concentration to facilitate the redox process, such as PANI, which makes them incompatible with Zn anodes. Generally, it is necessary to introduce functional groups such as $-SO_3H$,[252] −COOH, or redox-active phenothiazine derivatives[253] into PANI to maintain the high localized H^+ concentration around the polymer backbone. The addition of these functional groups could help promote the redox process at the electrode and endow PANI with excellent electrochemical performance, thus solving the problem of the different active conditions between the PANI cathode and the Zn anode.

Quinones, as a type of material in organic electrodes, can be compatible with electrolytes under acidic, neutral, and alkaline conditions (Figure 16a). Liang et al.[254] proved that the pH value of the electrolyte has a great influence on the cyclic stability of quinone anodes. PTO displayed 80% capacity decay after 2 cycles in a neutral electrolyte, which could be attributed to its high solubility in the electrolyte at that pH. After increasing the acidity of the electrolyte, operation of the battery with a PTO anode and a PbO_2 cathode resulted in a sustained high initial capacity of 395 mAh g^{-1} and a capacity retention of 96% after

https://doi.org/10.1021/acs.chemrev.2c00374
Chem. Rev. 2023, 123, 1712−1773

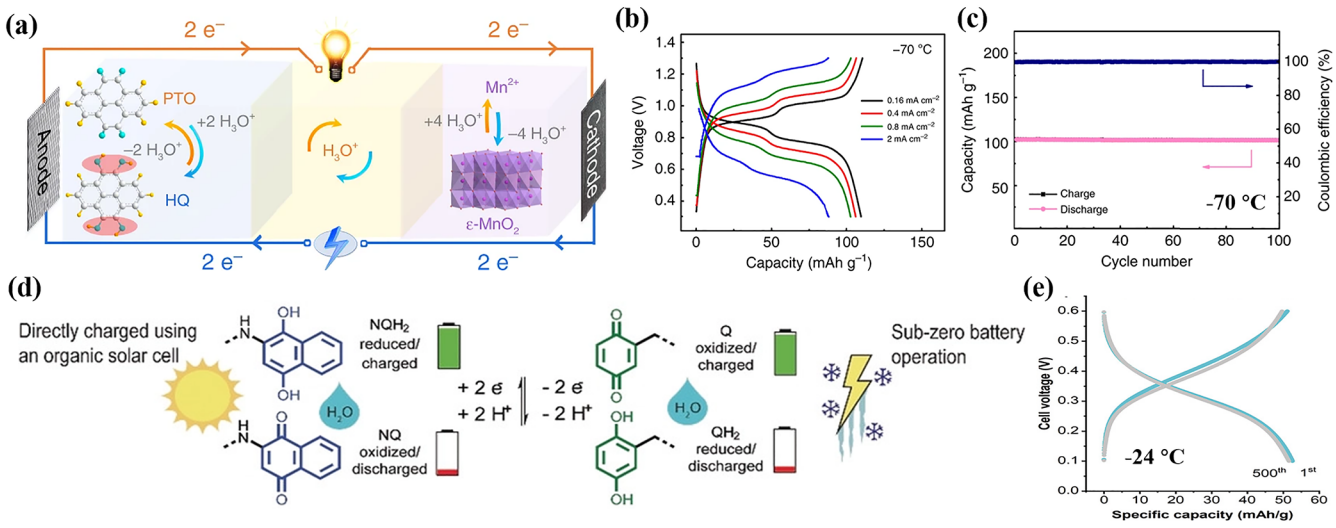

Figure 17. Application of hydronium-ion batteries based on organic electrodes. (a) Schematic illustration of the redox reaction for PTO-MnO_2@GF hydronium-ion battery. (b) Galvanostatic discharge−charge profiles of PTO-MnO_2@GF battery with different current densities at −70 °C. (c) Cycle performance of PTO-MnO_2@GF battery at −70 °C. Reproduced with permission from ref 260. Copyright 2020 Springer Nature. (d) Schematic illustration of the working mechanism for the all-organic hydronium-ion battery. (e) Galvanostatic discharge−charge profiles of the all-organic hydronium-ion battery after different cycles at −24 °C. Reproduced with permission from ref 261. Copyright 2020 Wiley-VCH.

1500 cycles at 2C, along with an average Coulombic efficiency of 99.6%. The robust cyclic stability and good rate capability of PTO in acidic electrolytes may be attributable to the prolific proton diffusivity, high electrochemical activity, and low electrode solubility.

To curtail dissolution concerns, a polymerized PTO (namely PPTO) was proposed. The prepared PPTO exhibited excellent cyclic stability in weakly acidic, neutral, and alkaline electrolytes, indicating PPTO is stable over a relatively wide pH range. In an alkaline environment (pH = 13), PPTO showed an excellent cycling stability with 83% capacity retention after 700 cycles, which could be attributed to the chemical inertness of the quinone core, the poor solubility of PPTO, and the apparent inertness of the amide bond toward hydrolysis. The researchers also studied the effect of pH on the reduction potentials of PTO, PPTO, and PAQS, with the results shown in Figure 16b.[254] In a pH range from −1 to +1, the reduction potentials of all three quinone compounds depended on pH. Increasing the pH value caused the reduction potential to decrease proportionally, indicating a proton storage mechanism. When the pH exceeded 3, the concentration of protons decreased below a threshold value and the reduction potential subsequently became independent of pH. At this pH range, the energy storage mainly depended on the concentration and presence of metal-ions, which was consistent with previous studies.[255] In addition, they explored the capacity and cyclic stability of PAQS and poly(benzo[1,2-*b*:4,5-*b*′]dithiophene-4,8-dione-2,6-diyl sulfide) at different pH values. Only at pH values far exceeding the acid dissociation constants of the corresponding hydroquinones, was the proton-coupled electron-transfer process effectively avoided such that organic electrodes could exhibit the highest capacity and most stable cycle life.[256] This study provided an informative method for determining the optimal pH of aqueous electrolytes in organic batteries.

Due to the fast dynamics of H^+ insertion/extraction in inorganic materials,[257,258] proton storage in rechargeable aqueous organic batteries has also attracted widespread attention. Recently, researchers have tried to use the uptake/removal reaction of H^+ in mild or acidic electrolytes with organic electrodes to prepare the hydronium-ion battery and hybrid battery which could store both proton (H^+) and metal ions. Resorting to the CV test, *in situ* XRD characterization, and DFT calculation, Wang et al.[259] first revealed that H_3O^+ and $H_5O_2^+$ ions could be reversibly stored in PTCDA electrodes operating with 1 M H_2SO_4 as the electrolyte. Guo et al.[260] designed a hydronium-ion battery based on H_3O^+ charge carriers with a MnO_2@graphite anode, a PTO cathode, and 2 M $MnSO_4$+2 M H_2SO_4 electrolyte, with the working mechanism shown in Figure 17a. The battery exhibited high energy densities and a long cycle life of more than 5000 cycles. In addition, due to the absence of intercalation and the dissolution processes related to H_3O^+, the proton battery is well suited to maintain excellent rate performance at the ultralow temperatures (Figure 17b,c). As shown in Figure 17d,e, similar results were reported in an all-organic hydronium-ion battery with the mechanism of proton insertion chemistry shown in Figure 1d.[261] Furthermore, it was found that the Zn-organic battery with sulfur heterocyclic quinone dibenzo[b,i]thianthrene-5,7,12,14-tetraone (DTT) cathode could store H^+ and Zn^{2+} simultaneously, which exhibited excellent flexibility and ultralong cycle life up to 23 000 cycles.[262]

3.2.3. Concentration Optimization. Previous studies have shown that in aqueous electrolytes, changing the concentration of the electrolyte has a considerable effect on the insertion/extraction potential of ions and the stability of electrode materials. Increasing the salt concentration could reduce the activity of water molecules and suppress the dissolution of active materials, thereby improving the cycling stability of the organic battery.[263]

"Water-in-salt" (WIS) electrolytes provide a new solution to widen the electrochemical stability window of aqueous electrolytes. In 2015, Suo et al.[264] first proposed the concept of WIS and reported a highly concentrated aqueous electrolyte (21 m LiTFSI) whose electrochemical window expanded to 3.0 V (1.9−4.9 V vs Li^+/Li) with the formation of the stable electrode−electrolyte interphase. The evolution of the Li^+

https://doi.org/10.1021/acs.chemrev.2c00374
Chem. Rev. 2023, 123, 1712−1773

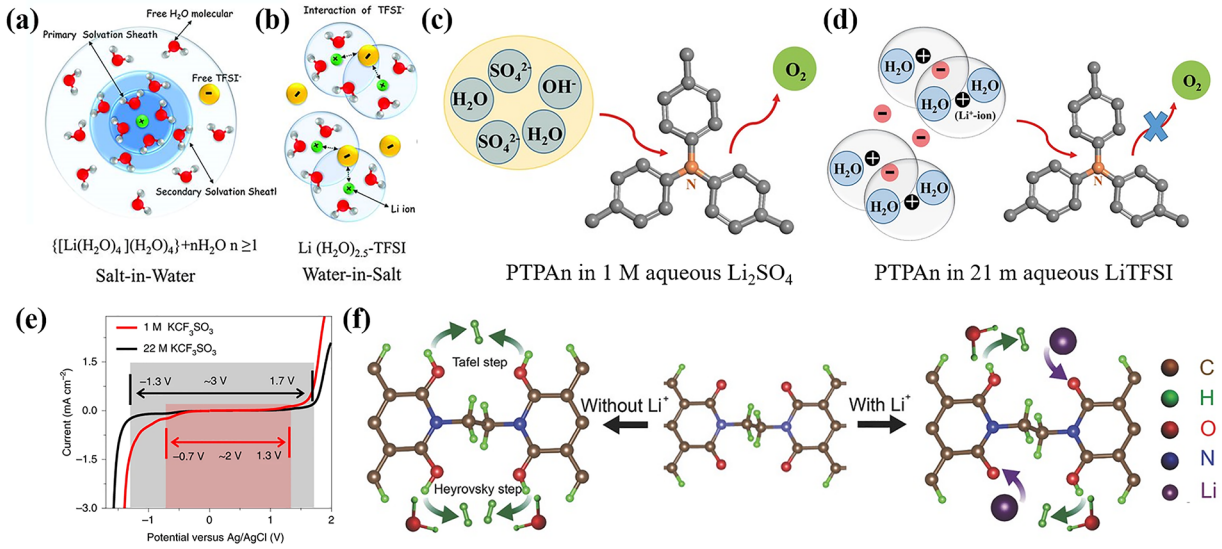

Figure 18. Different solvation structures in aqueous electrolytes. Schematic illustrations of the change of the Li^+ primary solvation sheath in (a) "salt-in-water" and (b) "water-in-salt" solutions. Reproduced with permission from ref 264. Copyright 2015 The American Association for the Advancement of Science. Schematic diagrams of PTPAn reaction in (c) 1 M Li_2SO_4 and (d) 21 m LiTFSI aqueous electrolytes during the charge process. Reproduced with permission from ref 272. Copyright 2017 Wiley-VCH. (e) Linear sweep voltammetry plots of 1 and 22 M KCF_3SO_3 electrolytes at the scan rate of 10 mV s^{-1}. Reproduced with permission from ref 273. Copyright 2019 Springer Nature. (f) Schematic illustration of hydrogen evolution reaction on PNFE surface with or without Li^+. Reproduced with permission from ref 274. Copyright 2016 Wiley-VCH.

primary solvation sheath in diluted and WIS electrolytes is shown in Figure 18a,b. For WIS electrolyte, the average number of water molecules actively solvating each ion is less than in dilute solutions, precluding H_2O molecules from effectively neutralizing the electrostatic field generated by the positive charge on Li^+. Therefore, the H_2O solvation sheath is partially replaced by an anion-containing Li^+ solvation sheath, and the electrochemical activity of water is reduced substantially, inhibiting the reduction of water and continuous hydrogen evolution. Furthermore, the increase of salt concentration is conducive to the preferential reduction of $TFSI^-$, which could form a dense interphase on the anode surface, alleviating the continuous reduction of both water and $TFSI^-$. As a result of the reduced water activity combined with the inhibition of hydrogen evolution, the electrochemical stability window of the electrolyte was extended to 3 V. The researchers then introduced the concept of WIS to aqueous NIBs, in which a dense Na^+ conductive SEI was observed to form on the surface of the $NaTi_2(PO_4)_3$ anode. In the NIB with the WIS electrolyte, the researchers additionally observed a wide electrochemical stability window of 2.5 V.[32] Recently, a series of WIS electrolytes with a broad electrochemical stability window based on superconcentrated conductive salts,[265,266] double salts,[267] hybrid solvents,[268−270] and inhomogeneous additives[271] have been reported, which could form effective protecting layers on the electrode surface, reduce the activity of water and water-induced side reactions, thus improving the cycling stability and energy density of the battery.

The use of WIS electrolytes has successfully extended the electrochemical window of aqueous LIBs to the range of 3−4 V, making it possible to match with the low-voltage graphite anode and high-voltage cathodes. However, the limited intercalation capacity of traditional transition metal oxides (less than 200 mAh g^{-1}) restricts the realization of higher energy density. The effective use of organic electrode materials instead of graphite or transition metal oxide electrodes is expected to further improve the energy density of the battery.

Dong et al.[272] introduced the high-concentration aqueous LiTFSI electrolyte in all organic batteries and successfully solved the irreversible challenge of the PTPAn electrode in a neutral aqueous electrolyte. As shown in Figure 18c, in a 1 M Li_2SO_4 aqueous electrolyte, both H_2O molecules and SO_4^{2-} anions were adsorbed on the N^+ site of PTPAn, and the adsorbed H_2O molecules were continuously oxidized to O_2 during the charging process, resulting in a low capacity and irreversible charge/discharge cycle of PTPAn. When replaced with a high concentration WIS electrolyte of 21 m LiTFSI, the free H_2O molecules in the system are bonded by ions from the salt (Figure 18d), effectively suppressing H_2O oxidation, allowing the Coulombic efficiency of the PTPAn electrode to reach 100%. The maximum operating voltage of the all-organic battery composed of a PNTCDA anode and a PTPAn cathode could reach 2.1 V, and the energy density could approach 52.8 Wh kg^{-1}. Jiang et al.[273] used a 22 M KCF_3SO_3 electrolyte instead of a 1 M KCF_3SO_3 electrolyte to widen the electrochemical stability window of the aqueous electrolyte from 2 to 3 V (Figure 18e). In addition, the aqueous electrolyte with high salt concentration also exhibited high ionic conductivity (7.6×10^{-2} S cm^{-1} at 25 °C and 1×10^{-2} S cm^{-1} at −20 °C), low viscosity (6.5×10^{-3} Pa s at 25 °C), and inhibited dissolution of electrodes. The K-ion full battery with a $K_xFe_{0.35}Mn_{0.65}[Fe(CN)_6]_w.zH_2O$ cathode and a 3,4,9,10-perylenetetracarboxylic diimide (PTCDI) anode exhibited high energy and power densities, which could achieve 80 Wh kg^{-1} and 1612 W kg^{-1}, respectively.[273]

However, high cost and low reaction kinetics pose challenges for practical applications of batteries using highly concentrated electrolytes, and designing organic batteries with a wide voltage window in medium or even low concentration electrolytes has become a hot topic for researchers. Wang et al.[274] found that in 0.5 M Li_2SO_4 electrolyte, the poly(naphthalene four formyl ethylenediamine) (PNFE)-$LiMn_2O_4$ full battery displayed a

https://doi.org/10.1021/acs.chemrev.2c00374
Chem. Rev. 2023, 123, 1712−1773

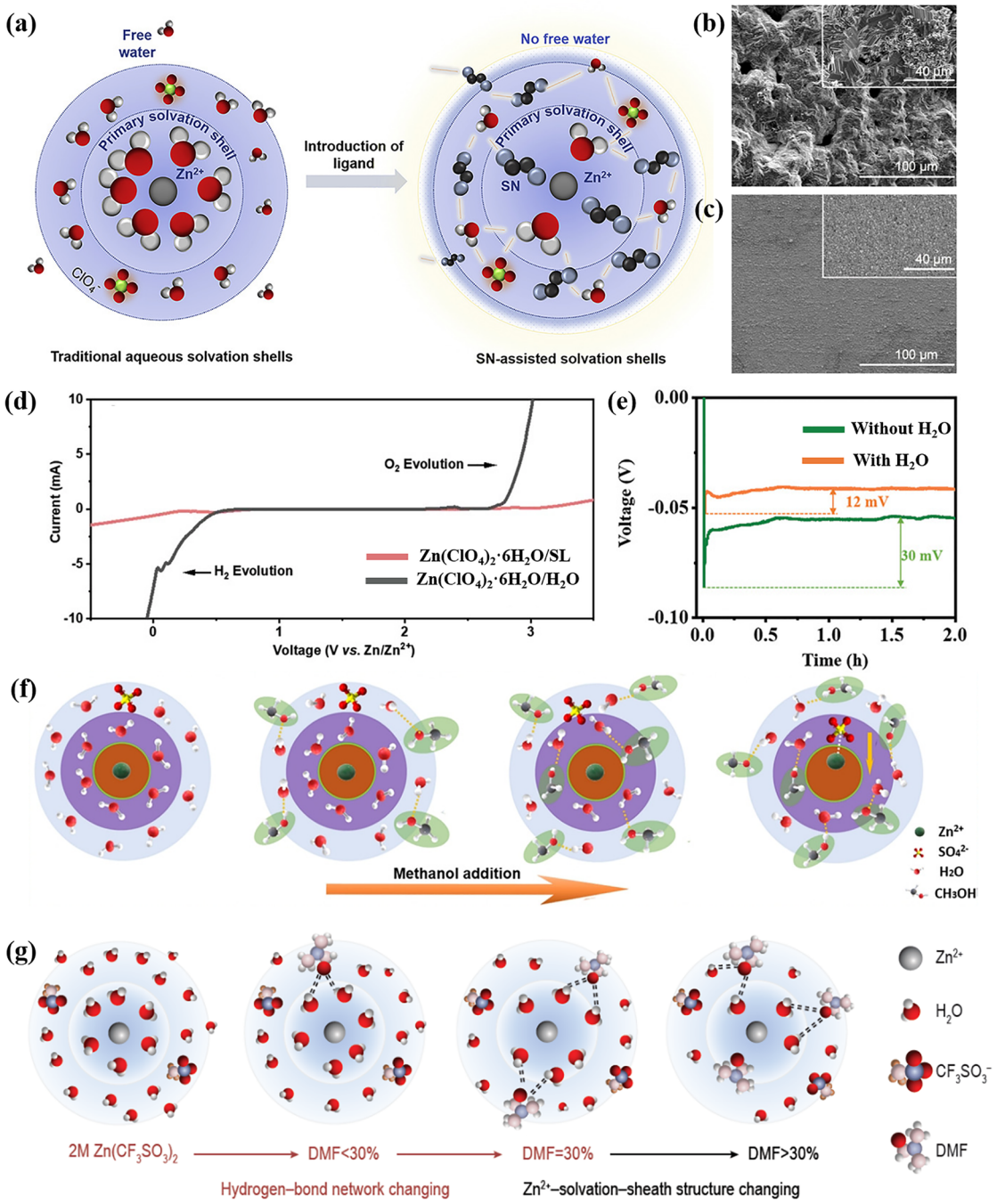

Figure 19. Effects of the addition of organic additives in aqueous electrolytes for organic batteries. (a) Schematic diagrams of Zn^{2+} solvation structure in traditional aqueous Zn electrolyte ($Zn(ClO_4)_2{\cdot}6H_2O/H_2O$) and hydrated eutectic electrolyte ($Zn(ClO_4)_2{\cdot}6H_2O$/SN). Typical SEM images of Zn metal after plating for 0.5 h at −0.3 V (versus Zn/Zn^{2+}) using (b) $Zn(ClO_4)_2{\cdot}6H_2O/H_2O$ and (c) $Zn(ClO_4)_2{\cdot}6H_2O$/SN electrolytes. Reproduced with permission from ref 283. Copyright 2020 Elsevier. (d) Electrochemical stability windows for $Zn(ClO_4)_2{\cdot}6H_2O$/SL and $Zn(ClO_4)_2{\cdot}6H_2O/H_2O$ electrolytes determined by linear sweep voltammetry tests. Reproduced with permission from ref 284. Copyright 2021 Wiley-VCH. (e) Nucleation overpotentials of Zn deposition on Cu at 0.1 mA cm^{-2} using electrolytes with and without H_2O. Reproduced with permission from ref 285. Copyright 2021 Wiley-VCH. (f) Schematic of changes in Zn^{2+} solvent sheath with the addition of methanol. Reproduced with permission from ref 291. Copyright 2021 Wiley-VCH. (g) Schematic of changes in Zn^{2+} solvent sheath and local hydrogen-bonding network with the addition of DMF. Reproduced with permission from ref 292. Copyright 2022 China Science Publishing & Media Ltd.

wide voltage range of 2 V. The improved working voltage window could be attributed to two aspects: 1) the passivation of the PNFE/carbon nanotube networks to effectively reduce hydrogen-evolution and 2) the action of Li^+ in the electrolyte to reduce the active sites and increase the hydrogen-evolution overpotentials (Figure 18f), effectively suppressing hydrogen-evolution. The research provided a new way to broaden the electrochemical stability window of the organic battery in low-concentration electrolytes.

https://doi.org/10.1021/acs.chemrev.2c00374
Chem. Rev. 2023, 123, 1712−1773

3.2.4. Effects of the Solvent. In fact, most salts in WIS electrolytes do not participate in battery reactions, but only play a role in maintaining the solvation sheath structure. Hence, determining how to reduce the content of free water in aqueous electrolytes and change the metal ions coordination environment without incurring a high cost has become a defining challenge for researchers.

3.2.4.1. Hydrated Eutectic Electrolytes. The introduction of hydrated eutectic electrolytes offers a possibility to reduce the activity of water and broaden the electrochemical stability window of aqueous electrolytes.

Eutectic electrolytes, as a kind of deep eutectic solvents, have attracted significant attention in the fields of advanced energy storage and conversion devices owing to their excellent electrochemical stability, nonflammability, compositional tunability, wide operating temperature window and good thermal and chemical stability.[275−277] Like ILs, eutectic electrolytes are composed of charged ion pairs without independent molecules and play an active role in constructing stable SEI and promoting uniform and reversible metal plating/stripping.[278−280] In contrast to standard aqueous electrolytes, in hydrated eutectic electrolytes, all water molecules participate in the formation of the eutectic structure and are confined in hydrogen-bonding. Due to the immobility and binding environment of the water molecules, the decomposition of water is inhibited, thereby resulting in a wider electrochemical window relative to ordinary, noneutectic, aqueous electrolytes.[281]

Due to the high solubility of metal oxides in the eutectic electrolytes, the eutectic electrolytes are currently more inclined toward batteries with organic electrode materials, mostly for Zn-ion batteries.[282] A novel hydrated eutectic electrolyte was prepared by a simple and low-cost formula via a mixture of an inexpensive and highly soluble Zn salt, ($Zn(ClO_4)_2·6H_2O$), and a neutral ligand, succinonitrile (SN). The hydrated eutectic electrolyte effectively protects the Zn anode, suppresses the hydrogen-evolution reaction and reduces the irreversible dissolution of organic cathode materials.[283] As shown in Figure 19a, SN can enter the primary solvation shell of Zn^{2+} and form a room temperature eutectic liquid with $Zn(ClO_4)_2·6H_2O$ in the hydrated eutectic electrolyte, altering the solvation structure of the hydrated Zn-ions from $[Zn(OH_2)_6]^{2+}$ to $[Zn(OH_2)_x(SN)_y]^{2+}$. The unique structure of the zinc aqua complex solvated with the SN-assisted solvation shell are beneficial for mitigating the parasitic reactions on the Zn/aqueous electrolyte interface and enabling smooth and dendrite-free Zn plating/stripping with an average Coulombic efficiency of 98.4%. The SEM images of the morphologies of Zn platting indicated that the hydrated eutectic electrolyte of $Zn(ClO_4)_2·6H_2O$/SN enabled highly uniform and compact Zn coating, which was in sharp contrast to the severe cracking and irregular protuberances observed on the surface of stainless steel using traditional aqueous Zn electrolyte (Figure 19b,c). In addition, all water molecules are bound in the eutectic network, resulting in a delayed oxidation and suppressed dissolution of the organic cathode materials. Similarly, the mixing of sulfolane (SL) and $Zn(ClO_4)_2·6H_2O$ could form a hydrated eutectic electrolyte due to the strong coordination between SL and Zn^{2+}.[284] The bound water molecules in the eutectic electrolyte help increase ionic diffusion, promote Zn^{2+} deposition, and reduce water activity, thereby extending the electrochemical stability window (Figure 19d) and stabilizing Zn plating/stripping. As a result, the PANI-Zn battery exhibited excellent cycling performance with a stable capacity of 72 mAh g^{-1} at a high current density of 3 A g^{-1} for more than 2500 cycles. In addition, the introduction of H_2O molecules in a $ZnCl_2$-acetamide eutectic electrolyte has proved to regulate the Zn^{2+} solvation structure and reduce the nucleation overpotential from 30 mV to 12 mV (Figure 19e), aiding facile Zn^{2+} desolvation and uniform Zn nucleation.[285]

Recently, a hydrated eutectic electrolyte consisting of $Mg(NO_3)_2·6H_2O$ and acetamide was developed for aqueous Mg-ion batteries.[286] The presence of solvated water molecules in the electrolyte facilitates fast Mg^{2+} transport, while the lack of free water molecules suppresses the dissolution of the PTCDA anode, ensuring excellent cycling stability. Hence, the PTCDA anode with fast reaction kinetics and the copper hexacyanoferrate cathode with an open-framework promote Mg^{2+} (de)-intercalation without serious structural changes, leading to superior rate capability.

3.2.4.2. Other Organic Additives. In addition, some organic additives can optimize the solvation structure of the electrolyte, expanding the electrochemical stability window and inhibiting the hydrogen evolution reaction and dendrite growth.[287−289] Specifically, the introduction of organic solvents may cause two solvation effects. First, the organic additives could interact with H_2O, affecting structures resulting from hydrogen-bonding in the electrolyte. In addition, they may also be inserted into the inner solvation sheath of the metal ions and occupy the position of H_2O, resulting in the alterations to the "normal" solvation structure.

For example, dimethyl sulfoxide (DMSO), with a higher Gutmann donor number than H_2O, can preferentially coordinate with Zn^{2+} ions and exclude water from the Zn^{2+} solvation sheath, weakening the bonding strength between Zn^{2+} ions and H_2O. The resulting electrolyte was observed to then form a dense SEI on Zn anodes.[290] Furthermore, the strong interaction between DMSO and H_2O could reduce the water reactivity. Similarly, by adding an antisolvent like methanol, into the $ZnSO_4$ aqueous electrolyte, the solvation structure of Zn^{2+} ions is regulated via the formation of hydrogen bonds between methanol and H_2O (Figure 19f). The water activity was observed to diminish and the Zn electrode reversibility was increased.[291] The PANI-Zn battery, with methanol-based antisolvent electrolyte, exhibited stable cycling capacity and high Coulombic efficiency as a result of inhibited dendrite growth, H_2 evolution and other side reactions. To further explore the inhibitory effects of altered hydrogen bonds and modulation of the inner Zn^{2+} solvation sheath on the hydrogen-evolution reaction, Ma et al. introduced different amounts of DMF in the 2 M $Zn(CF_3SO_3)_2$ aqueous electrolyte.[292] As shown in Figure 19g, the added DMF preferentially forms hydrogen bonds with water molecules, reducing the water activity and effectively inhibiting the deprotonation of the electrolyte. Notably, after increasing the volume fraction of DMF by more than 30%, some DMF is inserted into the inner Zn^{2+} solvation sheath, resulting in a diminishment of the electrochemical stability of the electrolyte. The optimal Zn reversibility can be obtained in the electrolyte with a critical concentration of 30% DMF. With the optimized electrolyte, a PANI-Zn battery successfully operated over a wide temperature range from −40 to +25 °C. The above results indicate that parasitic interfacial reactions can be inhibited via solvent effects, providing new strategies for the design of low-cost and efficient aqueous electrolytes.

3.2.5. Aqueous Batteries for Special Applications. Compared to the high mechanical rigidity of inorganic electrode materials, organic compounds exhibit flexibility and deform-

https://doi.org/10.1021/acs.chemrev.2c00374
Chem. Rev. 2023, 123, 1712−1773

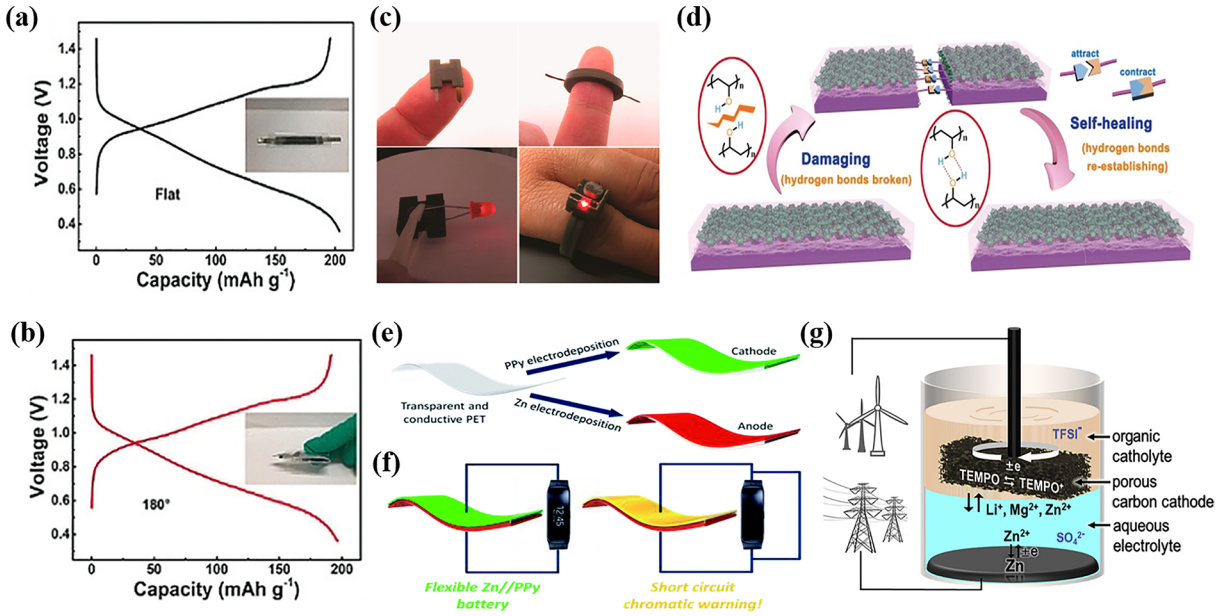

Figure 20. Aqueous batteries with special performances. The discharge/charge curves of the belt-shaped PTO-Zn battery (a) at flat state and (b) folded 180° after 100 times. Reproduced with permission from ref 295. Copyright 2018 Wiley-VCH. (c) The rechargeable batteries with various shapes. Reproduced from ref 73. Copyright 2018 American Chemical Society. (d) Illustration of the mechanism of the self-healing Zn-ion battery. Reproduced with permission from ref 298. Copyright 2019 Wiley-VCH. Schematics of (e) the structure and (f) demonstration of the Zn-PPy battery with a unique function of short-circuit warning. Reproduced with permission from ref 301. Copyright 2018 Royal Society of Chemistry. (g) Schematic illustration of the stirred self-stratified battery. Reproduced with permission from ref 302. Copyright 2020 Elsevier.

ability, which provide necessary conditions for the preparation of flexible batteries for wearable and portable electronic devices. Considering the high safety requirements for flexible wearables, using aqueous electrolytes instead of highly toxic and flammable organic electrolytes is expected to achieve a safe energy storage system which exhibits environmental friendliness, low cost and excellent performance.[293,294] In addition, by modifying the electrode materials or electrolytes of aqueous batteries, it is expected to achieve more functions like self-healing, biocompatibility and electrochromicity, which paves the way for the further development of smart flexible electronics.

Guo et al.[295] used PTO, an organic material with a high theoretical specific capacity, as the cathode material, and assembled a flexible Zn battery with a 2 M $ZnSO_4$ aqueous electrolyte, to avoid corrosion of the Zn anode. As a candidate for wearable electronics, the belt-shaped PTO-Zn battery showed excellent flexibility and strong mechanical performance against repeated bending. Compared to the flat battery (Figure 20a), the flexible battery showed no obvious capacity loss after repeated folding of 180° up to 100 times (Figure 20b) and maintained excellent cycling stability under various continuous bending degrees. However, low electronic conductivity and Zn dendrite formation are still relevant concerns. Similarly, the combination of a PANI-coated carbon fiber cathode, a Zn anode and the aqueous electrolyte enabled the design of small rechargeable batteries with various polygonal geometries such as rectangle, cylinder, H-, ring-, and cylindrical shapes (Figure 20c). These geometries demonstrated desirable integrations of energy storage devices and electronic equipment.[73] To further improve the flexibility of the electrodes, a nanostructural PANI-cellulose paper and a Zn-grown graphite paper were used as the cathode and the anode, respectively.[296] Together with a gel electrolyte based on a cellulose nanofiber and an aqueous electrolyte, the flexible Zn-ion battery showed outstanding electrochemical performance, and the specific capacity changed little under mechanical deformation, with only 9% loss after 1000 bending cycles. These studies indicate that aqueous organic batteries have great potential in flexible displays and wearable electronic devices through the reasonable design of electrode materials and energy-storage devices.

Although the flexible aqueous battery can withstand certain bending or tensile strain, it is still relatively easy to damage under exceedingly large deformation regimes, resulting in severe performance degradation. The flexible battery which possesses self-repair functions can automatically recover its performance after being mechanically damaged, not only extending the lifetime of the device, but also reducing electronic waste and economic cost. The development of self-healing polymer electrolytes plays a critical role in the development of self-healing batteries. The self-repair action of the polymer network operates normally according to the dynamic reorganization of hydrogen bonds or ionic bonds in the system.[297] A self-healing poly(vinyl alcohol) (PVA)/$Zn(CF_3SO_3)_2$ hydrogel electrolyte with a three-dimensional (3D) porous network structure was developed by a facile freezing/thawing strategy.[298] Due to extensive hydrogen bonding networks between the chains of PVA, the hydrogel electrolyte has excellent self-healing characteristics without any external stimulation (Figure 20d). Even after several cutting/self-healing processes, the Zn-ion batteries automatically repair themselves and recover electrochemical performance completely, showing an excellent repeatability of the self-healing performance. The self-healing Zn-ion battery is particularly suitable for low-cost and high-efficiency wearable products, which promotes the development of smart flexible electronics.

Through the combination of aqueous electrolytes and organic electrolyte materials with excellent biocompatibility, the prepared biobattery has a broad application prospect in

https://doi.org/10.1021/acs.chemrev.2c00374
Chem. Rev. 2023, 123, 1712−1773

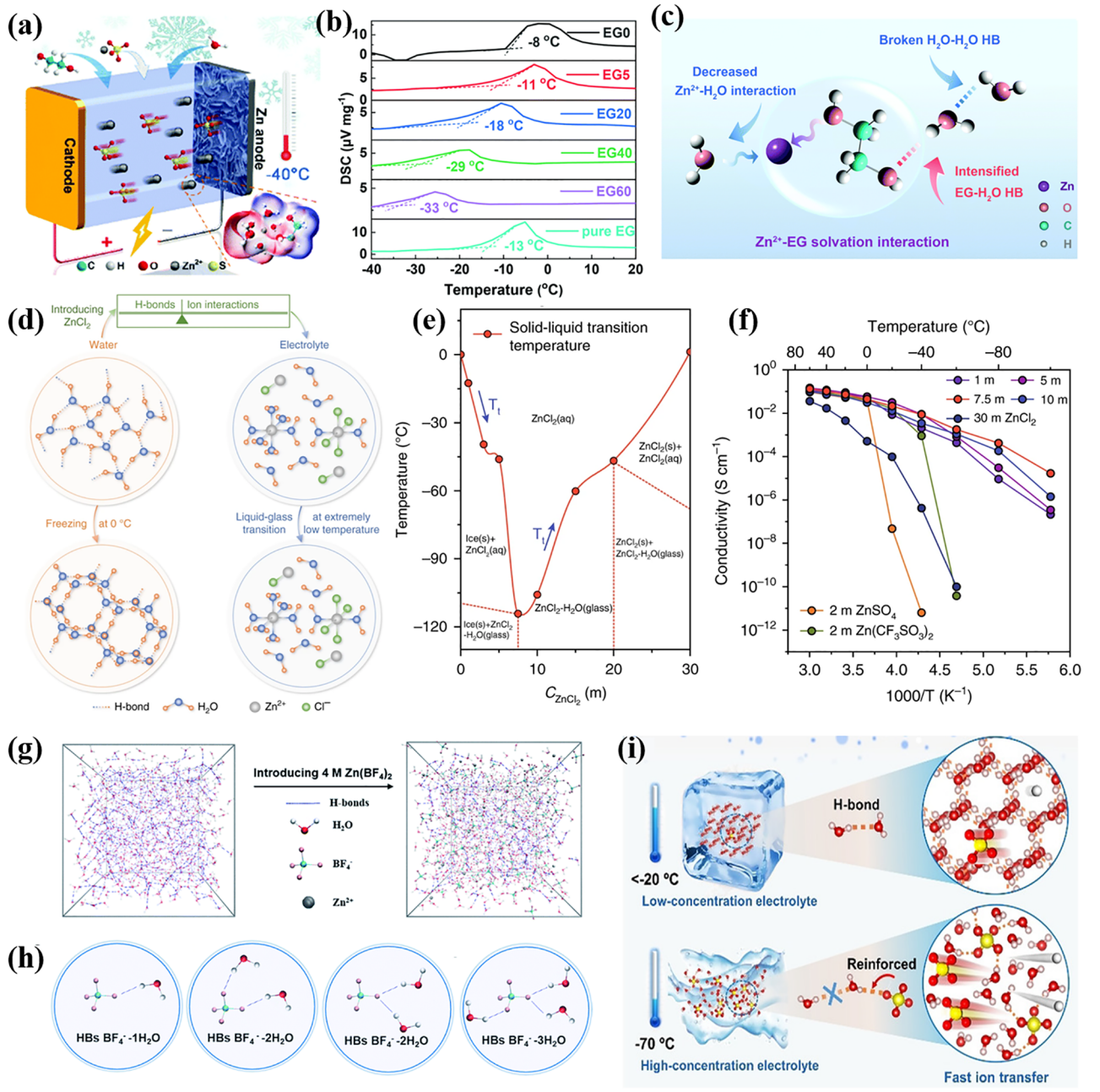

Figure 21. Design of aqueous electrolytes for low-temperature organic batteries. (a) Schematic of low-temperature Zn-ion battery with $ZnSO_4$-based hybrid electrolytes. (b) The freezing points of electrolytes with pure EG solvent and hybrid solvents of EG and H_2O obtained from the differential scanning calorimetry curves. (c) Schematic diagram of a possible antifreezing mechanism in the hybrid electrolyte. Reproduced with permission from ref 308. Copyright 2020 Royal Society of Chemistry. (d) schematic of the structure evolutions of water and electrolyte after addition of $ZnCl_2$. (e) The value of T_t and the phase composition of $ZnCl_2$ solution at different salt concentrations and temperatures. (f) The ionic conductivities of various electrolytes at different temperatures. Reproduced with permission from ref 310. Copyright 2020 Springer Nature. (g) Snapshots of the MD simulation of water and 4 M $Zn(BF_4)_2$ aqueous electrolyte. (h) Different types of hydrogen bonds between BF_4^- anion and H_2O molecules. Reproduced with permission from ref 311. Copyright 2021 Royal Society of Chemistry. (i) Illustration of the mechanism of how the addition of SO_4^{2-} impacts the original hydrogen-bonding networks. Reproduced with permission from ref 312. Copyright 2021 Wiley-VCH.

implantable biomedical devices. Biobatteries offer the possibility of developing implantable biomedical devices that can derive power provided by energy sources in the living body without requiring periodic power supply replacement. Among many organic materials, PPy is an excellent candidate as an active component in bioelectric batteries, because of its high specific capacity, good biocompatibility and excellent performance when implanted into the human body. Kong[299] and Li[300] et al. studied the performance of different biocompatible aqueous electrolytes in Mg-based and Zn-based bioelectric batteries using the PPy cathode and selected electrolyte systems of phosphate buffered saline and 0.1 M NaCl aqueous solution, respectively.

Wang et al.[301] reported a flexible, electrochromic and rechargeable battery for the first time. Researchers successfully deposited an electrochromic PPy cathode and Zn anode on a flexible, transparent, conductive PET substrate by a simple

https://doi.org/10.1021/acs.chemrev.2c00374
Chem. Rev. 2023, 123, 1712−1773

method of electrodeposition. The electrodes were matched with a PVA-based hydrogel electrolyte (Figure 20e). The battery could provide a high specific capacity of 123 mAh g^{-1} and exhibit a unique function of short-circuit warning. As shown in Figure 20f, when the battery voltage drops from 1.2 to 0 V, the color changes from black to yellow indicating the possibility of short circuit.

In addition, Meng et al.[302] proposed a stirred self-stratified Zn-organic battery without multilayer stacking, which greatly reduced the manufacturing cost of the battery (Figure 20g). The battery was designed according to the principles of phase separation and the inherent difference in solubilities of electrode materials. The structure is characterized as a thermodynamically stable sandwich with three layers of material, "liquid-liquid-solid" from top to bottom. The layers are specifically, an organic cathode phase, an aqueous electrolyte phase and a Zn anode. Due to the differential density of the cell components, the battery always recovers to its initial state after mechanical disturbance or charge−discharge reactions. The battery can exhibit accelerated charge/discharge process under stirring conditions with excellent cyclic reversibility and safety, and provide a new direction in the development of energy storage devices.

3.2.6. Low-Temperature Aqueous Batteries. It is widely known that the freezing point of water is 0 °C at standard atmospheric pressure,[303] which imposes a strict window of feasible operation conditions for aqueous batteries. Therefore, the most significant challenge for developing aqueous batteries that can operate under low-temperature conditions is the lack of advanced aqueous electrolytes which do not become prohibitively viscous or solidify at low temperature.[304]

Up to now, various strategies have been reported to inhibit the freezing of aqueous electrolytes. Well-known antifreeze agents, dimethyl sulfoxide (DMSO),[305,306] DMF,[292] and liquid alcohols[291,307−309] can preferentially form hydrogen-bonding networks with water molecules effectively outcompeting water to water hydrogen-bonding, thus providing a hybrid electrolyte with a relatively low freezing point and high ionic conductivity at low temperature. Due to the advantages of high boiling point, low freezing point, low volatility and high solubility in water, ethylene glycol (EG) was reported as a cosolvent in $ZnSO_4$-based hybrid electrolytes for low-temperature Zn-ion batteries (Figure 21a).[308] As shown in Figure 21b, with the increase of EG content (from EG0 to EG60), the freezing point of the hybrid electrolyte decreased to −33 °C gradually. The freezing point depression can be attributed to the disruption of the H_2O-H_2O hydrogen-bonding network via the action of EG molecules. The EG-H_2O hydrogen-bonding can dramatically decrease the solvation interaction of Zn^{2+} with H_2O (Figure 21c), resulting in less side reactions between the Zn anode and the electrolyte. However, increasing the amount of organic solvent additives directly leads to a serious decline in the intrinsic safety of aqueous batteries. Similarly, the addition of methanol in the $ZnSO_4$ electrolyte could disrupt hydrogen-bonding networks between H_2O molecules.[291] When the volume ratio of methanol reached 50%, the corresponding battery could maintain good fluidity at temperatures approaching to −40 °C, while the pure $ZnSO_4$ aqueous electrolyte froze at a higher temperature of −20 °C.

In addition, some electrolyte salts exhibit strong ionic interactions with water molecules, which could also significantly disrupt hydrogen-bonding networks in pure H_2O. As illustrated in Figure 21d, with the addition of $ZnCl_2$ in water, the strong intermolecular ion-dipole force between Zn^{2+} and H_2O molecules, via coordination with oxygen atoms in H_2O, ultimately reduces the hydrogen-bonding content in the solution.[310] When the concentration of $ZnCl_2$ gradually increased to 7.5 m, the lowest solid-liquid conversion temperature (T_t) of −114 °C and the highest ionic conductivity of 1.79 × 10^{-3} S cm^{-1} at −70 °C were obtained due to the reduced hydrogen-bonding content of the solution (Figure 21e,f). However, further increasing the content of $ZnCl_2$ would lead to the increase of T_t due to the more significant Coulombic interactions between cations and anions. Thus, it is important to balance the hydrogen-bonding and cation−anion interactions. As a result, the PANI-Zn battery was successfully operated over a wide temperature range from −90 to +60 °C. In addition to metal ions, some anions in electrolyte salts could disrupt the original hydrogen-bonding networks through the formation of new hydrogen bonds with H_2O molecules, so as to significantly reduce the freezing point of the electrolyte.[311,312] As illustrated in the results of molecular dynamics (MD) simulations (Figure 21g,h), the hydrogen bonds between H_2O molecules decreased rapidly after the addition of the $Zn(BF_4)_2$ salt, and numerous O−H···F hydrogen bonds between the BF_4^- anions and H_2O molecules were formed.[311] The introduction of BF_4^- anions can form four relatively weak hydrogen bonds with H_2O molecules, which efficiently prevents the H_2O molecules from forming an ordered hydrogen-bonding network. Benefiting from the ultralow freezing point of −122 °C and the high ionic conductivity of 1.47 × 10^{-3} S cm^{-1} at −70 °C of the 4 M $Zn(BF_4)_2$ electrolyte, the tetrachlorobenzoquinone-Zn battery exhibited excellent electrochemical performance over a wide temperature range from −95 to +25 °C. The strong interaction between SO_4^{2-} and H_2O molecules could result in an electrolyte that exhibits similar characteristics to the $Zn(BF_4)_2$ system, short-listing the antifreezing H_2SO_4 electrolyte as a promising electrolyte in the development of low-temperature aqueous batteries (Figure 21i).[312]

Deep eutectic solvents, in which the melting point of the eutectic mixture is significantly lower than that of individual constituents, are also a promising strategy for use in batteries operating at low temperatures. The hydrated eutectic electrolytes of $Zn(ClO_4)_2{\cdot}6H_2O$/SN[283] and $Zn(ClO_4)_2{\cdot}6H_2O$/SL[284] were reported to achieve stable low-temperature performance in organic batteries at −20 and −30 °C, respectively. However, a large number of organic solvents in these systems not only aggravate environmental degradation, but also lead to low ionic conductivity and high viscosity at low temperatures. The design of an aqueous-salt eutectic electrolyte without organic compounds is considered to be an effective way to solve the above problems. Therefore, Sun et al.[313] designed a deep eutectic electrolyte of 3.5 M $Mg(ClO_4)_2$ and 1 M $Zn(ClO_4)_2$, in which the formation of hydrogen bonds between ClO_4^- and H_2O molecules, combined with the strong electrostatic attraction between Mg^{2+} and the O atom of H_2O, significantly reduced the amount of hydrogen-bonding between H_2O molecules, resulting in an ultralow freezing point of −121 °C. Due to the high ionic conductivity and low viscosity of the electrolyte at low temperature, organic batteries of PTO-Zn and phenazine-Zn exhibited excellent cycling stability at the temperature approaching to −70 °C.

3.3. Inorganic Solid Electrolytes

In addition to optimizing the solvent and increasing the salt concentration in the liquid electrolyte, developing solid-state

https://doi.org/10.1021/acs.chemrev.2c00374
Chem. Rev. 2023, 123, 1712−1773

Table 3. Summary of Reported Inorganic and Polymer-Based Electrolytes for Organic Batteries

Electrolyte	Ionic conductivity (S cm^{-1})	Electrochemical stable window (V)	Battery system	Cycling stability: capacity retention [%], cycles, current	Rate performance	Ref
c-Na_3PS_4	3.9×10^{-4}	-	$Na_4C_6O_6$-$Na_{15}Sn_4$	76%, 100, 0.1C (60 °C)	0.1C→0.5C, 57%	325
Li_3PS_4	-	-	PBALS-Li	69%, 120, 0.1C	0.05C→0.4C, 63%	326
Li_3PS_4	-	-	PTO-Li	61%, 1000, 0.3C (60 °C)	0.1C→1C, 35%	327
c-Na_3PS_4	3.9×10^{-4}	-	PTO-$Na_{15}Sn_4$	89%, 500, 0.3C	0.1C→1C, 62%	74
$Li_7P_3S_{11}$	1.38×10^{-3} (60 °C)	-	PT-Li	82%, 370, 1C (60 °C)	0.1C→2C, 67% (60 °C)	75
$Li_7P_3S_{11}$	-	-	PTTCA-Li	83%, 100, 0.1C	0.1C→1.1C, 33%	329
β-Al_2O_3	3×10^{-3} (60 °C)	3.5	PTO-Na	80%, 50, 0.1C (60 °C)	0.1C→0.5C, 50%	330
LiPON	-	-	BQ-Li_2TP	74%, 100, 0.5C	-	335
PEO+LiTFSI	0.1 (100 °C)	-	TMQ-Li	77%, 40, 1C (100 °C)	0.03C→4.5C, 43%	338
SN+x-PS@PSTFSI-Li^+	2×10^{-4}	5.5	P4VC-Li	77%, 500, 2C	0.2C→2C, 52%	346
PPC-KFSI+BC	1.36×10^{-5} (20 °C)	4.15	PTCDA-K	84%, 40, 0.14C	0.07C→0.7C, 67%	351
PMA/PEG+0.7 M $LiClO_4$-DMSO	5.7×10^{-4}	-	C4Q-Li	85%, 100, 0.2C	0.2C→1C, 52%	352
PVDF-HFP+1 M $LiPF_6$-EC/DMC	7.3×10^{-3}	-	PTMA-Li	91%, 100, 1C	1C→50C, 88%	353
PVDF-HFP+1 M $NaClO_4$-EC/PC/5%FEC	5×10^{-4}	4.8	PNTCDA-Na	80%, 1000, 0.2C	0.2C→20C, 44%	354
PI+1.5 M $NaClO_4$-EC/DEC	2.1×10^{-3}	> 4	hard carbon-PTVE	95%, 100, 0.5C	0.5C→10C, 53%	355
Poly(DOL)+1 M LiTFSI-DOL/DME	1.04×10^{-4}	-	TAQB-Li	50%, 10000, 10C	0.5C→100C, 88%	356
PMMA+0.8 M KPF_6-EC/DEC/FEC	4.3×10^{-3}	4.9	AIBN-K	98%, 100, 0.4C	0.1C→1.5C, 70%	359
PMA/PEG+3wt % SiO_2+$LiClO_4$	2.6×10^{-4}	-	P5Q-Li	94.7%, 50, 0.5C	0.3C→1C, 55%	361
PEO/PEG+10wt % γ$LiAlO_2$+$LiClO_4$	8.21×10^{-4} (65 °C)	-	AQ-Li	54%, 100, 0.1C (65 °C)	0.1C→1C, 47%	362
PEO-$LiClO_4$-10 wt% LLTO	7.99×10^{-4} (70 °C)	5	PCTB-Li	90%, 300, 0.3C (70 °C)	0.13C→2.6C, 44%	363
PEO+LiTFSI//SiO_2+BMPTFSI	-	-	TCNQ-Li	79%, 100, 0.2C	0.2C→2C, 93%	364
PEO+LiTFSI //SiO_2+EMITFSI	-	-	DHBQ-Li	86%, 10, 0.2C	0.2C→1C, 55%	365
PEO+LiTFSI //SiO_2+EMITFSI	-	-	3Q-Li	80%, 30, 0.2C	0.05C→0.2C, 60%	366
MOF@PAN/PEO/IL	2.57×10^{-4}	4.6	IDAQ-Li	95%, 150, 0.24C	-	371
methacrylate-based polymer+BMITFSI+SiO_2	7.4×10^{-1}	-	PTMA-poly(TCAQ)	77%, 1000, 1C	1C→5C, 78%	372
polyDADMATFSI iongel+Al_2O_3 NPs	1.1×10^{-2} (50 °C)	4	PEDOT-Zn	89%, 13, 50 mA g^{-1} (50 °C)	25 mA g^{-1} → 50 mA g^{-1}, 68%	373
PolyDADMATFSI+Py_{14}TFSI+LiTFSI	2.1×10^{-4}	4.5	DB-DB	62%, 50, 0.5C	0.2C→5C, 33%	374

organic batteries is considered as another effective strategy to improve the performance of organic electrode materials. Besides their inherent high safety, excellent thermal, and mechanical stability, inorganic solid-state electrolytes are expected to completely circumvent the challenge of the organic electrode dissolution, resulting in improved cycling stability. Solid-state electrolytes offer beneficial solutions to certain battery operation problems but they also introduce their own unique operation challenges. Although it is generally believed that the inorganic solid-state electrolyte can inhibit dendrite growth, recent reports have found that the formation of dendrites is still observed in some solid-state batteries, which may be attributed to the high electronic conductivity of the solid-state electrolytes,[83] and/or the high local ionic resistivity of the grain boundary.[314,315] Furthermore, the poor interfacial contact between the electrolyte and the electrode, ubiquitous in solid-state batteries, cannot be ignored. To obtain high-performance solid-state batteries, the chemical and mechanical compatibility between the solid-state electrolyte and the electrode materials must be optimized. Currently, there are relatively few studies on combining organic

https://doi.org/10.1021/acs.chemrev.2c00374
Chem. Rev. 2023, 123, 1712−1773

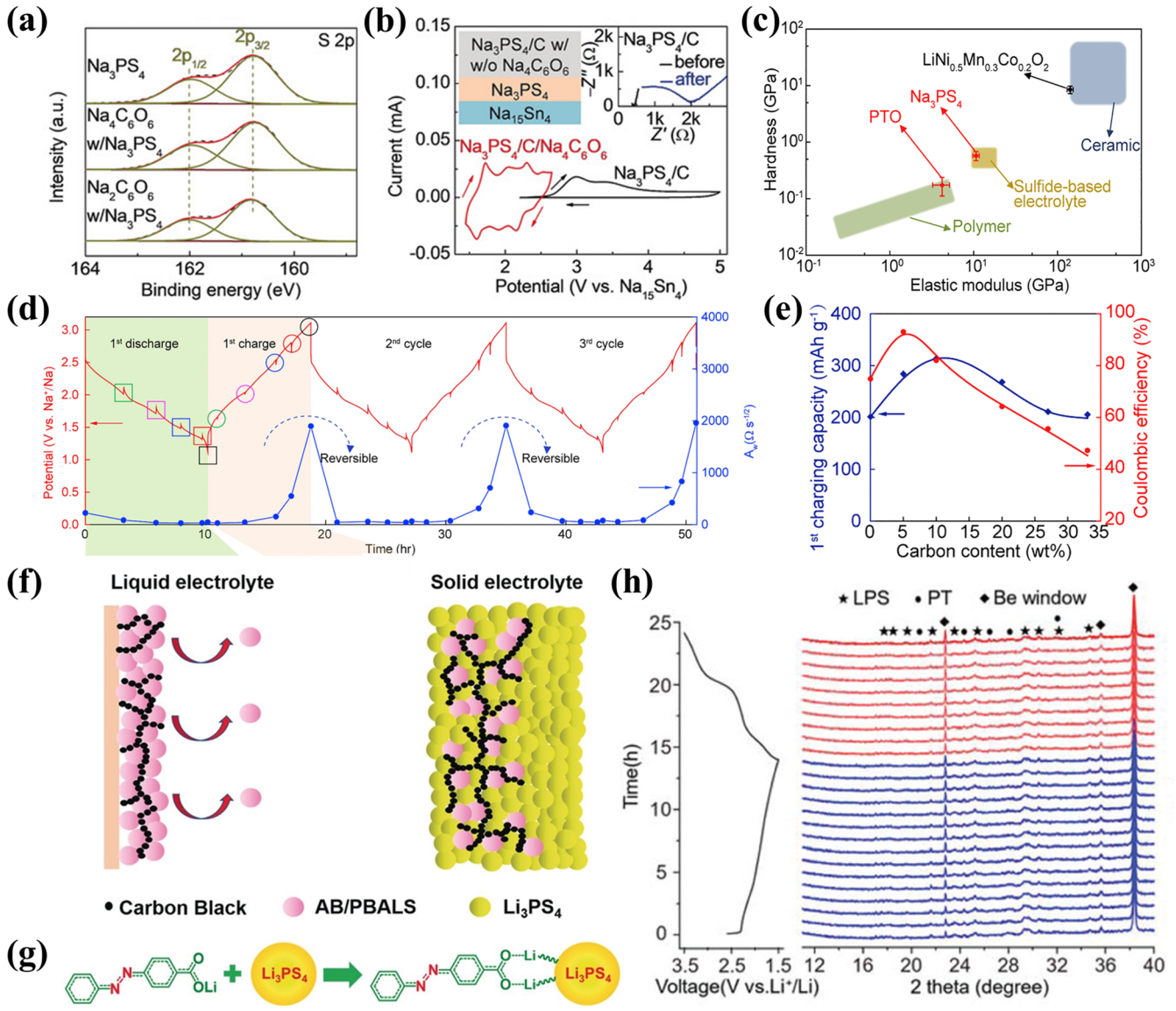

Figure 22. Interfacial compatibility analysis between sulfide solid electrolytes and organic electrodes. (a) S 2p spectra of pristine Na_3PS_4 and the mixtures with electrodes. (b) Operating window of $Na_4C_6O_6$ cathode and electrochemical stability window of Na_3PS_4 electrolyte via CV test at a scan rate of 0.05 mV s^{-1}. Left inset: structural diagram of the full cell for CV test; Right inset: EIS spectra of the cell before and after the CV test. Reproduced with permission from ref 325. Copyright 2018 Wiley-VCH. (c) Comparison of hardness and elastic modulus of some electrode and electrolyte materials. (d) Distribution of the Warburg coefficient (A_w) of PTO-based battery with Na_3PS_4 electrolyte under different voltages in the first three cycles. (e) Plot of the charging capacity and Coulombic efficiency in the first cycle as the function of carbon content. Reproduced with permission from ref 74. Copyright 2019 Elsevier. (f) Schematic presentation of AB/PBALS dissolution in the liquid electrolyte and Li_3PS_4 solid electrolyte. (g) Diagrammatic sketch of the interaction between PBALS electrode and Li_3PS_4 electrolyte. Reproduced with permission from ref 326. Copyright 2018 Wiley-VCH. (h) *In situ* XRD patterns of all-solid-state Li-PT cell during the first discharge/charge cycle. Reproduced with permission from ref 75. Copyright 2022 Wiley-VCH.

electrodes with inorganic solid-state electrolytes. The results are limited to mainly sulfide electrolytes, LiPON and β-Al_2O_3, which are all summarized in Table 3.

3.3.1. Sulfide-Based Electrolytes. Compared with the commercial organic liquid electrolytes, the relatively high ionic conductivity of solid-state sulfide electrolytes makes them attractive for practical applications in batteries.[316,317] Additionally, sulfide electrolytes could form excellent contact with electrodes through a simple cold pressing process, showing low boundary resistance and excellent ductility.[318,319] However, research has shown that sulfide electrolytes are not stable with alkali metal anodes (Li, Na, etc.) and high-voltage cathodes. Due to the narrow electrochemical stability windows of sulfide electrolytes and high Young's modulus of transitional metal oxide cathodes, the continuous accumulation of poor ion conductivity interfacial decomposition products and the formation of cracks between cathode materials and electrolyte would result in low Coulombic efficiency and ultimately, mechanical failure.[88,320,99] In 2018, Asano et al.[95] reported a new lithium halide solid-electrolyte material, Li_3YBr_6. It exhibits a high ionic conductivity (>1.0 × 10^{-3} S cm^{-1}) and good compatibility with the high-voltage metal oxide cathode. Since then, halide solid-state electrolytes have been regarded as promising electrolytes for high-voltage all-solid-state batteries

https://doi.org/10.1021/acs.chemrev.2c00374
Chem. Rev. 2023, 123, 1712−1773

due to their intrinsically high oxidative stability.[321,322] It is worth noting that most sulfide and halide electrolytes are reactive with alkali metals, thus increasing the interfacial resistance, hindering uniform deposition of alkali metals, and leading to deterioration of the battery performance.[323,324]

To avoid the side reaction between the Na metal and the Na_3PS_4 sulfide electrolyte, Yao et al.[74,325] replaced the Na metal anode with a $Na_{15}Sn_4$ alloy and developed a series of organic cathodes that were compatible with the Na_3PS_4 solid-state electrolyte. First, they converted the commercially available $Na_2C_6O_6$ to an ambipolar organic electrode material of tetrahydroxybenzoquinone ($Na_4C_6O_6$) and investigated its compatibility with the Na_3PS_4 electrolyte using XPS (Figure 22a) and CV (Figure 22b) measurements.[325] The results indicated that $Na_4C_6O_6$ was chemically and electrochemically compatible with the electrolyte because of: 1) the unchanged peaks corresponding to sulfur 2p electrons in Na_3PS_4 after mixing with the cathode and 2) the lower operating voltage window of the battery. The results showed that the solid-state full cell with the $Na_4C_6O_6$ cathode and the $Na_{15}Sn_4$ anode maintained about 70% initial capacity after 400 cycles at 0.2 C. Researchers attributed the modest capacity fading to the formation of microcracks in the cathode during cycling. However, the rate performance of the battery was unsatisfactory. In addition, considering the low average voltage of the $Na_4C_6O_6$ electrode material (2.15 V vs Na^+/Na), they proposed a new organic cathode material of PTO to further improve the energy density of the battery.[74] As shown in Figure 22c, the Young's modulus of PTO (4.2 ± 0.2 GPa) is about 2 orders of magnitude lower than that of traditional inorganic oxide cathodes (100−200 GPa), which could relieve the interfacial stress of the battery and help maintain consistently intimate contact between the sulfide solid-state electrolyte and PTO. More importantly, although the charge cutoff voltage of PTO slightly exceeded the oxidative decomposition potential of Na_3PS_4 electrolyte, it was found that the interfacial resistance layer between PTO and Na_3PO_4 was reversible during the battery cycles (Figure 22d). The decomposition of the electrolyte did not cause a net increase in the interfacial resistance, thus ensuring stable cycling of the battery. The excellent chemical, mechanical and electrochemical compatibilities between organic cathode materials and sulfide electrolytes enables the PTO-based battery to exhibit a high specific energy (587 Wh kg^{-1}) and record cycling stability (89% retention after 500 cycles).[74] It is worth noting that the content of conductive carbon has a significant impact on the first-cycle specific capacity and Coulombic efficiency of PTO (Figure 22e). When the carbon content was less than 5 wt %, the charge transfer resistance is large due to the electronically insulating nature of PTO. The insufficient electron transfer increases the charging overpotential, leading to a premature end of charging and a low Coulombic efficiency in the first cycle. This indicates that the addition of carbon into the composite electrode is essential for providing adequate electron transport. However, too much conductive carbon would accelerate the oxidation of electrolyte at the interface. When the carbon content was increased to 10 wt % and even 20 wt %, significant accumulation of resistive products caused by the oxidation of Na_3PS_4 leads to the continuous decrease in Coulombic efficiency and large capacity loss. In addition, unlike the batteries using liquid electrolytes, solid-state organic batteries suffer from low specific energy due to the high content of conductive carbon and low content of active materials in order to reduce the high electrode−electrolyte interfacial resistance.

Similarly, the Li_3PS_4 solid-state electrolyte has been reported in Li-organic batteries.[326,327] As shown in Figure 22f, the application of Li_3PS_4 eliminated the dissolution problem and shuttle effect of 4-(phenylazo) benzoic acid lithium salt (PBALS) in the liquid electrolyte.[326] Compared to the azobenzene without the carboxylate group (AB), the electrochemical performance of PBALS was much better due to the strong ionic bonding between PBALS and the Li_3PS_4 electrolyte as shown in Figure 22g. The more significant interaction between PBALS and Li_3PS_4 was confirmed by Raman spectra, Fourier-transform infrared spectroscopy (FTIR) spectra, and DFT calculations. The ionic bond supported intimate contact between active materials and the solid-state electrolyte, thus enabling Li_3PS_4 to accommodate the large volume change of PBALS during the cycling process and maintain low interfacial resistance. Excepting for the low initial Coulombic efficiency, caused by the decomposition of the Li_3PS_4 electrolyte, in the first few cycles, the Coulombic efficiency remained at 100% during long-term cycling, indicating mutually beneficial compatibility between PBALS and the Li_3PS_4 electrolyte.

One investigated strategy for increasing the compatibility between active materials and electrolytes is to change the physical structure of the active materials via ensuring smaller uniform "particle" size and distribution. Considering that traditional hand-milling and ball-milling methods cannot effectively reduce the size of the active material, the cryomilling technique is beneficial to decreasing the size of the active materials and suppress side reactions between Li_3PS_4 and the PTO electrode simultaneously, thus improving the electrochemical performance of the battery.[327] Recently, the chemical and electrochemical compatibilities between PT electrodes and $Li_7P_3S_{11}$ electrolytes were investigated, in depth, by spectroscopic and electrochemical characterizations.[75] According to *in situ* XRD results, no new peak or halos developed during the first cycle, indicating a lack of detectable decomposition products (Figure 22h). With continued cycling, the peak intensity associated with the electrolyte $Li_7P_3S_{11}$ was observed to decrease. Researchers speculated the amorphization of the electrolyte could be responsible and as a result the ion-conductive glass in the electrolyte also increases. Benefiting from the limited decomposition of $Li_7P_3S_{11}$, the reversible interlayer resistance and the mechanically soft characteristics of PT, all-solid-state battery with the PT-$Li_7P_3S_{11}$-Super P composite electrode exhibited a high specific capacity and an excellent cyclic stability.

Another strategy for increasing compatibility between active materials and solid electrolytes is to consider the reactivity, based on electronic structure, between the materials that occurs during cycling. Based on the soft and hard acid/base theory,[328] the hard base O, present in discharged carbonyl groups (C−O^-), readily reacts with the hard acid P, of the sulfide electrolyte, hindering the redox reaction of carbonyl-type active materials. Therefore, Yang et al.[329] designed a new organodisulfide cathode material with soft electroactive groups, which showed much better interfacial compatibility with the $Li_7P_3S_{11}$ electrolyte than carbonyl-type electrodes.

3.3.2. β-Al_2O_3 and LIPON Electrolytes. The interface between the inorganic solid electrolyte and the anode in organic batteries is also worthy of attention. Yao and co-workers[330] used the oxide-based solid electrolyte, β-Al_2O_3, in a PTO-Na battery and achieved an all-solid-state organic battery with high specific

https://doi.org/10.1021/acs.chemrev.2c00374
Chem. Rev. 2023, 123, 1712−1773

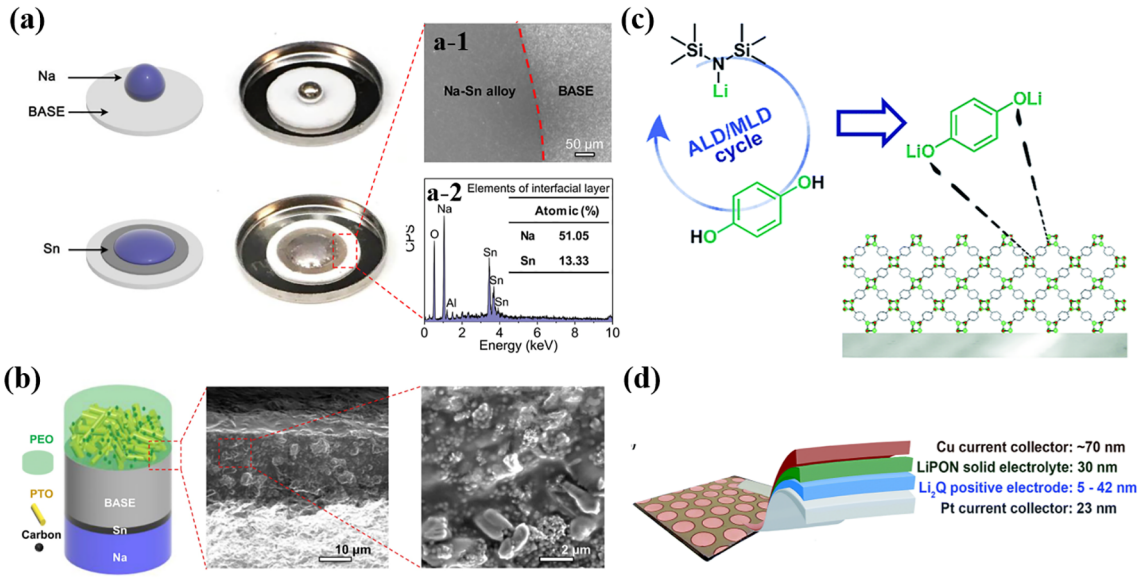

Figure 23. Measures to improve the interfacial contact between the inorganic solid electrolyte and two electrodes. (a) The wetting behavior of the molten Na with BASE with or without Sn coating. Inset: SEM image (a-1) and corresponding energy dispersive spectroscopy (EDS) analysis (a-2) at the interface. (b) Schematic diagram of PTO/BASE/Na battery with improved interface and SEM images of the cathode and the cathode/electrolyte interface. Reproduced with permission from ref 330. Copyright 2019 Elsevier. (c) The preparation of dilithium-1,4-benzenediolate thin film cathode by ALD/MLD technique. (d) Structure diagram of the thin-film battery. Reproduced with permission from ref 335. Copyright 2018 Royal Society of Chemistry.

energy (~900 Wh kg^{-1}). As shown in Figure 23a, the Sn film between the Na anode and the β-Al_2O_3 solid electrolyte successfully supported the reduction of the interfacial resistance. The formation of a $Na_{15}Sn_4$ alloy interlayer changed the wettability behavior of molten Na metal on β-Al_2O_3 from sodiophobic to sodiophilic contact, which was beneficial to aid in the plating/stripping process of Na. Furthermore, as an ion conductive polymer auxiliary agent, poly(ethylene oxide) (PEO) was added in the cathode material to form interpenetrating ionic and electronic channels, resulting in the maximal utilization of the PTO electrode (Figure 23b). The well-designed electrolyte/electrode interfaces, with low interfacial resistance, provided a good reference for the successful application of inorganic solid electrolytes in organic batteries.

Low current devices such as sensors, microelectronics, and micromechanical systems are considered to be target applications for thin-film batteries owing to the batteries' small size, low self-discharge rate, and high gravimetric energy density.[331,332] Furthermore, improvements in atomic/molecular layer deposition (ALD/MLD) technology has instigated accelerated preparation of all-solid-state thin-film batteries, mainly as a result of the unique advantages for interfacial modification.[333,334] Nisula et al.[335] used the ALD/MLD technology to achieve *in situ* deposition of a quinone cathode in its lithiated state, without any postdeposition lithiation treatments (Figure 23c). As shown in Figure 23d, the solid-state electrolyte LiPON and the organic cathode were integrated, by directly depositing LiPON, with a thickness of about 30 nm, onto the thin-film cathode. As a result of the deposition strategy, interfacial contact between the electrolyte and the cathode was significantly increased. When matched with an ALD/MLD-grown lithium terephthalate (Li_2TP) anode, the thin-film battery maintained 74% of the initial capacity after 100 cycles, which was much higher than that of the *in situ* plated Li and thermally evaporated Ge. The improved cyclic performance could be attributed to the relatively high compatibility between the Li_2TP anode and the LiPON electrolyte, and the high stability of the current collector. In addition, ultrathin batteries prepared via the ALD/MLD technology, with high redox reaction rates, are expected to unify the goals of achieving high energy density and high power density.

3.4. Polymer-Based Electrolytes

Polymer electrolytes have attracted widespread attention due to their flexibility, lightweight, facile fabrication into different shapes, and good interfacial contact with electrodes.[336] The ideal polymer electrolyte should simultaneously exhibit comparable ionic conductivity with liquid electrolytes, high ion transference number, low interfacial resistance, excellent thermal and electrochemical stability, a wide electrochemical window, and sufficient mechanical strength. In addition, the solid-state or quasi-solid-state polymer electrolytes are expected to satisfy special requirements for organic batteries such as suppressing the dissolution and shuttle effect of organic active materials.

Polymer-based electrolytes are mainly composed of organic polymer matrices and dissolved salts. In addition, they may also contain some liquid solvents (such as PC, EC, DOL, DME, DMSO, etc.) and inorganic fillers (such as inert fillers like SiO_2, Al_2O_3, etc. and active fillers like $Li_7La_3Zr_2O_{12}$ (LLZO), $Li_{0.33}La_{0.557}TiO_3$ (LLTO), etc.). Furthermore, IL-based ionogel electrolytes and poly(ionic liquid) (PIL) electrolytes also exhibit excellent properties and have attracted considerable research interests. The composition of polymer electrolytes, as well as the cyclic and rate performance of corresponding organic batteries are summarized in Table 3.

Depending on whether organic solvents are added, polymer electrolytes can be divided into the solvent-free solid polymer electrolyte (SPE) and the gel polymer electrolyte (GPE). Although SPEs can completely mitigate the dissolution of organic active materials, most reported SPEs exhibited low ionic

https://doi.org/10.1021/acs.chemrev.2c00374
Chem. Rev. 2023, 123, 1712−1773

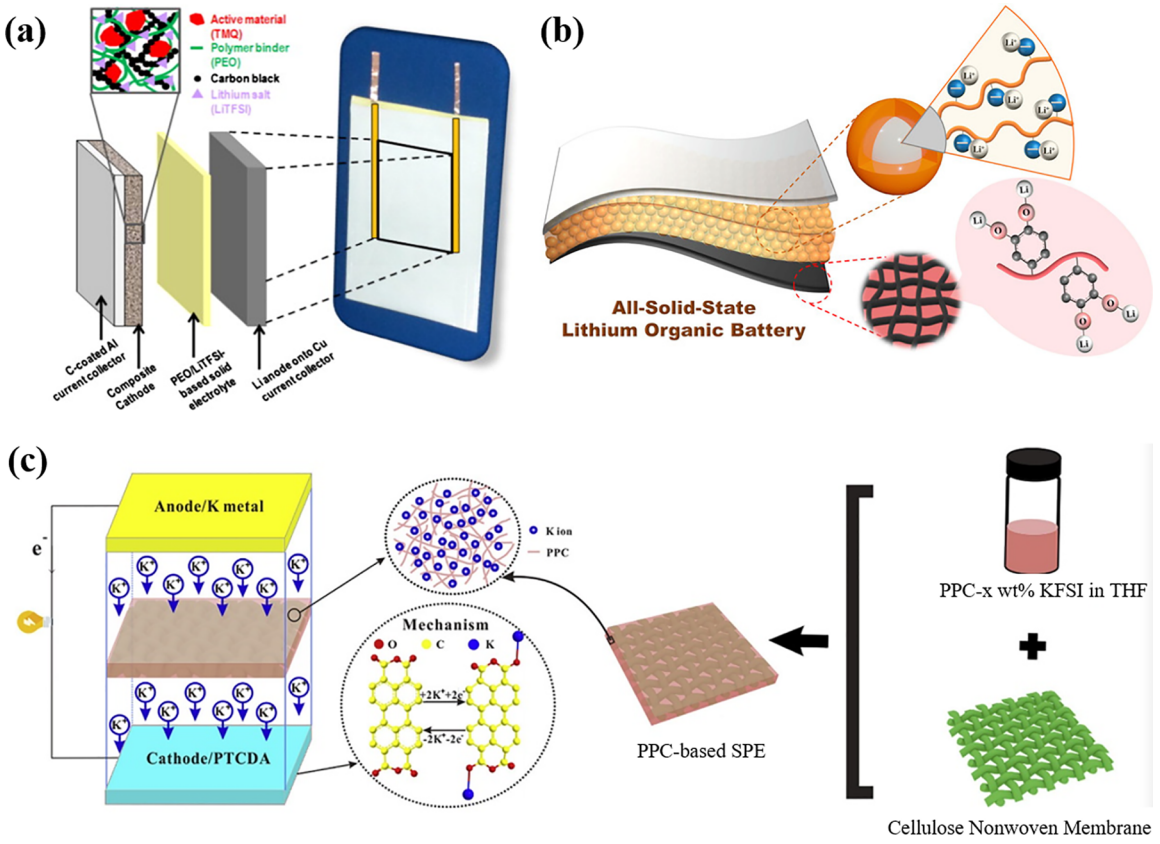

Figure 24. (a) Schematic representation of the TMQ-Li cell using solid polymer electrolyte. Reproduced with permission from ref 338. Copyright 2015 Elsevier. (b) Schematic diagram of the solid-state P4VC-Li battery with a single-ion polymer-SN electrolyte. Reproduced with permission from ref 346. Copyright 2020 Wiley-VCH. (c) Schematic diagrams of K-PTCDA battery composition and the preparation of the composite electrolyte. Reproduced with permission from ref 351. Copyright 2018 Elsevier.

conductivity (10^{-8}–10^{-5} S cm^{-1}) at room temperature and poor interfacial contact with the electrodes. Recently, SPEs based on covalent organic frameworks (COFs) have garnered attention due to their unique ion-diffusion mechanism compared to traditional linear polymer electrolytes. The COF-based SPEs are expected to achieve rapid ion transport at extremely low temperatures.[337] In addition to SPEs, GPEs have also attracted substantial research interest, because GPEs integrate the advantages of organic liquid electrolytes and solid-state electrolytes. Replacing traditional liquid electrolytes with GPEs is expected to improve the electrochemical performance of organic batteries and reduce the risk of liquid components leakage. However, the high organic solvent content in GPEs may result in undesirable dissolution of organic active materials. To overcome this challenge, the development of quasi (or all)-solid-state organic–inorganic composite electrolytes and PIL electrolytes has become the primary research direction.

3.4.1. Solid Polymer Electrolytes. SPEs usually consists of a polymer like PEO, poly(vinylidene difluoride-cohexafluoropropylene (PVDF-HFP) or polyacrylonitrile (PAN) as a matrix and some salts without the addition of organic solvents. Although SPEs have advantages of lightweight, good mechanical flexibility and high safety, the drawbacks of poor ionic conductivity at room temperature and poor interfacial compatibility with the electrode cannot be ignored. To address these challenges, the battery needs to be operated at elevated temperatures, which further complicates the practical application requirements and brings safety hazards.

For instance, Lécuyer et al.[338] used a commercial PEO-based SPE in Li metal batteries with tetramethoxy-*p*-benzoquinone (TMQ) as the cathode and tested the cyclic performance of the battery at 100 °C (Figure 24a). Compared with carbonate-based electrolytes, the all-solid-state PEO-LiTFSI electrolyte doubled the capacity of TMQ and significantly improved the capacity retention and rate performance of the battery. However, the diffusion of the organic active material was not completely inhibited, and a significant capacity loss was still observed with different cycling rates at 100 °C. Since the operating temperature of the battery is much higher than the melting point of the PEO-based electrolyte (about 60 °C), the active material will inevitably diffuse into the melted electrolyte, causing capacity fading. In addition, long-term cycling of the battery at elevated temperatures approaching to 100 °C will result in the genesis of new challenges, such as accelerated battery aging and diminishing mechanical properties. Therefore, the development of SPEs with high ionic conductivity at room temperature has become a future research direction.

To obtain solid-state electrolytes with exceptional performance at room temperature, SN, a typical molecular plastic crystal that possess positional order but orientational disorder in the temperature range from −35 to +62 °C, has been used as a solid plasticizer.[339,340] Compared with the traditional rigid crystals, SN displays higher diffusivity and plasticity, and its high polarity enables the dissolution of various salts, which is beneficial to obtaining high ionic conductivities.[341−344] However, the mechanical strength of SN is poor, making it difficult to form

https://doi.org/10.1021/acs.chemrev.2c00374
Chem. Rev. 2023, 123, 1712−1773

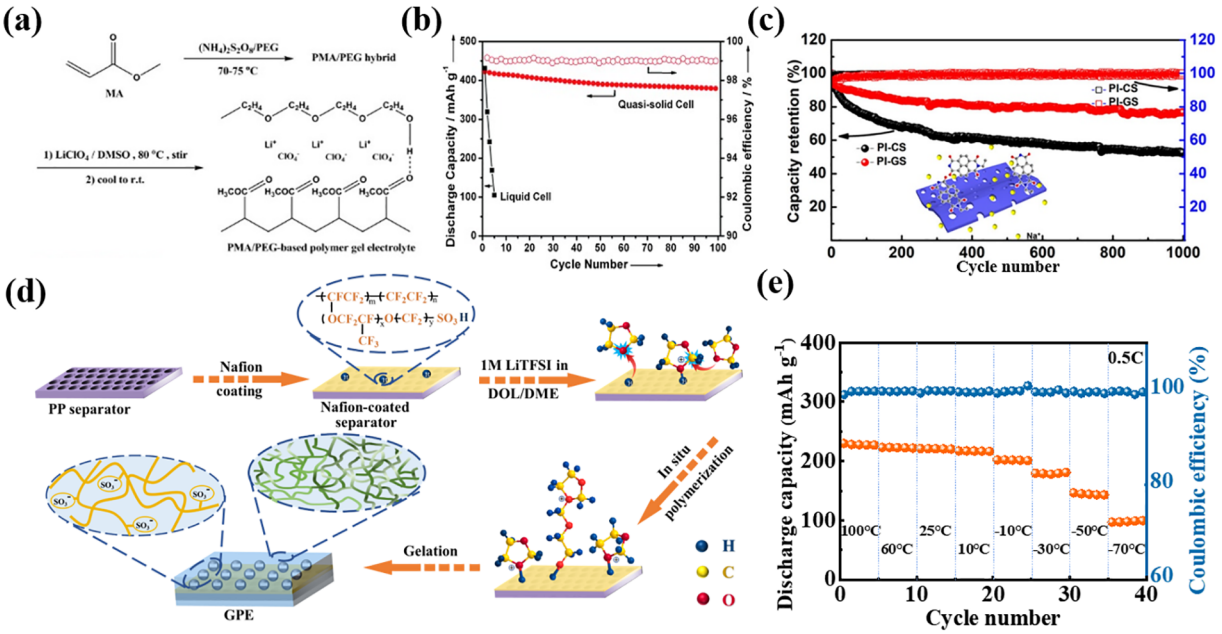

Figure 25. Organic batteries with GPEs. (a) Preparation process of the PMA/PEG-based GPE. (b) Cycle performance of the C4Q-Li batteries with the liquid electrolyte and PMA/PEG based GPE. Reproduced with permission from ref 352. Copyright 2013 Wiley-VCH. (c) Cycle performance of the PI-Na batteries with the liquid electrolyte (PI-CS) and PVDF-HFP based GPE (PI-GS). Inset: Schematic diagram of PVDF-HFP membrane blocking the shuttle effect of the dissolved organic materials. Reproduced from ref 354. Copyright 2015 American Chemical Society. (d) Schematic diagram of the preparation of Nafion-coated separator and *in situ* polymerization of DOL. (e) Specific capacity and Coulombic efficiency of the TAQB-Li battery using the *in situ* formed GPE at a wide range of operating temperatures. Reproduced with permission from ref 356. Copyright 2022 Wiley-VCH.

films by itself. To date, blending SN with a polymer matrix[339,345] has been the method to improve the mechanical properties of the SN-based electrolytes. A solid-state Li-organic battery was reported containing a bioinspired poly(4-vinylcatechol) (P4VC) cathode and a single ion conducting polymer nanoparticle electrolyte, in which SN was added to offer high Li^+ conductivity and thermal stability (Figure 24b). The hybridization of single-ion conducting polymer nanoparticles with SN resulted in a wide electrochemical window of up to 5.5 V, a high Li-ion transference number close to 1, and good mechanical performance over a wide temperature range between 25 and 90 °C.[346] In addition, the electrostatic repulsion between the redox intermediates and the nanoparticles could also mitigate the dissolution and diffusion of active materials. Compared with the P4VC-Li battery using a pure SN-based electrolyte, the battery with the hybrid electrolyte demonstrated better cyclic stability and rate performance.

SPEs with a single-component matrix usually exhibit low oxidation stability, limited thermal stability, a low ionic transference number, and unsatisfactory electrical conductivity. Methods to modify the polymer matrices have been reported recently, including copolymerization, cross-linking and interpenetration, and blending different polymers to combine their advantages.[336,347] To further improve the performance of SPEs, composite electrolytes with excellent comprehensive performance were reported by directly combining liner polymers with 3D polymer substrates such as electrospun PVDF,[348] nanoporous PI,[349] and various cellulose membranes.[350] A poly(propylene carbonate) (PPC)-based solid-state composite electrolyte with a cellulose nonwoven framework was used in K-organic batteries (Figure 24c).[351] The addition of cellulose membrane in SPEs not only increased the mechanical strength of the electrolyte, but also formed 3D continuous and uniform ion transport pathways. Due to the negligible solubility of PTCDA in the SPEs, the battery with the PTCDA cathode maintained a high capacity of 91.17 mAh g^{-1} after 40 cycles with a slow capacity decay rate of about 0.4% per cycle. Furthermore, the proposed SPE exhibited good compatibility with the organic cathode, which was verified by the high-rate performance of the organic battery.

Recently, a new hydrazone COF with single ion conduction and excellent thermal stability was used in solid-state organic batteries.[337] In contrast to the chain movement-based ion transport mechanism in linear polymer electrolytes, the high porosity and large surface area of COFs provided abundant free volume even at a low temperature, enabling a high ionic conductivity of 10^{-5} S cm^{-1} at −40 °C. The resulting all-solid-state Li-organic battery with 1,4-benzoquione (BQ) cathode could be cycled for 500 cycles with a high capacity retention of 87.7%, indicating that COF-based solid-state electrolytes can effectively inhibit the dissolution of small organic molecules. Therefore, developing high conductivity, high stability, and high compatibility SPEs is a promising approach to addressing the solubility challenge of organic batteries.

3.4.2. Gel Polymer Electrolytes. As an intermediate state between liquid electrolytes and SPEs, GPEs were proposed to solve the challenges of low ambient-temperature ionic conductivity and large electrolyte/electrode interfacial resistance of SPEs as well as the dissolution issue of organic electrode materials in liquid electrolytes. Many studies have been conducted by using GPEs in organic batteries, and promising performance was obtained.

Huang et al.[352] reported a quasi-solid-state organic battery using poly(methacrylate) (PMA)/PEG-based GPE with a solvent of DMSO and a lithium salt of $LiClO_4$ (Figure 25a). When the concentration of $LiClO_4$ in DMSO reached 0.7 M, the

https://doi.org/10.1021/acs.chemrev.2c00374
Chem. Rev. 2023, 123, 1712−1773

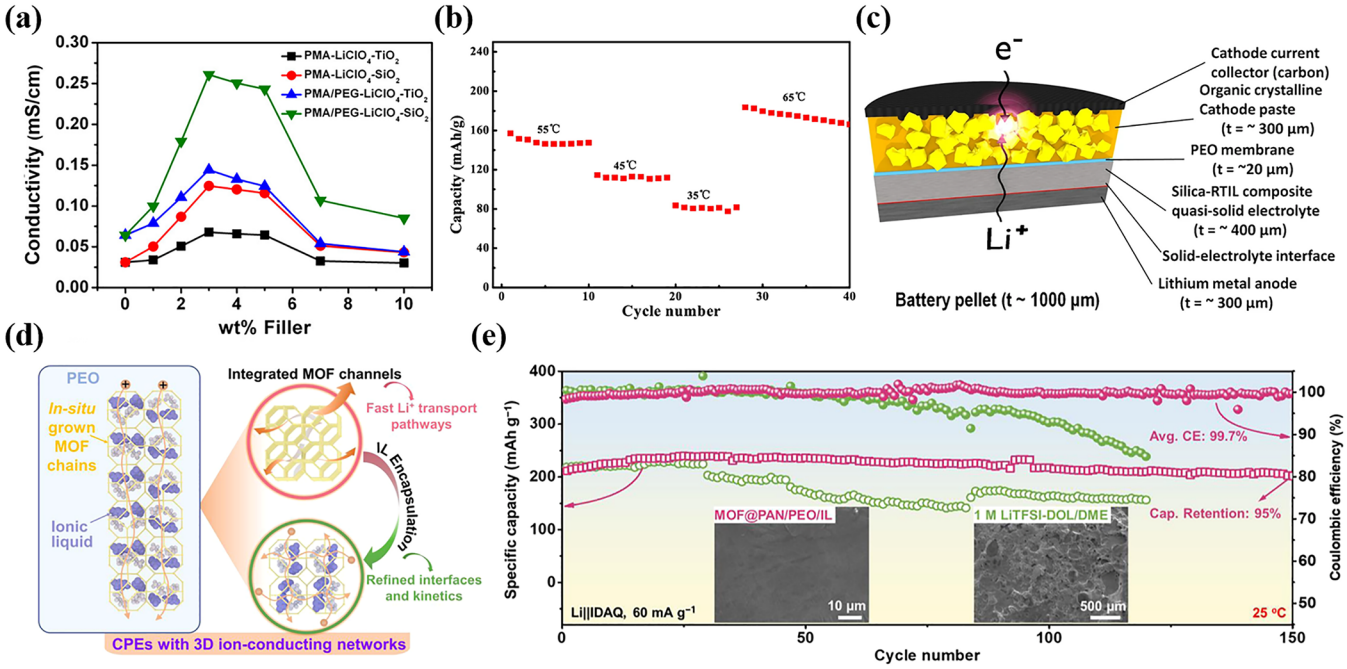

Figure 26. Organic batteries with polymer-inorganic composite electrolytes. (a) Effect of the amount and type of inorganic fillers on ionic conductivity of the electrolytes. Reproduced from ref 361. Copyright 2014 American Chemical Society. (b) Influence of the operating temperature on cycle stability of Li-AQ battery with solid composite electrolyte. Reproduced with permission from ref 362. Copyright 2016 Elsevier. (c) Structure and composition of the quasi-solid Li-organic battery with a multilayer composite electrolyte. Reproduced with permission from ref 364. Copyright 2012 Springer Nature. (d) Schematic illustration of the Li^+ transport in MOF@PAN/PEO/IL composite electrolyte. (e) Cycling performance of the Li-IDAQ batteries using commercial liquid electrolyte and MOF@PAN/PEO/IL composite electrolyte. Inset: SEM images of the surface of Li anodes recovered from the cycled batteries. Reproduced with permission from ref 371. Copyright 2022 Elsevier.

highest ionic conductivity of 5.7×10^{-4} S cm^{-1} was obtained. As shown in Figure 25b, the quasi-solid cell with a C4Q cathode delivered a high initial discharge capacity (422 mAh g^{-1}) and excellent cycling stability (89.8% capacity retention after 100 cycles), which are much better than those with traditional liquid electrolytes. The improved cycling stability was also observed in the 2,2′-bi(1,4-naphthoquinone)-Li battery with this GPE. These results show a great potential for GPEs in solving the dissolution issue of organic batteries. Similarly, PVDF-HFP based GPEs with interconnected pores and high specific surface area were also reported to improve the cycling stability and rate performance of PTMA and PI electrodes.[353,354] The unique porous structure of the PVDF-HFP membrane endows it with a high liquid absorption capability, which provides sufficient electrolyte for the electrochemical reaction. In contrast to the rapid capacity degradation of PI electrode using liquid electrolytes, the cycling stability of the electrode with PVDF-HFP-based GPE was significantly enhanced, indicating that the GPE blocked the diffusion of dissolved active materials (Figure 25c).[354] Besides being used as the electrode material, PI could also be applied in the preparation of GPEs. Using an electrospinning technique, PI membranes with a porous 3D network structure can be obtained, which show a high liquid absorption capability and a good mechanical property when used as the matrix of GPEs.[355] Organic batteries using the PI-based GPE and the CNTs-modified organic electrode realized excellent cycling stability and high rate performance. Recently, Li et al.[356] designed a multifunctional GPE with molecular sieving and charge repulsion, which was fabricated via Nafion-initiated *in situ* ring opening polymerization of the DOL solvent in electrolytes (Figure 25d). The *in situ* polymerization process provides an efficient method to fabricate batteries with GPEs, that can be seamlessly adopted in the current assembly route of commercial LIBs.[357,358] The obtained GPE provides intimate contact with electrodes, and prevents the shuttle of the dissolved organic molecules and redox intermediates while retaining fast reaction kinetics. In addition, by changing the content of DOL and introducing additional polymers like PEO, the shielding capability of the GPE can be tailored to sieve different sized small-molecule electrode materials. With such gel electrolytes, the small-molecule organic electrodes of 1,3,5-tri(9,10-anthraquinonyl)benzene (TAQB) and PTCDA demonstrate exceptional electrochemical performance with long cycle life, excellent rate capability and a wide working temperature range from −70 to +100 °C (Figure 25e).

In addition, GPEs can effectively suppress the dendrite growth and reduce the parasitic reaction between the electrolyte and the alkali metal anode. Using the GPE composed of cross-linked poly(methyl methacrylate), a stable electrode/electrolyte interface was established in AIBN-K batteries.[359] Unlike the cycled K metal anode with obvious dendrite growth in the liquid electrolyte, the surface of the cycled K metal anode in the GPE was covered by nodule-like depositions without dendrite formation, and the battery showed much higher cycling stability and Coulombic efficiency. These results indicate that GPEs play a critical role in preventing dissolution of organic electrode molecules, establishing stable SEI and improving cycling stability of batteries.

3.4.3. Polymer-Inorganic Composite Electrolytes. To further improve the ionic conductivity, mechanical performance, and thermal stability of the polymer-based electrolytes, composite electrolytes are often fabricated by adding inorganic

https://doi.org/10.1021/acs.chemrev.2c00374
Chem. Rev. 2023, 123, 1712−1773

fillers into the polymer matrix. To date, there are two types of inorganic fillers for polymer-inorganic composite electrolytes, including nonconductive passive fillers and conductive active fillers. For nonconductive passive fillers such as TiO_2, SiO_2, and Al_2O_3, the increase of the ionic conductivity is mainly attributed to the reduced crystallinity of the polymer and the accelerated dissociation of the metal salt via interactions between the salt and the surface groups of the ceramic nanoparticles. Ultimately, the free ion concentration is increased. For active fillers like LLZO, LLTO, $Li_{1.3}Al_{0.3}Ti_{1.7}(PO_4)_3$ (LATP), and $Li_{1.4}Al_{0.4}Ge_{1.6}(PO_4)_3$, the ionic conductivity is improved due to the establishment of a highly conductive pathways for Li-ion transport.[360]

Based on the previously designed PMA/PEG electrolyte,[352] Zhu et al.[361] optimized the gel electrolyte by adding SiO_2 fillers and prepared a hybrid solid electrolyte by a hot pressing method. As shown in Figure 26a, the ionic conductivity of the electrolyte with SiO_2 fillers was higher than that with TiO_2 fillers under the same contents of additives, which could be a result of the smaller size, higher aspect ratio, and inherent acidity of SiO_2. The composite electrolyte showed great promise for the application of the Li-P5Q battery, delivering a high initial capacity of 418 mAh g^{-1} at 0.2 C and excellent cyclic stability of 94.7% capacity retention after 50 cycles. Similarly, the capacity loss of the AQ electrode in PEO/PEG-γ-$LiAlO_2$ composite electrolyte was smaller than that in the liquid electrolyte, indicating that the dissolution of AQ was more effectively suppressed.[362] It is worth noting that obvious capacity decay was still observed at 65 °C (Figure 26b), which may be caused by the melting of the polymer and the accelerated dissolution of the active material at high temperatures. In other words, even for all-solid-state composite electrolytes, the operating temperature for organic batteries should not be higher than the melting temperature of the polymers in the electrolytes. Compared with inert ceramic fillers, ion-conductive fillers provide more ion transport channels, thus improving the overall ionic conductivity of the electrolyte. Wei et al.[363] blended PEO with the LLTO powder to prepare a PEO-$LiClO_4$-10 wt % LLTO composite electrolyte and achieved an all-solid-state organic battery with excellent cycling performance.

Although the direct blending process is simple to operate, it is difficult to achieve the uniform dispersion of inorganic fillers in the hybrid solid electrolyte. Once the content of inorganic fillers reaches a critical value, they will exhibit increased agglomeration to hinder effective ion transport in the electrolyte, resulting in the decrease of ionic conductivity. Stacking electrolytes with different properties for a multilayer composite electrolyte can better coordinate the interactions between the electrolyte and electrodes.

Hanyu et al.[364] designed a multilayer composite electrolyte by combining a PEO layer, a quasi-solid-state layer based on SiO_2-IL, and an artificial SEI layer (Figure 26c). The introduction of IL into the electrolyte could improve the ionic conductivity at room temperature.[365] After battery assembly, the PEO layer near the cathode dissolved in the IL and formed a thin matrix with high viscosity, which prevents the dissolution of the organic cathode and improves the interfacial contact. The intermediate layer of the loose quasi-solid electrolyte could provide a high ionic conductivity and separate the anode and cathode materials. The artificial SEI layer was used to stabilize the anode. Thanks to the ingenious structure design, the battery achieved a high capacity retention of 79% after 100 cycles. In addition, the quasi-solid electrolyte also has a good versatility, and can be used to improve the cycling performance of other organic electrodes based on hexaazatrinaphthylene and hexaazatriphenylenehexacarbonitrile.[366] The effects of the operating temperature on cyclic stability was also investigated, and the results showed that a high temperature was beneficial to obtaining a high initial capacity, but resulted in accelerated dissolution of the organic cathode and poor cycling performance.

Another promising method to reduce the aggregation of active fillers is to construct a 3D network skeleton, in which the polymer and salt are directly poured into a 3D ion-conducting framework, and the composite electrolyte is formed by volatilizing the solvent or lowering the temperature. 3D frameworks such as electrospun LLTO,[367] LLZO,[368] LATP@PAN,[369] and metal organic framework (MOF)@PAN[370] nanofiber membranes not only exhibit good mechanical integrity, high thermal stability, and superior flame resistance, but also provide continuous ion transport pathways to promote rapid and uniform metal-cation transport. Recently, Zhang et al.[371] designed a PEO-based composite electrolyte with a 3D ion-conducting MOF-based network. As shown in Figure 26d, the *in situ* growth of MOFs on PAN fibers provides fast and continuous pathways for Li^+ transport, and the IL confined in the pores of MOFs significantly reduces the interfacial resistance between MOFs and PEO, affording fast Li^+ migration kinetics and excellent interfacial compatibility. In addition, the Li-1,1′-iminodianthraquinone (IDAQ) battery with the MOF@PAN/PEO/IL composite electrolyte effectively suppressed the shuttle effect of organic active materials, and the cycling stability was drastically improved (Figure 26e). This study provides a critical research direction for further development of high-performance and sustainable organic batteries. Therefore, polymer-inorganic composite electrolytes are promising alternatives to SPEs for developing high-conductivity and high-mechanical-strength solid-state electrolytes to address the dissolution challenge in organic batteries at room temperature.

3.4.4. Ionogel and Poly(ionic liquid) Electrolytes. Ionogels and PIL electrolytes exhibit unique characteristics of high salt solubility, a wide electrochemical stability window, and high thermal stability, all of which are critical for the broad application prospects in solid-state batteries. Ionogel electrolytes are formed by mixing polar polymers and ILs directly, or via *in situ* polymerization of monomers in ILs. In ionogel electrolytes, the added ILs act as both plasticizers and ion transport carriers, and have high ionic conductivity, superior flame retardancy and the characteristic of inhibiting the dissolution of active materials, which can significantly improve the safety and cycling stability of organic batteries.

Recently, Muench et al.[372] reported a printable ionogel electrolyte for all-organic batteries, which was obtained by *in situ* polymerization of two acrylate-based monomers in 1-butyl-3-methylimidazolium bis(trifluoromethyl sulfonyl)imide (BMITFSI) via a UV-curing technique (Figure 27a). Within the ionogel electrolyte, the IL supports the high ionic conductivity and offers counterions for the redox process of the electrodes. Coupled with a cross-linked polymer with sufficient mechanical strength, the ionogel electrolyte exhibit attractive application prospects in organic batteries. In addition, researchers also employed an integrated preparation method to deposit the ionogel electrolyte on the cathode directly. It was found that compared with the traditional preparation method, *in situ* polymerization inside the battery could optimize the interfacial contact between the electrode and the electrolyte, as well as improve the initial specific capacity of the battery.

https://doi.org/10.1021/acs.chemrev.2c00374
Chem. Rev. 2023, 123, 1712−1773

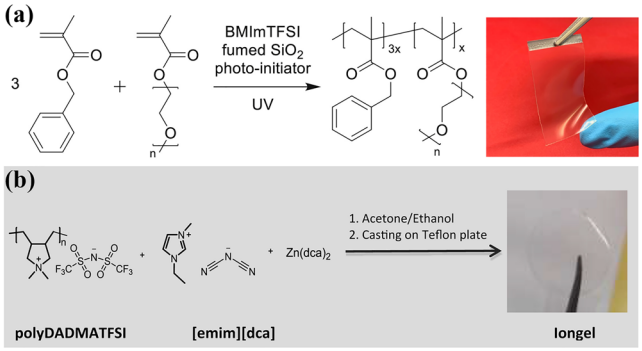

Figure 27. Application of ionogel and PIL electrolytes in organic batteries. (a) The polymerization reaction equation of ionogel electrolyte and its optical photograph. Reproduced with permission from ref 372. Copyright 2020 Elsevier. (b) Chemical structure of the components in PIL electrolyte and its preparation method. Reproduced with permission from ref 373. Copyright 2018 Elsevier.

However, the capacity retention was lower, which may be due to the large amount of unpolymerized residual monomers in the battery.

PILs have been regarded as a promising polymer electrolyte owing to their excellent processability, impermeability, mechanical stability, and flexible structural design. However, considering their low ionic conductivity, PILs and ionogel electrolytes are often mixed to form electrolytes with excellent performance. As shown in Figure 27b, Fdz De Anastro et al.[373] designed a PIL electrolyte with poly(dimethyldiallylammonium bis(trifluoromethanesulfonyl) imide (polyDADMATFSI) as the polymer matrix and EMIDCA as the conductive phase. Furthermore, the addition of $Zn(DCA)_2$ salt and Al_2O_3 nanoparticles improved the ionic conductivity of the electrolyte to 1.1×10^{-2} S cm^{-1}, which was close to that of pure IL-based electrolytes (4.1×10^{-2} S cm^{-1}). However, the initial capacity of the Zn-PEDOT battery using the PIL electrolyte was only 60 mAh g^{-1} at the current density of 0.01 mA cm^{-2}, followed with obvious capacity fading after a few cycles. Further optimization of PIL electrolytes is needed to enhance the electrochemical performance of organic batteries for practical applications.

To increase the contact area between the PIL electrolyte and the organic electrode, Leung et al.[374] used a "layer-by-layer" spray printing technique to prepare porous organic electrodes and deposited a highly conductive PIL electrolyte on these electrodes. SEM images of the electrode cross sections showed that the PIL electrolyte were fully infiltrated into the porous electrode. The preparation method can achieve favorable interfacial contact and low charge transfer resistance, which is beneficial to obtaining fast charge and discharge performance of the high-loading electrode. However, the large interfacial contact area promotes active material dissolution, resulting in more significant capacity decay and lower Coulombic efficiency compared to the nonporous electrode. Therefore, it is necessary to synergize this technique with other methods to inhibit the dissolution of organic electrodes for high-performance solid-state organic batteries.

With the in-depth study of ionogel and PIL electrolytes, excellent comprehensive properties are pursued to meet the demands for safer batteries with high performance. However, the application of these electrolytes in organic batteries is still at an early stage. It is necessary to further optimize the electrolyte formula, such as combining with solid frameworks like the MOF to improve mechanical properties, adjusting the IL components in electrolytes to reduce the dissolution of active materials and improve the cycling stability of organic batteries.

3.5. Interface Engineering

As the most important and least understood component in batteries, interphase regions have attracted widespread attention. Like many solid-state batteries based on inorganic electrode materials, the cyclability of solid-state organic batteries may be more limited by the interfacial properties between the active material and the electrolyte than the active material.

The chemical and electrochemical stability and good interfacial contact between the electrode and the solid-state electrolyte are absolutely key for fabricating effective solid-state organic batteries with excellent performances. For organic cathodes, the working potentials are generally lower than that of inorganic intercalated compound-based cathodes and the high oxidation potential of the solid-state electrolyte is uniquely suitable to ensure electrochemical and chemical stability with the electrode. Interfacial research is mainly concentrated on the following two aspects: 1) Replacing all-solid-state electrolytes with gel/quasi-solid electrolytes or increasing the operating temperature of the battery to the melting point of the polymer matrix in the electrolyte, converting "solid-solid" contact to "solid-liquid" contact. However, the inhibitory effect of the solid-state electrolyte on the dissolution of the organic electrode may be weakened or even disappear.[338,362,364] 2) Adding polymers, metal salts,[330,338,362] or inorganic electrolytes[325,326] to active materials during the preparation of the electrode. The combination of the polymer or inorganic electrolyte with the organic electrode is expected to support effective interfacial contact. In addition, it also promotes uniform distribution of the active components and form interpenetrating ionic and electronic channels to favor the full utilization of the active materials.[330] However, the addition of too many inactive materials in the electrode inevitably reduces the energy density of the whole battery.

In organic batteries, the selection range of the anode materials is relatively wide, mainly divided into active carbon materials, metal materials, and organic compounds. Carbon materials usually exhibit large volume expansion during cycling, leading to interface delamination and contact loss. For metal anodes, although ceramic solid-state electrolytes possess high mechanical strength, recent studies have shown that dendrites tend to nucleate and grow at the grain boundaries and defects in ceramic crystals.[314,375,376] The protection of metal anodes in organic batteries could refer to the previous strategies for suppressing dendrites in Li or Na metal batteries. Such strategies include adding inorganic fillers to enhance the mechanical property of polymer electrolytes, preparing single-crystal ceramics to eliminate the effects of grain boundaries and voids, and constructing a buffer layer or an artificial SEI layer at the interface. To overcome the poor wettability between the inorganic solid-state electrolyte and the metal anode, the introduction of an alloy buffer layer can reduce the surface roughness and tension of the metal, improving the interfacial wettability and providing necessary ion/electron conduction for metal plating/stripping.[330] It is noteworthy that most sulfide electrolytes and plastic crystal electrolytes are incompatible with alkali metals. Using Li-In,[377] Li-Al,[378] and Na-Sn[74,325] alloys instead of alkali metal anodes can tune the operating potential of the anodes into the electrochemical stability window of the sulfide electrolytes, preventing the reductive decomposition of the electrolyte. Furthermore, the use of organic electrode

https://doi.org/10.1021/acs.chemrev.2c00374
Chem. Rev. 2023, 123, 1712−1773

Table 4. Summary of Electrolyte Selections Based on Different Organic Electrolytes

Organic electrodes	Counter electrodes	Electrolytes	Cycling stability: capacity retention [%], cycles	Ref
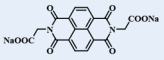 Na2BNDI (n-type)	Na	1 M $NaPF_6$-EC/DEC	76.7%, 300	120
		1 M $NaPF_6$-DEGDME	94.1%, 10000	
 K_2TP (n-type)	K	1 M KPF_6-PC	20%, 50	118
		1 M KPF_6-DME	94.6%, 500	
 DHBQDS (n-type)	Na	1 M $NaClO_4$-EC/DMC	42%, 240	124
		1 M $NaClO_4$-FEC/DMC	87%, 300	
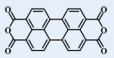 PTCDA (n-type)	Li	1 M LiTFSI-DOL/DME	28%, 1000	213
		3 M LiTFSI-DOL/DME	87%, 1000	
		Poly(DOL)+PEO+1 M LiTFSI-DOL/DME	93%, 200	356
	K	0.8 M KPF_6-EC/DEC	24%, 100	106
		2 M KFSI-TEP	70%, 100	
		KFSI-TMP (3:8 mol/mol)	56%, 200	107
	Graphite	3.5 m $Ca(FSI)_2$-EC/PC/DMC/EMC	85%, 350	221
	Mg	4.8 M $Mg(NO_3)_2$-H_2O	70%, 10	148
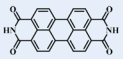 PTCDI (n-type)	$K_xFe_{0.35}Mn_{0.65}[Fe(CN)_6]_{w\cdot z}H_2O$	22 M KCF_3SO_3-H_2O	73%, 2000	273
 PTO (n-type)	Zn	2 M $ZnSO_4$-H_2O	70%, 1000	295
	Li	Li_3PS_4	61%, 1000	327
	Na	β-Al_2O_3	80%, 50	330
	$Na_{15}Sn_4$	Na_3PS_4	89%, 500	74
 PTPAn (p-type)	Graphite	0.5 M $NaPF_6$-G2	70%, 400 (−40 °C)	169
		0.8 M KPF_6-EC/DEC	76%, 500	379
	PI5	EMITFSI	75%, 5000	170
		1 M EMITFSI-MA/AN	Nearly 100%, 2000 (−60 °C)	163
	PNTCDA	21 m LiTFSI-H_2O	85%, 700	272
		2 m LiTFSI-EA	83%, 500	52
		1 M $Mg(ClO)_4$-AN	88%, 5000	140
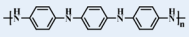 PANI (bipolar-type)	Zn	1 M $ZnCl_2$-H_2O	85%, 100	73
		2 M $Zn(CF_3SO_3)_2$-H_2O/DMF	92%, 350	292
		2 M $ZnSO_4$-H_2O	40%, 3700	125
		4.45 M $ZnCl_2$-EG	78%, 10000	
		2 M $ZnSO_4$-H_2O/methanol	86%, 2000	291
	K	0.8 M KPF_6-EC/DEC/FEC	80%, 100	359
		PMMA+0.8 M KPF_6-EC/DEC/FEC	98%, 100	
 PTMA (bipolar-type)	Graphite	1 M $LiPF_6$-EC/DEC	82%, 100	380
	Activated carbon	$Py_{14}TFSI$	87%, 10000	230
	Li	PVDF-HFP+1 M $LiPF_6$-EC/DMC	91%, 100	353

materials instead of alkali metal anodes can achieve excellent compatibility with sulfide electrolytes.

3.6. Electrolyte Selection for Different Organic Batteries

Although there are a number of reviews on organic electrode materials, there is a lack of guiding descriptors for electrolyte design in organic batteries. It is costly and time-consuming to identify the optimized electrolyte for newly devised organic electrode materials because of their various physicochemical properties and reaction mechanisms. Different electrolyte systems have been investigated for different organic electrodes

https://doi.org/10.1021/acs.chemrev.2c00374
Chem. Rev. 2023, 123, 1712−1773

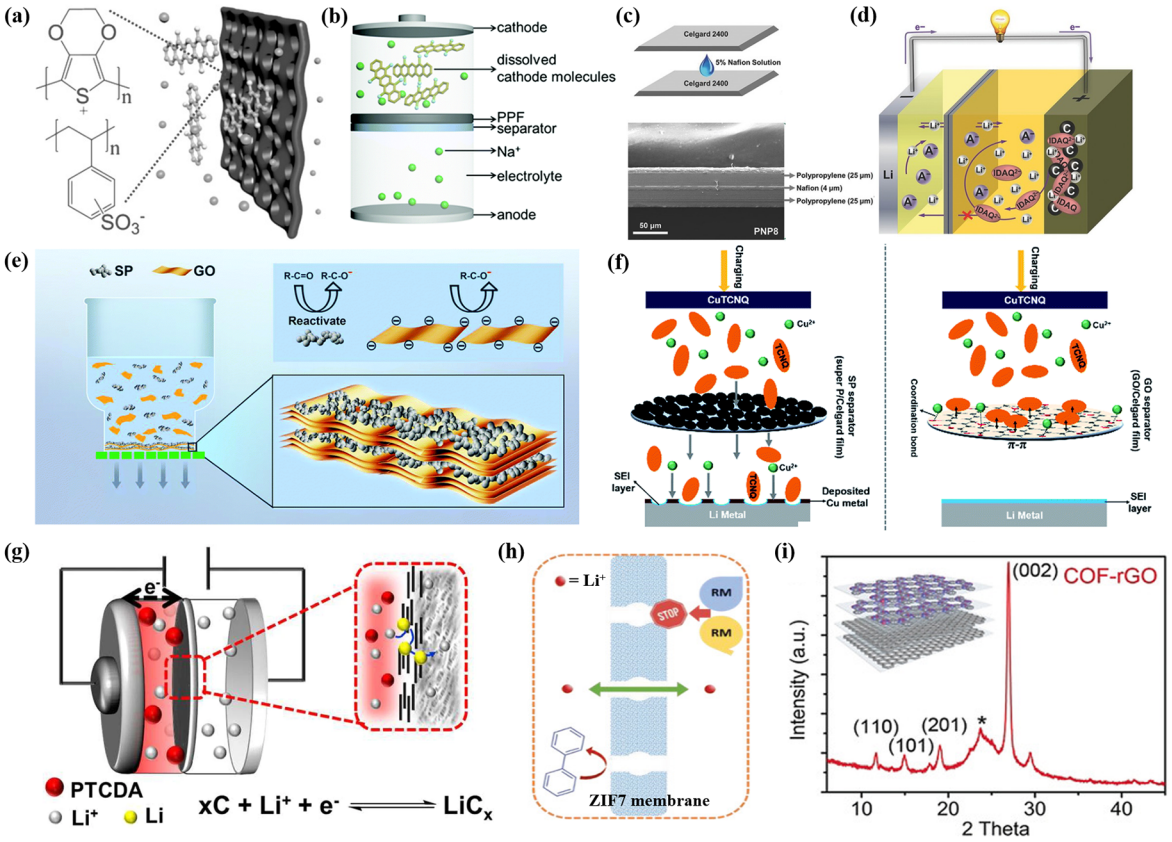

Figure 28. Application of ion-selective separators in organic batteries. (a) Composition of a PEDOT:PSS separator and its functioning mechanism in inhibiting the pass of active materials. Reproduced with permission from ref 388. Copyright 2016 Wiley-VCH. (b) Diagram of the inhibition of the shuttle effect of dissolved cathode molecules in PPF protective films. Reproduced with permission from ref 389. Copyright 2019 Royal Society of Chemistry. (c) The structural composition and the cross-section SEM image of the PNP separator. (d) Schematic illustration of a Li-organic battery with PNP separator. Reproduced with permission from ref 390. Copyright 2016 Wiley-VCH. (e) The fabrication process of the bicomponent layered coated separator and schematic diagram illustrating the inhibition of the passage of electroactive organic cations. Reproduced with permission from ref 393. Copyright 2018 Royal Society of Chemistry. (f) Schematic illustration of the differences between Super P-coated and GO-coated separators in blocking soluble organic molecules and Cu^{2+}. Reproduced with permission from ref 394. Copyright 2019 Royal Society of Chemistry. (g) Schematic illustration of the Li-PTCDA battery containing the separator with graphite coating. Reproduced with permission from ref 395. Copyright 2019 Springer Nature. (h) Schematic illustration of the ZIF7 membrane selectively penetrating Li^+ but blocking eluting redox mediators (RMs). Reproduced with permission from ref 398. Copyright 2020 Wiley-VCH. (i) XRD patterns of the ordered COF in COF-rGO. Inset is the schematic diagram of COF-rGO. Reproduced with permission from ref 400. Copyright 2018 Wiley-VCH.

with n-, p-, and bipolar types (Table 4). The performances of selected organic electrodes with different electrolytes are compared, and the solubility of active materials in the electrolytes and the stability of SEI formed on the organic electrodes are discussed. Although it is difficult to extract a universal descriptor on electrolyte selection and design to all organic electrode materials, we hope the discussion can provide some guidance.

The redox potentials of n-type organic electrode materials are typically below 3.5 V vs Li^+/Li, and the organic liquid electrolytes composed of metal salts and carbonate- or ether solvents have been widely used as ion conducting media. N-type organic electrode materials, especially carbonyl compounds, often suffer from rapid capacity loss and low energy efficiency due to their high solubility in organic solvents with similar chemical properties, thus limiting their practical application. From the perspective of electrodes, salinization and polymerization are effective methods to address the solubility problem. However, it was found that the performance of insoluble organic salt cathode materials like Na_2BNDI in conventional carbonate-based electrolytes was unsatisfactory, which could be attributed to the uncontrollable dendrite growth and infinite volume change of alkali metal anodes, resulting in low Coulombic efficiency and battery thermal runaway. Using ether-based electrolytes instead of carbonate-based ones[118,120] or adding film formation additives like FEC[124] is conducive to the formation of a thin and stable SEI layer. For organic compounds with high solubility in ether-based electrolytes, high-concentration organic electrolytes[106,107,213] and WIS aqueous electrolytes[273] can effectively reduce the content of uncoordinated solvent molecules in the system, thereby decreasing the dissolution of organic active materials and forming an anion-derived inorganic-rich SEI. Recently, the development of solid-state organic batteries based on inorganic solid electrolytes[74,327,330] and solid/quasi-solid polymer electrolytes[356] has also attracted great attention.

The p-type organic electrode materials are often used as the battery cathodes, and the counter electrodes are mostly graphite or low-voltage n-type organic materials. Since the p-type electrode materials react with anions from the electrolyte,

https://doi.org/10.1021/acs.chemrev.2c00374
Chem. Rev. 2023, 123, 1712−1773

single-cation conductors such as solid-state ceramic and single-ion conducting polymer electrolytes are not applicable. The selection of electrolytes is based on organic liquid, ILs, aqueous and polymer-based electrolytes. The high redox voltages of the p-type electrode materials (>3.5 V vs Li^+/Li) often require excellent oxidation stability of the organic liquid electrolytes. Therefore, carbonate-based electrolytes are often selected over ether-based electrolytes. Notably, the practical redox voltage of the p-type electrodes can be altered by changing the types of the solvents, which increases with the Gutmann donor numbers of the electrolytes.[127] In addition, the type of anions employed in the electrolyte also affects the redox voltages, charge transfer kinetics, and cycling stability of the electrodes. Generally, larger anion size triggers greater polarization and leads to higher redox potential of the electrode during the charge/discharge process. Considering the specific capacity of the battery with the p-type organic electrode is significantly influenced by the mass of the anions from the salt, an electrolyte salt with a low anionic mass can be selected on the promise of obtaining excellent electrochemical performance. Due to the fast redox kinetics and the absence of desolvation in the discharge process, some p-type electrode materials like PTPAn are often used as the cathodes in low-temperature batteries, that require electrolyte systems with low freezing points.[163,169] In addition, most of studies on electrolytes for p-type organic electrodes are focused on broadening the electrochemical stable window,[272] studies on the interface behaviors between electrolytes and p-type electrodes are currently lacking and needed.

Depending on the redox reaction of the electrode, the bipolar-type organic electrode can be regarded as n-type and/or p-type, and an appropriate electrolyte can be selected accordingly. The most studied bipolar-type electrode materials are nitronyl nitroxide polymers, which are usually used as p-type electrodes to obtain high discharge voltage and stable electrochemical performance. Therefore, electrolytes with wide electrochemical stability windows such as carbonate-based or IL-based electrolytes are usually selected. PTMA, the first organic radical reported as an electrode material for LIBs,[64] exhibited excellent cycling and rate performance due to the stable polymer structure and fast reaction kinetics. However, the low specific capacity, expensive raw materials and complex synthesis greatly hinder the application of nitronyl nitroxide-based electrode materials.

4. SEPARATORS IN ORGANIC BATTERIES

In addition to inherent interfacial problems, the preparation process of polymer and inorganic solid electrolytes is complicated, and great effort is still required to achieve industrialization. Certain methods of surface modification of separators and replacement with ion permselective membranes are expected to suppress the shuttle of active materials based on the size confinement effect or charge repulsion. In addition, the modified separators are often simple to prepare and fully fit the current battery preparation process. In fact, ion permselective separators play a critical role in the rapid transport of charge-carrying ions and isolation of the chemical reactions in separate electrodes,[381] and have been widely used in Li-S batteries,[382] Na-S batteries,[383] vanadium flow batteries,[384,385] and oxy-hydrogen fuel cells.[386,387] The ideal ion permselective membrane should have high-efficiency screening of ions, excellent chemical and mechanical properties, and competitive costs. In organic batteries, there is a common challenge caused by the shuttle effect of active materials, leading to the capacity degradation of the battery during the cycling process. Therefore, using ion permselective membranes instead of traditional separators is an effective way to isolate the dissolved active material on one side of the membrane.

Wang et al.[388] introduced the concept of pinhole-free polymeric dielectric layers in organic electronics into the field of Na-organic batteries. A Na^+-conductive thin membrane of PEDOT:PSS (PSS: poly(styrenesulfonate)) was coated on the glass fiber membrane near the PT cathode. As shown in Figure 28a, the permselective membrane allows the transport of Na^+ ions but blocks the dissolved organic molecules. This inhibits the diffusion of the dissolved PT molecules between the cathode and the Na anode, thus greatly improving the cycle life of the organic battery and opening a new path to minimize the dissolution of the active materials and the resulting shuttle effect. The results showed that compared with the battery using glass fiber separator, the battery with a PEDOT:PSS separator exhibited significantly enhanced cycling stability. However, the poor mechanical properties of the PEDOT:PSS membrane led to damage during the preparation and battery assembly process, resulting in a reduced capacity. Blending PEDOT:PSS with PEO, which has good film-forming characteristics and excellent mechanical properties, is expected to generate a free-standing protective layer that could inhibit the shuttle effect of organic electrodes (Figure 28b).[389] Using the composite film as the separator improved the capacity and cycling stability of the PT electrode compared to the single PEDOT:PSS film. However, the low ionic conductivity of PEO hindered the Na-ion transport. Although the thickness of the film can be reduced by adjusting the ratio of PEDOT:PSS and PEO to promote cation transport and improve the ionic conductivity, the rate performance of the battery was still unsatisfactory. A specific capacity of about 100 mAh g^{-1} was achieved at a current density of 1000 mA g^{-1}, corresponding to only 31.5% of the theoretical capacity.

In addition to PEDOT:PSS membranes, a commercial perfluorinated sulfonate ionomer (i.e., Nafion) with high proton conductivity, chemical stability, and excellent mechanical strength, was demonstrated to exhibit ion-selective permeability. Song et al.[390] combined Nafion with a polypropylene (PP) membrane to make a PP/Nafion/PP (PNP) sandwich-type separator (Figure 28c). The microporous PP membranes on both sides of the Nafion layer ensured the mechanical strength and avoided side reactions between Nafion and the electrodes while not significantly hindering the transport of Li ions. The results indicated that the PNP membrane showed significant selective permeability for ion transport, suggesting that the material did not affect the Li-ion transportation in the electrolyte, but blocked the migration of dissolved electroactive anions and molecules (Figure 28d), leading to significant improvement of the cyclability. In addition, the PNP separators exhibited good compatibility when applied to various organic battery systems.

However, designing selectively permeable membranes did not completely address the challenge of organic electrode dissolution. While using such membranes hindered the migration of active materials to the counter electrode, active materials could still be separated from the electrode. Therefore, the cyclic performance of the battery would tend to be stable only after the concentration of the dissolved active materials near the organic electrode reaches saturation. As a result, modified batteries with ion permselective separators still showed obvious capacity decay in the first few cycles due to the gradual dissolution of the active materials in the electrolyte. Therefore,

https://doi.org/10.1021/acs.chemrev.2c00374
Chem. Rev. 2023, 123, 1712−1773

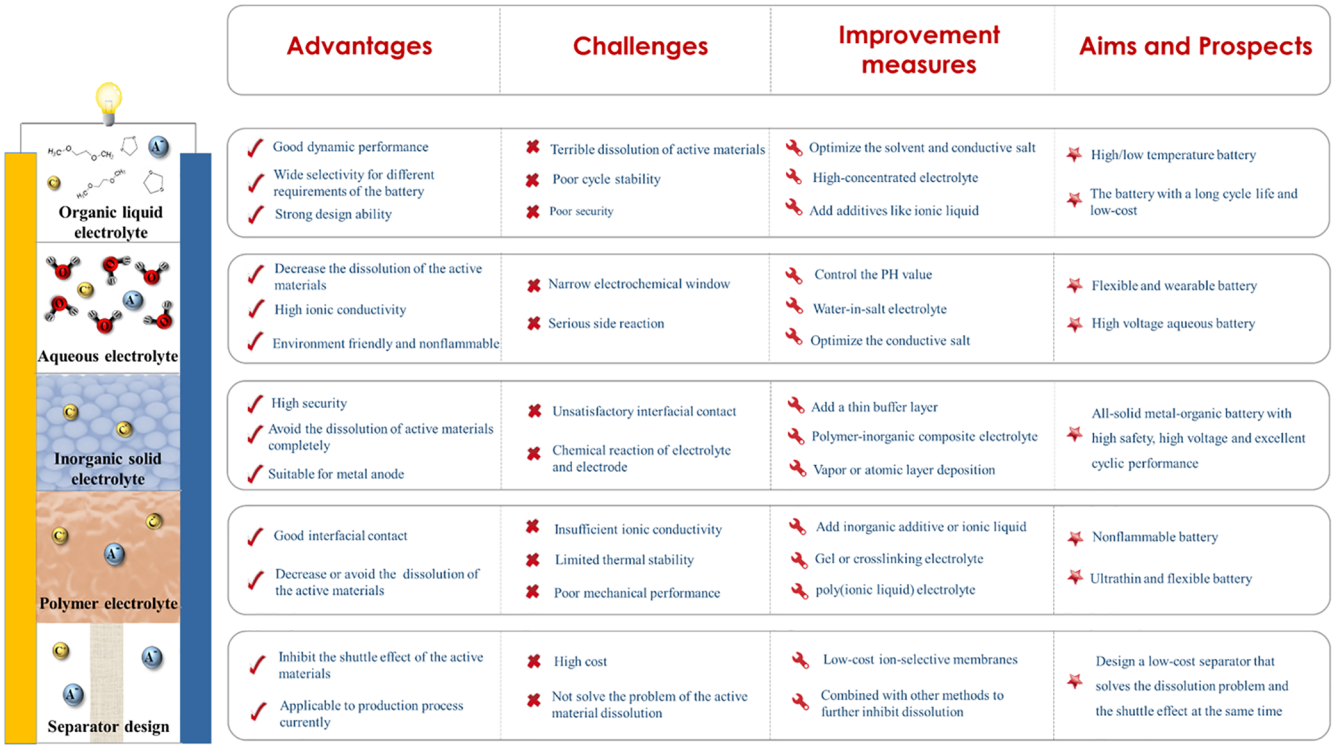

Figure 29. Advantages, challenges, improvement measures, and prospects of different types of electrolytes and modified separators in organic batteries.

for organic electrodes with high solubility such as AQ, improvement of the cycling stability requires to combine the ion permselective membrane with other complementary methods.[390]

Zhao et al.[245] replaced the organic liquid electrolyte with an aqueous electrolyte to reduce the solubility of quinone electrodes. Combined with the ion-selectively permeable separator of Nafion, the Zn-C4Q battery showed a more stable cycling performance compared with the battery using a filter paper as the separator. According to *in situ* UV−vis spectra and the observed color change of the electrolyte, researchers surmised the active material was dissolved in the aqueous electrolyte in the device with a filter paper separator. In contrast, for the Zn-C4Q battery with a Nafion separator, only weak absorption peaks were observed in the UV−vis curves and the color of the electrolyte was almost unchanged after cycling, indicating that the dissolution of the active material was inhibited. Furthermore, the result showed that the C4Q cathode coupled with a Nafion membrane exhibited a high capacity of 335 mAh g^{-1} at 20 mA g^{-1} and 87% of the capacity was retained after 1000 cycles at the current density of 500 mA g^{-1}, which was comparable to that of inorganic electrode materials.

Similar to Nafion, the large number of negatively charged nanopores in graphene oxide (GO) can result in cation transfer but prevent anion transfer.[139,391,392] As shown in Figure 28e, GO and Super P (or graphene) were directly filtered onto the Celgard separator by a simple vacuum filtration method to form a bicomponent layer-coated separator for Li-organic batteries.[393] The carboxylic acid and phenolic hydroxyl groups on GO could prevent dissolved electroactive anions from diffusing to the anode, while super P (or graphene), as the upper collector, could provide the reactivation sites, greatly improving the utilization rate of active materials. The implementation of GO and Super P (or graphene)-based separators significantly improved the open circuit voltage and cyclic stability of AQ and PTCDA cathodes. Recent research has shown that the separator modified by GO could also inhibit the shuttle reaction of neutral organic molecules. As shown in Figure 28f, due to the $\pi-\pi$ interaction between sp^2-hybridized carbon rings in GO and aromatic rings in organic molecules, the separator modified by GO could effectively immobilize the soluble active materials and prevent their transfer between electrodes, thus improving the capacity retention of the organic battery.[394] Furthermore, for metal-organic cathode materials like CuTCNQ, Cu^{2+} formed during the charging process could be trapped by coordination bonds with oxygen-containing groups on GO separators, which mitigates the corrosion of Cu^{2+} on the Li metal anode, and is conducive to the formation of uniform and dense SEI films.

In addition to ion-selective separators based on charge repulsion, the development of membranes with submicron or nanometric porous structures is also considered an effective way to hinder the passage of active materials. Belanger et al.[395] designed a double-layer separator with a porous, flexible and mechanically stable PP layer on one side and a thin, nonporous and continuous graphite layer on the other side. Since the submicron graphite layer is only permeable to Li ions, the diffusion of PTCDA is significantly inhibited (Figure 28g), benefiting the cycling stability and rate performance of the battery. Similarly, the development of MOFs and COFs with uniform and controllable nanopores holds promise for physically suppressing the shuttle effect of the electrode materials.[396,397] Theoretically, the uniform pores of MOF can be precisely adjusted by combining the appropriate inorganic and organic components so as to inhibit the shuttle reaction of organic active materials without affecting the permeability of other salts and solvents in the electrolyte. Recently, a MOF membrane based on ZIF7 nanoparticles and the PVDF-HFP binder was used as the separator in an organic-O_2 battery, which

https://doi.org/10.1021/acs.chemrev.2c00374
Chem. Rev. 2023, 123, 1712−1773

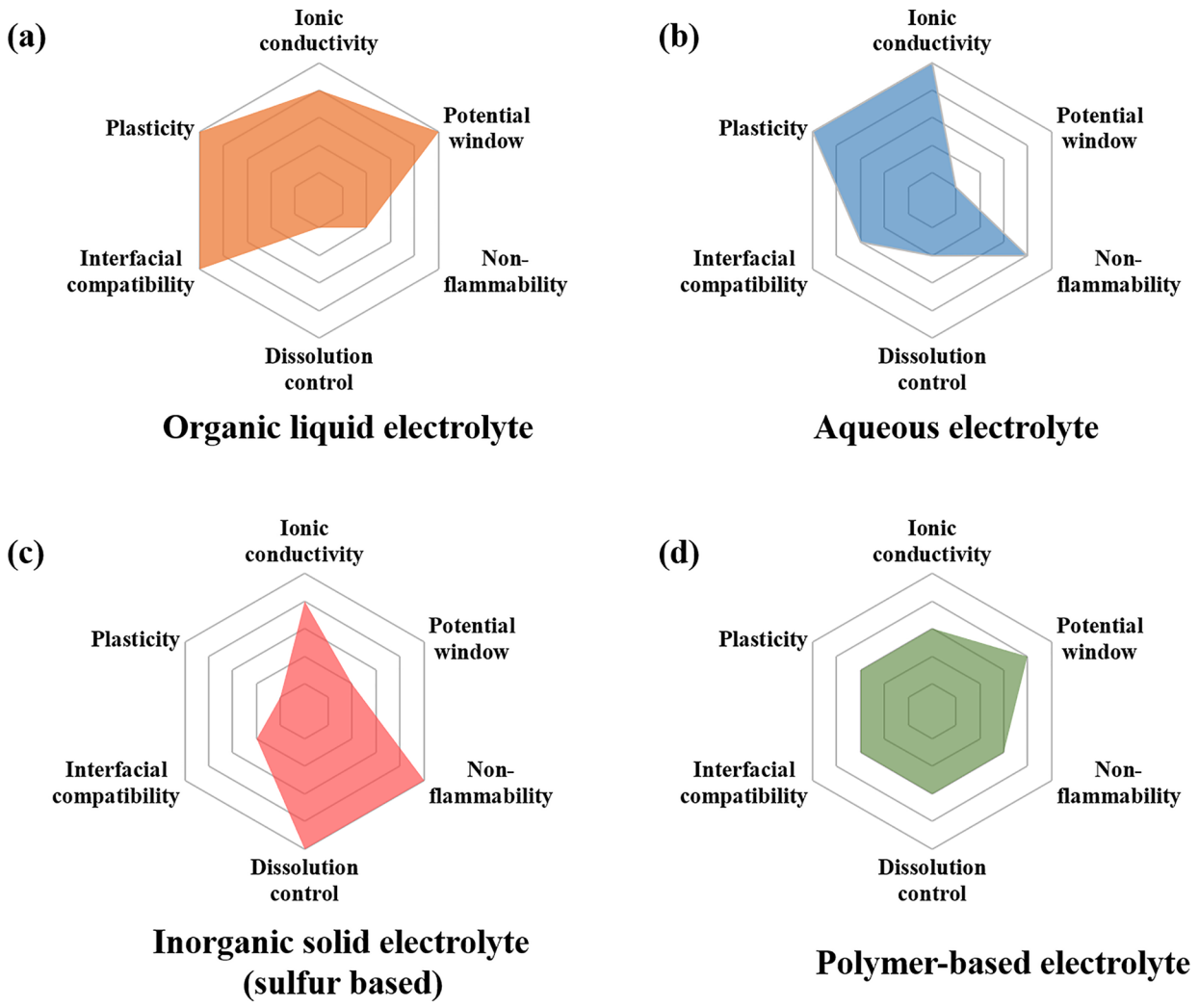

Figure 30. Performance profiles of different electrolytes. Radar plots of the properties of (a) organic liquid, (b) aqueous, (c) sulfur-based solid-state, and (d) polymer-based electrolytes.

could conduct Li ions and suppress organic intermediates shuttling in the system (Figure 28h).[398] However, the poor compatibility between inorganic MOF particles and organic polymer matrix causes inhomogeneous dispersion and large interfacial gaps, leading to the formation of nonselective permeation pathways. The research of self-assembled MOFs provided a possibility to prepare pure MOF-gel separators with homogeneous micropores. The intrinsic channel size between adjacent MOF cavities is smaller than that of organic intermediates but larger than that of other solvents or salts, which could alleviate the shuttling of organic molecules without sacrificing power.[399] Furthermore, giving the credit to the adjustable pore size, MOF-gel separators showed universal applicability for molecular and ionic sieving, which could be used to improve the cycling stability of organic molecules with various sizes.

Similarly, COF-based materials with high porosity, wide structural adjustability and stability can also be used as candidates for ion-selective membranes. However, the insolubility of COFs poses a challenge for the preparation of compact and ordered membranes. Jiang et al.[400] directly deposited COFs onto preobtained graphene and prepared an orderly stacked COF-graphene double-layer membrane (COF-rGO) to take advantage of the $\pi-\pi$ effect of graphene and COFs (Figure 28i). These interactions could be confirmed from the change of XRD peak patterns of the COF material in COF-rGO compared with the COF powders. The application of COF-rGO membranes is expected to inhibit the shuttle effect of polysulfide and PT, leading to excellent cycling stability and the capability to utilize both Li-S and organic NIBs. Furthermore, the rate performances of the batteries were also improved, indicating the ordered nanopores could facilitate the homogeneous and rapid metal ion transport.

Therefore, previous research has proved that fabricating ion permselective separators is an effective method to address the dissolution challenge and shuttle effect in organic batteries. More research efforts should be devoted to exploring the synergy of ion permselective separators and other complementary methods for high-performance organic batteries.

5. CHALLENGES AND PROSPECTS

In this work, we reviewed the components and properties of different electrolytes and summarized the advantages, challenges, improving strategies, and prospects of organic liquid electrolytes, aqueous electrolytes, inorganic solid electrolytes, polymer electrolytes, and special separators in organic batteries (Figure 29). The performance comparison of different types of electrolytes is summarized in Figure 30, in which each

https://doi.org/10.1021/acs.chemrev.2c00374
Chem. Rev. 2023, 123, 1712−1773

electrolyte system exhibits obvious weaknesses. Therefore, it is necessary to select appropriate electrolytes for different situations and modify them to achieve effective application in organic batteries.

At present, liquid electrolytes are still the main component of most organic batteries. The selection of solvents and salts has a significant effect on the electrochemical performance of the battery. Use of some special solvents can realize the successful operation of batteries in extreme environmental conditions, which expands their applications in high-altitude aircrafts, polar exploration, deep sea exploration, and so on. No matter it is in organic liquid electrolyte system or aqueous electrolyte system, highly concentrated electrolytes have shown excellent performances in improving the cyclic stability of the battery, reducing self-discharge of the electrode and widening the electrochemical window of the electrolyte. However, the high cost of the concentrated electrolyte and the poor wettability caused by the high viscosity are the main challenges for the commercial application of such electrolytes in the future. To address these challenges, it is necessary to control the concentration of the electrolyte accurately and explore practical methods to reduce the cost of the full battery under the precondition of ensuring excellent electrochemical performance. The development of new diluents, the design of localized high-concentration electrolytes, the use of hydrated deep eutectic electrolytes, and the exploration of cost-effective salts with high solubility have become the current research focus.

In addition to the liquid electrolytes, solid-state electrolytes are also developed to improve the cyclic stability and mitigate the self-discharge of organic batteries. Though some research process has been achieved, research of organic batteries using polymer-based electrolytes or inorganic solid electrolytes is still in its infancy, and there is much room for the improvement of all-solid-state organic batteries. For the polymer-based electrolyte, the low ionic conductivity is still a major obstacle for their application. Although it is possible to enhance the conductivity by preparing gel electrolytes or increasing the operating temperature, there is a risk of weakening or even eliminating the inhibition effect on the dissolution of organic electrode materials by the polymer-based electrolytes. To overcome this challenge, designing quasi-solid or all-solid organic-inorganic composite electrolytes with excellent performances and compatibility with organic electrode materials has become the future direction for the successful application of polymer-based electrolytes in organic batteries.

Inorganic solid electrolytes are another type of solid-state electrolytes, which could effectively avoid the capacity decay caused by the dissolution or shuttle effect of the organic active materials and the corresponding reaction intermediates. Sulfide-based electrolytes such as Li_3PS_4 and Na_3PS_4 have been proven to maintain good chemical and electrochemical compatibility with some organic electrodes. However, due to the electronically insulating nature of organic electrode materials and high ion transport resistance at the interface between the organic electrode and the solid-state electrolyte, a large amount (up to 70 wt %) of sulfide electrolytes is usually added in the electrodes. This is bound to decrease the energy density at the battery level. To further improve the performance of inorganic solid electrolyte-based organic batteries, the development of organic electrode materials with higher redox potentials, higher capacity, and better compatibility to enhance the energy density of the all-solid-state organic batteries has become a research focus.

Apart from developing organic electrode materials, the inorganic solid electrolytes also play a vital role in the performance of all-solid-state organic batteries. When the charge cutoff voltage of the organic battery is higher than the oxidation decomposition potential of the inorganic solid electrolyte, the sediment formed by the electrolyte decomposition may compromise the interphase between the electrolyte and the electrode, resulting in the degradation of battery performance. The development of halide electrolytes with high oxidative stability (~4.3 V vs Li^+/Li) offers an attractive strategy to solve the compatibility challenge with high-voltage (>4 V vs Li^+/Li) organic cathode materials in the future. In addition, the poor interfacial contact between the solid-state electrolyte and the organic electrode, combined with the low reaction kinetics and insufficient penetration of the electrode structure, would also make adverse effects on the battery. Although it is possible to realize the intimate contact between active materials and electrolyte by including additives like soft polymers, metal salts or inorganic electrolytes into the electrode, the rate performance of organic batteries based on solid-state electrolytes is still unsatisfactory. Furthermore, except for a few studies, most reported all-solid-state organic batteries are stably cycled for about 500 times, or even less, which is unacceptable for practical applications. For an organic battery based on metal anodes, it is very important to improve the stability of the anode and suppress dendrite formation. However, due to the lower cycle numbers achievable with such systems, this problem is often overlooked in organic battery research.

In recent years, the development of plastic crystal electrolytes and PIL electrolytes has provided a new direction for solid-state batteries. However, side reactions can occur in organic batteries between alkali metal anodes and electrolytes like the plastic crystal of SN. For example, the polymerization of nitriles catalyzed by alkali metals can form a highly resistive interface,[341] which blocks ion transport and reduces capacity retention during cycling.[401] Research indicated that the addition of FEC could form a stable and uniform protective layer on the surface of the metal and avoid the continuous polymerization of SN. However, the introduction of FEC may have adverse impacts on the electrochemical reaction of the organic molecules.[131] Therefore, the application of plastic crystal electrolytes in organic batteries needs further research to optimize the electrolyte-electrode interphase and mitigate the dendrite growth on metal anodes.

Besides the electrolytes, another critical component that closely contact with the electrodes in organic batteries is the membrane, but the impact of the membrane to the organic battery performance remains elusive. The ion conductivity and selective ion permeability of the membranes are often affected by many factors, but it lacks in-depth study to gain insight into the correlation between membrane structure and battery performance. There are a few reports about ion-selective membranes, but the application of ion-selective membranes in organic batteries is still immature. The significance of membranes to the energy storage devices has been extensively studied in the other fields such as fuel cells and flow batteries. Researchers have proposed a variety of methods to optimize the performances of ion-selective membranes. These include, but are not limited to, introducing dense sulfonation and regulating the topological structure of the main and side chains to increasing the ionic conductivity, using the restricted pore sieving effect to improve the ion selectivity of the membrane, and mixing with inorganic fillers to enhance the inhibition of the

https://doi.org/10.1021/acs.chemrev.2c00374
Chem. Rev. 2023, 123, 1712−1773

shuttle effect. These methods provide valuable experience and reference for optimizing the performance of ion-selective separators for organic batteries. In addition, some commercially available ion-selective membranes, such as Nafion membranes, are very expensive, and the development of low-cost sulfonated polymers as cation exchange membranes has also gained interest. Some separators or electrolyte designs that inhibited the dissolution and shuttle of polysulfides in Li-S batteries may also be suitable for organic batteries.[402,403] The synergy of advanced liquid electrolytes and ion-selective membranes offer numerous opportunities for developing high-performance and sustainable organic batteries.

In summary, organic batteries are promising alternatives to conventional LIBs due to the low cost, abundance, high sustainability and recyclability of organic materials. However, the understanding toward the correlation between electrolyte structure and battery performance, as well as the electrode–electrolyte interphase in organic batteries, is still at the infant stage, impeding the commercial application for energy storage and conversion. This review provides a guidance and roadmap for the electrolyte development in organic batteries. With the design and synthesis of new electrode materials and electrolytes, as well as the thorough investigation of their mechanism, the utility of organic batteries will shine and they will gradually shift from solely being of academic interest to being crucial for practical applications.

AUTHOR INFORMATION

Corresponding Authors

Chao Luo − *Department of Chemistry and Biochemistry, George Mason University, Fairfax, Virginia 22030, United States;* orcid.org/0000-0001-8497-8548; Email: cluo@gmu.edu

Juchen Guo − *Department of Chemical and Environmental Engineering, University of California−Riverside, Riverside, California 92521, United States; Materials Science and Engineering Program, University of California−Riverside, Riverside, California 92521, United States;* orcid.org/0000-0001-9829-1202; Email: juguo@ucr.edu

Yunhua Xu − *School of Materials Science and Engineering, Key Laboratory of Advanced Ceramics and Machining Technology (Ministry of Education), and Tianjin Key Laboratory of Composite and Functional Materials, Tianjin University, Tianjin 300072, China;* orcid.org/0000-0003-1818-3661; Email: yunhua.xu@tju.edu.cn

Authors

Mengjie Li − *School of Materials Science and Engineering, Key Laboratory of Advanced Ceramics and Machining Technology (Ministry of Education), and Tianjin Key Laboratory of Composite and Functional Materials, Tianjin University, Tianjin 300072, China*

Robert Paul Hicks − *Department of Chemical and Environmental Engineering, University of California−Riverside, Riverside, California 92521, United States*

Zifeng Chen − *School of Materials Science and Engineering, Key Laboratory of Advanced Ceramics and Machining Technology (Ministry of Education), and Tianjin Key Laboratory of Composite and Functional Materials, Tianjin University, Tianjin 300072, China*

Chunsheng Wang − *Department of Chemical and Biomolecular Engineering, University of Maryland, College Park, Maryland 20742, United States;* orcid.org/0000-0002-8626-6381

Complete contact information is available at: https://pubs.acs.org/10.1021/acs.chemrev.2c00374

Author Contributions

CRediT: **Mengjie Li** writing-original draft, writing-review & editing; **Robert Paul Hicks** writing-review & editing; **Zifeng Chen** writing-review & editing; **Chao Luo** funding acquisition, writing-review & editing; **Juchen Guo** writing-review & editing; **Chunsheng Wang** writing-review & editing; **Yunhua Xu** conceptualization, investigation, resources, supervision, writing-review & editing.

Notes

The authors declare no competing financial interest.

Biographies

Mengjie Li obtained her B.E. degree from the College of Polymer Science and Engineering at Sichuan University in 2016. Then she received her M.S. degree from the School of Materials Science and Engineering at Beijing University of Chemical Technology in 2019. She is currently a Ph.D. student at the School of Material Science and Engineering, Tianjin University. Her research interests focus on lithium-based energy storage materials, especially polymer electrolytes.

Robert Paul Hicks received his B.S. in Chemistry from North Carolina State University in 2016 followed by his M.S. in Physical Chemistry from Boston College, where he researched electrocatalytic processes via structure-specific spectroscopies, in 2019. He joined Professor Juchen Guo's group in the Chemical and Environmental Engineering department at UCR in 2021. His current research interests include developing and studying electrolytes for application in lithium and nonlithium ion rechargeable batteries.

Zifeng Chen received his B.E. degree from the School of Materials Science and Engineering at Tianjin University in 2015. Then he conducted his Ph.D. research on organic batteries under the supervision of Prof. Yanhou Geng and Yunhua Xu at Tianjin University. After receiving his Ph.D. in 2022, he worked as a postdoctoral fellow with Prof. Xianhe Bu at the School of Materials Science and Engineering, Nankai University. Currently his research interests mainly focus on the novel organic electrode materials and the applications of MOFs in energy storage batteries.

Chao Luo is an Assistant Professor at George Mason University. He received his Bachelor's degree in Chemistry from Wuhan University in 2008, and then he joined Prof. Xuesong Wang's group and received his Master's degree in Organic Chemistry from Technical Institute of Chemistry and Physics, Chinese Academy of Sciences in 2011. Afterward, he joined Prof. Chunsheng Wang's group and obtained his Ph.D. in Chemical Engineering from University of Maryland, College Park in 2015. He also worked as a postdoc at University of Maryland, College Park from 2016 to 2019 and joined George Mason University as an Assistant Professor in 2019. He was the recipient of NSF CAREER Award. His current research interests focus on developing new organic materials and new chemistries for high-performance and sustainable energy storage devices.

Juchen Guo is an Associate Professor at University of California–Riverside. He earned his Bachelor's degree in Chemical Engineering from Zhejiang University in 1999 and his Ph.D. in Chemical Engineering from University of Maryland in 2007 under the supervision of Prof. Timothy A. Barbari. From 2007 to 2011, he performed postdoctoral studies at University of Maryland under the direction of Profs. F. Joseph Schork and Chunsheng Wang. He also performed postdoctoral study at Cornell University from 2011 to 2012 under the direction of Prof. Lynden A. Archer prior to joining the Department of

https://doi.org/10.1021/acs.chemrev.2c00374
Chem. Rev. 2023, 123, 1712−1773

Chemical and Environmental Engineering at UC Riverside in 2012. He was the recipient of 2014 Hellman Fellowship and 2018 NSF CAREER Award. His research interests are interfacial phenomena and material properties in electrochemical energy storage systems.

Chunsheng Wang is a Robert Franklin and Frances Riggs Wright Distinguished Chair Professor in the Chemical & Biomolecular Engineering, Department of Chemistry and Biochemistry, at the University of Maryland. He is an Associate Editor of *ACS Applied Energy Materials* and UMD Director of the UMD-ARL Center for Research in Extreme Battery. His research focuses on reachable batteries and fuel cells. He was ranked as the Global Highly Cited Researchers (top 1% by citation) by Clarivate Analytics in 2018−2019.

Yunhua Xu is a Professor in the School of Materials Science and Engineering of Tianjin University. He received his Ph.D. degree in Materials Physics and Chemistry from South China University of Technology in 2008. Prior to joining Tianjin University, he worked as a visiting student and then a researcher at the University of California, Santa Barbara, Iowa State University, and the University of Maryland, College Park, from 2006 to 2015. His research interests focus on electrochemical storage materials and devices.

ACKNOWLEDGMENTS

Y.X. acknowledges the support of the National Key Research and Development Program of China (Grant No.: 2019YFE0118800) and the National Natural Science Foundation of China (Grant No.: 22179092). C.L. acknowledges the US National Science Foundation (Award No.: 2000102).

REFERENCES

(1) Kittner, N.; Lill, F.; Kammen, D. M. Energy Storage Deployment and Innovation for the Clean Energy Transition. *Nat. Energy* **2017**, *2*, 17125.
(2) Xu, K. A Long Journey of Lithium : From the Big Bang to Our Smartphones. *Energy Environ. Mater.* **2019**, *2*, 229−233.
(3) Janek, J.; Zeier, W. G. A Solid Future for Battery Development. *Nat. Energy* **2016**, *1*, 16141.
(4) Liu, J.; Bao, Z.; Cui, Y.; Dufek, E. J.; Goodenough, J. B.; Khalifah, P.; Li, Q.; Liaw, B. Y.; Liu, P.; Manthiram, A.; et al. Pathways for Practical High-Energy Long-Cycling Lithium Metal Batteries. *Nat. Energy* **2019**, *4*, 180−186.
(5) Whittingham, M. S. Ultimate Limits to Intercalation Reactions for Lithium Batteries. *Chem. Rev.* **2014**, *114*, 11414−11443.
(6) Zhang, K.; Han, X.; Hu, Z.; Zhang, X.; Tao, Z.; Chen, J. Nanostructured Mn-Based Oxides for Electrochemical Energy Storage and Conversion. *Chem. Soc. Rev.* **2015**, *44*, 699−728.
(7) Huang, B.; Pan, Z.; Su, X.; An, L. Recycling of Lithium-Ion Batteries: Recent Advances and Perspectives. *J. Power Sources* **2018**, *399*, 274−286.
(8) Wang, Y.; An, N.; Wen, L.; Wang, L.; Jiang, X.; Hou, F.; Yin, Y.; Liang, J. Recent Progress on the Recycling Technology of Li-Ion Batteries. *J. Energy Chem.* **2021**, *55*, 391−419.
(9) Lee, S.; Kwon, G.; Ku, K.; Yoon, K.; Jung, S. K.; Lim, H. D.; Kang, K. Recent Progress in Organic Electrodes for Li and Na Rechargeable Batteries. *Adv. Mater.* **2018**, *30*, 1704682.
(10) Tarascon, J.-M.; Armand, M. Building Better Batteries. *Nature* **2008**, *451*, 652−657.
(11) Nguyen, T. P.; Easley, A. D.; Kang, N.; Khan, S.; Lim, S. M.; Rezenom, Y. H.; Wang, S.; Tran, D. K.; Fan, J.; Letteri, R. A.; et al. Polypeptide Organic Radical Batteries. *Nature* **2021**, *593*, 61−66.
(12) Larcher, D.; Tarascon, J. M. Towards Greener and More Sustainable Batteries for Electrical Energy Storage. *Nat. Chem.* **2015**, *7*, 19−29.
(13) Miroshnikov, M.; Divya, K. P.; Babu, G.; Meiyazhagan, A.; Reddy Arava, L. M.; Ajayan, P. M.; John, G. Power from Nature: Designing Green Battery Materials from Electroactive Quinone Derivatives and Organic Polymers. *J. Mater. Chem. A* **2016**, *4*, 12370−12386.
(14) Leguizamon, S.; Díaz-Orellana, K. P.; Velez, J.; Thies, M. C.; Roberts, M. E. High Charge-Capacity Polymer Electrodes Comprising Alkali Lignin from the Kraft Process. *J. Mater. Chem. A* **2015**, *3*, 11330−11339.
(15) Lu, Y.; Hou, X.; Miao, L.; Li, L.; Shi, R.; Liu, L.; Chen, J. Cyclohexanehexone with Ultrahigh Capacity as Cathode Materials for Lithium-Ion Batteries. *Angew. Chem., Int. Ed.* **2019**, *58*, 7020−7024.
(16) Fan, X.; Wang, F.; Ji, X.; Wang, R.; Gao, T.; Hou, S.; Chen, J.; Deng, T.; Li, X.; Chen, L.; et al. A Universal Organic Cathode for Ultrafast Lithium and Multivalent Metal Batteries. *Angew. Chem., Int. Ed.* **2018**, *57*, 7146−7150.
(17) Xie, J.; Zhang, Q. Recent Progress in Multivalent Metal (Mg, Zn, Ca, and Al) and Metal-Ion Rechargeable Batteries with Organic Materials as Promising Electrodes. *Small* **2019**, *15*, 1805061.
(18) Zhao, Q.; Wang, J.; Lu, Y.; Li, Y.; Liang, G.; Chen, J. Oxocarbon Salts for Fast Rechargeable Batteries. *Angew. Chem., Int. Ed.* **2016**, *55*, 12528−12532.
(19) Liang, Y.; Dong, H.; Aurbach, D.; Yao, Y. Current Status and Future Directions of Multivalent Metal-Ion Batteries. *Nat. Energy* **2020**, *5*, 646−656.
(20) Wang, H. G.; Yuan, S.; Ma, D. L.; Huang, X. L.; Meng, F. L.; Zhang, X. B. Tailored Aromatic Carbonyl Derivative Polyimides for High-Power and Long-Cycle Sodium-Organic Batteries. *Adv. Energy Mater.* **2014**, *4*, 1301651.
(21) Wu, X.; Jin, S.; Zhang, Z.; Jiang, L.; Mu, L.; Hu, Y. S.; Li, H.; Chen, X.; Armand, M.; Chen, L.; et al. Unraveling the Storage Mechanism in Organic Carbonyl Electrodes for Sodium-Ion Batteries. *Sci. Adv.* **2015**, *1*, No. e1500330.
(22) Liang, Y.; Luo, C.; Wang, F.; Hou, S.; Liou, S. C.; Qing, T.; Li, Q.; Zheng, J.; Cui, C.; Wang, C. An Organic Anode for High Temperature Potassium-Ion Batteries. *Adv. Energy Mater.* **2019**, *9*, 1802986.
(23) Tang, M.; Zhu, S.; Liu, Z.; Jiang, C.; Wu, Y.; Li, H.; Wang, B.; Wang, E.; Ma, J.; Wang, C. Tailoring π-Conjugated Systems: From π-π Stacking to High-Rate-Performance Organic Cathodes. *Chem.* **2018**, *4*, 2600−2614.
(24) Peng, C.; Ning, G.-H.; Su, J.; Zhong, G.; Tang, W.; Tian, B.; Su, C.; Yu, Di.; Zu, L.; Yang, J.; et al. Reversible Multi-Electron Redox Chemistry of π-Conjugated N-Containing Heteroaromatic Molecule-Based Organic Cathodes. *Nat. Energy* **2017**, *2*, 17074.
(25) Chen, Y.; Li, J.; Zhu, Q.; Fan, K.; Cao, Y.; Zhang, G.; Zhang, C.; Gao, Y.; Zou, J.; Zhai, T.; et al. Two-Dimensional Organic Supramolecule via Hydrogen Bonding and π-π Stacking for Ultrahigh Capacity and Long-Life Aqueous Zinc-Organic Batteries. *Angew. Chem., Int. Ed.* **2022**, *61*, No. e202116289.
(26) Wu, M.; Luu, N. T. H.; Chen, T.; Lyu, H.; Huang, T.; Dai, S.; Sun, X.; Ivanov, A. S.; Lee, J.; Popovs, I.; et al. Supramolecular Self-Assembled Multi-Electron-Acceptor Organic Molecule as High-Performance Cathode Material for Li-Ion Batteries. *Adv. Energy Mater.* **2021**, *11*, 2100330.
(27) Zhang, K.; Guo, C.; Zhao, Q.; Niu, Z.; Chen, J. High-Performance Organic Lithium Batteries with an Ether-Based Electrolyte and 9,10-Anthraquinone (AQ)/CMK-3 Cathode. *Adv. Sci.* **2015**, *2*, 1500018.
(28) Hong, J.; Lee, M.; Lee, B.; Seo, D. H.; Park, C. B.; Kang, K. Biologically Inspired Pteridine Redox Centres for Rechargeable Batteries. *Nat. Commun.* **2014**, *5*, 5335.
(29) Xu, K. Nonaqueous Liquid Electrolytes for Lithium-Based Rechargeable Batteries. *Chem. Rev.* **2004**, *104*, 4303−4417.
(30) Xu, K. Electrolytes and Interphases in Li-Ion Batteries and Beyond. *Chem. Rev.* **2014**, *114*, 11503−11618.
(31) Manthiram, A.; Yu, X.; Wang, S. Lithium Battery Chemistries Enabled by Solid-State Electrolytes. *Nat. Rev. Mater.* **2017**, *2*, 16103.
(32) Suo, L.; Borodin, O.; Wang, Y.; Rong, X.; Sun, W.; Fan, X.; Xu, S.; Schroeder, M. A.; Cresce, A. V.; Wang, F.; et al. Water-in-Salt" Electrolyte Makes Aqueous Sodium-Ion Battery Safe, Green, and Long-Lasting. *Adv. Energy Mater.* **2017**, *7*, 1701189.

https://doi.org/10.1021/acs.chemrev.2c00374
Chem. Rev. 2023, 123, 1712−1773

(33) Liang, Y.; Yao, Y. Positioning Organic Electrode Materials in the Battery Landscape. *Joule* **2018**, *2*, 1690−1706.
(34) Han, C.; Li, H.; Shi, R.; Zhang, T.; Tong, J.; Li, J.; Li, B. Organic Quinones towards Advanced Electrochemical Energy Storage: Recent Advances and Challenges. *J. Mater. Chem. A* **2019**, *7*, 23378−23415.
(35) Bhosale, M. E.; Chae, S.; Kim, J. M.; Choi, J. Y. Organic Small Molecules and Polymers as an Electrode Material for Rechargeable Lithium Ion Batteries. *J. Mater. Chem. A* **2018**, *6*, 19885−19911.
(36) Lu, Y.; Chen, J. Prospects of Organic Electrode Materials for Practical Lithium Batteries. *Nat. Rev. Chem.* **2020**, *4*, 127−142.
(37) Lu, Y.; Zhang, Q.; Li, L.; Niu, Z.; Chen, J. Design Strategies toward Enhancing the Performance of Organic Electrode Materials in Metal-Ion Batteries. *Chem.* **2018**, *4*, 2786−2813.
(38) Shea, J. J.; Luo, C. Organic Electrode Materials for Metal Ion Batteries. *ACS Appl. Mater. Interfaces* **2020**, *12*, 5361−5380.
(39) Poizot, P.; Gaubicher, J.; Renault, S.; Dubois, L.; Liang, Y.; Yao, Y. Opportunities and Challenges for Organic Electrodes in Electrochemical Energy Storage. *Chem. Rev.* **2020**, *120*, 6490−6557.
(40) Lu, Y.; Cai, Y.; Zhang, Q.; Chen, J. Insights into Redox Processes and Correlated Performance of Organic Carbonyl Electrode Materials in Rechargeable Batteries. *Adv. Mater.* **2022**, *34*, 2104150.
(41) Rajagopalan, R.; Tang, Y.; Jia, C.; Ji, X.; Wang, H. Understanding the Sodium Storage Mechanisms of Organic Electrodes in Sodium Ion Batteries: Issues and Solutions. *Energy Environ. Sci.* **2020**, *13*, 1568−1592.
(42) Xu, S.; Chen, Y.; Wang, C. Emerging Organic Potassium-Ion Batteries: Electrodes and Electrolytes. *J. Mater. Chem. A* **2020**, *8*, 15547−15574.
(43) Heiska, J.; Nisula, M.; Karppinen, M. Organic Electrode Materials with Solid-State Battery Technology. *J. Mater. Chem. A* **2019**, *7*, 18735−18758.
(44) Balducci, A.; Gerlach, P. A Critical Analysis about the Underestimated Role of the Electrolyte in Batteries Based on Organic Materials. *ChemElectroChem.* **2020**, *7*, 2364−2375.
(45) Chen, R.; Bresser, D.; Saraf, M.; Gerlach, P.; Balducci, A.; Kunz, S.; Schröder, D.; Passerini, S.; Chen, J. A Comparative Review of Electrolytes for Organic Material-based Energy Storage Devices Employing Solid Electrodes and Redox Fluids. *ChemSusChem* **2020**, *13*, 2205−2219.
(46) Tarascon, J. M.; Armand, M. Issues and Challenges Facing Rechargeable Lithium Batteries. *Nature* **2001**, *414*, 359−367.
(47) Song, Z.; Zhou, H. Towards Sustainable and Versatile Energy Storage Devices: An Overview of Organic Electrode Materials. *Energy Environ. Sci.* **2013**, *6*, 2280−2301.
(48) Wang, M.; Tang, Y. A Review on the Features and Progress of Dual-Ion Batteries. *Adv. Energy Mater.* **2018**, *8*, 1703320.
(49) Wang, H.-g.; Wang, Y.; Wu, Q.; Zhu, G. Recent Developments in Electrode Materials for Dual-Ion Batteries: Potential Alternatives to Conventional Batteries. *Mater. Today* **2022**, *52*, 269−298.
(50) Hagemann, T.; Winsberg, J.; Häupler, B.; Janoschka, T.; Gruber, J. J.; Wild, A.; Schubert, U. S. A Bipolar Nitronyl Nitroxide Small Molecule for an All-Organic Symmetric Redox-Flow Battery. *NPG Asia Mater.* **2017**, *9*, No. e340.
(51) Molina, A.; Patil, N.; Ventosa, E.; Liras, M.; Palma, J.; Marcilla, R. New Anthraquinone-Based Conjugated Microporous Polymer Cathode with Ultrahigh Specific Surface Area for High-Performance Lithium-Ion Batteries. *Adv. Funct. Mater.* **2020**, *30*, 1908074.
(52) Dong, X.; Guo, Z.; Guo, Z.; Wang, Y.; Xia, Y. Organic Batteries Operated at −70°C. *Joule* **2018**, *2*, 902−913.
(53) Song, S. H.; Cho, M.; Park, I.; Yoo, J. G.; Ko, K. T.; Hong, J.; Kim, J.; Jung, S. K.; Avdeev, M.; Ji, S.; et al. High-Voltage-Driven Surface Structuring and Electrochemical Stabilization of Ni-Rich Layered Cathode Materials for Li Rechargeable Batteries. *Adv. Energy Mater.* **2020**, *10*, 2000521.
(54) Li, G.; Ren, Z.; Li, Al. L.; Yu, R.; Quan, W.; Wang, C.; Lin, T.; Yi, D.; Liu, Y.; Zhang, Q.; et al. Highly Stable Surface and Structural Origin for Lithium-Rich Layered Oxide Cathode Materials. *Nano Energy* **2022**, *98*, 107169.
(55) Liang, Y.; Zhang, P.; Yang, S.; Tao, Z.; Chen, J. Fused Heteroaromatic Organic Compounds for High-Power Electrodes of Rechargeable Lithium Batteries. *Adv. Energy Mater.* **2013**, *3*, 600−605.
(56) Armand, M.; Grugeon, S.; Vezin, H.; Laruelle, S.; Ribière, P.; Poizot, P.; Tarascon, J. M. Conjugated Dicarboxylate Anodes for Li-Ion Batteries. *Nat. Mater.* **2009**, *8*, 120−125.
(57) Patil, N.; Aqil, A.; Ouhib, F.; Admassie, S.; Inganäs, O.; Jérôme, C.; Detrembleur, C. Bioinspired Redox-Active Catechol-Bearing Polymers as Ultrarobust Organic Cathodes for Lithium Storage. *Adv. Mater.* **2017**, *29*, 1703373.
(58) Kim, H.; Kwon, J. E.; Lee, B.; Hong, J.; Lee, M.; Park, S. Y.; Kang, K. High Energy Organic Cathode for Sodium Rechargeable Batteries. *Chem. Mater.* **2015**, *27*, 7258−7264.
(59) Wu, D.; Xie, Z.; Zhou, Z.; Shen, P.; Chen, Z. Designing High-Voltage Carbonyl-Containing Polycyclic Aromatic Hydrocarbon Cathode Materials for Li-Ion Batteries Guided by Clar's Theory. *J. Mater. Chem. A* **2015**, *3*, 19137−19143.
(60) Yang, H.; Lee, J.; Cheong, J. Y.; Wang, Y.; Duan, G.; Hou, H.; Jiang, S.; Kim, I. D. Molecular Engineering of Carbonyl Organic Electrodes for Rechargeable Metal-Ion Batteries: Fundamentals, Recent Advances, and Challenges. *Energy Environ. Sci.* **2021**, *14*, 4228−4267.
(61) Ren, L.; Su, L.; Chen, X. Influence of DC Conductivity of PPy Anode on Li/PPy Secondary Batteries. *J. Appl. Polym. Sci.* **2008**, *109*, 3458−3460.
(62) Zhu, L. M.; Lei, A. W.; Cao, Y. L.; Ai, X. P.; Yang, H. X. An All-Organic Rechargeable Battery Using Bipolar Polyparaphenylene as a Redox-Active Cathode and Anode. *Chem. Commun.* **2013**, *49*, 567−569.
(63) Feng, J. K.; Cao, Y. L.; Ai, X. P.; Yang, H. X. Polytriphenylamine: A High Power and High Capacity Cathode Material for Rechargeable Lithium Batteries. *J. Power Sources* **2008**, *177*, 199−204.
(64) Nakahara, K.; Iwasa, S.; Satoh, M.; Morioka, Y.; Iriyama, J.; Suguro, M.; Hasegawa, E. Rechargeable Batteries with Organic Radical Cathodes. *Chem. Phys. Lett.* **2002**, *359*, 351−354.
(65) Oyaizu, K.; Tatsuhira, H.; Nishide, H. Facile Charge Transport and Storage by a TEMPO-Populated Redox Mediating Polymer Integrated with Polyaniline as Electrical Conducting Path. *Polym. J.* **2015**, *47*, 212−219.
(66) Choi, W.; Ohtani, S.; Oyaizu, K.; Nishide, H.; Geckeler, K. E. Radical Polymer-Wrapped SWNTs at a Molecular Level: High-Rate Redox Mediation through a Percolation Network for a Transparent Charge-Storage Material. *Adv. Mater.* **2011**, *23*, 4440−4443.
(67) Sukegawa, T.; Sato, K.; Oyaizu, K.; Nishide, H. Efficient Charge Transport of a Radical Polyether/SWCNT Composite Electrode for an Organic Radical Battery with High Charge-Storage Density. *RSC Adv.* **2015**, *5*, 15448−15452.
(68) Song, Z.; Xu, T.; Gordin, M. L.; Jiang, Y. B.; Bae, I. T.; Xiao, Q.; Zhan, H.; Liu, J.; Wang, D. Polymer-Graphene Nanocomposites as Ultrafast-Charge and -Discharge Cathodes for Rechargeable Lithium Batteries. *Nano Lett.* **2012**, *12*, 2205−2211.
(69) Tian, J.; Cao, D.; Zhou, X.; Hu, J.; Huang, M.; Li, C. High-Capacity Mg-Organic Batteries Based on Nanostructured Rhodizonate Salts Activated by Mg-Li Dual-Salt Electrolyte. *ACS Nano* **2018**, *12*, 3424−3435.
(70) Liang, Y.; Chen, Z.; Jing, Y.; Rong, Y.; Facchetti, A.; Yao, Y. Heavily N-Dopable π-Conjugated Redox Polymers with Ultrafast Energy Storage Capability. *J. Am. Chem. Soc.* **2015**, *137*, 4956−4959.
(71) Fan, L.; Ma, R.; Wang, J.; Yang, H.; Lu, B. An Ultrafast and Highly Stable Potassium-Organic Battery. *Adv. Mater.* **2018**, *30*, 1805486.
(72) Lee, S.; Hong, J.; Jung, S. K.; Ku, K.; Kwon, G.; Seong, W. M.; Kim, H.; Yoon, G.; Kang, I.; Hong, K.; et al. Charge-Transfer Complexes for High-Power Organic Rechargeable Batteries. *Energy Storage Mater.* **2019**, *20*, 462−469.
(73) Kim, C.; Ahn, B. Y.; Wei, T. S.; Jo, Y.; Jeong, S.; Choi, Y.; Kim, I. D.; Lewis, J. A. High-Power Aqueous Zinc-Ion Batteries for Customized Electronic Devices. *ACS Nano* **2018**, *12*, 11838−11846.

https://doi.org/10.1021/acs.chemrev.2c00374
Chem. Rev. 2023, 123, 1712−1773

(74) Hao, F.; Chi, X.; Liang, Y.; Zhang, Y.; Xu, R.; Guo, H.; Terlier, T.; Dong, H.; Zhao, K.; Lou, J.; et al. Taming Active Material-Solid Electrolyte Interfaces with Organic Cathode for All-Solid-State Batteries. *Joule* **2019**, *3*, 1349−1359.
(75) Zhou, X.; Zhang, Y.; Shen, M.; Fang, Z.; Kong, T.; Feng, W.; Xie, Y.; Wang, F.; Hu, B.; Wang, Y. A Highly Stable Li-Organic All-Solid-State Battery Based on Sulfide Electrolytes. *Adv. Energy Mater.* **2022**, *12*, 2103932.
(76) Liu, X.; Zheng, B.; Zhao, J.; Zhao, W.; Liang, Z.; Su, Y.; Xie, C.; Zhou, K.; Xiang, Y.; Zhu, J.; et al. Electrochemo-Mechanical Effects on Structural Integrity of Ni-Rich Cathodes with Different Microstructures in All Solid-State Batteries. *Adv. Energy Mater.* **2021**, *11*, 2003583.
(77) de Vasconcelos, L. S.; Xu, R.; Xu, Z.; Zhang, J.; Sharma, N.; Shah, S. R.; Han, J.; He, X.; Wu, X.; Sun, H.; et al. Chemomechanics of Rechargeable Batteries : Status, Theories, and Perspectives. *Chem. Rev.* **2022**, *122*, 13043−13107.
(78) Turcheniuk, K.; Bondarev, D.; Singhal, V.; Yushin, G. Ten Years Left for Redesign Lithium-Ion Batteries. *Nature* **2018**, *559*, 467−471.
(79) U.S. Department of the Interior & U.S. Geological Survey. *Mineral Commodity Summaries 2021*; U.S. Department of the Interior & U.S. Geological Survey, 2021; https://pubs.er.usgs.gov/publication/mcs2021.
(80) Vaalma, C.; Buchholz, D.; Weil, M.; Passerini, S. A Cost and Resource Analysis of Sodium-Ion Batteries. *Nat. Rev. Mater.* **2018**, *3*, 18013.
(81) Park, Y.; Shin, D. S.; Woo, S. H.; Choi, N. S.; Shin, K. H.; Oh, S. M.; Lee, K. T.; Hong, S. Y. Sodium Terephthalate as an Organic Anode Material for Sodium Ion Batteries. *Adv. Mater.* **2012**, *24*, 3562−3567.
(82) Bachman, J. C.; Muy, S.; Grimaud, A.; Chang, H. H.; Pour, N.; Lux, S. F.; Paschos, O.; Maglia, F.; Lupart, S.; Lamp, P.; et al. Inorganic Solid-State Electrolytes for Lithium Batteries: Mechanisms and Properties Governing Ion Conduction. *Chem. Rev.* **2016**, *116*, 140−162.
(83) Han, F.; Westover, A. S.; Yue, J.; Fan, X.; Wang, F.; Chi, M.; Leonard, D. N.; Dudney, N. J.; Wang, H.; Wang, C. High Electronic Conductivity as the Origin of Lithium Dendrite Formation within Solid Electrolytes. *Nat. Energy* **2019**, *4*, 187−196.
(84) Zhao, Q.; Stalin, S.; Zhao, C. Z.; Archer, L. A. Designing Solid-State Electrolytes for Safe, Energy-Dense Batteries. *Nat. Rev. Mater.* **2020**, *5*, 229−252.
(85) Li, X.; Liang, J.; Yang, X.; Adair, K. R.; Wang, C.; Zhao, F.; Sun, X. Progress and Perspectives on Halide Lithium Conductors for All-Solid-State Lithium Batteries. *Energy Environ. Sci.* **2020**, *13*, 1429−1461.
(86) Kwak, H.; Wang, S.; Park, J.; Liu, Y.; Kim, K. T.; Choi, Y.; Mo, Y.; Jung, Y. S. Emerging Halide Superionic Conductors for All-Solid-State Batteries: Design, Synthesis, and Practical Applications. *ACS Energy Lett.* **2022**, *7*, 1776−1805.
(87) Lu, Y.; Li, L.; Zhang, Q.; Niu, Z.; Chen, J. Electrolyte and Interface Engineering for Solid-State Sodium Batteries. *Joule* **2018**, *2*, 1747−1770.
(88) Tian, Y.; Shi, T.; Richards, W. D.; Li, J.; Kim, J. C.; Bo, S. H.; Ceder, G. Compatibility Issues between Electrodes and Electrolytes in Solid-State Batteries. *Energy Environ. Sci.* **2017**, *10*, 1150−1166.
(89) Pan, H.; Hu, Y. S.; Chen, L. Room-Temperature Stationary Sodium-Ion Batteries for Large-Scale Electric Energy Storage. *Energy Environ. Sci.* **2013**, *6*, 2338−2360.
(90) Banerjee, A.; Park, K. H.; Heo, J. W.; Nam, Y. J.; Moon, C. K.; Oh, S. M.; Hong, S. T.; Jung, Y. S. Na3SbS4: A Solution Processable Sodium Superionic Conductor for All-Solid-State Sodium-Ion Batteries. *Angew. Chem., Int. Ed.* **2016**, *55*, 9634−9638.
(91) Hayashi, A.; Noi, K.; Tanibata, N.; Nagao, M.; Tatsumisago, M. High Sodium Ion Conductivity of Glass-Ceramic Electrolytes with Cubic Na3PS4. *J. Power Sources* **2014**, *258*, 420−423.
(92) Tang, H.; Deng, Z.; Lin, Z.; Wang, Z.; Chu, I. H.; Chen, C.; Zhu, Z.; Zheng, C.; Ong, S. P. Probing Solid-Solid Interfacial Reactions in All-Solid-State Sodium-Ion Batteries with First-Principles Calculations. *Chem. Mater.* **2018**, *30*, 163−173.
(93) Ohta, N.; Takada, K.; Sakaguchi, I.; Zhang, L.; Ma, R.; Fukuda, K.; Osada, M.; Sasaki, T. $LiNbO_3$-Coated $LiCoO_2$ as Cathode Material for All Solid-State Lithium Secondary Batteries. *Electrochem. commun.* **2007**, *9*, 1486−1490.
(94) Yubuchi, S.; Ito, Y.; Matsuyama, T.; Hayashi, A.; Tatsumisago, M. 5 V Class $LiNi_{0.5}Mn_{1.5}O_4$ Positive Electrode Coated with Li_3PO_4 Thin Film for All-Solid-State Batteries Using Sulfide Solid Electrolyte. *Solid State Ionics* **2016**, *285*, 79−82.
(95) Asano, T.; Sakai, A.; Ouchi, S.; Sakaida, M.; Miyazaki, A.; Hasegawa, S. Solid Halide Electrolytes with High Lithium-Ion Conductivity for Application in 4 V Class Bulk-Type All-Solid-State Batteries. *Adv. Mater.* **2018**, *30*, 1803075.
(96) Liang, J.; Li, X.; Adair, K. R.; Sun, X. Metal Halide Superionic Conductors for All-Solid-State Batteries. *Acc. Chem. Res.* **2021**, *54*, 1023−1033.
(97) Xu, R.; Sun, H.; de Vasconcelos, L. S.; Zhao, K. Mechanical and Structural Degradation of $LiNi_xMn_yCo_zO_2$ Cathode in Li-Ion Batteries: An Experimental Study. *J. Electrochem. Soc.* **2017**, *164*, A3333−A3341.
(98) Koerver, R.; Aygün, I.; Leichtweiß, T.; Dietrich, C.; Zhang, W.; Binder, J. O.; Hartmann, P.; Zeier, W. G.; Janek, J. Capacity Fade in Solid-State Batteries: Interphase Formation and Chemomechanical Processes in Nickel-Rich Layered Oxide Cathodes and Lithium Thiophosphate Solid Electrolytes. *Chem. Mater.* **2017**, *29*, 5574−5582.
(99) Koerver, R.; Zhang, W.; De Biasi, L.; Schweidler, S.; Kondrakov, A. O.; Kolling, S.; Brezesinski, T.; Hartmann, P.; Zeier, W. G.; Janek, J. Chemo-Mechanical Expansion of Lithium Electrode Materials-on the Route to Mechanically Optimized All-Solid-State Batteries. *Energy Environ. Sci.* **2018**, *11*, 2142−2158.
(100) Li, M.; Wang, C.; Chen, Z.; Xu, K.; Lu, J. New Concepts in Electrolytes. *Chem. Rev.* **2020**, *120*, 6783−6819.
(101) Yan, C.; Xu, R.; Xiao, Y.; Ding, J.-F.; Xu, L.; Li, B.-Q.; Huang, J.-Q. Toward Critical Electrode/Electrolyte Interfaces in Rechargeable Batteries. *Adv. Funct. Mater.* **2020**, *30*, 1909887.
(102) Wang, H.; Zhai, D.; Kang, F. Solid Electrolyte Interphase (SEI) in Potassium Ion Batteries. *Energy Environ. Sci.* **2020**, *13*, 4583−4608.
(103) Nokami, T.; Matsuo, T.; Inatomi, Y.; Hojo, N.; Tsukagoshi, T.; Yoshizawa, H.; Shimizu, A.; Kuramoto, H.; Komae, K.; Tsuyama, H.; et al. Polymer-Bound Pyrene-4,5,9,10-Tetraone for Fast-Charge and -Discharge Lithium-Ion Batteries with High Capacity. *J. Am. Chem. Soc.* **2012**, *134*, 19694−19700.
(104) Amanchukwu, C. V.; Yu, Z.; Kong, X.; Qin, J.; Cui, Y.; Bao, Z. A New Class of Ionically Conducting Fluorinated Ether Electrolytes with High Electrochemical Stability. *J. Am. Chem. Soc.* **2020**, *142*, 7393−7403.
(105) Yu, Z.; Wang, H.; Kong, X.; Huang, W.; Tsao, Y.; Mackanic, D. G.; Wang, K.; Wang, X.; Huang, W.; Choudhury, S.; et al. Molecular Design for Electrolyte Solvents Enabling Energy-Dense and Long-Cycling Lithium Metal Batteries. *Nat. Energy* **2020**, *5*, 526−533.
(106) Liu, S.; Mao, J.; Zhang, Q.; Wang, Z.; Pang, W. K.; Zhang, L.; Du, A.; Sencadas, V.; Zhang, W.; Guo, Z. An Intrinsically Non-Flammable Electrolyte for High-Performance Potassium Batteries. *Angew. Chem., Int. Ed.* **2020**, *59*, 3638−3644.
(107) Liu, S.; Mao, J.; Zhang, L.; Pang, W. K.; Du, A.; Guo, Z. Manipulating the Solvation Structure of Nonflammable Electrolyte and Interface to Enable Unprecedented Stability of Graphite Anodes beyond 2 Years for Safe Potassium-Ion Batteries. *Adv. Mater.* **2021**, *33*, 2006313.
(108) Liu, K.; Liu, W.; Qiu, Y.; Kong, B.; Sun, Y.; Chen, Z.; Zhuo, D.; Lin, D.; Cui, Y. Electrospun Core-Shell Microfiber Separator with Thermal-Triggered Flame-Retardant Properties for Lithium-Ion Batteries. *Sci. Adv.* **2017**, *3*, No. e1601978.
(109) Zhou, M.; Bai, P.; Ji, X.; Yang, J.; Wang, C.; Xu, Y. Electrolytes and Interphases in Potassium Ion Batteries. *Adv. Mater.* **2021**, *33*, 2003741.
(110) Hosaka, T.; Kubota, K.; Hameed, A. S.; Komaba, S. Research Development on K-Ion Batteries. *Chem. Rev.* **2020**, *120*, 6358−6466.
(111) Perner, V.; Diddens, D.; Otteny, F.; KüPers, V.; Bieker, P.; Esser, B.; Winter, M.; Kolek, M. Insights into the Solubility of

https://doi.org/10.1021/acs.chemrev.2c00374
Chem. Rev. 2023, 123, 1712−1773

Poly(Vinylphenothiazine) in Carbonate-Based Battery Electrolytes. *ACS Appl. Mater. Interfaces* **2021**, *13*, 12442−12453.
(112) Xie, J.; Wang, Z.; Xu, Z. J.; Zhang, Q. Toward a High-Performance All-Plastic Full Battery with a Single Organic Polymer as Both Cathode and Anode. *Adv. Energy Mater.* **2018**, *8*, 1703509.
(113) Sieuw, L.; Jouhara, A.; Quarez, É.; Auger, C.; Gohy, J.-F.; Poizot, P.; Vlad, A. A H-Bond Stabilized Quinone Electrode Material for Li-Organic Batteries: The Strength of Weak Bonds. *Chem. Sci.* **2019**, *10*, 418−426.
(114) Renault, S.; Geng, J.; Dolhem, F.; Poizot, P. Evaluation of Polyketones with N-Cyclic Structure as Electrode Material for Electrochemical Energy Storage: Case of Pyromellitic Diimide Dilithium Salt. *Chem. Commun.* **2011**, *47*, 2414−2416.
(115) Phadke, S.; Cao, M.; Anouti, M. Approaches to Electrolyte Solvent Selection for Poly-Anthraquinone Sulfide Organic Electrode Material. *ChemSusChem* **2018**, *11*, 965−974.
(116) Hansen, C. M. *Hansen Solubility Parameters A User's Handbook*; CRC Press, 2007. DOI: 10.1201/9781420006834.
(117) Hansen, C. M. Aspects of Solubility, Surfaces and Diffusion in Polymers. *Prog. Org. Coatings* **2004**, *51*, 55−66.
(118) Lei, K.; Li, F.; Mu, C.; Wang, J.; Zhao, Q.; Chen, C.; Chen, J. High K-Storage Performance Based on the Synergy of Dipotassium Terephthalate and Ether-Based Electrolytes. *Energy Environ. Sci.* **2017**, *10*, 552−557.
(119) Li, B.; Zhao, J.; Zhang, Z.; Zhao, C.; Sun, P.; Bai, P.; Yang, J.; Zhou, Z.; Xu, Y. Electrolyte-Regulated Solid-Electrolyte Interphase Enables Long Cycle Life Performance in Organic Cathodes for Potassium-Ion Batteries. *Adv. Funct. Mater.* **2019**, *29*, 1807137.
(120) Wang, Y.; Bai, P.; Li, B.; Zhao, C.; Chen, Z.; Li, M.; Su, H.; Yang, J.; Xu, Y. Ultralong Cycle Life Organic Cathode Enabled by Ether-Based Electrolytes for Sodium-Ion Batteries. *Adv. Energy Mater.* **2021**, *11*, 2101972.
(121) Liang, H. J.; Gu, Z. Y.; Zhao, X. X.; Guo, J. Z.; Yang, J. L.; Li, W. H.; Li, B.; Liu, Z. M.; Li, W. L.; Wu, X. L. Ether-Based Electrolyte Chemistry Towards High-Voltage and Long-Life Na-Ion Full Batteries. *Angew. Chem., Int. Ed.* **2021**, *60*, 26837−26846.
(122) Ba, D.; Gui, Q.; Liu, W.; Wang, Z.; Li, Y.; Liu, J. Robust Cathode-Ether Electrolyte Interphase on Interfacial Redox Assembled Fluorophosphate Enabling High-Rate and Ultrastable Sodium Ion Full Cells. *Nano Energy* **2022**, *94*, 106918.
(123) Castillo-Martínez, E.; Carretero-González, J.; Armand, M. Polymeric Schiff Bases as Low-Voltage Redox Centers for Sodium-Ion Batteries. *Angew. Chem., Int. Ed.* **2014**, *53*, 5341−5345.
(124) Luo, C.; Wang, J.; Fan, X.; Zhu, Y.; Han, F.; Suo, L.; Wang, C. Roll-to-Roll Fabrication of Organic Nanorod Electrodes for Sodium Ion Batteries. *Nano Energy* **2015**, *13*, 537−545.
(125) Geng, L.; Meng, J.; Wang, X.; Han, C.; Han, K.; Xiao, Z.; Huang, M.; Xu, P.; Zhang, L.; Zhou, L.; et al. Eutectic Electrolyte with Unique Solvation Structure for High-Performance Zinc-Ion Batteries. *Angew. Chem., Int. Ed.* **2022**, *134*, No. e202206717.
(126) Lee, M.; Hong, J.; Lee, B.; Ku, K.; Lee, S.; Park, C. B.; Kang, K. Multi-Electron Redox Phenazine for Ready-to-Charge Organic Batteries. *Green Chem.* **2017**, *19*, 2980−2985.
(127) Lee, S.; Lee, K.; Ku, K.; Hong, J.; Park, S. Y.; Kwon, J. E.; Kang, K. Utilizing Latent Multi-Redox Activity of P-Type Organic Cathode Materials toward High Energy Density Lithium-Organic Batteries. *Adv. Energy Mater.* **2020**, *10*, 2001635.
(128) Cui, H.; Wang, T.; Huang, Z.; Liang, G.; Chen, Z.; Chen, A.; Wang, D.; Yang, Q.; Hong, H.; Fan, J.; et al. High-Voltage Organic Cathodes for Zinc-Ion Batteries through Electron Cloud and Solvation Structure Regulation. *Angew. Chem., Int. Ed.* **2022**, *61*, No. e202203453.
(129) Lee, M.; Hong, J.; Lopez, J.; Sun, Y.; Feng, D.; Lim, K.; Chueh, W. C.; Toney, M. F.; Cui, Y.; Bao, Z. High-Performance Sodium-Organic Battery by Realizing Four-Sodium Storage in Disodium Rhodizonate. *Nat. Energy* **2017**, *2*, 861−868.
(130) Zhang, S. W.; Cao, T.; Lv, W.; Zhang, J.; Tao, Y.; Kang, F.; Wang, D. W.; Yang, Q. H. High-Performance Graphene/Disodium Terephthalate Electrodes with Ether Electrolyte for Exceptional Cooperative Sodiation/Desodiation. *Nano Energy* **2020**, *77*, 105203.
(131) Sun, P.; Bai, P.; Chen, Z.; Su, H.; Yang, J.; Xu, K.; Xu, Y. A Lithium-Organic Primary Battery. *Small* **2020**, *16*, 1906462.
(132) Chen, Z.; Su, H.; Sun, P.; Bai, P.; Yang, J.; Li, M.; Deng, Y.; Liu, Y.; Geng, Y.; Xu, Y. A Nitroaromatic Cathode with an Ultrahigh Energy Density Based on Six-Electron Reaction per Nitro Group for Lithium Batteries. *Proc. Natl. Acad. Sci. U. S. A.* **2022**, *119*, No. e2116775119.
(133) Pan, B.; Huang, J.; Feng, Z.; Zeng, L.; He, M.; Zhang, L.; Vaughey, J. T.; Bedzyk, M. J.; Fenter, P.; Zhang, Z.; et al. Polyanthraquinone-Based Organic Cathode for High-Performance Rechargeable Magnesium-Ion Batteries. *Adv. Energy Mater.* **2016**, *6*, 1600140.
(134) NuLi, Y.; Guo, Z.; Liu, H.; Yang, J. A New Class of Cathode Materials for Rechargeable Magnesium Batteries: Organosulfur Compounds Based on Sulfur-Sulfur Bonds. *Electrochem. commun.* **2007**, *9*, 1913−1917.
(135) Pan, B.; Zhou, D.; Huang, J.; Zhang, L.; Burrell, A. K.; Vaughey, J. T.; Zhang, Z.; Liao, C. 2,5-Dimethoxy-1,4-Benzoquinone (DMBQ) as Organic Cathode for Rechargeable Magnesium-Ion Batteries. *J. Electrochem. Soc.* **2016**, *163*, A580−A583.
(136) Zhao, X.; Zhao, Z.; Miao, Y. Chloride Ion-Doped Polypyrrole Nanocomposite as Cathode Material for Rechargeable Magnesium Battery. *Mater. Res. Bull.* **2018**, *101*, 1−5.
(137) Ha, S. Y.; Lee, Y. W.; Woo, S. W.; Koo, B.; Kim, J. S.; Cho, J.; Lee, K. T.; Choi, N. S. Magnesium(II) Bis(Trifluoromethane Sulfonyl) Imide-Based Electrolytes with Wide Electrochemical Windows for Rechargeable Magnesium Batteries. *ACS Appl. Mater. Interfaces* **2014**, *6*, 4063−4073.
(138) Bitenc, J.; Pirnat, K.; Mali, G.; Novosel, B.; Randon Vitanova, A.; Dominko, R. Poly(Hydroquinoyl-Benzoquinonyl Sulfide) as an Active Material in Mg and Li Organic Batteries. *Electrochem. commun.* **2016**, *69*, 1−5.
(139) Dong, H.; Tutusaus, O.; Liang, Y.; Zhang, Y.; Lebens-Higgins, Z.; Yang, W.; Mohtadi, R.; Yao, Y. High-Power Mg Batteries Enabled by Heterogeneous Enolization Redox Chemistry and Weakly Coordinating Electrolytes. *Nat. Energy* **2020**, *5*, 1043−1050.
(140) Lu, D.; Liu, H.; Huang, T.; Xu, Z.; Ma, L.; Yang, P.; Qiang, P.; Zhang, F.; Wu, D. Magnesium Ion Based Organic Secondary Batteries. *J. Mater. Chem. A* **2018**, *6*, 17297−17302.
(141) Kundu, D.; Hosseini Vajargah, S.; Wan, L.; Adams, B.; Prendergast, D.; Nazar, L. F. Aqueous: Vs. Nonaqueous Zn-Ion Batteries: Consequences of the Desolvation Penalty at the Interface. *Energy Environ. Sci.* **2018**, *11*, 881−892.
(142) Guerfi, A.; Trottier, J.; Boyano, I.; De Meatza, I.; Blazquez, J. A.; Brewer, S.; Ryder, K. S.; Vijh, A.; Zaghib, K. High Cycling Stability of Zinc-Anode/Conducting Polymer Rechargeable Battery with Non-Aqueous Electrolyte. *J. Power Sources* **2014**, *248*, 1099−1104.
(143) Tie, Z.; Niu, Z. Design Strategies for High-Performance Aqueous Zn/Organic Batteries. *Angew. Chem., Int. Ed.* **2020**, *59*, 21293−21303.
(144) Wang, Y.; Wang, N.; Dong, X.; Wang, B.; Guo, Z.; Wang, Z.; Wang, R.; Qiu, X. Zinc-organic Battery with a Wide Operation-temperature Window from −70 to 150 °C. *Angew. Chem., Int. Ed.* **2020**, *59*, 14577−14583.
(145) Simons, T. J.; Salsamendi, M.; Howlett, P. C.; Forsyth, M.; Macfarlane, D. R.; Pozo-Gonzalo, C. Rechargeable Zn/PEDOT Battery with an Imidazolium-Based Ionic Liquid as the Electrolyte. *ChemElectroChem.* **2015**, *2*, 2071−2078.
(146) Ponrouch, A.; Frontera, C.; Bardé, F.; Palacín, M. R. Towards a Calcium-Based Rechargeable Battery. *Nat. Mater.* **2016**, *15*, 169−172.
(147) Wang, D.; Gao, X.; Chen, Y.; Jin, L.; Kuss, C.; Bruce, P. G. Plating and Stripping Calcium in an Organic Electrolyte. *Nat. Mater.* **2018**, *17*, 16−20.
(148) Rodríguez-Pérez, I. A.; Yuan, Y.; Bommier, C.; Wang, X.; Ma, L.; Leonard, D. P.; Lerner, M. M.; Carter, R. G.; Wu, T.; Greaney, P. A.; et al. Mg-Ion Battery Electrode: An Organic Solid's Herringbone Structure Squeezed upon Mg-Ion Insertion. *J. Am. Chem. Soc.* **2017**, *139*, 13031−13037.

(149) Gheytani, S.; Liang, Y.; Wu, F.; Jing, Y.; Dong, H.; Rao, K. K.; Chi, X.; Fang, F.; Yao, Y. An Aqueous Ca-Ion Battery. *Adv. Sci.* **2017**, *4*, 1700465.
(150) Elia, G. A.; Marquardt, K.; Hoeppner, K.; Fantini, S.; Lin, R.; Knipping, E.; Peters, W.; Drillet, J. F.; Passerini, S.; Hahn, R. An Overview and Future Perspectives of Aluminum Batteries. *Adv. Mater.* **2016**, *28*, 7564−7579.
(151) Walter, M.; Kravchyk, K. V.; Böfer, C.; Widmer, R.; Kovalenko, M. V. Polypyrenes as High-Performance Cathode Materials for Aluminum Batteries. *Adv. Mater.* **2018**, *30*, 1705644.
(152) Bitenc, J.; Lindahl, N.; Vizintin, A.; Abdelhamid, M. E.; Dominko, R.; Johansson, P. Concept and Electrochemical Mechanism of an Al Metal Anode - Organic Cathode Battery. *Energy Storage Mater.* **2020**, *24*, 379−383.
(153) Kim, D. J.; Yoo, D. J.; Otley, M. T.; Prokofjevs, A.; Pezzato, C.; Owczarek, M.; Lee, S. J.; Choi, J. W.; Stoddart, J. F. Rechargeable Aluminium Organic Batteries. *Nat. Energy* **2019**, *4*, 51−59.
(154) Gong, K.; Fang, Q.; Gu, S.; Li, S. F. Y.; Yan, Y. Nonaqueous Redox-Flow Batteries: Organic Solvents, Supporting Electrolytes, and Redox Pairs. *Energy Environ. Sci.* **2015**, *8*, 3515−3530.
(155) Dong, X.; Lin, Y.; Li, P.; Ma, Y.; Huang, J.; Bin, D.; Wang, Y.; Qi, Y.; Xia, Y. High Energy Rechargeable Metallic Lithium Battery at −70 °C Enabled by a Cosolvent Electrolyte. *Angew. Chem., Int. Ed.* **2019**, *58*, 5623−5627.
(156) Wu, J.; Rui, X.; Wang, C.; Pei, W. B.; Lau, R.; Yan, Q.; Zhang, Q. Nanostructured Conjugated Ladder Polymers for Stable and Fast Lithium Storage Anodes with High-Capacity. *Adv. Energy Mater.* **2015**, *5*, 1402189.
(157) Wu, J.; Rui, X.; Long, G.; Chen, W.; Yan, Q.; Zhang, Q. Pushing Up Lithium Storage through Nanostructured Polyazaacene Analogues as Anode. *Angew. Chem., Int. Ed.* **2015**, *54*, 7354−7358.
(158) Guo, R.; Che, Y.; Lan, G.; Lan, J.; Li, J.; Xing, L.; Xu, K.; Fan, W.; Yu, L.; Li, W. Tailoring Low-Temperature Performance of a Lithium-Ion Battery via Rational Designing Interphase on an Anode. *ACS Appl. Mater. Interfaces* **2019**, *11*, 38285−38293.
(159) Li, Q.; Lu, D.; Zheng, J.; Jiao, S.; Luo, L.; Wang, C. M.; Xu, K.; Zhang, J. G.; Xu, W. Li+-Desolvation Dictating Lithium-Ion Battery's Low-Temperature Performances. *ACS Appl. Mater. Interfaces* **2017**, *9*, 42761−42768.
(160) Jones, J.-P.; Smart, M. C.; Krause, F. C.; Bugga, R. V. The Effect of Electrolyte Additives upon Lithium Plating during Low Temperature Charging of Graphite-LiNiCoAlO2 Lithium-Ion Three Electrode Cells. *J. Electrochem. Soc.* **2020**, *167*, 020536.
(161) Zhang, Q.; Cai, W.; Yao, Y. X.; Zhu, G. L.; Yan, C.; Jiang, L. L.; He, C.; Huang, J. Q. A Review on Energy Chemistry of Fast-Charging Anodes. *Chem. Soc. Rev.* **2020**, *49*, 3806−3833.
(162) Zhang, S. S.; Xu, K.; Jow, T. R. Low Temperature Performance of Graphite Electrode in Li-Ion Cells. *Electrochim. Acta* **2002**, *48*, 241−246.
(163) Qin, J.; Lan, Q.; Liu, N.; Zhao, Y.; Song, Z.; Zhan, H. A Metal-Free Battery Working at −80 °C. *Energy Storage Mater.* **2020**, *26*, 585−592.
(164) Holoubek, J.; Yin, Y.; Li, M.; Yu, M.; Meng, Y. S.; Liu, P.; Chen, Z. Exploiting Mechanistic Solvation Kinetics for Dual-Graphite Batteries with High Power Output at Extremely Low Temperature. *Angew. Chem., Int. Ed.* **2019**, *58*, 18892−18897.
(165) Dong, X.; Yang, Y.; Wang, B.; Cao, Y.; Wang, N.; Li, P.; Wang, Y.; Xia, Y. Low-Temperature Charge/Discharge of Rechargeable Battery Realized by Intercalation Pseudocapacitive Behavior. *Adv. Sci.* **2020**, *7*, 2000196.
(166) Fan, X.; Ji, X.; Chen, L.; Chen, J.; Deng, T.; Han, F.; Yue, J.; Piao, N.; Wang, R.; Zhou, X.; et al. All-Temperature Batteries Enabled by Fluorinated Electrolytes with Non-Polar Solvents. *Nat. Energy* **2019**, *4*, 882−890.
(167) Xu, J.; Wang, X.; Yuan, N.; Ding, J.; Qin, S.; Razal, J. M.; Wang, X.; Ge, S.; Gogotsi, Y. Extending the Low Temperature Operational Limit of Li-Ion Battery to −80 °C. *Energy Storage Mater.* **2019**, *23*, 383−389.
(168) Holoubek, J.; Liu, H.; Wu, Z.; Yin, Y.; Xing, X.; Cai, G.; Yu, S.; Zhou, H.; Pascal, T. A.; Chen, Z.; et al. Tailoring Electrolyte Solvation for Li Metal Batteries Cycled at Ultra-Low Temperature. *Nat. Energy* **2021**, *6*, 303−313.
(169) Chen, J.; Peng, Y.; Yin, Y.; Fang, Z.; Cao, Y.; Wang, Y.; Dong, X.; Xia, Y. A Desolvation-Free Sodium Dual-Ion Chemistry for High Power Density and Extremely Low Temperature. *Angew. Chem., Int. Ed.* **2021**, *60*, 23858−23862.
(170) Qin, J.; Lan, Q.; Liu, N.; Men, F.; Wang, X.; Song, Z.; Zhan, H. A Metal-Free Battery with Pure Ionic Liquid Electrolyte. *iScience* **2019**, *15*, 16−27.
(171) Zheng, Y.; Qian, T.; Ji, H.; Xia, X.; Liu, J.; Zhu, Y.; Yan, C. Accelerating Ion Dynamics Under Cryogenic Conditions by the Amorphization of Crystalline Cathodes. *Adv. Mater.* **2021**, *33*, 2102634.
(172) Eftekhari, A.; Corrochano, P. Electrochemical Energy Storage by Aluminum as a Lightweight and Cheap Anode/Charge Carrier. *Sustain. Energy Fuels* **2017**, *1*, 1246−1264.
(173) Lin, M. C.; Gong, M.; Lu, B.; Wu, Y.; Wang, D. Y.; Guan, M.; Angell, M.; Chen, C.; Yang, J.; Hwang, B. J.; et al. An Ultrafast Rechargeable Aluminium-Ion Battery. *Nature* **2015**, *520*, 324−328.
(174) Read, J. A.; Cresce, A. V.; Ervin, M. H.; Xu, K. Dual-Graphite Chemistry Enabled by a High Voltage Electrolyte. *Energy Environ. Sci.* **2014**, *7*, 617−620.
(175) Qiao, Y.; Jiang, K.; Li, X.; Deng, H.; He, Y.; Chang, Z.; Wu, S.; Guo, S.; Zhou, H. A Hybrid Electrolytes Design for Capacity-Equivalent Dual-Graphite Battery with Superior Long-Term Cycle Life. *Adv. Energy Mater.* **2018**, *8*, 1801120.
(176) Li, W. H.; Liang, H. J.; Hou, X. K.; Gu, Z. Y.; Zhao, X. X.; Guo, J. Z.; Yang, X.; Wu, X. L. Feasible Engineering of Cathode Electrolyte Interphase Enables the Profoundly Improved Electrochemical Properties in Dual-Ion Battery. *J. Energy Chem.* **2020**, *50*, 416−423.
(177) Aurbach, D.; Lu, Z.; Schechter, A.; Gofer, Y.; Gizbar, H.; Turgeman, R.; Cohen, Y.; Moshkovich, M.; Levi, E. Prototype Systems for Rechargeable Magnesium Batteries. *Nature* **2000**, *407*, 724−727.
(178) Chen, Q.; Nuli, Y. N.; Guo, W.; Yang, J.; Wang, J. L.; Guo, Y. G. PTMA/Graphene as a Novel Cathode Material for Rechargeable Magnesium Batteries. *Acta Phys. Chim. Sin.* **2013**, *29*, 2295−2299.
(179) Lee, K.; Serdiuk, I. E.; Kwon, G.; Min, D. J.; Kang, K.; Park, S. Y.; Kwon, J. E. Phenoxazine as a High-Voltage p-Type Redox Center for Organic Battery Cathode Materials: Small Structural Reorganization for Faster Charging and Narrow Operating Voltage. *Energy Environ. Sci.* **2020**, *13*, 4142−4156.
(180) Suga, T.; Sugita, S.; Ohshiro, H.; Oyaizu, K.; Nishide, H. P- and n-Type Bipolar Redox-Active Radical Polymer: Toward Totally Organic Polymer-Based Rechargeable Devices with Variable Configuration. *Adv. Mater.* **2011**, *23*, 751−754.
(181) Nauroozi, D.; Pejic, M.; Schwartz, P. O.; Wachtler, M.; Bäuerle, P. Synthesis and Solvent-Free Polymerisation of Vinyl Terephthalate for Application as an Anode Material in Organic Batteries. *RSC Adv.* **2016**, *6*, 111350−111357.
(182) Gerlach, P.; Burges, R.; Lex-Balducci, A.; Schubert, U. S.; Balducci, A. Influence of the Salt Concentration on the Electrochemical Performance of Electrodes for Polymeric Batteries. *Electrochim. Acta* **2019**, *306*, 610−616.
(183) Deunf, É.; Moreau, P.; Quarez, É.; Guyomard, D.; Dolhem, F.; Poizot, P. Reversible Anion Intercalation in a Layered Aromatic Amine: A High-Voltage Host Structure for Organic Batteries. *J. Mater. Chem. A* **2016**, *4*, 6131−6139.
(184) Rajesh, M.; Dolhem, F.; Davoisne, C.; Becuwe, M. Reversible Anion Insertion in Molecular Phenothiazine-Based Redox-Active Positive Material for Organic Ion Batteries. *ChemSusChem* **2020**, *13*, 2364−2370.
(185) Chen, Z.; Xu, N.; Li, W.; Zhao, R.; Dong, Y.; Liu, J.; Su, C.; Wang, J.; Zhang, C. Effect of Trace Hydrofluoric Acid in a LiPF6 Electrolyte on the Performance of a Li-Organic Battery with an N-Heterocycle Based Conjugated Microporous Polymer as the Cathode. *J. Mater. Chem. A* **2019**, *7*, 16347−16355.

https://doi.org/10.1021/acs.chemrev.2c00374
Chem. Rev. 2023, 123, 1712−1773

(186) Adams, B. D.; Zheng, J.; Ren, X.; Xu, W.; Zhang, J. Accurate Determination of Coulombic Efficiency for Lithium Metal Anodes and Lithium Metal Batteries. *Adv. Energy Mater.* **2018**, *8*, 1702097.
(187) Miao, R.; Yang, J.; Feng, X.; Jia, H.; Wang, J.; Nuli, Y. Novel Dual-Salts Electrolyte Solution for Dendrite-Free Lithium-Metal Based Rechargeable Batteries with High Cycle Reversibility. *J. Power Sources* **2014**, *271*, 291−297.
(188) Martinez-Ibañez, M.; Sanchez-Diez, E.; Qiao, L.; Zhang, Y.; Judez, X.; Santiago, A.; Aldalur, I.; Carrasco, J.; Zhu, H.; Forsyth, M.; et al. Unprecedented Improvement of Single Li-Ion Conductive Solid Polymer Electrolyte Through Salt Additive. *Adv. Funct. Mater.* **2020**, *30*, 2000455.
(189) Jiao, S.; Ren, X.; Cao, R.; Engelhard, M. H.; Liu, Y.; Hu, D.; Mei, D.; Zheng, J.; Zhao, W.; Li, Q.; et al. Stable Cycling of High-Voltage Lithium Metal Batteries in Ether Electrolytes. *Nat. Energy* **2018**, *3*, 739−746.
(190) Geng, Z.; Lu, J.; Li, Q.; Qiu, J.; Wang, Y.; Peng, J.; Huang, J.; Li, W.; Yu, X.; Li, H. Lithium Metal Batteries Capable of Stable Operation at Elevated Temperature. *Energy Storage Mater.* **2019**, *23*, 646−652.
(191) Xu, G.; Shangguan, X.; Dong, S.; Zhou, X.; Cui, G. Key Scientific Issues in Formulating Blended Lithium Salts Electrolyte for Lithium Batteries. *Angew. Chem., Int. Ed.* **2020**, *59*, 3400−3415.
(192) Lu, Z.; Schechter, A.; Moshkovich, M.; Aurbach, D. On the Electrochemical Behavior of Magnesium Electrodes in Polar Aprotic Electrolyte Solutions. *J. Electroanal. Chem.* **1999**, *466*, 203−217.
(193) Cheng, Y.; Stolley, R. M.; Han, K. S.; Shao, Y.; Arey, B. W.; Washton, N. M.; Mueller, K. T.; Helm, M. L.; Sprenkle, V. L.; Liu, J.; et al. Highly Active Electrolytes for Rechargeable Mg Batteries Based on a $[Mg_2(\mu\text{-}Cl)_2]^{2+}$ Cation Complex in Dimethoxyethane. *Phys. Chem. Chem. Phys.* **2015**, *17*, 13307−13314.
(194) Bitenc, J.; Pirnat, K.; Bančič, T.; Gaberšček, M.; Genorio, B.; Randon-Vitanova, A.; Dominko, R. Anthraquinone-Based Polymer as Cathode in Rechargeable Magnesium Batteries. *ChemSusChem* **2015**, *8*, 4128−4132.
(195) Cui, L.; Zhou, L.; Zhang, K.; Xiong, F.; Tan, S.; Li, M.; An, Q.; Kang, Y. M.; Mai, L. Salt-Controlled Dissolution in Pigment Cathode for High-Capacity and Long-Life Magnesium Organic Batteries. *Nano Energy* **2019**, *65*, 103902.
(196) Lu, Y.; Tu, Z.; Archer, L. A. Stable Lithium Electrodeposition in Liquid and Nanoporous Solid Electrolytes. *Nat. Mater.* **2014**, *13*, 961−969.
(197) Biswal, P.; Kludze, A.; Rodrigues, J.; Deng, Y.; Moon, T.; Stalin, S.; Zhao, Q.; Yin, J.; Kourkoutis, L. F.; Archer, L. A. The Early-Stage Growth and Reversibility of Li Electrodeposition in Br-Rich Electrolytes. *Proc. Natl. Acad. Sci. U.S.A.* **2021**, *118*, No. e2012071118.
(198) Liao, C.; Sa, N.; Key, B.; Burrell, A. K.; Cheng, L.; Curtiss, L. A.; Vaughey, J. T.; Woo, J. J.; Hu, L.; Pan, B.; et al. The Unexpected Discovery of the $Mg(HMDS)_2/MgCl_2$ Complex as a Magnesium Electrolyte for Rechargeable Magnesium Batteries. *J. Mater. Chem. A* **2015**, *3*, 6082−6087.
(199) Wang, Y.; Liu, Z.; Wang, C.; Hu, Y.; Lin, H.; Kong, W.; Ma, J.; Jin, Z. π-Conjugated Polyimide-Based Organic Cathodes with Extremely-Long Cycling Life for Rechargeable Magnesium Batteries. *Energy Storage Mater.* **2020**, *26*, 494−502.
(200) Gao, T.; Han, F.; Zhu, Y.; Suo, L.; Luo, C.; Xu, K.; Wang, C. Hybrid Mg^{2+}/Li^+ Battery with Long Cycle Life and High Rate Capability. *Adv. Energy Mater.* **2015**, *5*, 1401507.
(201) Cheng, Y.; Chang, H. J.; Dong, H.; Choi, D.; Sprenkle, V. L.; Liu, J.; Yao, Y.; Li, G. Rechargeable Mg-Li Hybrid Batteries: Status and Challenges. *J. Mater. Res.* **2016**, *31*, 3125−3141.
(202) Wang, P.; Yan, X. Recent Advances in Mg-Li and Mg-Na Hybrid Batteries. *Energy Storage Mater.* **2022**, *45*, 142−181.
(203) Sun, X.; Duffort, V.; Nazar, L. F. Prussian Blue Mg-Li Hybrid Batteries. *Adv. Sci.* **2016**, *3*, 1600044.
(204) Cheng, Y.; Shao, Y.; Parent, L. R.; Sushko, M. L.; Li, G.; Sushko, P. V.; Browning, N. D.; Wang, C.; Liu, J. Interface Promoted Reversible Mg Insertion in Nanostructured Tin-Antimony Alloys. *Adv. Mater.* **2015**, *27*, 6598−6605.
(205) Rashad, M.; Asif, M.; Wang, Y.; He, Z.; Ahmed, I. Recent Advances in Electrolytes and Cathode Materials for Magnesium and Hybrid-Ion Batteries. *Energy Storage Mater.* **2020**, *25*, 342−375.
(206) Hu, Y.-S.; Lu, Y. The Mystery of Electrolyte Concentration: From Superhigh to Ultralow. *ACS Energy Lett.* **2020**, *5*, 3633−3636.
(207) Li, Y.; Yang, Y.; Lu, Y.; Zhou, Q.; Qi, X.; Meng, Q.; Rong, X.; Chen, L.; Hu, Y. S. Ultralow-Concentration Electrolyte for Na-Ion Batteries. *ACS Energy Lett.* **2020**, *5*, 1156−1158.
(208) Wu, F.; Chu, F.; Ferrero, G. A.; Sevilla, M.; Fuertes, A. B.; Borodin, O.; Yu, Y.; Yushin, G. Boosting High-Performance in Lithium-Sulfur Batteries via Dilute Electrolyte. *Nano Lett.* **2020**, *20*, 5391−5399.
(209) Yamada, Y.; Yamada, A. Review—Superconcentrated Electrolytes for Lithium Batteries. *J. Electrochem. Soc.* **2015**, *162*, A2406−A2423.
(210) Yamada, Y.; Wang, J.; Ko, S.; Watanabe, E.; Yamada, A. Advances and Issues in Developing Salt-Concentrated Battery Electrolytes. *Nat. Energy* **2019**, *4*, 269−280.
(211) Luo, C.; Borodin, O.; Ji, X.; Hou, S.; Gaskell, K. J.; Fan, X.; Chen, J.; Deng, T.; Wang, R.; Jiang, J.; et al. Azo Compounds as a Family of Organic Electrode Materials for Alkali-Ion Batteries. *Proc. Natl. Acad. Sci. U.S.A.* **2018**, *115*, 2004−2009.
(212) Xiong, M.; Tang, W.; Cao, B.; Yang, C.; Fan, C. A Small-Molecule Organic Cathode with Fast Charge-Discharge Capability for K-Ion Batteries. *J. Mater. Chem. A* **2019**, *7*, 20127−20131.
(213) Cai, T.; Han, Y.; Lan, Q.; Wang, F.; Chu, J.; Zhan, H.; Song, Z. Stable Cycling of Small Molecular Organic Electrode Materials Enabled by High Concentration Electrolytes. *Energy Storage Mater.* **2020**, *31*, 318−327.
(214) Luo, C.; Ji, X.; Hou, S.; Eidson, N.; Fan, X.; Liang, Y.; Deng, T.; Jiang, J.; Wang, C. Azo Compounds Derived from Electrochemical Reduction of Nitro Compounds for High Performance Li-Ion Batteries. *Adv. Mater.* **2018**, *30*, 1706498.
(215) Guo, C.; Zhang, K.; Zhao, Q.; Pei, L.; Chen, J. High-Performance Sodium Batteries with the 9,10-Anthraquinone/CMK-3 Cathode and an Ether-Based Electrolyte. *Chem. Commun.* **2015**, *51*, 10244−10247.
(216) Xu, Z.; Ye, H.; Li, H.; Xu, Y.; Wang, C.; Yin, J.; Zhu, H. Enhanced Lithium Ion Storage Performance of Tannic Acid in LiTFSI Electrolyte. *ACS Omega* **2017**, *2*, 1273−1278.
(217) Qian, J.; Henderson, W. A.; Xu, W.; Bhattacharya, P.; Engelhard, M.; Borodin, O.; Zhang, J.-G. High Rate and Stable Cycling of Lithium Metal Anode. *Nat. Commun.* **2015**, *6*, 6362.
(218) Yamada, Y.; Furukawa, K.; Sodeyama, K.; Kikuchi, K.; Yaegashi, M.; Tateyama, Y.; Yamada, A. Unusual Stability of Acetonitrile-Based Superconcentrated Electrolytes for Fast-Charging Lithium-Ion Batteries. *J. Am. Chem. Soc.* **2014**, *136*, 5039−5046.
(219) Tong, Z.; Tian, S.; Wang, H.; Shen, D.; Yang, R.; Lee, C. S. Tailored Redox Kinetics, Electronic Structures and Electrode/Electrolyte Interfaces for Fast and High Energy-Density Potassium-Organic Battery. *Adv. Funct. Mater.* **2020**, *30*, 1907656.
(220) Huang, Y.; Fang, C.; Zhang, W.; Liu, Q.; Huang, Y. Sustainable Cycling Enabled by a High-Concentration Electrolyte for Lithium-Organic Batteries. *Chem. Commun.* **2019**, *55*, 608−611.
(221) Li, J.; Han, C.; Ou, X.; Tang, Y. Concentrated Electrolyte for High-Performance Ca-Ion Battery Based on Organic Anode and Graphite Cathode. *Angew. Chem., Int. Ed.* **2022**, *61*, No. e202116668.
(222) Zhang, W.; Sun, H.; Hu, P.; Huang, W.; Zhang, Q. Double-effect of Highly Concentrated Acetonitrile-based Electrolyte in Organic Lithium-ion Battery. *EcoMat* **2021**, *3*, No. e12128.
(223) Chen, S.; Zheng, J.; Mei, D.; Han, K. S.; Engelhard, M. H.; Zhao, W.; Xu, W.; Liu, J.; Zhang, J. G. High-Voltage Lithium-Metal Batteries Enabled by Localized High-Concentration Electrolytes. *Adv. Mater.* **2018**, *30*, 1706102.
(224) MacFarlane, D. R.; Forsyth, M.; Howlett, P. C.; Kar, M.; Passerini, S.; Pringle, J. M.; Ohno, H.; Watanabe, M.; Yan, F.; Zheng, W.; et al. Ionic Liquids and Their Solid-State Analogues as Materials for Energy Generation and Storage. *Nat. Rev. Mater.* **2016**, *1*, 15005.
(225) Gurkan, B. E.; Qiang, Z.; Chen, Y. M.; Zhu, Y.; Vogt, B. D. Enhanced Cycle Performance of Quinone-Based Anodes for Sodium

https://doi.org/10.1021/acs.chemrev.2c00374
Chem. Rev. 2023, 123, 1712−1773

Ion Batteries by Attachment to Ordered Mesoporous Carbon and Use of Ionic Liquid Electrolyte. *J. Electrochem. Soc.* **2017**, *164*, H5093−H5099.
(226) Casado, N.; Hilder, M.; Pozo-Gonzalo, C.; Forsyth, M.; Mecerreyes, D. Electrochemical Behavior of PEDOT/Lignin in Ionic Liquid Electrolytes: Suitable Cathode/Electrolyte System for Sodium Batteries. *ChemSusChem* **2017**, *10*, 1783−1791.
(227) Liang, Y.; Zhang, P.; Chen, J. Function-Oriented Design of Conjugated Carbonyl Compound Electrodes for High Energy Lithium Batteries. *Chem. Sci.* **2013**, *4*, 1330−1337.
(228) Wylie, L.; Seeger, Z. L.; Hancock, A. N.; Izgorodina, E. I. Increased Stability of Nitroxide Radicals in Ionic Liquids: More than a Viscosity Effect. *Phys. Chem. Chem. Phys.* **2019**, *21*, 2882−2888.
(229) Wang, X.; Shang, Z.; Yang, A.; Zhang, Q.; Cheng, F.; Jia, D.; Chen, J. Combining Quinone Cathode and Ionic Liquid Electrolyte for Organic Sodium-Ion Batteries. *Chem.* **2019**, *5*, 364−375.
(230) Gerlach, P.; Burges, R.; Lex-Balducci, A.; Schubert, U. S.; Balducci, A. The Influence of the Electrolyte Composition on the Electrochemical Behaviour of Cathodic Materials for Organic Radical Batteries. *J. Power Sources* **2018**, *405*, 142−149.
(231) Fang, Y.; Chen, C.; Fan, J.; Zhang, M.; Yuan, W.; Li, L. Reversible Interaction of 1-Butyl-1-Methylpyrrolidinium Cations with 5,7,12,14-Pentacenetetrone from a Pure Ionic Liquid Electrolyte for Dual-Ion Batteries. *Chem. Commun.* **2019**, *55*, 8333−8336.
(232) Li, W.; Yao, H.; Yan, K.; Zheng, G.; Liang, Z.; Chiang, Y. M.; Cui, Y. The Synergetic Effect of Lithium Polysulfide and Lithium Nitrate to Prevent Lithium Dendrite Growth. *Nat. Commun.* **2015**, *6*, 7436.
(233) Zhang, X.-Q.; Chen, X.; Cheng, X.-B.; Li, B.-Q.; Shen, X.; Yan, C.; Huang, J.-Q.; Zhang, Q. Highly Stable Lithium Metal Batteries Enabled by Regulating the Solvation of Lithium Ions in Nonaqueous Electrolytes. *Angew. Chem., Int. Ed.* **2018**, *130*, 5275−5275.
(234) Liu, H.; Yue, X.; Xing, X.; Yan, Q.; Huang, J.; Petrova, V.; Zhou, H.; Liu, P. A Scalable 3D Lithium Metal Anode. *Energy Storage Mater.* **2019**, *16*, 505−511.
(235) Chen, D.; Avestro, A. J.; Chen, Z.; Sun, J.; Wang, S.; Xiao, M.; Erno, Z.; Algaradah, M. M.; Nassar, M. S.; Amine, K.; et al. A Rigid Naphthalenediimide Triangle for Organic Rechargeable Lithium-Ion Batteries. *Adv. Mater.* **2015**, *27*, 2907−2912.
(236) Xie, J.; Chen, W.; Wang, Z.; Jie, K. C. W.; Liu, M.; Zhang, Q. Synthesis and Exploration of Ladder-Structured Large Aromatic Dianhydrides as Organic Cathodes for Rechargeable Lithium-Ion Batteries. *Chem. Asian J.* **2017**, *12*, 868−876.
(237) Ma, T.; Zhao, Q.; Wang, J.; Pan, Z.; Chen, J. A Sulfur Heterocyclic Quinone Cathode and a Multifunctional Binder for a High-Performance Rechargeable Lithium-Ion Battery. *Angew. Chem., Int. Ed.* **2016**, *128*, 6538−6542.
(238) Hu, Y.; Tang, W.; Yu, Q.; Wang, X.; Liu, W.; Hu, J.; Fan, C. Novel Insoluble Organic Cathodes for Advanced Organic K-Ion Batteries. *Adv. Funct. Mater.* **2020**, *30*, 2000675.
(239) Luo, J. Y.; Cui, W. J.; He, P.; Xia, Y. Y. Raising the Cycling Stability of Aqueous Lithium-Ion Batteries by Eliminating Oxygen in the Electrolyte. *Nat. Chem.* **2010**, *2*, 760−765.
(240) Tang, W.; Zhu, Y.; Hou, Y.; Liu, L.; Wu, Y.; Loh, K. P.; Zhang, H.; Zhu, K. Aqueous Rechargeable Lithium Batteries as an Energy Storage System of Superfast Charging. *Energy Environ. Sci.* **2013**, *6*, 2093−2104.
(241) Kim, H.; Hong, J.; Park, K. Y.; Kim, H.; Kim, S. W.; Kang, K. Aqueous Rechargeable Li and Na Ion Batteries. *Chem. Rev.* **2014**, *114*, 11788−11827.
(242) Liu, Z.; Huang, Y.; Huang, Y.; Yang, Q.; Li, X.; Huang, Z.; Zhi, C. Voltage Issue of Aqueous Rechargeable Metal-Ion Batteries. *Chem. Soc. Rev.* **2020**, *49*, 180−232.
(243) Li, W.; Dahn, J. R.; Wainwright, D. S. Rechargeable Lithium Batteries with Aqueous Electrolytes. *Science* **1994**, *264*, 1115.
(244) He, P.; Liu, J. L.; Cui, W. J.; Luo, J. Y.; Xia, Y. Y. Investigation on Capacity Fading of LiFePO4 in Aqueous Electrolyte. *Electrochim. Acta* **2011**, *56*, 2351−2357.
(245) Zhao, Q.; Huang, W.; Luo, Z.; Liu, L.; Lu, Y.; Li, Y.; Li, L.; Hu, J.; Ma, H.; Chen, J. High-Capacity Aqueous Zinc Batteries Using Sustainable Quinone Electrodes. *Sci. Adv.* **2018**, *4*, No. eaao1761.
(246) Dong, X.; Chen, L.; Liu, J.; Haller, S.; Wang, Y.; Xia, Y. Environmentally-Friendly Aqueous Li (or Na)-Ion Battery with Fast Electrode Kinetics and Super-Long Life. *Sci. Adv.* **2016**, *2*, No. e1501038.
(247) Qin, H.; Song, Z. P.; Zhan, H.; Zhou, Y. H. Aqueous Rechargeable Alkali-Ion Batteries with Polyimide Anode. *J. Power Sources* **2014**, *249*, 367−372.
(248) Yan, L.; Zhao, C.; Sha, Y.; Li, Z.; Liu, T.; Ling, M.; Zhou, S.; Liang, C. Electrochemical Redox Behavior of Organic Quinone Compounds in Aqueous Metal Ion Electrolytes. *Nano Energy* **2020**, *73*, 104766.
(249) Wan, F.; Zhang, L.; Wang, X.; Bi, S.; Niu, Z.; Chen, J. An Aqueous Rechargeable Zinc-Organic Battery with Hybrid Mechanism. *Adv. Funct. Mater.* **2018**, *28*, 1804975.
(250) Luo, Y.; Zheng, F.; Liu, L.; Lei, K.; Hou, X.; Xu, G.; Meng, H.; Shi, J.; Li, F. A High-Power Aqueous Zinc-Organic Radical Battery with Tunable Operating Voltage Triggered by Selected Anions. *ChemSusChem* **2020**, *13*, 2239−2244.
(251) Haüpler, B.; Rössel, C.; Schwenke, A. M.; Winsberg, J.; Schmidt, D.; Wild, A.; Schubert, U. S. Aqueous Zinc-Organic Polymer Battery with a High Rate Performance and Long Lifetime. *NPG Asia Mater.* **2016**, *8*, No. e283.
(252) Shi, H.-Y.; Ye, Y.-J.; Liu, K.; Song, Y.; Sun, X. A Long-Cycle-Life Self-Doped Polyaniline Cathode for Rechargeable Aqueous Zinc Batteries. *Angew. Chem., Int. Ed.* **2018**, *57*, 16359−16363.
(253) Li, P.; Fang, Z.; Zhang, Y.; Mo, C.; Hu, X.; Jian, J.; Wang, S.; Yu, D. A High-Performance, Highly Bendable Quasi-Solid-State Zinc-Organic Battery Enabled by Intelligent Proton-Self-Buffering Copolymer Cathodes. *J. Mater. Chem. A* **2019**, *7*, 17292−17298.
(254) Liang, Y.; Jing, Y.; Gheytani, S.; Lee, K.-Y.; Liu, P.; Facchetti, A.; Yao, Y. Universal Quinone Electrodes for Long Cycle Life Aqueous Rechargeable Batteries. *Nat. Mater.* **2017**, *16*, 841−848.
(255) Lin, K.; Chen, Q.; Gerhardt, M. R.; Tong, L.; Kim, S. B.; Eisenach, L.; Valle, A. W.; Hardee, D.; Gordon, R. G.; Aziz, M. J.; et al. Alkaline Quinone Flow Battery. *Science* **2015**, *349*, 1529−1532.
(256) Jing, Y.; Liang, Y.; Gheytani, S.; Yao, Y. A Quinone Anode for Lithium Ion Batteries in Mild Aqueous Electrolytes. *ChemSusChem* **2020**, *13*, 2250−2255.
(257) Pan, H.; Shao, Y.; Yan, P.; Cheng, Y.; Han, K. S.; Nie, Z.; Wang, C.; Yang, J.; Li, X.; Bhattacharya, P.; et al. Reversible Aqueous Zinc/Manganese Oxide Energy Storage from Conversion Reactions. *Nat. Energy* **2016**, *1*, 16039.
(258) Huang, J.; Wang, Z.; Hou, M.; Dong, X.; Liu, Y.; Wang, Y.; Xia, Y. Polyaniline-Intercalated Manganese Dioxide Nanolayers as a High-Performance Cathode Material for an Aqueous Zinc-Ion Battery. *Nat. Commun.* **2018**, *9*, 2906.
(259) Wang, X.; Bommier, C.; Jian, Z.; Li, Z.; Chandrabose, R. S.; Rodríguez-Pérez, I. A.; Greaney, P. A.; Ji, X. Hydronium-Ion Batteries with Perylenetetracarboxylic Dianhydride Crystals as an Electrode. *Angew. Chem., Int. Ed.* **2017**, *56*, 2909−2913.
(260) Guo, Z.; Huang, J.; Dong, X.; Xia, Y.; Yan, L.; Wang, Z.; Wang, Y. An Organic/Inorganic Electrode-Based Hydronium-Ion Battery. *Nat. Commun.* **2020**, *11*, 959.
(261) Strietzel, C.; Sterby, M.; Huang, H.; Strømme, M.; Emanuelsson, R.; Sjödin, M. An Aqueous Conducting Redox-Polymer-Based Proton Battery That Can Withstand Rapid Constant-Voltage Charging and Sub-Zero Temperatures. *Angew. Chem., Int. Ed.* **2020**, *132*, 9718−9725.
(262) Wang, Y.; Wang, C.; Ni, Z.; Gu, Y.; Wang, B.; Guo, Z.; Wang, Z.; Bin, D.; Ma, J.; Wang, Y. Binding Zinc Ions by Carboxyl Groups from Adjacent Molecules toward Long-Life Aqueous Zinc-Organic Batteries. *Adv. Mater.* **2020**, *32*, 2000338.
(263) Dražević, E.; Andersen, A. S.; Wedege, K.; Henriksen, M. L.; Hinge, M.; Bentien, A. Investigation of Low-Cost Oligoanthraquinones for Alkaline, Aqueous Rechargeable Batteries with Cell Potential up to 1.13 V. *J. Power Sources* **2018**, *381*, 94−100.

https://doi.org/10.1021/acs.chemrev.2c00374
Chem. Rev. 2023, 123, 1712−1773

(264) Suo, L.; Borodin, O.; Gao, T.; Olguin, M.; Ho, J.; Fan, X.; Luo, C.; Wang, C.; Xu, K. Water-in-Salt" Electrolyte Enables High-Voltage Aqueous Lithium-Ion Chemistries. *Science* **2015**, *350*, 938−943.
(265) Jiang, L.; Liu, L.; Yue, J.; Zhang, Q.; Zhou, A.; Borodin, O.; Suo, L.; Li, H.; Chen, L.; Xu, K.; et al. High-Voltage Aqueous Na-Ion Battery Enabled by Inert-Cation-Assisted Water-in-Salt Electrolyte. *Adv. Mater.* **2020**, *32*, 1904427.
(266) Chen, L.; Zhang, J.; Li, Q.; Vatamanu, J.; Ji, X.; Pollard, T. P.; Cui, C.; Hou, S.; Chen, J.; Yang, C.; et al. A 63 m Superconcentrated Aqueous Electrolyte for High-Energy Li-Ion Batteries. *ACS Energy Lett.* **2020**, *5*, 968−974.
(267) Suo, L.; Borodin, O.; Sun, W.; Fan, X.; Yang, C.; Wang, F.; Gao, T.; Ma, Z.; Schroeder, M.; von Cresce, A.; et al. Advanced High-Voltage Aqueous Lithium-Ion Battery Enabled by "Water-in-Bisalt" Electrolyte. *Angew. Chem., Int. Ed.* **2016**, *55*, 7136−7141.
(268) Wang, F.; Borodin, O.; Ding, M. S.; Gobet, M.; Vatamanu, J.; Fan, X.; Gao, T.; Eidson, N.; Liang, Y.; Sun, W.; et al. Hybrid Aqueous/Non-Aqueous Electrolyte for Safe and High-Energy Li-Ion Batteries. *Joule* **2018**, *2*, 927−937.
(269) Dou, Q.; Lei, S.; Wang, D. W.; Zhang, Q.; Xiao, D.; Guo, H.; Wang, A.; Yang, H.; Li, Y.; Shi, S.; et al. Safe and High-Rate Supercapacitors Based on an "Acetonitrile/Water in Salt" Hybrid Electrolyte. *Energy Environ. Sci.* **2018**, *11*, 3212−3219.
(270) Chen, J.; Vatamanu, J.; Xing, L.; Borodin, O.; Chen, H.; Guan, X.; Liu, X.; Xu, K.; Li, W. Improving Electrochemical Stability and Low-Temperature Performance with Water/Acetonitrile Hybrid Electrolytes. *Adv. Energy Mater.* **2020**, *10*, 1902654.
(271) Yang, C.; Chen, J.; Qing, T.; Fan, X.; Sun, W.; von Cresce, A.; Ding, M. S.; Borodin, O.; Vatamanu, J.; Schroeder, M. A.; et al. 4.0 V Aqueous Li-Ion Batteries. *Joule* **2017**, *1*, 122−132.
(272) Dong, X.; Yu, H.; Ma, Y.; Bao, J. L.; Truhlar, D. G.; Wang, Y.; Xia, Y. All-Organic Rechargeable Battery with Reversibility Supported by "Water-in-Salt" Electrolyte. *Chem. Eur. J.* **2017**, *23*, 2560−2565.
(273) Jiang, L.; Lu, Y.; Zhao, C.; Liu, L.; Zhang, J.; Zhang, Q.; Shen, X.; Zhao, J.; Yu, X.; Li, H.; et al. Building Aqueous K-Ion Batteries for Energy Storage. *Nat. Energy* **2019**, *4*, 495−503.
(274) Wang, Y.; Cui, X.; Zhang, Y.; Zhang, L.; Gong, X.; Zheng, G. Achieving High Aqueous Energy Storage via Hydrogen-Generation Passivation. *Adv. Mater.* **2016**, *28*, 7626−7632.
(275) Smith, E. L.; Abbott, A. P.; Ryder, K. S. Deep Eutectic Solvents (DESs) and Their Applications. *Chem. Rev.* **2014**, *114*, 11060−11082.
(276) Wu, J.; Liang, Q.; Yu, X.; Lu, Q.-F.; Ma, L.; Qin, X.; Chen, G.; Li, B. Deep Eutectic Solvents for Boosting Electrochemical Energy Storage and Conversion: A Review and Perspective. *Adv. Funct. Mater.* **2021**, *31*, 2011102.
(277) Zhang, C.; Zhang, L.; Yu, G. Eutectic Electrolytes as a Promising Platform for Next-Generation Electrochemical Energy Storage. *Acc. Chem. Res.* **2020**, *53*, 1648−1659.
(278) Qiu, H.; Du, X.; Zhao, J.; Wang, Y.; Ju, J.; Chen, Z.; Hu, Z.; Yan, D.; Zhou, X.; Cui, G. Zinc Anode-Compatible in-Situ Solid Electrolyte Interphase via Cation Solvation Modulation. *Nat. Commun.* **2019**, *10*, 5374.
(279) Zhao, J.; Zhang, J.; Yang, W.; Chen, B.; Zhao, Z.; Qiu, H.; Dong, S.; Zhou, X.; Cui, G.; Chen, L. Water-in-Deep Eutectic Solvent" Electrolytes Enable Zinc Metal Anodes for Rechargeable Aqueous Batteries. *Nano Energy* **2019**, *57*, 625−634.
(280) Jaumaux, P.; Liu, Q.; Zhou, D.; Xu, X.; Wang, T.; Wang, Y.; Kang, F.; Li, B.; Wang, G. Deep Eutectic Solvent-Based Self-Healing Polymer Electrolyte for Safe and Long-Life Lithium Metal Batteries. *Angew. Chem., Int. Ed.* **2020**, *59*, 9134−9142.
(281) Jiang, P.; Chen, L.; Shao, H.; Huang, S.; Wang, Q.; Su, Y.; Yan, X.; Liang, X.; Zhang, J.; Feng, J.; et al. Methylsulfonylmethane-Based Deep Eutectic Solvent as a New Type of Green Electrolyte for a High-Energy-Density Aqueous Lithium-Ion Battery. *ACS Energy Lett.* **2019**, *4*, 1419−1426.
(282) Geng, L.; Wang, X.; Han, K.; Hu, P.; Zhou, L.; Zhao, Y.; Luo, W.; Mai, L. Eutectic Electrolytes in Advanced Metal-Ion Batteries. *ACS Energy Lett.* **2022**, *7*, 247−260.
(283) Yang, W.; Du, X.; Zhao, J.; Chen, Z.; Li, J.; Xie, J.; Zhang, Y.; Cui, Z.; Kong, Q.; Zhao, Z.; et al. Hydrated Eutectic Electrolytes with Ligand- Oriented Solvation Shells for Long-Cycling Zinc-Organic Batteries Hydrated Eutectic Electrolytes with Ligand-Oriented Solvation Shells for Long-Cycling Zinc-Organic Batteries. *Joule* **2020**, *4*, 1557−1574.
(284) Lin, X.; Zhou, G.; Robson, M. J.; Yu, J.; Kwok, S. C. T.; Ciucci, F. Hydrated Deep Eutectic Electrolytes for High-Performance Zn-Ion Batteries Capable of Low-Temperature Operation. *Adv. Funct. Mater.* **2022**, *32*, 2109322.
(285) Shi, J.; Sun, T.; Bao, J.; Zheng, S.; Du, H.; Li, L.; Yuan, X.; Ma, T.; Tao, Z. Water-in-Deep Eutectic Solvent" Electrolytes for High-Performance Aqueous Zn-Ion Batteries. *Adv. Funct. Mater.* **2021**, *31*, 2102035.
(286) Zhu, Y.; Guo, X.; Lei, Y.; Wang, W.; Emwas, A. H.; Yuan, Y.; He, Y.; Alshareef, H. N. Hydrated Eutectic Electrolytes for High-Performance Mg-Ion Batteries. *Energy Environ. Sci.* **2022**, *15*, 1282−1292.
(287) Xu, J.; Ji, X.; Zhang, J.; Yang, C.; Wang, P.; Liu, S.; Ludwig, K.; Chen, F.; Kofinas, P.; Wang, C. Aqueous Electrolyte Design for Super-Stable 2.5 V $LiMn_2O_4$ || $Li_4Ti_5O_{12}$ Pouch Cells. *Nat. Energy* **2022**, *7*, 186−193.
(288) Nian, Q.; Zhang, X.; Feng, Y.; Liu, S.; Sun, T.; Zheng, S.; Ren, X.; Tao, Z.; Zhang, D.; Chen, J. Designing Electrolyte Structure to Suppress Hydrogen Evolution Reaction in Aqueous Batteries. *ACS Energy Lett.* **2021**, *6*, 2174−2180.
(289) Wang, D.; Li, Q.; Zhao, Y.; Hong, H.; Li, H.; Huang, Z.; Liang, G.; Yang, Q.; Zhi, C. Insight on Organic Molecules in Aqueous Zn-Ion Batteries with an Emphasis on the Zn Anode Regulation. *Adv. Energy Mater.* **2022**, *12*, 2102707.
(290) Cao, L.; Li, D.; Hu, E.; Xu, J.; Deng, T.; Ma, L.; Wang, Y.; Yang, X. Q.; Wang, C. Solvation Structure Design for Aqueous Zn Metal Batteries. *J. Am. Chem. Soc.* **2020**, *142*, 21404−21409.
(291) Hao, J.; Yuan, L.; Ye, C.; Chao, D.; Davey, K.; Guo, Z.; Qiao, S. Z. Boosting Zinc Electrode Reversibility in Aqueous Electrolytes by Using Low-Cost Antisolvents. *Angew. Chem., Int. Ed.* **2021**, *60*, 7366−7375.
(292) Ma, Y.; Zhang, Q.; Liu, L.; Li, Y.; Li, H.; Yan, Z.; Chen, J. N,N-Dimethylformamide Tailors Solvent Effect to Boost Zn Anode Reversibility in Aqueous Electrolyte. *Natl. Sci. Rev.* **2022**, No. *9*, nwac051.
(293) Guo, Z.; Zhao, Y.; Ding, Y.; Dong, X.; Chen, L.; Cao, J.; Wang, C.; Xia, Y.; Peng, H.; Wang, Y. Multi-Functional Flexible Aqueous Sodium-Ion Batteries with High Safety. *Chem.* **2017**, *3*, 348−362.
(294) Song, W. J.; Lee, S.; Song, G.; Park, S. Stretchable Aqueous Batteries: Progress and Prospects. *ACS Energy Lett.* **2019**, *4*, 177−186.
(295) Guo, Z.; Ma, Y.; Dong, X.; Huang, J.; Wang, Y.; Xia, Y. An Environmentally Friendly and Flexible Aqueous Zinc Battery Using an Organic Cathode. *Angew. Chem., Int. Ed.* **2018**, *57*, 11737−11741.
(296) Ma, Y.; Xie, X.; Lv, R.; Na, B.; Ouyang, J.; Liu, H. Nanostructured Polyaniline-Cellulose Papers for Solid-State Flexible Aqueous Zn-Ion Battery. *ACS Sustain. Chem. Eng.* **2018**, *6*, 8697−8703.
(297) Huang, Y.; Liu, J.; Wang, J.; Hu, M.; Mo, F.; Liang, G.; Zhi, C. An Intrinsically Self-Healing NiCo||Zn Rechargeable Battery with a Self-Healable Ferric-Ion-Crosslinking Sodium Polyacrylate Hydrogel Electrolyte. *Angew. Chem., Int. Ed.* **2018**, *57*, 9810−9813.
(298) Huang, S.; Wan, F.; Bi, S.; Zhu, J.; Niu, Z.; Chen, J. A Self-Healing Integrated All-in-One Zinc-Ion Battery. *Angew. Chem., Int. Ed.* **2019**, *131*, 4357−4361.
(299) Kong, Y.; Wang, C.; Yang, Y.; Too, C. O.; Wallace, G. G. A Battery Composed of a Polypyrrole Cathode and a Magnesium Alloy Anode - Toward a Bioelectric Battery. *Synth. Met.* **2012**, *162*, 584−589.
(300) Li, S.; Sultana, I.; Guo, Z.; Wang, C.; Wallace, G. G.; Liu, H. K. Polypyrrole as Cathode Materials for Zn-Polymer Battery with Various Biocompatible Aqueous Electrolytes. *Electrochim. Acta* **2013**, *95*, 212−217.
(301) Wang, J.; Liu, J.; Hu, M.; Zeng, J.; Mu, Y.; Guo, Y.; Yu, J.; Ma, X.; Qiu, Y.; Huang, Y. A Flexible, Electrochromic, Rechargeable Zn//PPy

https://doi.org/10.1021/acs.chemrev.2c00374
Chem. Rev. 2023, 123, 1712−1773

Battery with a Short Circuit Chromatic Warning Function. *J. Mater. Chem. A* **2018**, *6*, 11113−11118.
(302) Meng, J.; Tang, Q.; Zhou, L.; Zhao, C.; Chen, M.; Shen, Y.; Zhou, J.; Feng, G.; Shen, Y.; Huang, Y. A Stirred Self-Stratified Battery for Large-Scale Energy Storage. *Joule* **2020**, *4*, 953−966.
(303) Reaser, P. B.; Burch, G. E. Determination of Deuterium Oxide in Water by Measurement of Freezing Point. *Science* **1958**, *128*, 415−416.
(304) Nian, Q.; Sun, T.; Liu, S.; Du, H.; Ren, X.; Tao, Z. Issues and Opportunities on Low-Temperature Aqueous Batteries. *Chem. Eng. J.* **2021**, *423*, 130253.
(305) Nian, Q.; Wang, J.; Liu, S.; Sun, T.; Zheng, S.; Zhang, Y.; Tao, Z.; Chen, J. Aqueous Batteries Operated at −50 °C. *Angew. Chem., Int. Ed.* **2019**, *58*, 16994−16999.
(306) Ye, Y.; Zhang, Y.; Chen, Y.; Han, X.; Jiang, F. Cellulose Nanofibrils Enhanced, Strong, Stretchable, Freezing-Tolerant Ionic Conductive Organohydrogel for Multi-Functional Sensors. *Adv. Funct. Mater.* **2020**, *30*, 2003430.
(307) Rong, Q.; Lei, W.; Chen, L.; Yin, Y.; Zhou, J.; Liu, M. Anti-Freezing, Conductive Self-Healing Organohydrogels with Stable Strain-Sensitivity at Subzero Temperatures. *Angew. Chem., Int. Ed.* **2017**, *56*, 14159−14163.
(308) Chang, N.; Li, T.; Li, R.; Wang, S.; Yin, Y.; Zhang, H.; Li, X. An Aqueous Hybrid Electrolyte for Low-Temperature Zinc-Based Energy Storage Devices. *Energy Environ. Sci.* **2020**, *13*, 3527−3535.
(309) Wang, R.; Yao, M.; Huang, S.; Tian, J.; Niu, Z. An Anti-Freezing and Anti-Drying Multifunctional Gel Electrolyte for Flexible Aqueous Zinc-Ion Batteries. *Sci. China Mater.* **2022**, *65*, 2189−2196.
(310) Zhang, Q.; Ma, Y.; Lu, Y.; Li, L.; Wan, F.; Zhang, K.; Chen, J. Modulating Electrolyte Structure for Ultralow Temperature Aqueous Zinc Batteries. *Nat. Commun.* **2020**, *11*, 4463.
(311) Sun, T.; Yuan, X.; Wang, K.; Zheng, S.; Shi, J.; Zhang, Q.; Cai, W.; Liang, J.; Tao, Z. An Ultralow-Temperature Aqueous Zinc-Ion Battery. *J. Mater. Chem. A* **2021**, *9*, 7042−7047.
(312) Yue, F.; Tie, Z.; Deng, S.; Wang, S.; Yang, M.; Niu, Z. An Ultralow Temperature Aqueous Battery with Proton Chemistry. *Angew. Chem., Int. Ed.* **2021**, *60*, 13882−13886.
(313) Sun, T.; Zheng, S.; Du, H.; Tao, Z. Synergistic Effect of Cation and Anion for Low-Temperature Aqueous Zinc-Ion Battery. *Nano-Micro Lett.* **2021**, *13*, 204.
(314) Yu, S.; Siegel, D. J. Grain Boundary Contributions to Li-Ion Transport in the Solid Electrolyte $Li_7La_3Zr_2O_{12}$ (LLZO). *Chem. Mater.* **2017**, *29*, 9639−9647.
(315) Gao, B.; Jalem, R.; Tian, H.-K.; Tateyama, Y. Revealing Atomic-Scale Ionic Stability and Transport around Grain Boundaries of Garnet $Li_7La_3Zr_2O_{12}$ Solid Electrolyte. *Adv. Energy Mater.* **2022**, *12*, 2102151.
(316) Kato, Y.; Hori, S.; Saito, T.; Suzuki, K.; Hirayama, M.; Mitsui, A.; Yonemura, M.; Iba, H.; Kanno, R. High-Power All-Solid-State Batteries Using Sulfide Superionic Conductors. *Nat. Energy* **2016**, *1*, 16030.
(317) Zhang, Q.; Cao, D.; Ma, Y.; Natan, A.; Aurora, P.; Zhu, H. Sulfide-Based Solid-State Electrolytes: Synthesis, Stability, and Potential for All-Solid-State Batteries. *Adv. Mater.* **2019**, *31*, 1901131.
(318) Sakuda, A.; Hayashi, A.; Tatsumisago, M. Sulfide Solid Electrolyte with Favorable Mechanical Property for All-Solid-State Lithium Battery. *Sci. Rep.* **2013**, *3*, 2261.
(319) Chen, S.; Xie, D.; Liu, G.; Mwizerwa, J. P.; Zhang, Q.; Zhao, Y.; Xu, X.; Yao, X. Sulfide Solid Electrolytes for All-Solid-State Lithium Batteries: Structure, Conductivity, Stability and Application. *Energy Storage Mater.* **2018**, *14*, 58−74.
(320) Wang, C.; Hwang, S.; Jiang, M.; Liang, J.; Sun, Y.; Adair, K.; Zheng, M.; Mukherjee, S.; Li, X.; Li, R.; et al. Deciphering Interfacial Chemical and Electrochemical Reactions of Sulfide-Based All-Solid-State Batteries. *Adv. Energy Mater.* **2021**, *11*, 2100210.
(321) Zahiri, B.; Patra, A.; Kiggins, C.; Yong, A. X. B.; Ertekin, E.; Cook, J. B.; Braun, P. V. Revealing the Role of the Cathode-Electrolyte Interface on Solid-State Batteries. *Nat. Mater.* **2021**, *20*, 1392−1400.
(322) Zhou, L.; Zuo, T. T.; Kwok, C. Y.; Kim, S. Y.; Assoud, A.; Zhang, Q.; Janek, J.; Nazar, L. F. High Areal Capacity, Long Cycle Life 4 V Ceramic All-Solid-State Li-Ion Batteries Enabled by Chloride Solid Electrolytes. *Nat. Energy* **2022**, *7*, 83−93.
(323) Wenzel, S.; Leichtweiss, T.; Weber, D. A.; Sann, J.; Zeier, W. G.; Janek, J. Interfacial Reactivity Benchmarking of the Sodium Ion Conductors Na3PS4 and Sodium β-Alumina for Protected Sodium Metal Anodes and Sodium All-Solid-State Batteries. *ACS Appl. Mater. Interfaces* **2016**, *8*, 28216−28224.
(324) Li, X.; Liang, J.; Chen, N.; Luo, J.; Adair, K. R.; Wang, C.; Banis, M. N.; Sham, T. K.; Zhang, L.; Zhao, S.; et al. Water-Mediated Synthesis of a Superionic Halide Solid Electrolyte. *Angew. Chem., Int. Ed.* **2019**, *58*, 16427−16432.
(325) Chi, X.; Liang, Y.; Hao, F.; Zhang, Y.; Whiteley, J.; Dong, H.; Hu, P.; Lee, S.; Yao, Y. Tailored Organic Electrode Material Compatible with Sulfide Electrolyte for Stable All-Solid-State Sodium Batteries. *Angew. Chem., Int. Ed.* **2018**, *130*, 2660−2664.
(326) Luo, C.; Ji, X.; Chen, J.; Gaskell, K. J.; He, X.; Liang, Y.; Jiang, J.; Wang, C. Solid-State Electrolyte Anchored with a Carboxylated Azo Compound for All-Solid-State Lithium Batteries. *Angew. Chem., Int. Ed.* **2018**, *57*, 8567−8571.
(327) Hao, F.; Liang, Y.; Zhang, Y.; Chen, Z.; Zhang, J.; Ai, Q.; Guo, H.; Fan, Z.; Lou, J.; Yao, Y. High-Energy All-Solid-State Organic-Lithium Batteries Based on Ceramic Electrolytes. *ACS Energy Lett.* **2021**, *6*, 201−207.
(328) Sahu, G.; Lin, Z.; Li, J.; Liu, Z.; Dudney, N.; Liang, C. Air-Stable, High-Conduction Solid Electrolytes of Arsenic-Substituted Li_4SnS_4. *Energy Environ. Sci.* **2014**, *7*, 1053−1058.
(329) Yang, Z.; Wang, F.; Hu, Z.; Chu, J.; Zhan, H.; Ai, X.; Song, Z. Room-Temperature All-Solid-State Lithium-Organic Batteries Based on Sulfide Electrolytes and Organodisulfide Cathodes. *Adv. Energy Mater.* **2021**, *11*, 2102962.
(330) Chi, X.; Hao, F.; Zhang, J.; Wu, X.; Zhang, Y.; Gheytani, S.; Wen, Z.; Yao, Y. A High-Energy Quinone-Based All-Solid-State Sodium Metal Battery. *Nano Energy* **2019**, *62*, 718−724.
(331) Dudney, N. J. Solid-State Thin-Film Rechargeable Batteries. *Mater. Sci. Eng. B Solid-State Mater. Adv. Technol.* **2005**, *116*, 245−249.
(332) Patil, A.; Patil, V.; Wook Shin, D.; Choi, J. W.; Paik, D. S.; Yoon, S. J. Issue and Challenges Facing Rechargeable Thin Film Lithium Batteries. *Mater. Res. Bull.* **2008**, *43*, 1913−1942.
(333) Pearse, A. J.; Schmitt, T. E.; Fuller, E. J.; El-Gabaly, F.; Lin, C. F.; Gerasopoulos, K.; Kozen, A. C.; Talin, A. A.; Rubloff, G.; Gregorczyk, K. E. Nanoscale Solid State Batteries Enabled by Thermal Atomic Layer Deposition of a Lithium Polyphosphazene Solid State Electrolyte. *Chem. Mater.* **2017**, *29*, 3740−3753.
(334) Zhao, Y.; Zheng, K.; Sun, X. Addressing Interfacial Issues in Liquid-Based and Solid-State Batteries by Atomic and Molecular Layer Deposition. *Joule* **2018**, *2*, 2583−2604.
(335) Nisula, M.; Karppinen, M. In Situ Lithiated Quinone Cathode for ALD/MLD-Fabricated High-Power Thin-Film Battery. *J. Mater. Chem. A* **2018**, *6*, 7027−7033.
(336) Yue, L.; Ma, J.; Zhang, J.; Zhao, J.; Dong, S.; Liu, Z.; Cui, G.; Chen, L. All Solid-State Polymer Electrolytes for High-Performance Lithium Ion Batteries. *Energy Storage Mater.* **2016**, *5*, 139−164.
(337) Li, X.; Hou, Q.; Huang, W.; Xu, H.-S.; Wang, X.; Yu, W.; Li, R.; Zhang, K.; Wang, L.; Chen, Z.; et al. Solution-Processable Covalent Organic Framework Electrolytes for All-Solid-State Li-Organic Batteries. *ACS Energy Lett.* **2020**, *5*, 3498−3506.
(338) Lécuyer, M.; Gaubicher, J.; Barrès, A.-L.; Dolhem, F.; Deschamps, M.; Guyomard, D.; Poizot, P. A Rechargeable Lithium/Quinone Battery Using a Commercial Polymer Electrolyte. *Electrochem. commun.* **2015**, *55*, 22−25.
(339) Fan, L. Z.; Hu, Y. S.; Bhattacharyya, A. J.; Maier, J. Succinonitrile as a Versatile Additive for Polymer Electrolytes. *Adv. Funct. Mater.* **2007**, *17*, 2800−2807.
(340) Yu, X.; Xue, L.; Goodenough, J. B.; Manthiram, A. Ambient-Temperature All-Solid-State Sodium Batteries with a Laminated Composite Electrolyte. *Adv. Funct. Mater.* **2021**, *31*, 2002144.
(341) Alarco, P. J.; Abu-Lebdeh, Y.; Abouimrane, A.; Armand, M. The Plastic-Crystalline Phase of Succinonitrile as a Universal Matrix for Solid-State Ionic Conductors. *Nat. Mater.* **2004**, *3*, 476−481.

https://doi.org/10.1021/acs.chemrev.2c00374
Chem. Rev. 2023, 123, 1712−1773

(342) Braga, M. H.; M Subramaniyam, C.; Murchison, A. J.; Goodenough, J. B. Nontraditional, Safe, High Voltage Rechargeable Cells of Long Cycle Life. *J. Am. Chem. Soc.* **2018**, *140*, 6343−6352.
(343) Zhu, X.; Zhao, R.; Deng, W.; Ai, X.; Yang, H.; Cao, Y. An All-Solid-State and All-Organic Sodium-Ion Battery Based on Redox-Active Polymers and Plastic Crystal Electrolyte. *Electrochim. Acta* **2015**, *178*, 55−59.
(344) Huang, W.; Zheng, S.; Zhang, X.; Zhou, W.; Xiong, W.; Chen, J. Synthesis and Application of Calix[6] Quinone as a High-Capacity Organic Cathode for Plastic Crystal Electrolyte-Based Lithium-Ion Batteries. *Energy Storage Mater.* **2020**, *26*, 465−471.
(345) Lv, P.; Li, Y.; Wu, Y.; Liu, G.; Liu, H.; Li, S.; Tang, C.; Mei, J.; Li, Y. Robust Succinonitrile-Based Gel Polymer Electrolyte for Lithium-Ion Batteries Withstanding Mechanical Folding and High Temperature. *ACS Appl. Mater. Interfaces* **2018**, *10*, 25384−25392.
(346) Kim, B.; Kang, H.; Kim, K.; Wang, R. Y.; Park, M. J. All-Solid-State Lithium-Organic Batteries Comprising Single-Ion Polymer Nanoparticle Electrolytes. *ChemSusChem* **2020**, *13*, 2271−2279.
(347) Zhou, Q.; Ma, J.; Dong, S.; Li, X.; Cui, G. Intermolecular Chemistry in Solid Polymer Electrolytes for High-Energy-Density Lithium Batteries. *Adv. Mater.* **2019**, *31*, 1902029.
(348) Li, H.; Li, M.; Siyal, S. H.; Zhu, M.; Lan, J.-L.; Sui, G.; Yu, Y.; Zhong, W.; Yang, X. A Sandwich Structure Polymer/Polymer-Ceramics/Polymer Gel Electrolytes for the Safe, Stable Cycling of Lithium Metal Batteries. *J. Membr. Sci.* **2018**, *555*, 169−176.
(349) Wan, J.; Xie, J.; Kong, X.; Liu, Z.; Liu, K.; Shi, F.; Pei, A.; Chen, H.; Chen, W.; Chen, J.; et al. Ultrathin, Flexible, Solid Polymer Composite Electrolyte Enabled with Aligned Nanoporous Host for Lithium Batteries. *Nat. Nanotechnol.* **2019**, *14*, 705−711.
(350) Chen, L.; Fan, L. Z. Dendrite-Free Li Metal Deposition in All-Solid-State Lithium Sulfur Batteries with Polymer-in-Salt Polysiloxane Electrolyte. *Energy Storage Mater.* **2018**, *15*, 37−45.
(351) Fei, H.; Liu, Y.; An, Y.; Xu, X.; Zeng, G.; Tian, Y.; Ci, L.; Xi, B.; Xiong, S.; Feng, J. Stable All-Solid-State Potassium Battery Operating at Room Temperature with a Composite Polymer Electrolyte and a Sustainable Organic Cathode. *J. Power Sources* **2018**, *399*, 294−298.
(352) Huang, W.; Zhu, Z.; Wang, L.; Wang, S.; Li, H.; Tao, Z.; Shi, J.; Guan, L.; Chen, J. Quasi-Solid-State Rechargeable Lithium-Ion Batteries with a Calix[4]Quinone Cathode and Gel Polymer Electrolyte. *Angew. Chem., Int. Ed.* **2013**, *52*, 9162−9166.
(353) Kim, J.-K.; Cheruvally, G.; Choi, J.-W.; Ahn, J.-H.; Choi, D. S.; Song, C. E. Rechargeable Organic Radical Battery with Electrospun, Fibrous Membrane-Based Polymer Electrolyte. *J. Electrochem. Soc.* **2007**, *154*, A839.
(354) Zhang, Y.; An, Y.; Dong, S.; Jiang, J.; Dou, H.; Zhang, X. Enhanced Cycle Performance of Polyimide Cathode Using a Quasi-Solid-State Electrolyte. *J. Phys. Chem. C* **2018**, *122*, 22294−22300.
(355) Kim, H. W.; Kim, H.-J.; Byeon, H.; Kim, J.; Yang, J. W.; Kim, Y.; Kim, J.-K. Binder-Free Organic Cathode Based on Nitroxide Radical Polymer-Functionalized Carbon Nanotubes and Gel Polymer Electrolyte for High-Performance Sodium Organic Polymer Batteries. *J. Mater. Chem. A* **2020**, *8*, 17980−17986.
(356) Li, M.; Yang, J.; Shi, Y.; Chen, Z.; Bai, P.; Su, H.; Xiong, P.; Cheng, M.; Zhao, J.; Xu, Y. Soluble Organic Cathodes Enable Long Cycle Life, High Rate, and Wide-Temperature Lithium-Ion Batteries. *Adv. Mater.* **2022**, *34*, 2107226.
(357) Vijayakumar, V.; Anothumakkool, B.; Kurungot, S.; Winter, M.; Nair, J. R. In Situ Polymerization Process: An Essential Design Tool for Lithium Polymer Batteries. *Energy Environ. Sci.* **2021**, *14*, 2708−2788.
(358) Xiang, J.; Zhang, Y.; Zhang, B.; Yuan, L.; Liu, X.; Cheng, Z.; Yang, Y.; Zhang, X.; Li, Z.; Shen, Y.; et al. A Flame-Retardant Polymer Electrolyte for High Performance Lithium Metal Batteries with an Expanded Operation Temperature. *Energy Environ. Sci.* **2021**, *14*, 3510−3521.
(359) Gao, H.; Xue, L.; Xin, S.; Goodenough, J. B. A High-Energy-Density Potassium Battery with a Polymer-Gel Electrolyte and a Polyaniline Cathode. *Angew. Chem., Int. Ed.* **2018**, *57*, 5449−5453.
(360) Zheng, J.; Tang, M.; Hu, Y. Lithium Ion Pathway within $Li_7La_3Zr_2O_{12}$-Polyethylene Oxide Composite Electrolytes. *Angew. Chem., Int. Ed.* **2016**, *55*, 12538−12542.
(361) Zhu, Z.; Hong, M.; Guo, D.; Shi, J.; Tao, Z.; Chen, J. All-Solid-State Lithium Organic Battery with Composite Polymer Electrolyte and Pillar[5] Quinone Cathode. *J. Am. Chem. Soc.* **2014**, *136*, 16461−16464.
(362) Li, W.; Chen, L.; Sun, Y.; Wang, C.; Wang, Y.; Xia, Y. All-Solid-State Secondary Lithium Battery Using Solid Polymer Electrolyte and Anthraquinone Cathode. *Solid State Ionics* **2017**, *300*, 114−119.
(363) Wei, W.; Li, L.; Zhang, L.; Hong, J.; He, G. An All-Solid-State Li-Organic Battery with Quinone-Based Polymer Cathode and Composite Polymer Electrolyte. *Electrochem. commun.* **2018**, *90*, 21−25.
(364) Hanyu, Y.; Honma, I. Rechargeable Quasi-Solid State Lithium Battery with Organic Crystalline Cathode. *Sci. Rep.* **2012**, *2*, 453.
(365) Hanyu, Y.; Ganbe, Y.; Honma, I. Application of Quinonic Cathode Compounds for Quasi-Solid Lithium Batteries. *J. Power Sources* **2013**, *221*, 186−190.
(366) Hanyu, Y.; Sugimoto, T.; Ganbe, Y.; Masuda, A.; Honma, I. Multielectron Redox Compounds for Organic Cathode Quasi-Solid State Lithium Battery. *J. Electrochem. Soc.* **2014**, *161*, A6−A9.
(367) Wang, X.; Zhang, Y.; Zhang, X.; Liu, T.; Lin, Y. H.; Li, L.; Shen, Y.; Nan, C. W. Lithium-Salt-Rich PEO/$Li_{0.3}La_{0.557}TiO_3$ Interpenetrating Composite Electrolyte with Three-Dimensional Ceramic Nano-Backbone for All-Solid-State Lithium-Ion Batteries. *ACS Appl. Mater. Interfaces* **2018**, *10*, 24791−24798.
(368) Zhao, Y.; Yan, J.; Cai, W.; Lai, Y.; Song, J.; Yu, J.; Ding, B. Elastic and Well-Aligned Ceramic LLZO Nanofiber Based Electrolytes for Solid-State Lithium Batteries. *Energy Storage Mater.* **2019**, *23*, 306−313.
(369) Li, D.; Chen, L.; Wang, T.; Fan, L. Z. 3D Fiber-Network-Reinforced Bicontinuous Composite Solid Electrolyte for Dendrite-Free Lithium Metal Batteries. *ACS Appl. Mater. Interfaces* **2018**, *10*, 7069−7078.
(370) Li, Z.; Wang, S.; Shi, J.; Liu, Y.; Zheng, S.; Zou, H.; Chen, Y.; Kuang, W.; Ding, K.; Chen, L.; et al. A 3D Interconnected Metal-Organic Framework-Derived Solid-State Electrolyte for Dendrite-Free Lithium Metal Battery. *Energy Storage Mater.* **2022**, *47*, 262−270.
(371) Zhang, X.; Shen, F.; Long, X.; Zheng, S.; Ruan, Z.; Cai, P.; Hong, X.; Zheng, Q. Fast Li^+ Transport and Superior Interfacial Chemistry within Composite Polymer Electrolyte Enables Ultra-Long Cycling Solid-State Li-Metal Batteries. *Energy Storage Mater.* **2022**, *52*, 201−209.
(372) Muench, S.; Burges, R.; Lex-Balducci, A.; Brendel, J. C.; Jäger, M.; Friebe, C.; Wild, A.; Schubert, U. S. Printable Ionic Liquid-Based Gel Polymer Electrolytes for Solid State All-Organic Batteries. *Energy Storage Mater.* **2020**, *25*, 750−755.
(373) Fdz De Anastro, A.; Casado, N.; Wang, X.; Rehmen, J.; Evans, D.; Mecerreyes, D.; Forsyth, M.; Pozo-Gonzalo, C. Poly(Ionic Liquid) Iongels for All-Solid Rechargeable Zinc/PEDOT Batteries. *Electrochim. Acta* **2018**, *278*, 271−278.
(374) Leung, P.; Bu, J.; Quijano Velasco, P.; Roberts, M. R.; Grobert, N.; Grant, P. S. Single-Step Spray Printing of Symmetric All-Organic Solid-State Batteries Based on Porous Textile Dye Electrodes. *Adv. Energy Mater.* **2019**, *9*, 1901418.
(375) Cao, D.; Sun, X.; Li, Q.; Natan, A.; Xiang, P.; Zhu, H. Lithium Dendrite in All-Solid-State Batteries : Growth Mechanisms, Suppression Strategies, and Characterizations. *Matter* **2020**, *3*, 57−94.
(376) Ning, Z.; Jolly, D. S.; Li, G.; De Meyere, R.; Pu, S. D.; Chen, Y.; Kasemchainan, J.; Ihli, J.; Gong, C.; Liu, B.; et al. Visualizing Plating-Induced Cracking in Lithium-Anode Solid-Electrolyte Cells. *Nat. Mater.* **2021**, *20*, 1121−1130.
(377) Wan, J.; Song, Y. X.; Chen, W. P.; Guo, H. J.; Shi, Y.; Guo, Y. J.; Shi, J. L.; Guo, Y. G.; Jia, F. F.; Wang, F. Y.; et al. Micromechanism in All-Solid-State Alloy-Metal Batteries: Regulating Homogeneous Lithium Precipitation and Flexible Solid Electrolyte Interphase Evolution. *J. Am. Chem. Soc.* **2021**, *143*, 839−848.
(378) Pan, H.; Zhang, M.; Cheng, Z.; Jiang, H.; Yang, J.; Wang, P.; He, P.; Zhou, H. Carbon-Free and Binder-Free Li-Al Alloy Anode Enabling

an All-Solid-State Li-S Battery with High Energy and Stability. *Sci. Adv.* **2022**, *8*, No. eabn4372.
(379) Fan, L.; Liu, Q.; Xu, Z.; Lu, B. An Organic Cathode for Potassium Dual-Ion Full Battery. *ACS Energy Lett.* **2017**, *2*, 1614−1620.
(380) Nakahara, K.; Iriyama, J.; Iwasa, S.; Suguro, M.; Satoh, M.; Cairns, E. J. Al-Laminated Film Packaged Organic Radical Battery for High-Power Applications. *J. Power Sources* **2007**, *163*, 1110−1113.
(381) Jiang, C.; Wang, C. 2D Materials as Ionic Sieves for Inhibiting the Shuttle Effect in Batteries. *Chem. - An Asian J.* **2020**, *15*, 2294−2302.
(382) Ma, L.; Nath, P.; Tu, Z.; Tikekar, M.; Archer, L. A. Highly Conductive, Sulfonated, UV-Cross-Linked Separators for Li-S Batteries. *Chem. Mater.* **2016**, *28*, 5147−5154.
(383) Yu, X.; Manthiram, A. Ambient-Temperature Sodium-Sulfur Batteries with a Sodiated Nafion Membrane and a Carbon Nanofiber-Activated Carbon Composite Electrode. *Adv. Energy Mater.* **2015**, *5*, 1500350.
(384) Liu, J.; Yu, L.; Cai, X.; Khan, U.; Cai, Z.; Xi, J.; Liu, B.; Kang, F. Sandwiching H-BN Monolayer Films between Sulfonated Poly(Ether Ether Ketone) and Nafion for Proton Exchange Membranes with Improved Ion Selectivity. *ACS Nano* **2019**, *13*, 2094−2102.
(385) Ding, C.; Zhang, H.; Li, X.; Zhang, H.; Yao, C.; Shi, D. Morphology and Electrochemical Properties of Perfluorosulfonic Acid Ionomers for Vanadium Flow Battery Applications: Effect of Side-Chain Length. *ChemSusChem* **2013**, *6*, 1262−1269.
(386) Smitha, B.; Sridhar, S.; Khan, A. A. Solid Polymer Electrolyte Membranes for Fuel Cell Applications - A Review. *J. Membr. Sci.* **2005**, *259*, 10−26.
(387) Park, C. H.; Lee, C. H.; Guiver, M. D.; Lee, Y. M. Sulfonated Hydrocarbon Membranes for Medium-Temperature and Low-Humidity Proton Exchange Membrane Fuel Cells (PEMFCs). *Prog. Polym. Sci.* **2011**, *36*, 1443−1498.
(388) Wang, C.; Jiang, C.; Xu, Y.; Liang, L.; Zhou, M.; Jiang, J.; Singh, S.; Zhao, H.; Schober, A.; Lei, Y. A Selectively Permeable Membrane for Enhancing Cyclability of Organic Sodium-Ion Batteries. *Adv. Mater.* **2016**, *28*, 9182−9187.
(389) Zhu, S.; Tang, M.; Wu, Y.; Chen, Y.; Jiang, C.; Xia, C.; Zhuo, S.; Wang, B.; Wang, C. Free-Standing Protective Films for Enhancing the Cyclability of Organic Batteries. *Sustain. Energy Fuels* **2019**, *3*, 142−147.
(390) Song, Z.; Qian, Y.; Otani, M.; Zhou, H. Stable Li-Organic Batteries with Nafion-Based Sandwich-Type Separators. *Adv. Energy Mater.* **2016**, *6*, 1501780.
(391) Huang, J. Q.; Zhuang, T. Z.; Zhang, Q.; Peng, H. J.; Chen, C. M.; Wei, F. Permselective Graphene Oxide Membrane for Highly Stable and Anti-Self-Discharge Lithium-Sulfur Batteries. *ACS Nano* **2015**, *9*, 3002−3011.
(392) Shaibani, M.; Akbari, A.; Sheath, P.; Easton, C. D.; Banerjee, P. C.; Konstas, K.; Fakhfouri, A.; Barghamadi, M.; Musameh, M. M.; Best, A. S.; et al. Suppressed Polysulfide Crossover in Li-S Batteries through a High-Flux Graphene Oxide Membrane Supported on a Sulfur Cathode. *ACS Nano* **2016**, *10*, 7768−7779.
(393) Pan, Y.; Hao, J.; Zhu, X.; Zhou, Y.; Chou, S. Ion Selective Separators Based on Graphene Oxide for Stabilizing Lithium Organic Batteries. *Inorg. Chem. Front.* **2018**, *5*, 1869−1875.
(394) Fang, C.; Ye, Z.; Wang, Y.; Zhao, X.; Huang, Y.; Zhao, R.; Liu, J.; Han, J.; Huang, Y. Immobilizing an Organic Electrode Material through π-π Interaction for High-Performance Li-Organic Batteries. *J. Mater. Chem. A* **2019**, *7*, 22398−22404.
(395) Belanger, R. L.; Commarieu, B.; Paolella, A.; Daigle, J. C.; Bessette, S.; Vijh, A.; Claverie, J. P.; Zaghib, K. Diffusion Control of Organic Cathode Materials in Lithium Metal Battery. *Sci. Rep.* **2019**, *9*, 1213.
(396) Chang, Z.; Qiao, Y.; Wang, J.; Deng, H.; He, P.; Zhou, H. Fabricating Better Metal-Organic Frameworks Separators for Li-S Batteries: Pore Sizes Effects Inspired Channel Modification Strategy. *Energy Storage Mater.* **2020**, *25*, 164−171.
(397) Bai, S.; Liu, X.; Zhu, K.; Wu, S.; Zhou, H. Metal-Organic Framework-Based Separator for Lithium-Sulfur Batteries. *Nat. Energy* **2016**, *1*, 16094.
(398) Deng, H.; Chang, Z.; Qiu, F.; Qiao, Y.; Yang, H.; He, P.; Zhou, H. A Safe Organic Oxygen Battery Built with Li-Based Liquid Anode and MOFs Separator. *Adv. Energy Mater.* **2020**, *10*, 1903953.
(399) Bai, S.; Kim, B.; Kim, C.; Tamwattana, O.; Park, H.; Kim, J.; Lee, D.; Kang, K. Permselective Metal-Organic Framework Gel Membrane Enables Long-Life Cycling of Rechargeable Organic Batteries. *Nat. Nanotechnol.* **2021**, *16*, 77−84.
(400) Jiang, C.; Tang, M.; Zhu, S.; Zhang, J.; Wu, Y.; Chen, Y.; Xia, C.; Wang, C.; Hu, W. Constructing Universal Ionic Sieves via Alignment of Two-Dimensional Covalent Organic Frameworks (COFs). *Angew. Chem., Int. Ed.* **2018**, *57*, 16072−16076.
(401) Zhang, Q.; Liu, K.; Ding, F.; Li, W.; Liu, X.; Zhang, J. Safety-Reinforced Succinonitrile-Based Electrolyte with Interfacial Stability for High-Performance Lithium Batteries. *ACS Appl. Mater. Interfaces* **2017**, *9*, 29820−29828.
(402) Xiao, Y.; Han, B.; Zeng, Y.; Chi, S.-S.; Zeng, X.; Zheng, Z.; Xu, K.; Deng, Y. New Lithium Salt Forms Interphases Suppressing Both Li Dendrite and Polysulfide Shuttling. *Adv. Energy Mater.* **2020**, *10*, 1903937.
(403) Lu, H.; Chen, Z.; Yuan, Y.; Du, H.; Wang, J.; Liu, X.; Hou, Z.; Zhang, K.; Fang, J.; Qu, Y. A Rational Balance Design of Hybrid Electrolyte Based on Ionic Liquid and Fluorinated Ether in Lithium Sulfur Batteries. *J. Electrochem. Soc.* **2019**, *166*, A2453−A2458.

https://doi.org/10.1021/acs.chemrev.2c00374
Chem. Rev. 2023, 123, 1712−1773